LITHOSTRATIGRAPHY, SEDIMENTOLOGY, AND DIAGENESIS OF THE ORDOVICIAN CARBONATES, SOUTHERN THAILAND

by

Thanis Wongwanich, B.Sc.

Submitted in partial fulfilment of the requirements
for the degree of
Doctor of Philosophy
(Geology)
University of Tasmania
(October, 1990)

This thesis contains no material which has been accepted for the award of any other higher degree or graduate diploma in any tertiary institution and to the best of the author's knowledge and belief, the thesis contains no material previously published or written by another person, except when due reference is made in the text of the thesis.

Thanis Wongwanich

Thanis Wongwanich

ABSTRACT

The Ordovician Thung Song Group, in Satun Province, southern Thailand, is a 1,400 m thick sequence of tropical limestones, dolomites and calcareous shale ranging from the Upper Tremadoc to Upper Ashgill. The sequence conformably overlies the siliciclastic, Tarutao Group and is conformably overlain by black graptolitic shales and cherts with radiolarians of the Wang Tong Formation. The Ordovician-Silurian boundary is placed in the lower part of the Wang Tong Formation ~25 m above the Pa Kae Formation. At least seven distinctive lithostratigraphic units have been recognized and are formalised here as the Malaka Formation, Talo Dang Formation, La Nga Formation, Pa Nan Formation, Lae Tong Formation, Rung Nok Formation, and the Pa Kae Formation. The Pa Kae Formation is proposed for the uppermost formation of the Thung Song Group.

The Thung Song carbonates were deposited on a homoclinal ramp. Environments during a major marine transgression with minor eustatic fluctuation included large tidal flats, stromatolite reefs, lagoons, local buildup-barrier reefs, and deeper water carbonates. The rocks are composed of twelve microfacies including stromatolites, micrite to fossiliferous micrite, biomicrite, intramicrite, poorly washed to unsorted biosparite, biopelsparite and pelbiosparite, pelsparite, intrasparite, flat pebble conglomerate, oosparite, biolithite and limestone breccia, micro- to megadolomite and dolomite breccia. These indicate sedimentation in a wide range of environments from supratidal, intertidal, subtidal to deeper-water zones. The lower portion of the sequence was deposited in peritidal, lagoonal and carbonate buildup environments and stromatolites played a major role in the sedimentation. Flat pebble conglomerates with algal laminite clasts, intrasparite and small-scale hummocky cross-stratification indicate high-energy storm events.

The Pa Kae Formation is different from the underlying shallow water carbonates. It was deposited in a tropical setting, during a period of intense glaciation at high latitudes on Gondwanaland, as deeper water stromatolitic mounds. The rocks display rhythmic alternation of red stromatolitic limestones and dark red mudstones. The stromatolitic limestones are biomicrites with dense stromatolitic structures developed from flat laminites in the bottom to common columnar stromatolites, and some thrombolitic and oncolitic stromatolites on the top of each bed. They share several common features with the deep water stromatolites from the Canning Basin, Western Australia, such as fine lamination, rare or no fenestrae, and abundant pelagic faunas. They are different in the abundant ferromanganese micronodules, the

occurrence of glauconitic pellets, bored calcite cements and very abundant rhombic spars. Based on a new proposed model developed to predict the possible palaeobathymetry of the carbonate rocks in tropical to temperate regions, the Pa Kae stromatolites accreted on the very distal part of the Thai Ordovician carbonate ramp at about 175-300 m depths and at about 15°C. Their heavy isotopic signature (-3.1‰PDB of $\partial^{18}O$ and +3.4‰PDB of $\partial^{13}C$) and their cyclic nature suggest that the warm and cold climates repeated themselves many times throughout the Late Ordovician.

The Thung Song carbonates have undergone a long and complex diagenetic history including early marine, early to late meteoric, and burial cementation; dolomitization; physical and chemical compaction; and dedolomitization. Early cementation within the carbonate buildups of the Rung Nok Formation and the Pa Kae stromatolitic mounds are much more extensive than in the peritidal carbonates of the Malaka Formation and La Nga Formation but it is rare in the lagoonal facies of the Talo Dang Formation and Lae Tong Formation. Therefore, the degree of compaction of the lagoonal facies is extremely high in comparison with those of the peritidal buildups and deeper water stromatolitic mounds. Stylolites are very abundant in the Thung Song Group, especially in the peritidal carbonates and play a major role in the development of nodular structures in the limestone and shale of the lagoonal facies and of the deeper water stromatolitic facies.

Most of the dolomites in the lower formation including the Malaka Formation, and La Nga Formation are early diagenetic microdolomites with minor dolomite cement. Later diagenetic meso- to megadolomites are common in the Rung Nok Formation. The dolomitization of the Pa Kae Formation occurred locally throughout its diagenetic history but normal sea water dolomite is dominant. The isotopic field of the Thung Song dolomite overlaps the marine calcite diagenetic field and extends up to the meteoric diagenetic field, possibly suggesting that these dolomites formed from marine to mixed-water dolomitizing fluids.

ACKNOWLEDGEMENTS

I would like to thank all those who helped in the preparation of this thesis. In particular, I am indebted to Dr C.F. Burrett for suggesting the study and his advice throughout the project. I am grateful to Dr C.P. Rao who provided invaluable advice on many aspects of the sedimentology, geochemistry, and a critical review of this manuscript. Special thanks must go to Drs M.R. Banks, R.A. Fortey, J. Long, B. Rickards, J. Shergold, and B. Stait for their advice on stratigraphy and help in identification of many fossils from Thailand. To Dr R.F. Berry, I am indebted for his guidance on primary structures. To Dr E.G. Purdy for his helpful discussions on many aspects.

Acknowledgement is extended to the personnel of the Royal Thai Department of Mineral Resources, the Tarutao National Marine Park and the Phetra National Marine Park. They are Mr P. Polahan, Mr T. Japanakaset, Mr P. Angsuwanich, Mrs R. Ingkawat, Dr S. Bunopas, N. Nakornsri, Dr P. Sukato, Mr W. Laemwilae, Mrs B. Sektheera, Mr S. Muenlek, Mr and Mrs S. Maranate, Mr W. Tansathien, Mrs S. Vimuktanan, Mr C. Budmuong, Mrs Varaporn Sopa and Mr Sawai Chaitha.

I owe thanks to many graduate students, including M. Wallace, S. Eggins, T. Falloon, D. Huston, Y. Panjasawatwong, P. Chaodumrong, Sampan, Ai Yang, Salman Palgunady, Djojomihardjo Saetijoso, Rahmat Harmanto, Khin Zaw, Sjafra Dwipa, Udi Hartono, Baharuddin, and Wu Yongqian for their assistance with my research. Special gratitude is extended to a number of technical staff at the University of Tasmania, Mrs J.M. Beattie and Ms J. Pongratz who typed part of this report, and P. Cornish, P. Green, L. Hurd, W. Jablonski, B. Lewis, M. Power, P. Robinson, S. Stevens and K. Whelan.

The following people reviewed various portions of this manuscript and their editing is much appreciated : Drs M.R. Banks, C.P. Rao, C.F. Burrett and Ruth Lanyon. In addition, I would like to thank the examiners including Dr E.G. Purdy, Dr T.P. Scoffin and Prof. C.S. Nelson for the very helpful comments and corrections

It would have been impossible to undertake this study without the support of the Australian International Development Assistance Bureau, the University of Tasmania, and the Royal Thai Department of Mineral Resources. AIDAB officers provided invaluable support including John Baker, Robin Bowden, Cathy McCourt, Frank Williamson, and Kevin McCormack.

Finally, I would like to thank my wife for the patience, enthusiasm and support she has shown me throughout these years.

CONTENTS

LIST OF FIGURES AND TABLES

FIGURES

TABLES

ENCLOSURES

Appendix 1	General geology of study area.
Appendix 2	Map showing sample localities in area of study.
Appendix 3	Geology of Thailand.
Appendix 4	Detailed lithostratigraphic columns.
Appendix 5	Summary of microfacies, characteristics and inferred depositional environments.
Appendix 6	Oxygen and carbon isotopic ranges.
Appendix 7	Lower to Middle Palaeozoic stratigraphy of mainland Satun province, southern Thailand.

Chapter 1
INTRODUCTION

The Ordovician carbonates of Southern Thailand are known as the Thung Song Group (Javanaphet, 1969) and are well exposed as an irregular and discontinuous north-south mountain belt in central peninsular Thailand (Fig. 1), from the Thai-Malay border in Satun province northward to Amphoe La Ngu, Amphoe Thung Wa, along both flanks of the Mesozoic granite mountain ranges between Trang-Phattalung provinces and Amphoe Thung Song, and both flanks of Khao Luong northward toward Amphoe Khanom in Nakhon Si Thamarat province.

The Thung Song Group can be traced throughout the west and northwest of Thailand (Kobayashi, 1964; Bunopas, 1976, 1983; Wongwanich and Burrett, 1983). Similar units of the Ordovician limestone extend northward to the Shan States of Burma and southward to north Malaysia (Jones, 1968, 1981; Kobayashi, 1973, 1984; Piyasin, 1980; Wongwanich *et al.*, 1983, 1990).

The Thung Song Group lies conformably with gradational contact on the red siliciclastics of the Tarutao Group and is sharply and conformably overlain by the black shales and cherts, siliciclastics and carbonates of Siluro-Devonian age, the Kanchanaburi Group, in Satun Province.

1.1 General Information of the Study Area

Because of granite intrusion during the Mesozoic, most of the rocks in the north and in the area adjacent to the granite mass in the south of southern peninsular Thailand are strongly recrystallized and highly deformed by the extensive contact metamorphism so that its original features have been largely obscured. The rocks are also strongly folded (Burton, 1974; Bunopas *et al.*, 1980) and faulted. Therefore, suitable areas for working on sedimentology, stratigraphy and palaeontology are areas far from the granite intrusions (Appendix 1,2,3). The study area, with the best development of the Thung Song Group, is situated in the west and northwest of Satun province, which has long been a prime location for studying the lower Palaeozoic rocks of South- East Asia (Bunopas *et al.*, 1980; Teraoka *et al.*, 1982; Wongwanich *et al.*, 1990).

The study area lies in the extreme south of Thailand in Satun province between lat. 6°30'00"N and 7°00'00"N and long. 99°31'44"E to 99°46'8"E, in the area of 756 square kilometres, covered by U.S. Army Service 1:250,000 sheet NB. 47-7, Changwat Satun; 1:50,000, Series L 707 edition 3-RTSD, sheet 4922I, Amphoe La Ngu, sheet 4922III, Ko Tarutao, and sheet 4922IV, Ban Pak Bara.

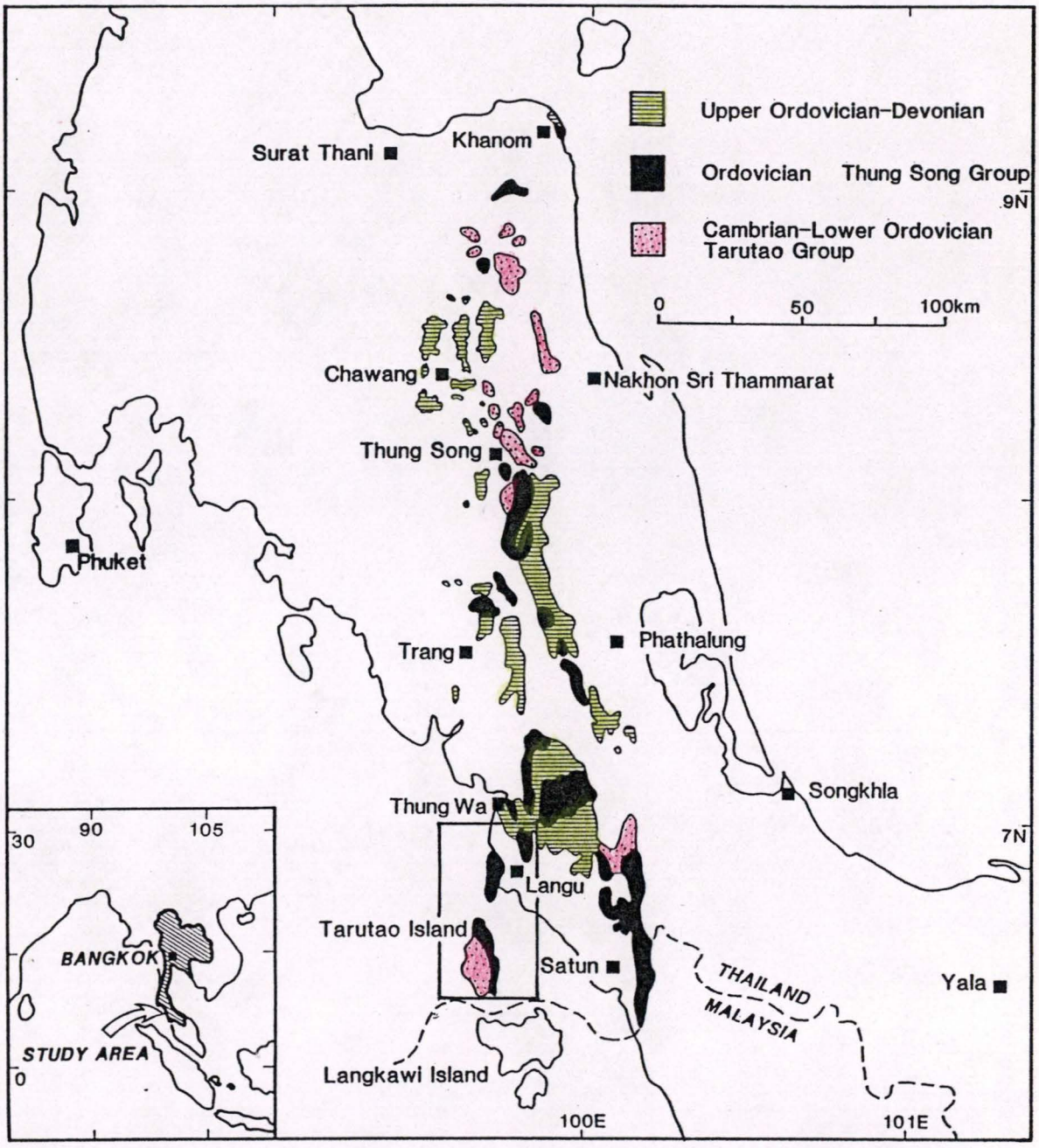

Fig. 1 Map showing locality and distribution of the Lower to Middle Palaeozoic rocks of southern Thailand and the study area.

Much of the mainland area is covered by the wide fertile coastal plain and the scattered rugged chain of N-S Ordovician carbonate mountains while the lower ground along the shoreline and the area between the mountains is cultivated for rice, coconut, oil palm, and rubber. Deposits of mud along estuaries and mangrove swamps are exposed at low water. The drainage is good through the short tidal channel system.

The part of Satun province under study includes most of the district of Amphoe La Ngu. A good system of roads runs north from Satun province through Amphoe La Ngu and Amphoe Thung Wa to Trang province, before connecting with the well developed road system of the south. The chief industries of the area are fishing and rubber plantations.

Ko Tarutao, Ko Khao Yai and other small islands are incorporated into the Turutao National Marine Park and Phetra National Marine Park of the Royal Thai Forest Department.

The tropical climate of the region is seasonally influenced by two monsoons. The dry season corresponding to the northeast monsoon is during October to March before the wet season of the southeast monsoon during April to September. The field season is usually good for four months between November to February. The mean daily maximum temperature is 32°C and a mean daily minimum is 24°C.

1.2 Previous Work and Literature

The Ordovician carbonates of the study area have received international attention over the past three decades since the discovery of an upper Cambrian fauna in the red siliciclastic rocks underlying the Ordovician carbonates on Ko Tarutao was reported by Buravas (1957) and Kobayashi (1957). Subsequent studies before 1980, dealt mainly with the upper Cambrian red sandstone of the Tarutao Group on Ko Tarutao and the palaeontology and general geology of the study area (Kobayashi, 1958; Kobayashi and Hamada, 1964; Bunopas, 1974).

Burton (1974) named the passage beds, above the Tarutao Group, and Ordovician carbonates the Satun Group. Between 1978 and 1980, Tansuwan and others undertook regional mapping of the whole area. The unpublished report of investigation together with a geological map of Satun Province Quadrangle (1: 250,000) were submitted to the Geological Survey Division, Department of Mineral Resources of Thailand in 1982.

Until the work of Bunopas *et al.* (1980), the Ordovician carbonates, lying in the eastern part of Ko Tarutao , were named the Thung Song Formation and separated into two parts: the lower and middle parts are composed of laminated shale, limestone and graded up to reddish brown argillaceous limestone and stylolitic limestone. Later,

Teraoka *et al.* (1982), demonstrated that they range in age from lower Ordovician to Silurian and can be divided into five units representing platform margin to slope facies.

Wongwanich *et al.*, 1983, recognized at least five major lithostratigraphic subdivisions deposited from peritidal through lagoonal to reefal environment from the Ibexian to Lower Whiterockian. This interpretation was confirmed by Mason (1986) in general but he was able to subdivide the Ordovician carbonates on Ko Tarutao into eight units with the last unit representing the slope facies similar to Teraoka *et al.*'s conclusion.

Detailed palaeontological and paleobiogeographical studies on the Thung Song Group have been carried out by a number of researchers in the area (Hamada *et al.*,1975; Teraoka *et al.*, 1982; Wongwanich and Burrett, 1983; Stait *et al.*, 1984; Stait and Burrett, 1984, 1987; Jell *et al.*, 1984; Burrett and Stait, 1985, 1987; Shergold *et al.*, 1988; Burrett *et al.*, 1990). Based on conodonts and trilobites, it is clear that the Cambro-Ordovician boundary lies within the uppermost part of the Tarutao Group, at least on Ko Tarutao (Teraoka *et al.*, 1982; Stait *et al.*, 1984).

Recently, Wongwanich *et al.* (1990) discovered and proposed the Pa Kae Formation for the deeper-water, red, stromatolitic limestone, containing abundant Upper Caradoc to Lower Ashgill trilobites, as the uppermost formation of the Thung Song Group. The Ordovician-Silurian boundary has been identified within the black carbonaceous shale, just above the lower Dalmanitina horizon within *Dalmanitina* beds of the Wang Tong Formation which lies conformably on the Pa Kae Formation and is overlain by the Kuan Tung Formation.

1.3 Aims and Scope of Project

Although the general geology, palaeontology and broad stratigraphy of the study area are now moderately well known, there is a lack of research dealing with carbonate sedimentology, especially on the detailed petrology, petrography, diagenetic and on the depositional aspects of these rocks.

Therefore, the major objectives of this project are to:

1) establish the litho-stratigraphic sequence and the terminology of the Ordovician carbonates of the study area,
2) investigate the diagenetic history of the rocks, independently and collectively from field work, petrography and geochemical criteria,
3) reconstruct the depositional environments, and
4) investigate and discuss the association of stromatolitic structures in the deeper water limestone, the Pa Kae Formation, in order to clarify the possibility of stromatolites in deeper water conditions. In contrast to other studies on

stromatolites, this work integrates lithostratigraphy, palaeontology, sedimentology, diagenesis and geochemistry of the rocks themselves to interpret the palaeoenvironment of the Pa Kae stromatolites. An attempt has been made to establish a simple conceptual model to estimate a possible palaeobathymetry for the deeper water stromatolites.

Chapter 2
METHODS OF STUDY

2.1 Field Methods

Field work was carried out for four months during the field seasons in early 1982, 1985, 1987 and 1988; using 1: 50,000 base maps prepared by U.S. Army Topographic Command in 1978. Due to the discontinuous nature and intense tropical weathering, a simple continuous stratigraphic section could not be obtained. Therefore, many separated sections were measured by visual estimation and pacing in the areas of poor outcrop or steep cliffs on the islands, and occasionally by tape normal to strike in more detailed sections with good exposures on coastal outcrops, road cuttings and quarries.

Lithology, bedding, texture, primary and secondary structures, and fossils were noted in their correct vertical position in the field notebooks at a scale of about 1 or 5 m to 1 cm. Rocks containing dolomite were easily recognised in the field because of their pink to brown colour and lower effervescence after application of 10% HCl.

More than 1500 oriented rock samples were collected, wherever significant changes in lithologic or faunal properties are observed (Appendix 2,4). Many were also collected in the middle of units if the rocks exhibited a complex sedimentology. Large samples (5-7 kg) for conodont studies, were collected from the bottom, in the middle, and top of each rock unit, but closer spaced samples were collected in the Ordovician-Silurian boundary interval.

2.2 Laboratory Methods

2.2.1 Petrographic Analysis

All specimens were cut normal to bedding and polished in the laboratory. About 700 small polished slabs (5 x 5 x 0.5 cm) and 800 polished thin sections were prepared. More than one hundred and fifty large slabs (10 x 15 x 1.5 cm) were polished or etched in 1% HCl for the study of the morphology of stromatolites and sedimentary structure. Thin sections, and polished slabs for acetate peels were stained with Arizarin red-s and Potassium ferricyanide (Dickson, 1966). Peels were made using the cellulose acetate sheet method of Stewart and Taylor (1965).

Polished thin section analyses were carried out under the conventional microscope to determine the constituents and mineral composition of the rocks,

cementation, dolomitization, and other diagenetic features. The petrographic classifications and terminology of the rocks used throughout this report are Folk's (1962) carbonate classification and Choquette and Pray's (1970) porosity classification schemes. Thin sections for palaeontological study were also examined by an optical projector and microfiche reader/printer.

About 200 selected polished thin sections were examined under cathodoluminescence using a Nuclide ELM-2B Luminoscope. Luminoscope operating conditions were 12 to 15 KV beam energy and 0.6 to 0.8 mA beam current, and about 1cm focused beam at 100 mtorr vacuum.

In order to examine the fabric and texture of the very fine grained carbonate rocks which are too small to be observed by the ordinary optical microscope, the uncovered, etched thin sections of micrite, microdolomite, and deep water stromatolites were coated with carbon or gold, using an ionized spattering coater prior to SEM observation. Electron micrographs were taken on a Philips 505 SEM.

Microprobe analyses of the distribution of Fe, Mn and other elements in the deep water limestone were perfomed on a Jeol JXA 50A electron microprobe using an energy dispersive system with silicate standards and ZAF corrections. An analytical precision of 0.2 wt% is expected using this system.

2.2.2 Isotope and Trace Element Geochemistry

Isotopic studies are important in order to understand carbonate deposition and diagenesis. Therefore, 154 individual carbonate components and whole rocks were separated and sampled from both stained and unstained, smooth polished slabs using a binocular microscope and a dental drill for oxygen and carbon stable isotopic analyses. The powders were further finely grounded by agate mortar.

Powder of a fauna and non-skeletal grains, 10 marine cements, 4 spar in fenestral porosity, 8 later diagenetic spars, 6 spar in vein, 21 micrites, 11 red calcareous mudstones, 9 whole rocks, and 17 dolomites were allowed to react with 100% phosphoric acid at 25°C for 24 hours. Another 28 whole rock powders of dolomitic limestone were also allowed to react with 100% phosphoric acid at 25°C. The CO_2 extracted after three hours reaction was taken as coming from calcite. Further reaction was allowed to proceed and CO_2 collected after 20 to 48 hours was taken as coming from dolomite. The resulting CO_2 from each sample was analysed for isotopic composition of $\partial^{13}C$ and $\partial^{18}O$ on a Micromass VG 602D, mass spectrophotometer. This sequential analysis for coexisting calcite and dolomite is based on the method proposed by Epstein *et al.*(1964) and Sheppard and Schwarcz (1970).

The isotopic results are presented as parts per thousand (‰) in δ-notation relative to the PDB (Pedee Belemite) -1 standard. The correction for ^{17}O was made by using the standard procedures proposed by Craig (1957) and Mook and Grootes (1973). The precision was determined by daily analysis of the calcite standards TKL-1 (Te Kuiti limestone No. 1) and Biggenden.

Major and minor element (Ca, Mg, Sr, Na, Mn, Fe) analyses of 55 carbonate components from the Pa Kae and Lae Tong Formation were performed on a Varian AA6 atomic absorption spectrometer using 50 mg samples based on the method described by Robinson (1980). GFS401, GFS402 limestone standards were used to monitor the precision of results. Minor contamination from clay minerals can be expected for the iron results (Robinson, 1980). The analyses for Ti, Ba, and P_2O_5 have been done on a Siemens SR 1 automated XRF on pressed pellets. The accuracy and precision were monitored using a variety of international and in-house standard rocks.

Chapter 3
STRATIGRAPHY

3.1 Introduction

On the basis of reconnaissance geological investigation for mineral deposits along the west flank of the main granite mountain range in central peninsular Thailand, from Surat Thani Province to Satun Province in the south (Fig.1,Appendix 3), dark grey to black Ordovician limestones of the area were named the Thung Song Limestone by Brown, *et al.* (1951). They were later upgraded to the Thung Song Group by Javanaphet (1969) whilst compiling the 1:1,000,000, 2nd Geological map of Thailand.

In the following discussion of geography, the Thai words for district (amphoe), village (ban), hill (khao), bay (ao) and island (ko) will be used as this system is used on the published (Javanaphet, 1964; Tansuwan *et al.*, 1979) and on most unpublished maps.

The first broad stratigraphy of the area was given by Burton (1974) who recognized the presence of two separate units: the Nai Tak Formation and the Thung Song Formation respectively. He grouped them together under a new name: the Satun Group. Later Bunopas *et al.* (1980) took an opposing view and regarded the Thung Song Formation as a component of their new La Ngu Group composed of the red siliciclastic Tarutao Formation and the Thung Song Formation (Fig. 3.1). The stratigraphic status of the Thung Song is unclear and remains controversial in Thailand. It will be referred to here as the Thung Song Group.

In general, the Thung Song Group in Satun Province is characterized by an alternating sequence of limestones, dolomitic limestones, dolomites and minor calcareous mudstone, with a thickness of about 900-1,410 m and ranging in age from Middle Tremadoc to Ashgill. The group is well exposed on the eastern coast of Ko Tarutao, Ko Khao Yai , and the other small islands between Ko Tarutao and Ban Pak Bara, extending northward to the mainland at Amphoe La Ngu and further north along the rugged mountain range to Amphoe Thung Wa (Fig. 1, Appendix 1).

The Thung Song Group conformably overlies the red siliciclastic, Tarutao Group on Ko Tarutao (Bunopas *et al.*, 1980; Teraoka *et al.*, 1982; Lee, 1983; Wongwanich and Burrett, 1983; Mason, 1986) and is conformably overlain by a sequence of chert, black shale and siltstone, the Wang Tong Formation at Ban Pa Kae, 11 km north of Amphoe La Ngu (Wongwanich *et al.*, 1990; Appendix 7).

At least eight distinctive, conformable lithostratigraphic units are present in the Thung Song Group of the study area. The rock unit on Ko Tarutao consists of six

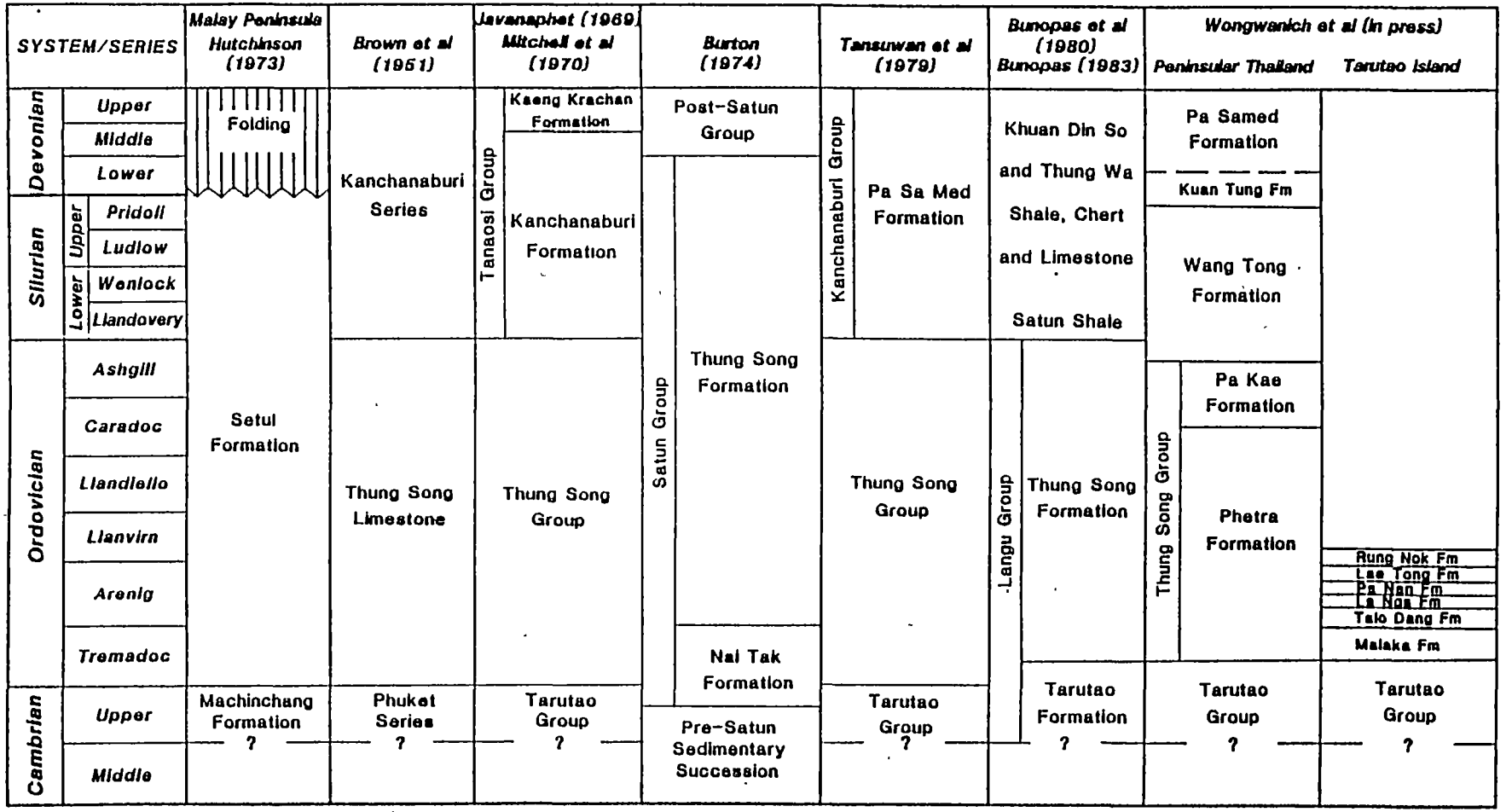

Fig.3.1 Stratigraphic subdivisions of the Lower to Middle Palaeozoic of Satun Province and the adjacent area in central peninsular Thailand including west Malaysia.

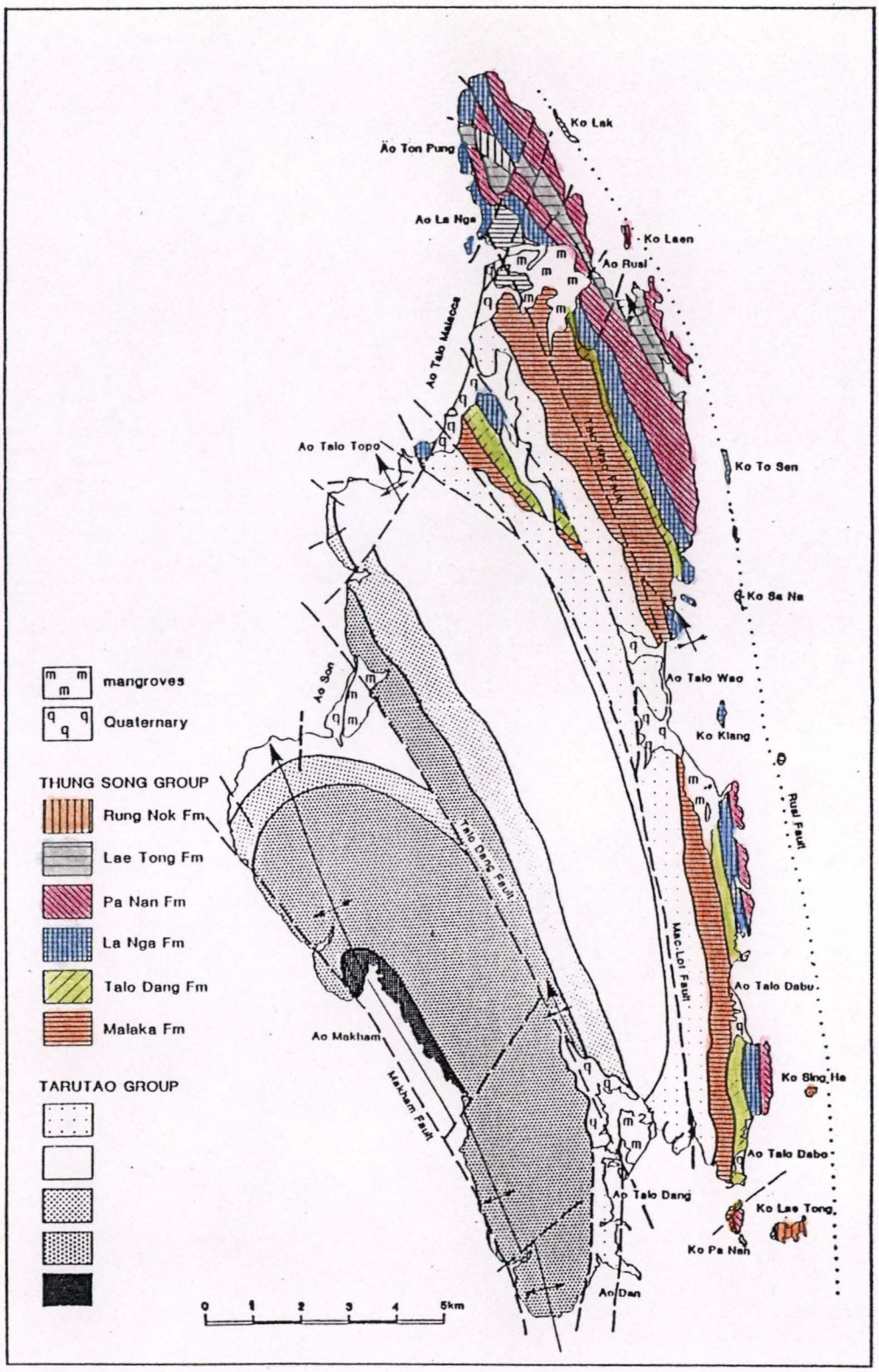

Fig. 3.2 Geological map of Tarutao Island, showing the distribution of all formations of the Thung Song Group and Tarutao Group. Formations in the Tarutao Group have not been named as yet (revised from Mason, 1986).

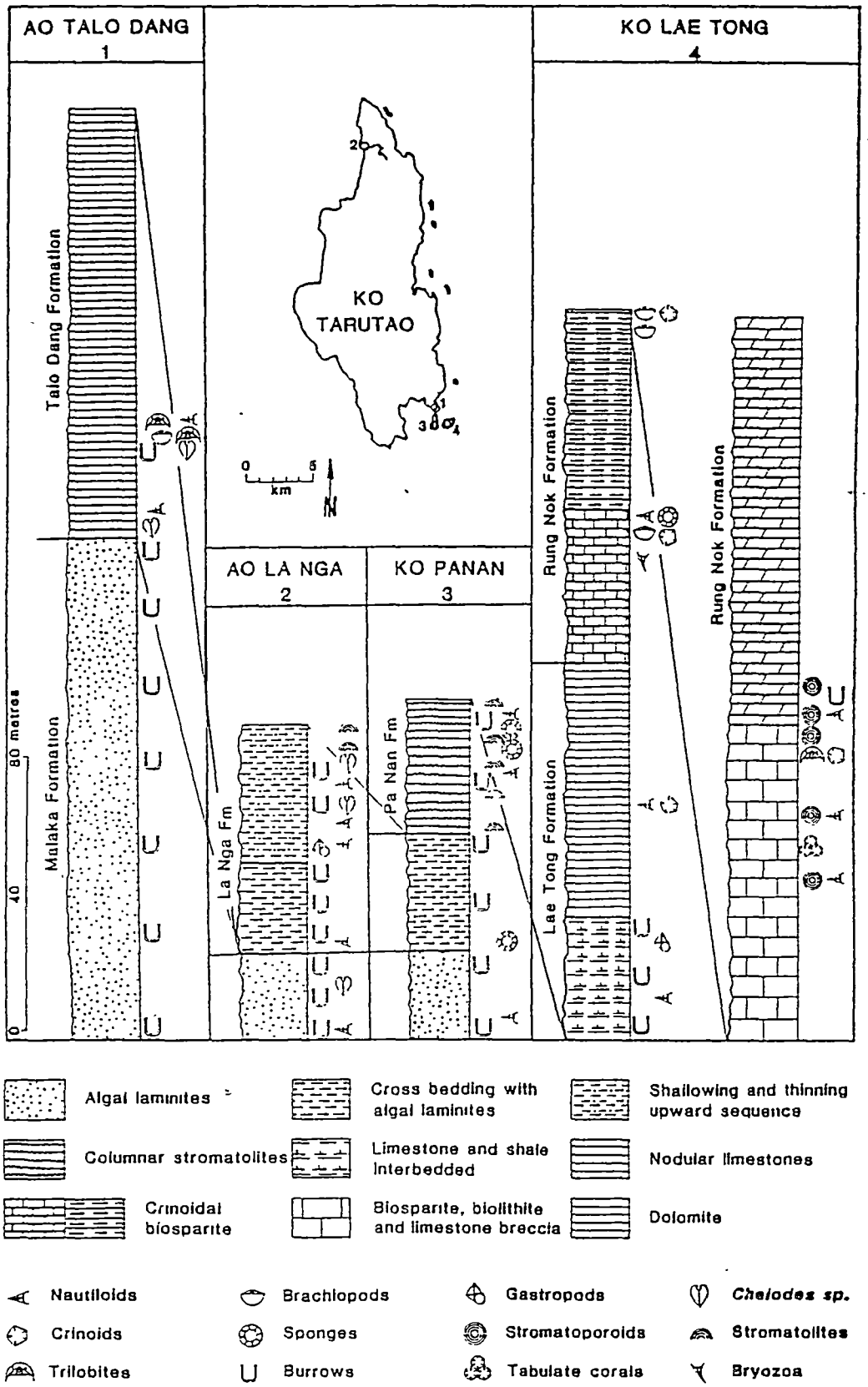

Fig. 3.3 Stratigraphic column of the Thung Song Group on Tarutao Island, Location, lithologic subdivision, faunal content and correlation are indicated. (Revised from Wongwanich *et al.*, 1983)

formations which are from the base: the Malaka Formation, Talo Dang Formation, La Nga Formation, Pa Nan Formation, Lae Tong Formation, Rung Nok Formation. On the adjacent islands and on the mainland the Phetra and Pa Kae Formation are mapped but only the Pa Kae Formation is defined because of time constraints and the complex structure of the Phetra area. Furthermore, palaeontological study on the Phetra Formation is needed prior the stratigraphical and sedimentological consideration.

Based on lithological and palaeontological evidence, the rocks of southern Thailand can be correlated confidently with the Ordovician carbonates of the lower Setul Limestone of the Setul Formation in west Malaysia (Jones, 1973, 1981; Kobayashi, 1973, 1984; Burton, 1974; Wongwanich *et al.*, 1983, 1990; Wyatt, 1983.

3.2 The Malaka Formation

The Malaka Formation takes its name from Malaka Creek, the biggest creek on the N.W.-side of Ko Tarutao. The type section is situated on the north bank of Malaka Creek forming the Tarutao National Marine Park Headquarters, at grid ref. 712, 411, on 1:50,000 map sheet 4922III, Ko Tarutao.

The formation is well exposed along a rocky shoreline and in a small sea-cliff in its type area and can be traced along a strike distance of about 20 km S.E. of the type section passing through Ao Talo Wao to Ao Talo Dang, at the south end of Ko Tarutao (Fig. 3.2). The Malaka Formation is also well exposed on the northern side of Ao Phante Malaka, at the base of Khao Ta Bo, east of Ao Dan, Ko Lek, Ko To Sen, Ko Sana, Ko Klua Lo within the Tarutao National Marine Park, and extending northwards to Ko Khao Yai, west of Ban Pak Bara.

The Malaka Formation in its type locality consists of 30m of alternating beds of very thinly bedded grey argillaceous and dolomitic limestone, which is characterized by wavy, continuous and partly discontinuous lenticular bedding 10-100 mm thick, brown and grey algal lamellae, occasionally developing small stromatolitic domes, with abundant vertical burrows, trace fossils, and some mud cracks (Fig. 3.3, 3.4).

The lower portion of the Malaka Formation at the base of Khao Ta Bo and Ao Talo Dang, the limestone beds have sharp bases and grade up to brown shale layers but the main part of the formation is algal laminate (Fig. 3.4B).

Algal laminations are frequently eroded into the various shapes of intraclasts. Small scale cross bedding and cross lamination with a scoured, truncated surface are present.

Taraoka *et al.* (1982) reported a 1m tuff layer intercalated in the basal part of their S1 member. This probably lies within the section along Malaka Creek where volcanogenic quartz detrital grained sandstones are recognized in the lower part of the

Fig. 3.4 A. The thinly bedded limestone of the Malaka Formation at type locality, Ao Phante Malaka, Ko Tarutao.

B. The brown weathering algal laminae with abundant vertical burrows (arrow). Most of laminites (stratiform stromatolite microfacies I) are wavy, partly discontinuous to continuous throughout the outcrop.

C. Mould of worm tracks (arrow) filled by brown microdolomites on the upper surface of limestone layers in the Malaka Formation.

D. Mud cracks partly filled by brown microdolomites (arrow), and commonly associated with large intraclasts (arrow).

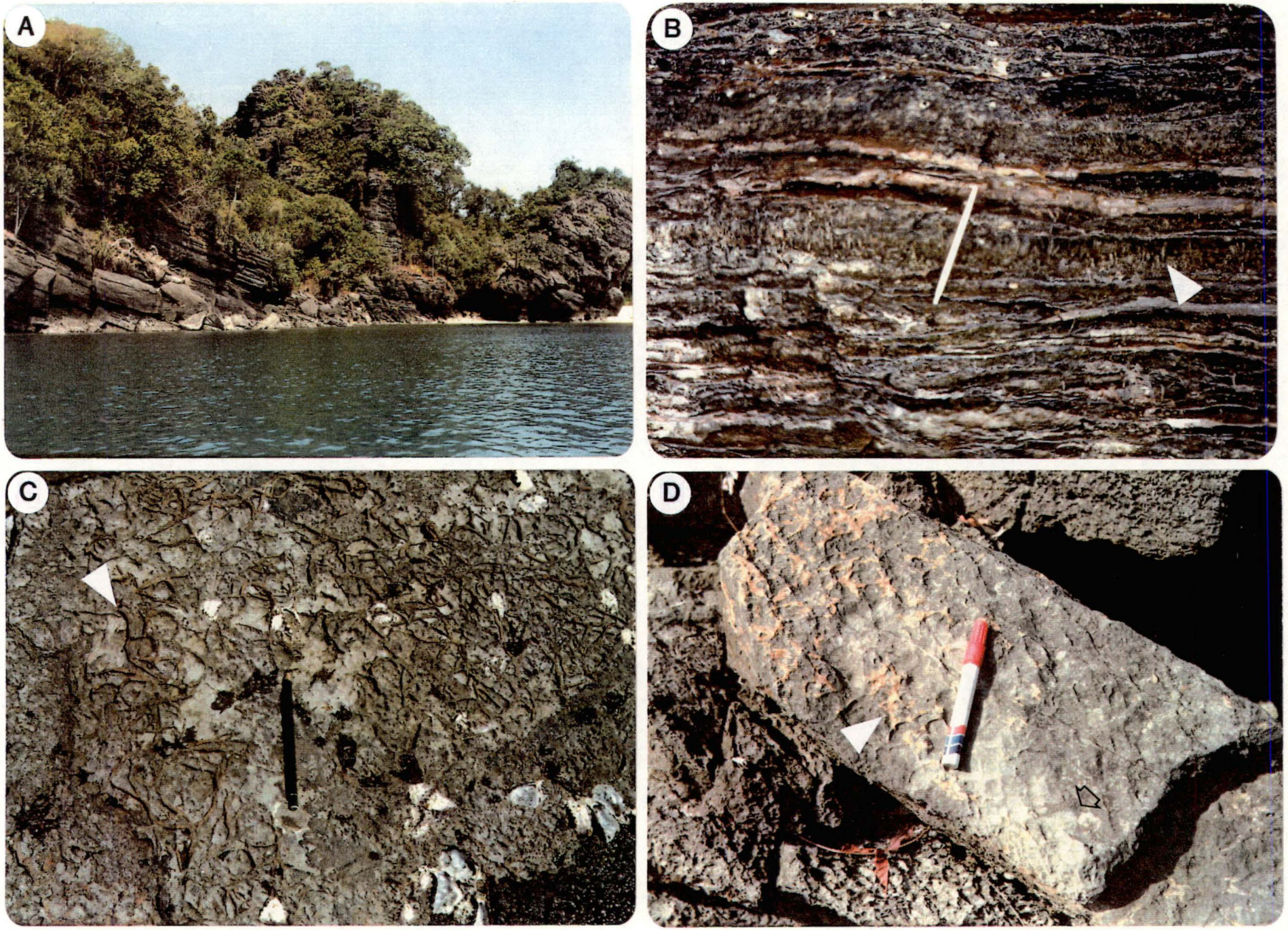
A
B
C
D

formation. A 450–800 mm thick bed of siliceous tuff with feldspar phenocrysts is also found interbedded with stratiform stromatolites in the middle part of the Phetra Formation at Ko Khao Yai, west of Ban Pak Bara.

The Malaka Formation thickens southward from the type locality, attaining a maximum of 410 m at Ao Talo Wao and decreasing to 150 m at Ao Talo Dang (Fig. 3.3). The formation is faulted against the red siliciclastic Tarutao Formation along the north shore of Malaka Creek and at Ao Talo Dang but it conformably overlies the Tarutao Group at Ao Talo Wao and in the interior reaches of Malaka Creek. The contact between the Malaka Formation and the overlying Talo Dang Formation is a conformable and gradational contact at grid ref. 768, 216, east of Ao Talo Dang, and as the gradational contact to the La Nga Formation, without the Talo Dang Formation, at grid ref. 712, 412, south of Ao La Nga.

A very similar sequence is well exposed on the south coast of Ko Khao Yai, about 13 km NE of the type locality and in the Langkawi Islands, NW Malaysia, referred to as unit A of the Lower Setul Limestone (Wongwanich, 1983; Wyatt, 1983; Mason, 1986).

Palaeontology and Age

The Malaka Formation contains a moderate abundance of fossils including nautiloids, gastropods, and the polyplacophoran *Chelodes*. Trilobite, bivalve, calcareous algae and echinoderm debris are observed in thin sections. Stait and Burrett (1984a) identified the many polyphacophoran valves from this formation as *Chelodes whitehousei* which is indicative of the Lower Ordovician. The valves occur with *Euchasma* and a conodont fauna including *Scolopodus quadraplicatus* and *Acontiodus latus*, suggesting a Late Tremadoc age for this assemblage. *Chelodes whitehousei* also occurs in the Ninmaroo Formation in western Queensland (Stait and Burrett, 1984a). Stait and Burrett (1984b) also identified the orthoconic nautiloids within the lowest formation of the Thung Song Group on Ko Tarutao as Endoceratidae gen. et sp. indet, indicating a Late Ibexian age (Late Tremadoc).

3.3 The Talo Dang Formation

The Talo Dang Formation is named after Ao Talo Dang, situated at the southern end of Ko Tarutao. The type section is on the small bay, east of Ao Talo Dang, between grid ref. 767,216 to 769,216, on 1:50,000 map sheet 4922III, Ko Tarutao. The area contains the bulk of the outcrop area of the Malaka Formation and Talo Dang Formation (Fig. 3.2).

The Talo Dang Formation can be mapped for a strike distance of about 18 km along the east coast of Ko Tarutao from the type locality extending northwards to Ao Talo Wao and further northwestwards across the island to Malaka Creek. The total thickness of this formation is 130 m at the type section and becomes gradually thinner to about 80 m at Ao Bin La, on the opposite coast of the Ko Sa Na, and it pinches out at Malaka Creek (Fig. 3.2, 3.3). The gradational contact of the Talo Dang Formation and the Malaka Formation below occurs over a 5-10m interval (Mason, 1986). It is overlain by the La Nga Formation and may in part be a lateral equivalent of it (Fig. 3.3).

The Talo Dang Formation consists, principally, of the very thinly bedded (10-50 mm) of grey to pink, continuous to discontinuous nodular limestone interbedded with green, greyish green and red weathering calcareous shale. The lower part begins with 6m brown, massively to thickly bedded, fine grained, brownish gray, feldspathic sandstone and siliceous tuff with tabular cross bedding and channel structure before abruptly changing to the thick sequence of the nodular limestone and calcareous shale (Fig. 3.5A,B).

The upper part, the main part, consists of alternating cycles of lime-rich nodular limestone layers and darker greenish grey to red weathering calcareous shale layers, with the limestone increasing upwards. Each cycle starts from the calcareous shale dominated horizons with sparse isolated, irregular to elongate-lenticular limestone nodules and develops upward into strata-bound nodules in the middle and up to the continuous irregular or lenticular limestone beds with minor calcareous shale parting at the top. At least 6 cycles are observed at the type section, with the average thickness of a cycle about 2-10m. The upper 30m at the top of the sequence is strongly deformed and has developed strong cleavage. The secondary quartz is occasionally replaced at the rim of some limestone nodules in this part (Fig. 3.5D).

The limestone exhibits micritic texture or occurs as calcisiltite at the base and gradually transforms to coarser calcarenite with abundant fossil fragments and mainly horizontal burrows at the top of the cycle. Some cycles in the middle part of the sequence display a cross lamination in the limestone layers and are well laminated in the interbedded shale. The faunas are well preserved in the irregular or lenticular limestones at the top of the sequence but are rare in the lower limestone nodules and absent in calcareous shales.

This formation has been correlated with the upper part of the member A of the Lower Setul Limestone (Wongwanich *et al.*, 1983; Wyatt, 1983) in the Langkawi Islands, N.W. Malaysia.

Palaeontology and Age

Fig. 3.5 A. Nodular limestones interbedded with green calcareous shales. Note the generally periodical development of limestone nodules from isolated nodules (1) at the base to strata-bound (2) and irregular or lenticular beds (3) on the top of cycles.

B. Thickly bedded to massively feldsparthic sandstones with tabular cross-bedding and scour bases (arrow) in lower portion of the Talo Dang Formation.

C. Relatively uncompacted, isolated and strata-bound nodules in laminated calcareous shale. Note the deflection of lamination (arrow) around nodule and the breakage of nodules in upper layers.

D. The replacement of quartz at the rims of lenticular limestones (arrow) interbedded with gray shales on the top of the Talo Dang Formation.

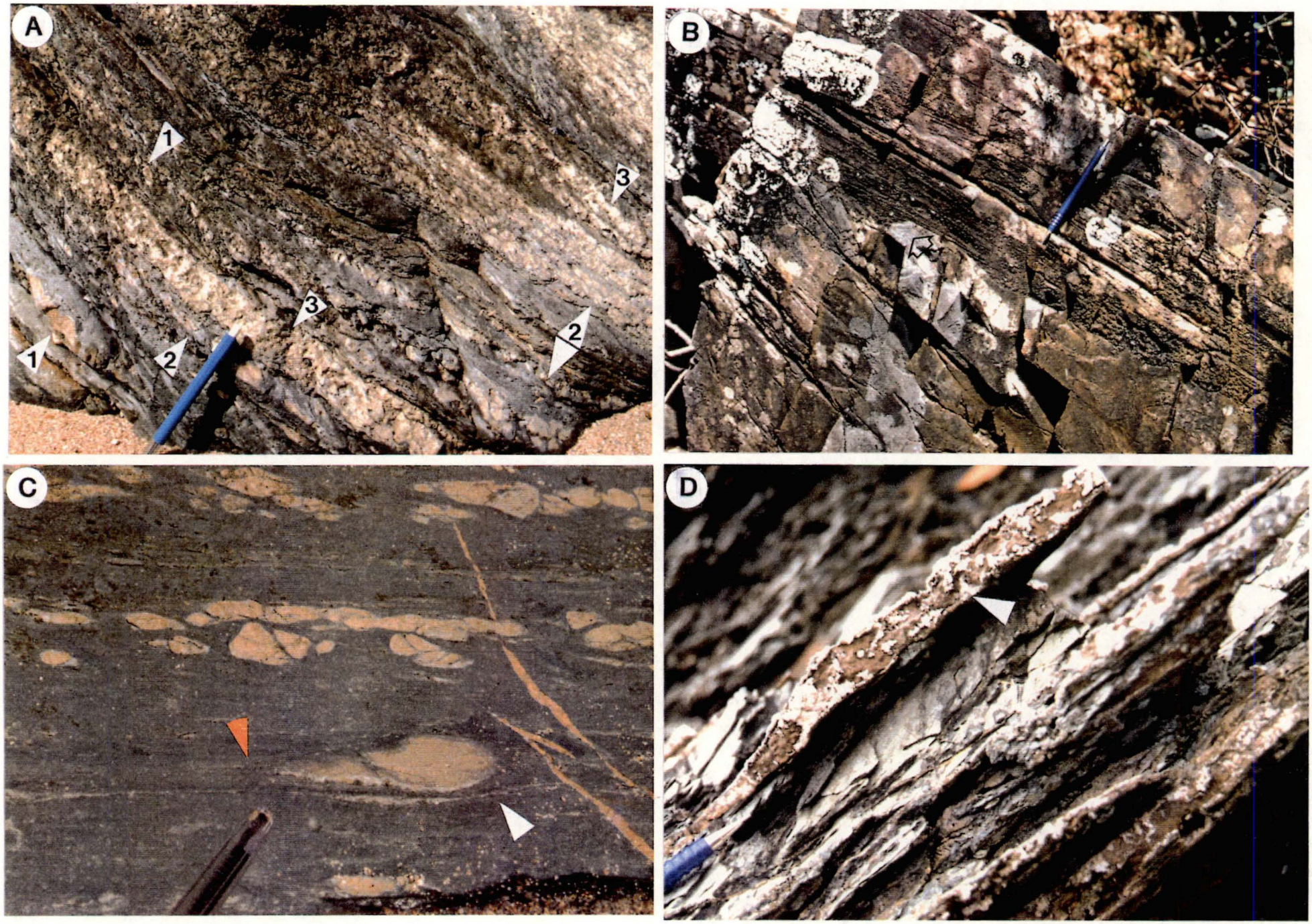
A
1
2
3
1
2
3
B
C
D

Fossils of the Talo Dang Formation are rare and restricted to a few horizons in the type section. Orthoconic nautiloids and *Chelodes* are found in the lower part of the formation. The small brachiopods, *Chelodes*, trilobite fragments and straight nautiloids occur at the 25m and 30m horizons above the base of the formation. Distinctive curved and 30cm long straight nautiloids also occur on the north side of Ao Talo Dabu, 4.7km north of the type section.

Based on the occurrence of *Chelodes* and orthoconic nautiloids in the Talo Dang Formation, the age of this rock unit is probably Late Tremadoc (Stait and Burrett, 1984a,b).

3.4 The La Nga Formation

The La Nga Formation takes its name from Ao La Nga, north of Malaka Creek, west of Ko Tarutao, where the distinctive primary features of this formation have been clearly developed. The type section is in a small cliff on the south side of the bay, at grid ref. 213,413 on 1:50,000 map sheet 4922II, Ko Tarutao (Fig. 3.2).

The formation can be traced for 21 km southeastward to the east coast at Ao Talo Wao, and further south to Ao Talo Dabo. The total thickness of the formation at the type section is 75 m and it gradually becomes thicker to the east where it is 170 m thick at Ao Talo Dabo. The formation is also exposed at the south end of Ao Talo Malaka. The La Nga Formation is conformably overlain by the Pa Nan Formation throughout the east coast (Fig. 3.2) with an abrupt and sometimes scoured contact.

The La Nga Formation is composed of two conformable members: the lower member and the upper member (Fig. 3.3).

The lower member is a 27 m thick sequence of thick to massive cross-bedded and channelled grey dolosiltite and calcarenite. A complex network of trough and minor planar, cross-bedding occur in lenticular sets that vary in thickness from 150-400 mm with an average of 200 mm (Fig. 3.6A,B). Cross-bedding is bi-modal. This formation at Ao Talo Wao contains well developed but smaller scale (100-200 mm) herring-bone cross bedding with spectacular channel within channel structure (Fig. 3.6C).

The lower surface of each set of festoon cross bedding is disconformable and probably represents channel scour. Reactivation surfaces, minor lag deposits, horizontal, vertical and u-shaped burrows are common. In general, the trough cross-bedding at the type section displays an upward decrease in cross-bed scale from decimetre at the bottom to centimetre at the top of the unit with a gradational change to planar cross bedding prior to normal bedding. The black weathering, very thin

Fig. 3.6 A. Thickly bedded to massive limestones in the lower portion of the La Nga Formation gradually grade up to thinly bedded limestones on the top of the sequence.

B. Trough cross-stratification in massive beds with a scour base (1) and reactivation surface (2). The cross-stratification changes to normal lamination on the upper part of lower member.

C. Channel within channel structures at Ao Talo Wao. Note the gray massive limestone (hammer) with abundant fossils cut through cross-bedded limestone.

D. Small-scale shallowing-upward sequence begins with massive limestone (1) to thick bedded and thin bedded on top of a cycle. Note the stromatolite laminites developed along cross lamination (2,3).

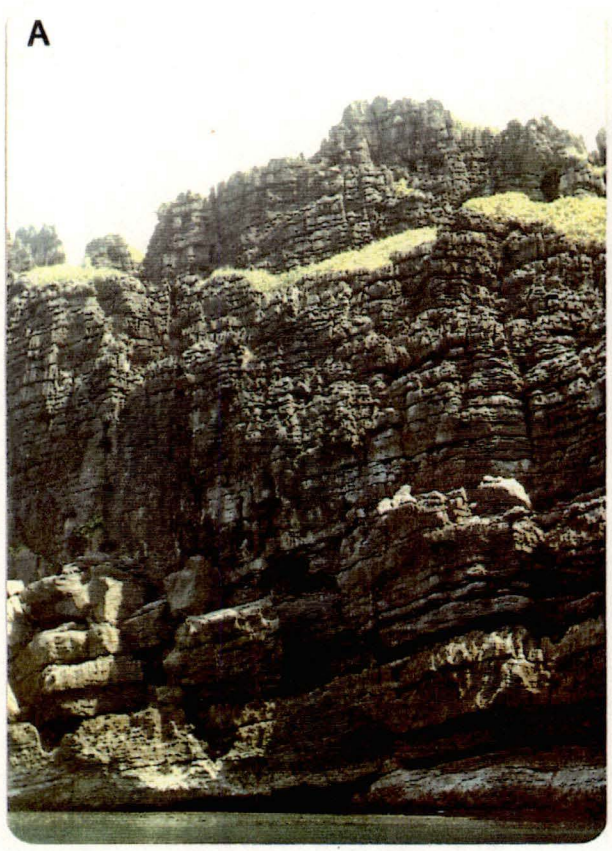
A

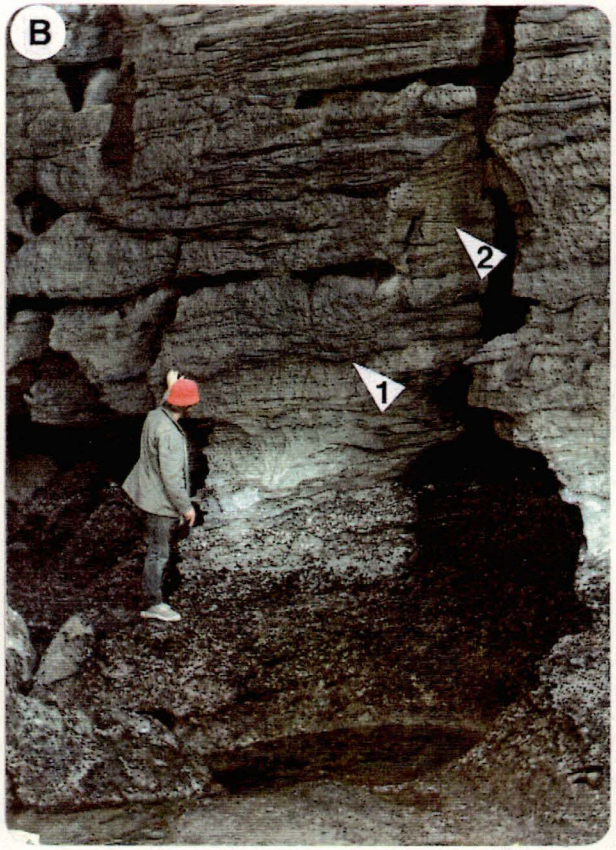
B
2
1

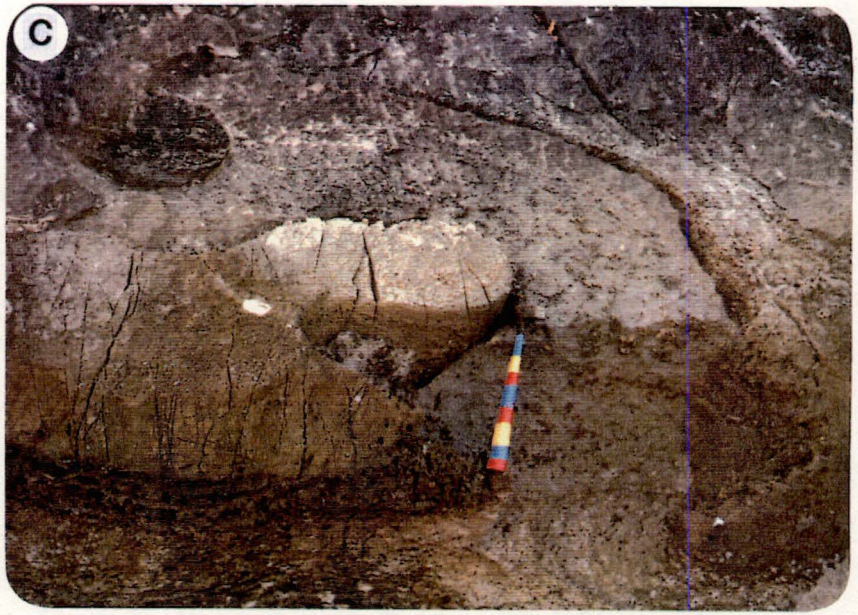
C


D
2
3
1
1

carbonaceous dolomitic layers along the foresets also decrease upwards. This complex trough cross-bedded unit grades up to the upper member.

The upper member is a 48m thick sequence of small scale shallowing and fining-upward sequences that vary in thickness from 10-25m. The sequence occurs three times at the type section. The basal unit of the sequence is massively bedded (1-3m), medium to coarse grey calcarenite and abruptly changes to the thickly bedded (0.3-1m) fine calcarenite with occasional planar cross-bedding and vertical and horizontal burrows (Fig. 3.6D). Some cycles further grade up to thinly bedded calcarenite (200-600 mm) with tabular cross bedding and to algal laminae at the top. The flat pebble conglomerate, mud cracks, wavy stromatolites (small domes), and extensive vertical burrows are present in the upper part of the sequence.

The similar shallowing upward sequence is well exposed at the south side of Khao Ngiap, 11 km north of Amphoe La Ngu. It can be also correlated with the upper part of the unit B of the Lower Setul Limestone on the Langkawi Island (Wongwanich et al., 1983; Wyatt, 1983).

Palaeontology and Age

The faunal assemblage of the La Nga Formation includes gastropods, orthoconic nautiloids, polyplacophorans *(Chelodes)* and *Nuia.* Bivalve, echinoderm and trilobite debris are observed in thin sections. The silicified gastropods from Ao Talo Dabu were identified by Kobayashi (1959, 1984) as *Sinuitopsis* cf. *kochiriensis* Kobayashi (1934) which he took to indicate the Llandeilo. However, Jell et al. (1984) identified the same gastropods from Ao Bin La, about 10km north of Kobayashi's locality 28, as *Peelerophon oehlerti* (Bergeron) indicating the Tremadoc-Arenig. The age of the associated conodonts is Early Arenig (Burrett, personal communication).

3.5 The Pa Nan Formation

The Pa Nan Formation is named after Ko Pa Nan, situated at the south end of Ko Tarutao. The type section is at the south bay of Ko Pa Nan, grid ref. 770,203 on 1: 50,000 map sheet 4922II, Ko Tarutao (Fig. 3.2).

This formation can be traced for 26 km along strike, northwards from the type locality along the whole of the east coast of Ko Tarutao (Fig. 3.2). The total thickness at the type section is 50 m. Mason (1986) suggested that it gradually increases to 210 m to the north, between grid ref. 442,720 and grid ref. 439,725 southeast of Laem Tanyong Mara. The Pa Nan Formation conformably overlies the La Nga Formation and is overlain by the Lae Tong Formation.

Fig. 3.7 A. Thinly, wavy bedded stromatolitic limestone, the Pa Nan Formation at the Ko Pa Nan, the type locality of this rock unit.

B. The dense LLH-C columnar stromatolites with branching digitate morphology (arrow) giving a wavy appearance to the bedding.

C. The concentric stromatolite heads on the upper surface of bedding at Ao Dan, Ko Tarutao.


A


B

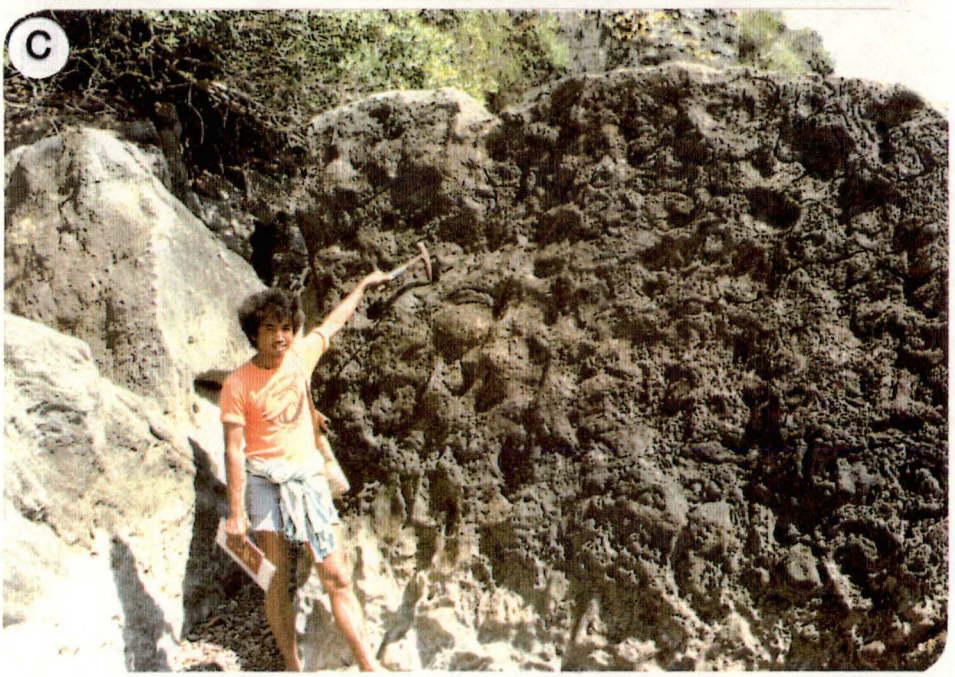
C

Teraoka et al. (1982) described the presence of *Ophiomorpha*-like burrows, with a diameter of 300-600 mm, within the upper part of their S3 member. These are stromatolites (Wongwanich and Burrett, 1983; Wongwanich *et al.*, 1983; Mason, 1986) and are the major component of the formation and occur throughout the unit. The small scale decimetre-sized columnar stromatolites give a characteristic wavy appearance to the bedding that can be observed at a considerable distance (Fig. 3.7A).

The most abundant form of the stromatolites in the Pa Nan Formation is the elongated, moderate branching, furcate columnar stromatolites. The branching digitate stromatolites (LLH-C) occur at only two localities at Ao Dan and Ko Pa Nan, at the southend of Ko Tarutao (Fig. 3.2; 3.7B,C). The elongation of the stromatolitic columns on the upper surface of bedding is varied from place to place. At the type section, they often align at 270°–90°, 35°–125° and 65°–295°, on the NE coast of Ko Tarutao the columns are aligned in 140°–30° and 20°–210° directions. The major alignment is in an E-W direction with the minor one NE-SW (Wongwanich *et al.*, 1983; Mason, 1986) and NW-SE.

The Pa Nan Formation typically consists of dolomitic calcisiltite and dark grey micrite. The dolomites give outcrops their distinctive bright yellowish brown vertical stripes. At 5 m below the top of the sequence at the type section, the stromatolitic limestone is intercalated with 3 m of thin lenticular bedded limestone (150-300 mm thick). The rock is a flat pebble conglomerate, grey coarse grain calcarenite, and dark grey dolosiltite laminae. Bi-modal trough cross laminations and channel scour are common and the depositional environment is interpreted as a channel deposit.

Palaeontology and Age

Fossils of the Pa Nan Formation are moderately abundant. The small sponges (<30 mm diameter), orthoconic nautiloids, gastropods, *Chelodes* valves, and trilobites may be seen between the stromatolite columns. The dolomitised u-shape and straight vertical burrows are common but horizontal burrows are restricted to the channel facies. Based on the stratigraphic position of the Pa Nan Formation, the age of this unit is probably Early Arenig.

3.6 The Lae Tong Formation

The Lae Tong Formation is named after Ko Lae Tong, immediately south of Ko Tarutao where the sequence shows a good vertical development of strata. The type section is on the west coast of the island, between grid ref. 775,205 to 776,203 on 1: 50,000 topographic map sheet 4922II, Ko Tarutao.

Fig. 3.8 A. Brown weathering, gray, thin bedded limestones interbedded with dark gray carbonaceous shale in the lower member of the Lae Tong Formation. Limestone beds have irregular nodules and lenticular bedding with erosional bed bases.

B. Red nodular limestones of the upper member are characterized by red and green calcareous shale containing nodules of buff to gray limestone.

C. The oblique view of interference ripple marks on hummocky cross-stratified bedding (B) in the lower member of the Lae Tong Formation at Ao Ton Pung.

D. Alternation of thinly bedded, brown weathering gray limestones with gray carbonaceous shale parting. Limestone beds show cross-lamination resembling small-scale hummocky stratification with erosional bases (arrow).


A

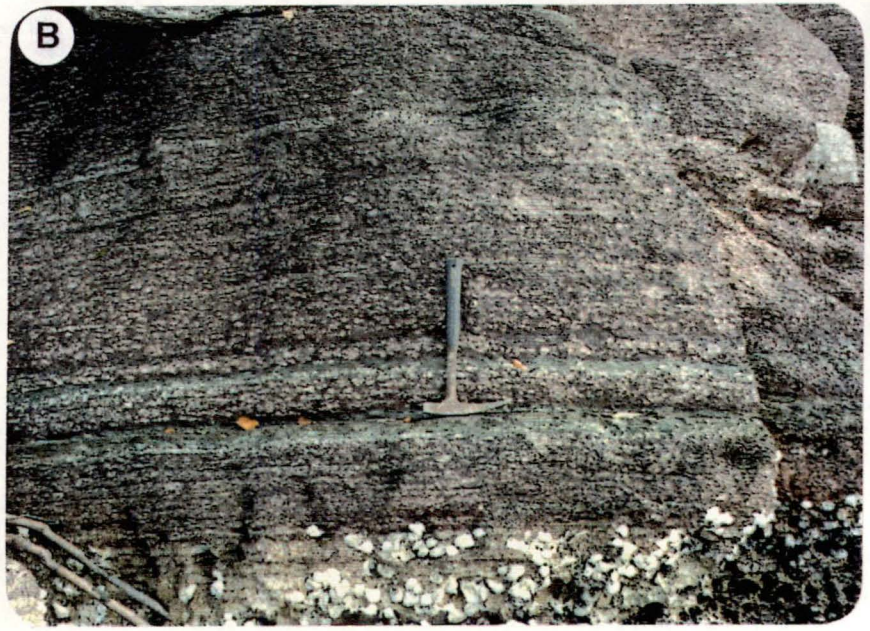
B


C


D

The formation in type section, is well exposed as a rocky shoreline and as a steep sea cliff. It can be traced as discontinuous outcrops for 22 km along the chain of small islands, east of Ko Tarutao, from Ko Lae Tong to Ko Laen in the north. The Lae Tong Formation is also exposed on Ko Tarutao at Ao Rusi on the east coast and at Ao Ton Pung, Ao Makham on the west (Fig. 3.2). The Lae Tong Formation ranges in thickness from 112 m at the type section to 40m at Ko Laen and about 100-120 m at the steep sea-cliff at Ao Ton Pung, about 3 km north of Malaka Creek. The lower contact of the Lae Tong Formation with the Pa Nan Formation is obscured but is probably gradational and conformable. The upper contact with the overlying Rung Nok Formation is clearly gradational and conformable (Fig. 3.3).

The argillaceous-rich sequence of the Lae Tong Formation consists of two distinctive conformable members: the thin-bedded limestone-shale member and the nodular limestone member respectively.

The lower member is 35 m thick and consists of the very thinly bedded (10-30 mm) limestone-shale alternations (Fig. 3.8). The limestone layer is brown weathering, grey, slightly argillaceous calcarenite, calcisiltite, and minor calcirudite and calcilutite. Bed geometries include small irregular nodules, lenses and wedges at the type section, with cross laminations and ripple beds at Ko Laen, but are dominated by irregularly bedded, continuous limestone sheets. Some layers are coarser near the base and display thin lags of shell debris (Fig. 3.8). Bed bases are often erosional and become ripple surfaces at the top (Fig. 3.8A,C). At Ao Ton Pung, bedding is more regular and lenticular with better continuity sharp bases, and an abundance of interference ripple marks and cross laminations resembling small-scale hummocky stratification in the dominant calcilutite texture. Dark grey calcareous-carbonaceous shale partings are laminated and fissile with more pyritic nodules and very rare skeletal debris. Only the coarse grained limestone contains abundant small fossil fragments including gastropods, echinoderms, trilobites, brachiopods and nautiloids. The burrows are both vertical and horizontal but mostly random and branching. This unit is gradational to the nodular limestone member.

The upper member is 77 m thick and consists of very thin-bedded (10-30 mm), grey, irregular, discontinuous to continuous nodular limestone interbedded with the red weathering greenish grey shale (Fig. 3.8B), resembling the Talo Dang Formation but without an alternating cycle. The sequence begins with calcareous shale dominated horizons having sparse isolated and irregular to elongated micritic limestone nodules which develop upwards to fast stratabound nodules and then to closely spaced nodular or continuous lenticular limestone layers having minor calcareous shale partings at the top.

No burrows or other distinctive primary structures have been observed at the type section. In thin sections and polished slabs, the shale partings display dewatering lamination.

Synaeresis cracks or probable mud-cracks associated with very thin calcite pseudomorphs after gypsum layers occur at Ao Makham. Pyrite nodules are common.

The fossil fragments, including trilobites, brachiopods, bryozoans, and echinoderms are sparse and restricted to limestone nodules. The distinctive fossils of the Lae Tong Formation are abundant orthoconic, cyrtoconic and gyroconic nautiloids and receptaculitids.

Palaeontology and Age

Teraoka *et al.* (1982) identified several conodonts from the upper member of this Formation. The conodonts include *Drepanodus basiovalis*, *Drepanodus forceps*, *Paroistodus parallelus*, *Baltoniodus oepiki* and *Prioniodus evae communis*, suggesting a Middle Arenig age (Teraoka *et al.*, 1982).

Stait and Burrett (1984) identified the nautiloids from the upper member of the Lae Tong Formation as *Hardmanoceras chrysanthimum* associated with conodonts of the *Prioniodus evae* zone of probable Middle Arenig age and correlated this with the same fauna in the Middle Arenig Emanuel Formation of Western Australia and in the probable Middle Arenig of North China.

3.7 The Rung Nok Formation

The Rung Nok Formation takes its name from the Rung Nok (swallow) cave, within the third member of this formation, on Ko Lae Tong, SE of Ko Tarutao. The type section is along the steep sea cliff and beach in the small bay south-side of Ko Lae Tong, between grid ref. 776,203 and 7825,2065 on 1:50,000 topographic map sheet 4922II, Ko Tarutao (Fig. 3.2).

The Rung Nok Formation consists of over 368 m of the fossiliferous thinly to thickly and massively bedded limestones, dolomitic limestones and dolomites, and overlies the Lae Tong Formation conformably (Fig. 3.9A). The upper boundary does not crop out anywhere on Ko Tarutao or Ko Lae Tong but the formation is thought to be conformably overlain by the younger Ordovician carbonates on mainland Satun Province. The rock is well exposed at Ko Lae Tong, Ko Sing Ha and Ko Laen in the north. Teraoka *et al.* (1982) reported the existence of this formation at the south side of Ao Makham, west of Ko Tarutao where the rock is highly deformed by extensive faulting. The Rung Nok Formation corresponds to the unit D of the Lower Setul

Fig. 3.9 A. Thinly well-bedded limestones of the Rung Nok Formation, Member 1, lie conformably lies on the red nodular limestones (arrow) at Ko Lae Tong.

B. Thinly well-bedded dolomitic limestones and dolomites of member 4 are conformably overlie (arrow) massively bedded limestones of member 3 at Ao Rung Nok, Ko Lae Tong.

C. Thinly bedded limestone of the second member of the Rung Nok Formation . Note stylolitic (Black) bedding seams.

D. Faulted thickly bedded, gray oolitic limestones of possibly the La Nga Formation overlie massive dolomite (arrow) at Ko Laen.

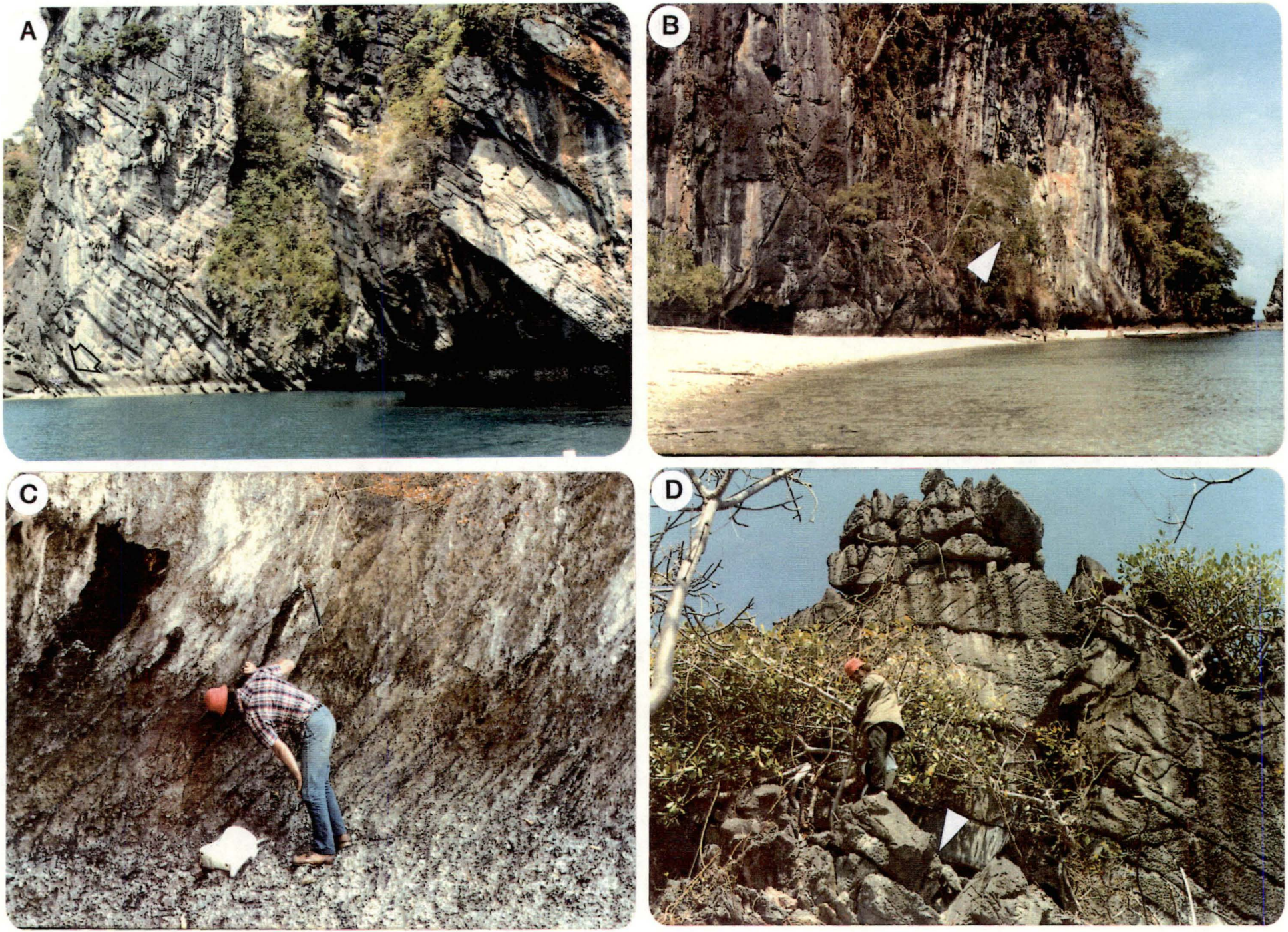
A
B
C
D

Limestone in the Langkawi Islands, NW Malaysia (Wongwanich *et al.*, 1983; Wyatt, 1983).

The Rung Nok Formation consists of four members. The lowest, member 1 consists of 45 m of well, very thinly bedded limestone (10-30 mm), light grey to white crinoidal calcarenite or biosparite (Fig. 3.9A). Bedding becomes slightly thicker upward (20-40 mm) with abundant sponges, receptaculatids and brachiopods.

Member 2 consists of 70 m of grey and pink, thinly bedded limestone (30-100 mm) and dolomitic limestone with brachiopods, bryozoans and crinoids (Fig. 3.9C).

Member 3 consists of 158 m of grey, thinly to massively bedded calcarenite and calcisiltite (Fig.3.9B) with abundant in situ laminar and high domical stromatoporoids, brachiopods, primitive tabulate corals, conical sponges, bryozoans, trilobites and echinoderm debris. The rock usually displays small channels filled with sparry calcite.

Member 4 consists of 105 m of grey to pink, well-bedded (50-150 mm) and massively bedded dolocalcarenite with pseudo-dolomite breccia at the bottom and in the middle of the sequence. The faunal assemblage includes crinoids, nautiloids, brachiopods and sponges. Fossil content decreases upward with increasing dolomitization.

At Ko Laen, the rock of the second member is thickly bedded (300- 800 mm), grey oocalcarenite and coarse grained, pink dolomite.

Palaeontology and Age

Teraoka *et al.* (1982) identified the conodonts from the first member as *Prioniodus navis, Prionioidus evae communis, Drepanoistodus forceps, Baltonioidus triangularis* and *Acodus longibasis*, suggesting the Early to Middle Arenig.

Based on the stratigraphic position and fauna, the most probable age range of the Rung Nok Formation is Middle to Late Arenig.

3.8 The Pa Kae Formation

Wongwanich *et al.* (in press) have proposed the Pa Kae Formation for the uppermost formation of the Thung Song Group in central peninsular Thailand. The type section is the small hill, about 0.3-0.7 km east of km 10.6 of the La Ngu-Thung Wa road, between grid ref. 8583,7122–8592,7085 on 1:50,000 map sheet 4922I, Amphoe Langu (Fig. 3.10). In the type area, the Pa Kae Formation is well exposed on the three small hills on the east side of the main road between Ban Wang Tong and Ban Pa Kae. It has been traced along a strike distance for about 2 km, northeast and

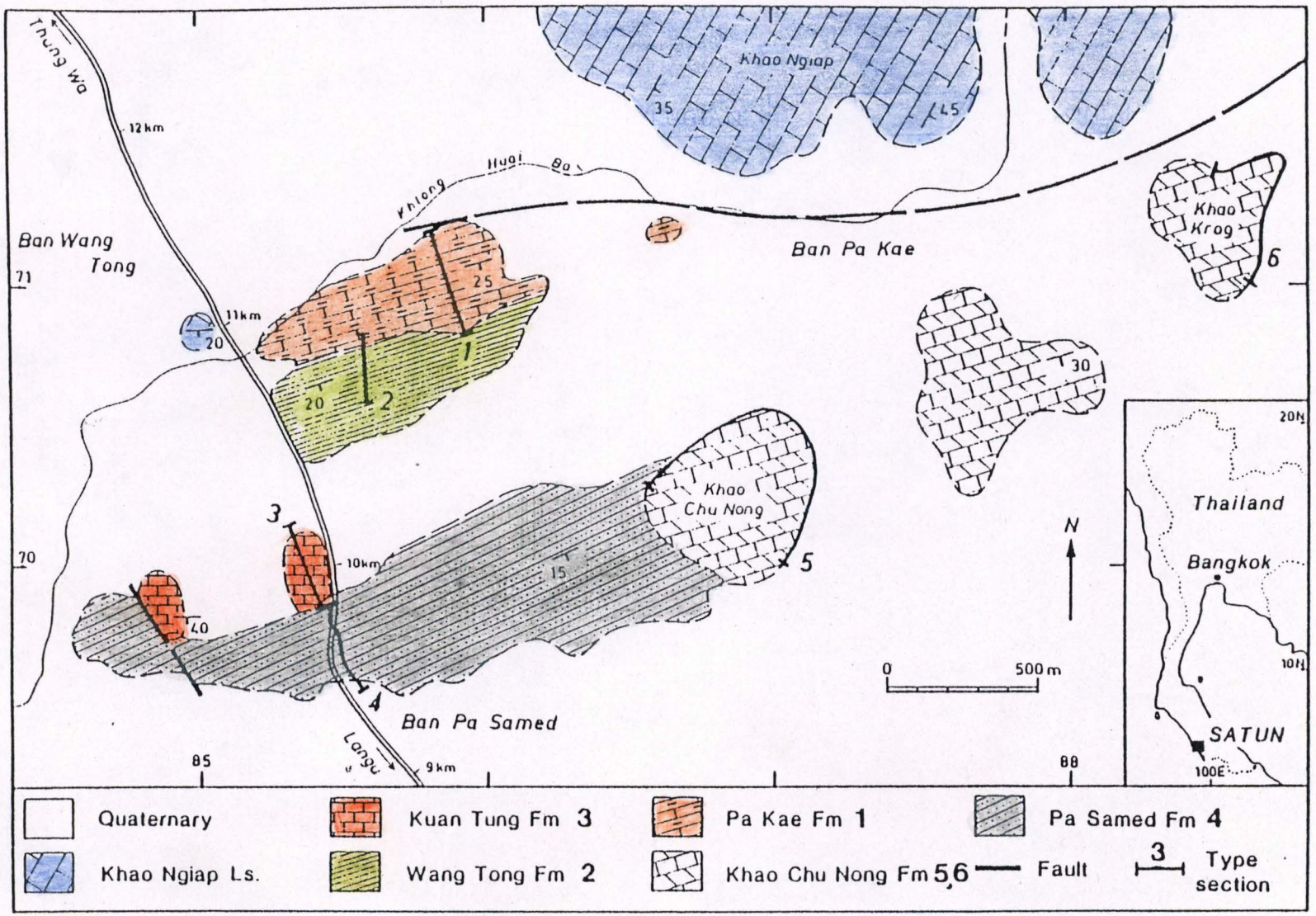

Fig. 3.10 Map showing type section and distribution of the Pa Kae Formation and the Silurian-Devonian rocks at type area Ban Pa Kae, Amphoe La Ngu, Satun Province.

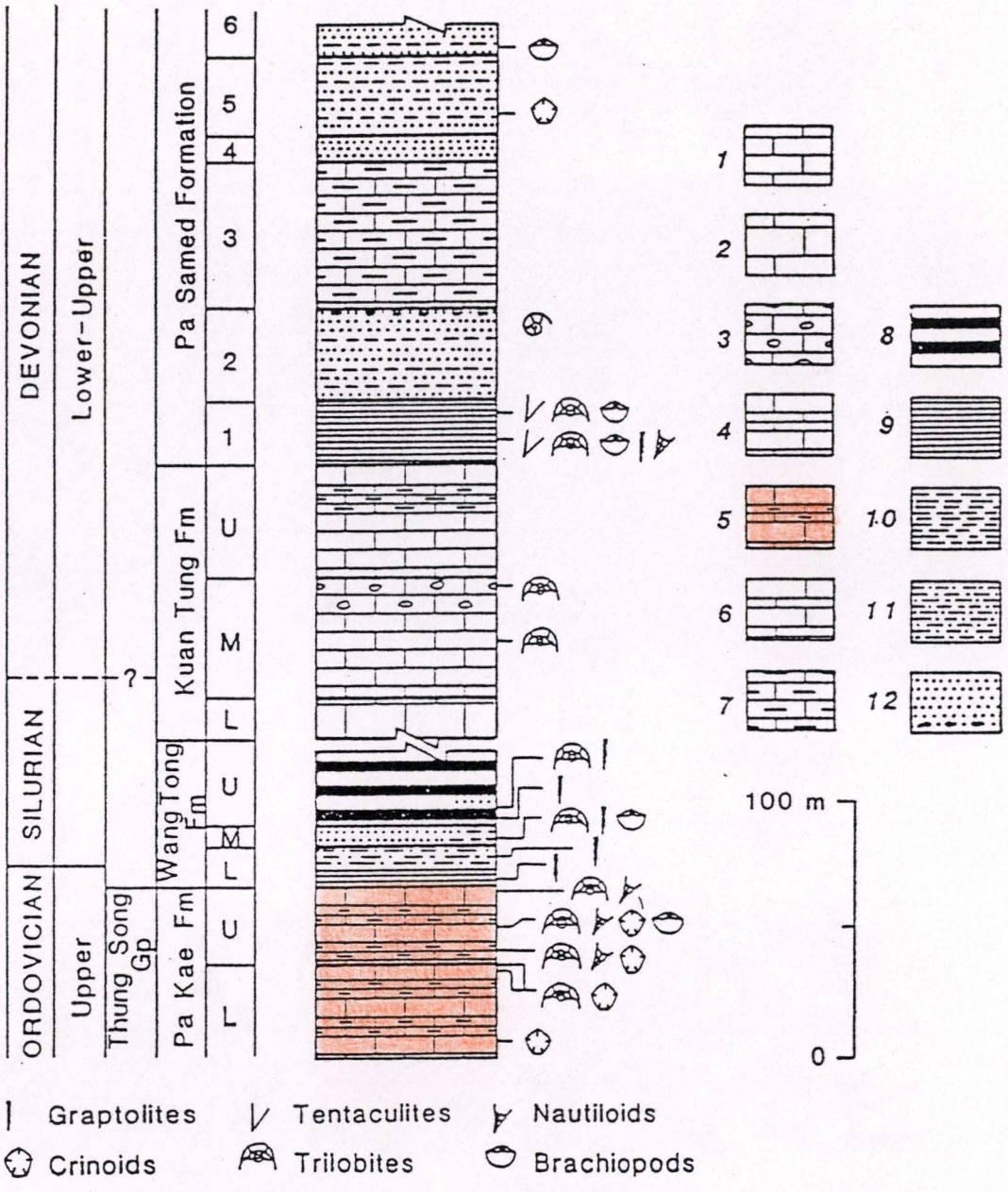

Fig. 3.11 Composite stratigraphic column of Upper Ordovician-Devonian rocks. 1) Thin bedded limestone, 2) Massive to thick bedded limestone, 3) Thin bedded limestone with chert nodules, 4) Thin bedded limestone interbedded with laminated limestone, 5) Red stromatolitic limestone, 6) Thin bedded limestone with finning-upward sequence, 7) Argillaceous limestone to decalcified shale, 8) Chert and black shale, 9) Black shale, 10) Brown, gray and red shale, 11) Siltstone, 12) Sandstone with in part well rounded pebbles.

southeast of the type section in this area. It is also well exposed at Khao Ao Nun, 16 km south of the type section.

The Pa Kae Formation is composed of 66 m of alternating beds of very thinly bedded (100-150 mm), red stromatolitic limestone and red silty mudstone with minor thrombolitic and rare oncolitic limestone. The unit is characterised by wavy bedding along stromatolite biostromes or bioherms, by phacoidal texture and by stromatolitic polygons on the upper bedding surfaces. The thickness increases considerably southward to 126 m at Khao Ao Nun. Part of the Pa Kae Formation is faulted against the typical Thung Song Group, grey dolomitic limestone and limestone at the south end of Khao Ngiap, but it conformably overlies the thinly bedded limestone with the orthoconic nautiloids at the small limestone quarry at km post 11. The upper contact between the Pa Kae Formation and the overlying chert, black shale and siltstone alternation of the Wang Tong Formation is conformable and extremely sharp (Fig. 3.11).

The Pa Kae Formation can be subdivided into lower and upper members (Fig. 3.11). The lower member is 34 m of poorly laminated to very thinly bedded (10-50 mm) red stromatolitic limestone with dark red calcareous silty mudstone partings. It appears more massive than the upper member (Fig. 3.12A) and contains a large amount of crinoid debris. But the stromatolitic polygons (Fig. 3.12C) are smaller than in the upper member.

The 32 m thick upper member is distinguished by an increasing predominance of stromatolitic limestone with layers about 50-250 mm thick and a decreasing number of silty argillaceous layers. The dark red polygonal concentration of ferruginous-argillaceous material is clearly preserved on bedding planes. The fauna includes a number of small well preserved deep-water trilobites, orthoconic nautiloids, gastropods, brachiopods (*Foliomena*), ostracods, calcispheres and echinoderms.

The dark red iron concretions enclosing intraclasts and bioclasts are common in both members. At the rear of the black shale quarry close to the type section, the thin bedded limestone on the top of the sequence gradually changes to grey limestone with abundant pyrite nodules.

A similar lithology to the Pa Kae Formation extends as far as Ban Na, Na Born District, Nakhon Si Thammarat Province, 140 km north of the type area where 12m of stromatolitic limestone with orthoconic nautiloids is well exposed in the Klong Rung Giad, grid ref. 734,236, map sheet 4925IV. A very similar sequence is exposed on the northwest coast of Pulau Langgon, Langkawi Islands, NW Malaysia (Jones, 1968; Igo and Koike, 1967; Wongwanich *et al.*, 1983; Wyatt, 1983). The approximately coeval Linwe Formation of the Pindaya Group in the southern Shan States and the

Fig. 3.12 A. Thin bedded, red stromatolitic limestones interbedded with dark red calcareous silty mudstone in the lower member of the Pa Kae Formation.

B. Red stromatolitic limestones with calcareous silty mudstone parting of the upper member showing thinly and wavy bedding, and small stromatolitic columns (arrow).

C. Typical stromatolitic polygons on the upper surface of red stromatolitic bedding within the Pa Kae Formation.

D. A polished slab of red stromatolitic limestone showing the development of stromatolites from stratiform stromatolites at the base to LLH-C columnar stromatolites on the top of bedding. Red intraclasts (arrow) are common.

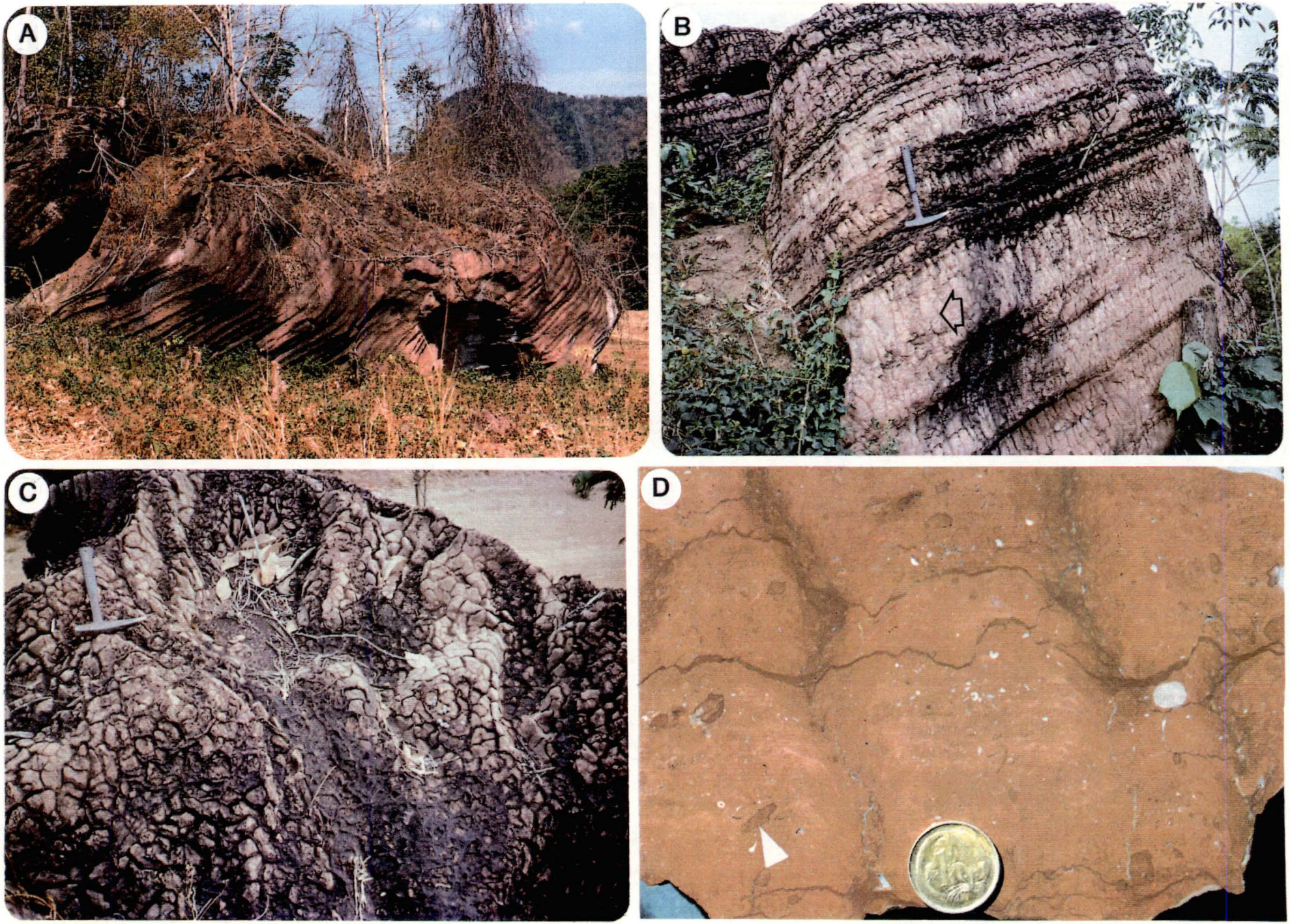
A
B
C
D

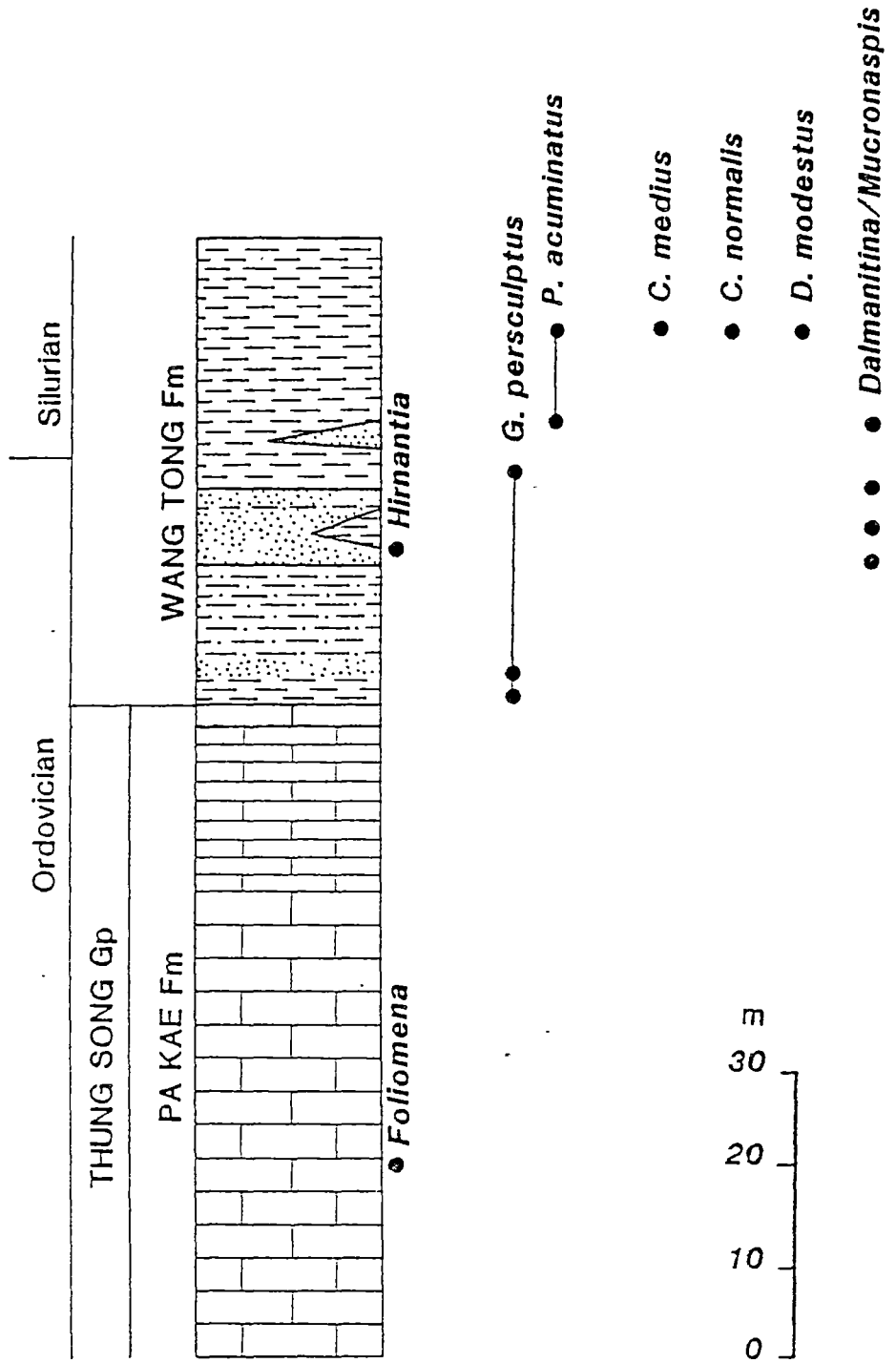

Fig. 3.13 General stratigraphic column of the Pa Kae Formation and Wang Tong Formation showing important faunal elements. A probable position of the Ordovician-Silurian boundary is shown.

Nyaungbaw Formation of the Naungkangi Group in the Northern Shan State of Burma also contain sequences of purple phacoidal limestones (Wolfart *et al.*, 1984).

Palaeontology and Age

R.A. Fortey (personal communication) has identified a dominantly pelagic trilobite fauna from the upper horizons of the type section including species of *Ovalocephalus*, *Orthorhachis*, *Nileus*, ?*Amphytrion*, and cyclopygidae which are indicative of the Late Ordovician, ranging from the Late Caradoc to Early Ashgill.

3.9 The Ordovician-Silurian Boundary

No attempts have been made to define the Ordovician-Silurian boundary in Thailand before this work (Wongwanich *et al.*, 1990). Traditionally this boundary is placed between the gray to dark gray Thung Song carbonates and the black shales interbedded with cherts. The discovery of the red stromatolitic limestones of the Pa Kae Formation, and the *Damanitina* beds within the Wang Tong Formation in 1985 provided an excellent opportunity to identify that boundary in southern peninsular Thailand (Wongwanich *et al.*, 1990).

Based on trilobites, and graptolites (which were identified by R.B. Rickards, personal communication) including *Glyptograptus persculptus, Glyptograptus exgr. persculptus* (small form), *Parakidograptus acuminatus, Climacograptus medius, Climacograptus normalis, Pseudoclimacograptus sp., and Climacograptus modestus* the Ordovician-Silurian boundary is placed at the base of the *acuminatus* Biozone and above the *persculptus* Biozone within the lower portion of the Wang Tong Formation (Fig. 3.13). This is just above the lower *Dalmanitina* beds (Wongwanich *et al.*, 1990)

Chapter 4
PETROGRAPHY AND MICROFACIES ANALYSIS

4.1 General Petrography

4.1.1 Mineral Composition

The major minerals of the Thung Song Group are calcite and dolomite while clay, quartz, feldspar, iron-minerals and organic matter comprise the subordinate components. The distinction between dolomite and calcite is mostly on the bases of 1) usually euhedral microrhombs, well defined rhombohedral cleavage, and 2) staining techniques (Dickson, 1966).

Calcite: Calcite, the major mineral component, occurs as microcrystalline calcite (micrite), sparry calcite, skeletal and non-skeletal varieties. Microcrystalline calcite, with or without sparry calcite within primary and secondary porosities, is extensive in the Malaka Formation, Talo Dang Formation, La Nga Formation, Pa Nan Formation, Lae Tong Formation, and Pa Kae Formation (Fig. 4.1 - 4.4B). In contrast, the Rung Nok Formation contains abundant sparry calcite as cementing material, with minor microcrystalline calcite forming envelopes or pore filling (Fig. 4.4B-4.7). Calcite veinlets and calcite pseudomorphs after gypsum (Fig. 4.5) are widely distributed in most of the lower formations.

Dolomite: Dolomite commonly occurs as 1) brown microdolomite, interlaminated or interbedded with micrite or other microfacies in the Malaka Formation, La Nga Formation, Pa Nan Formation and Lae Tong Formation (Fig. 3.4B, 3.12C), 2) brown microdolomite along stylolites, 3) microdolomite with or without iron zonation in worm burrows (Fig. 3.4D, 4.1A), 4) very fine brown dolomicrite associated with calcite pseudomorphs after gypsum in the upper member of the Lae Tong Formation (Fig. 4.9A), 5) large dolomite crystals, replacing micrite, sparry calcite and allochems (Fig. 4.9C), 6) saddle dolomite in large voids or veins, and 7) dolomite cement.

Quartz: This mineral is normally present as very small detrital grains (20-120 mm), especially in the Malaka Formation, La Nga Formation and in the lower member of the Lae Tong Formation (Fig. 4.3). Both authigenic quartz (19-70 μm) and silica replacement have been observed in the Pa Nan Formation, Talo Dang Formation, Lae Tong Formation and Phetra Formation.

Feldspar: Although detrital feldspar occurs only rarely in the lower formations of the Thung Song Group, it is abundant as detrital and authigenic minerals (albite, 80-120 μm) in some layers of the Lae Tong Formation

Iron Minerals: Within the Thung Song Group iron-bearing minerals occur 1) as a finely divided iron-oxide "Zonal rim" around some dolomite rhombs, especially the micro to mesodolomite in burrows as well as the saddle dolomite which infills large voids and veins, 2) as finely divided hematite grains within the Pa Kae Formation, 3) as ferromanganese micronodules or concretional layers enclosing intraclasts and bioclasts in the Pa Kae Formation (Fig. 4.2B), 4) as intergranular cement in the La Nga Formation (Fig. 4.5A), 5) as insoluble residue along stylolite zones, and 6) as single crystals (20-1500 μm) and/or spherulitic pyrite (5-15 mm) in the Malaka Formation, La Nga Formation, and especially the Lae Tong Formation.

Clay Minerals: In thin section, it is difficult to discriminate the clay minerals from either carbonaceous matter or very fine lime mud. However, the occurrence of clay minerals can be ascertained by the presence of 1) an extremely fine matrix (<4μ), and 2) widely disseminated prismatic mica- like minerals in argillaceous layers. The first category has been found in the Malaka Formation, while the latter is observed in argillaceous layers of the Lae Tong Formation,Talo Dang Formation and the Pa Kae Formation.

Carbonaceous Matter: Similar to the clay minerals, this material is difficult to distinguish because of its lack of structure and very fine grain size. Recognition of carbonaceous matter is therefore based on its very dark colour and fine grain size associated with other recognized fabric including cryptalgal laminae (Fig. 4.1D). Large amounts of carbonaceous matter have been observed infilling some burrows as well as within algal laminations in the Malaka Formation, La Nga Formation, Pa Nan Formation and Lae Tong Formation.

4.1.2 Cement

The cementing material of the Thung Song Group is usually composed of calcite, dolomite, and rare iron oxide. Occasionally, the cement also includes micrite.

Calcite normally forms an equant and blocky mosaic cement. Fibrous and radiaxial fibrous cement are only abundant in the coarse grained biosparite of the Rung Nok Formation and the oosparite microfacies of the Malaka Formation and the La Nga

Formation. Uneven drusy fibrous cement has precipitated initially within the rims of pore spaces in between particles, after floored interstices, followed by the inward growth of equant and/or blocky cement towards the centre of the pores. Some bioclasts, especially crinoid fragments are rimmed by syntaxial calcite cement.

4.2 Microfacies Analyses

Twelve microfacies have been recognised: 1) stromatolites, 2) micrite and fossiliferous micrite, 3) biomicrite, 4) intramicrite, 5) poorly washed to unsorted biosparite, 6) biopelsparite and pelbiosparite, 7) pelsparite, 8) intrasparite, 9) flat pebble conglomerate, 10) oosparite, 11) biolithite and limestone breccia, and 12) dolosparite, dolomicrite and dolomite breccia. The dismicrite microfacies is incorporated into the stromatolitic microfacies because of the usual occurrence of dismicrite along stromatolitic laminae.

4.2.1 Microfacies I - Stromatolites

Stromatolites are laminated organosedimentary structures built by the trapping and binding of sediment, and/or carbonate-precipitating activity of microbial communities (Kalkowsky, 1908; Buick *et al.*, 1981; Krumbein, 1983; Kennard and James, 1987). These structures are prominent in several formation of the Thung Song Group within the study area. Two principal types of stromatolites are recognized: stratiform stromatolites and columnar stromatolites (Fig. 3.4B, 3.7, 3.12). The stratiform stromatolites, cryptalgal laminites or algal laminites (Logan et al., 1964; Aitken, 1967; Hofmann, 1969 ; Walter, 1976) are most common and widespread in the Malaka Formation and the La Nga Formation whereas the columnar stromatolites are the major component of the Pa Nan Formation and the Pa Kae Formation. Thrombolitic stromatolites, oncolitic stromatolites and oncolites (Fig. 4.2A, C) are less abundant in the Pa Kae Formation. Folk (1959, p.29) proposed the term algal biolithite for this rock type.

4.2.1.1. Stratiform Stromatolites

This microfacies can be subdivided into two categories: the smooth flat stromatolites and the wavy, irregular and crinkled stromatolites that occasionally occur as small scale domal structures.

1. The smooth flat stromatolites are visible as brown to black coloured laminae along foresets of cross strata in both the lower and upper members of the La Nga

Fig. 4.1 A. Alternating layers of microdolomite (D) and pelmicrosparite (L) in a stratiform stromatolite. Note the flame structure, intraclast, and increasing grain size of microdolomite downwards within the burrow (arrow) in pelmicrosparite. Thin section no.396B 2, the Malaka formation.

B. Stratiform stromatolites with an occasional domal structure (centre top), developed on intrasparite at the lower portion of the picture. Note the microdolomite along the mud cracks (arrow).Thin section no.396B2, the Malaka formation.

C. Parasitic LLH-C—>LLH-V (V) growing on the top of the first order LLH-V laminae (L) in a columnar stromatolite. Thin section no. 15, the Pa Nan Formation.

D. Alternating layers of microdolomite (brownish gray), micrite (brownish black) with microdolomite infilling a burrow (arrow) in a columnar stromatolite. Note the scattered tubular fenestrae. Thin section no. PN, the Pa Nan Formation.

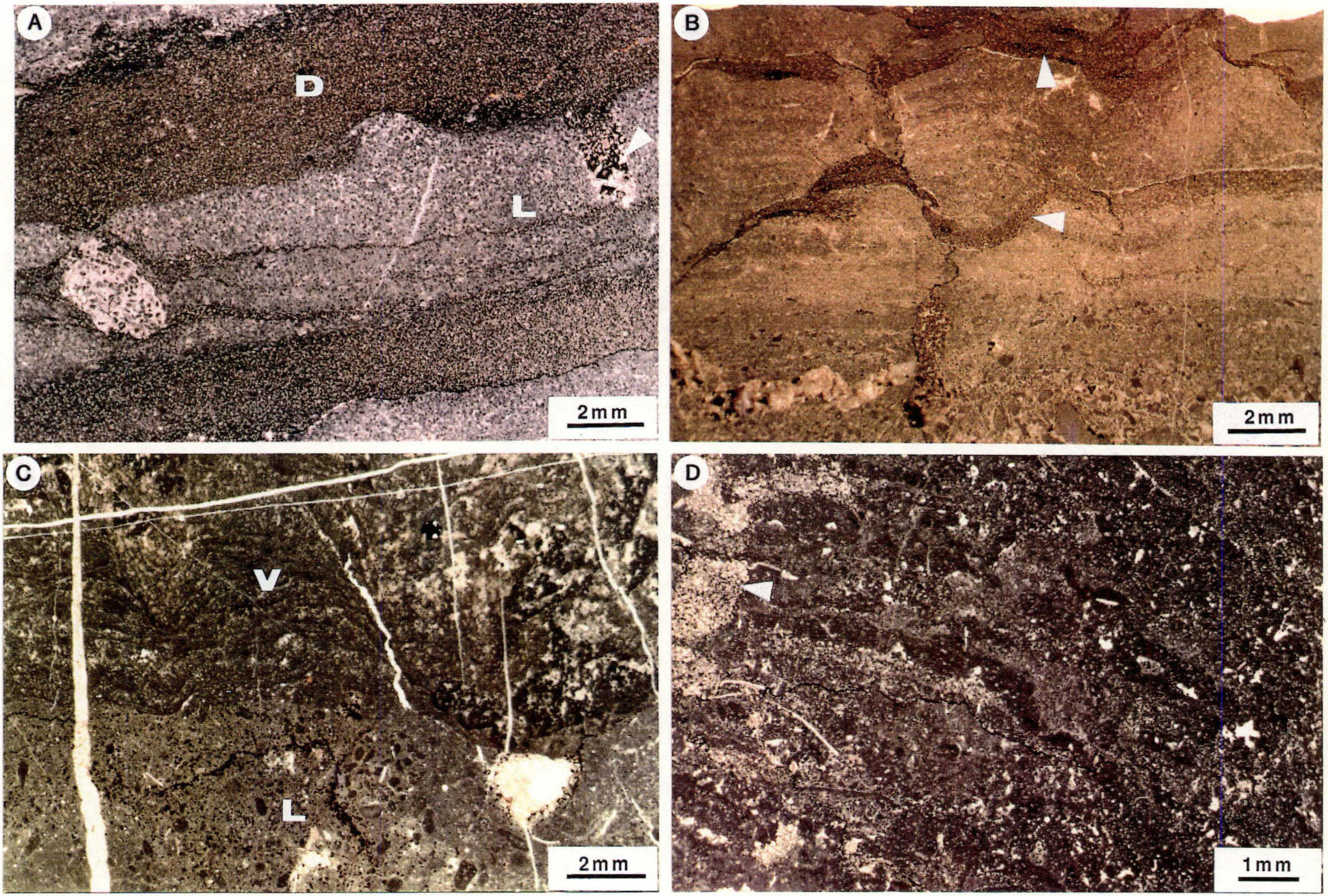
A
D
L
2mm
B
2mm
C
V
L
2mm
D
1mm

Formation; along the algal laminites and cross laminations of the Malaka Formation; and on top of some cycles in the upper member of the La Nga Formation (Fig. 3.4B, 3.6B,D). The rock comprises alternating laminations of microdolomite and limestone (Fig. 4.1A) which commonly form primary structure such as cross strata and flame structures. Some beds contain mud cracks. Bioclasts, intraclasts (Fig. 4.4D), and fenestral fabrics are very rare whereas vertical and U-shaped burrows are abundant (Fig. 3.4B).

The microdolomite layers are generally uniform along their length, and range from 0.5-5 mm in thickness. They are composed of very fine grained, tightly interlocking, primary or early diagenetic, brown idiotopic microdolomite rhombs (20-100 mm) surrounded by abundant black organic matter (Fig. 4.1A). These layers are commonly smooth but may protrude into the overlying limestone.

The limestone layers (0.5-30 mm thick) comprise grey micrite and pelsparite, containing very small ovoid and elliptical peloids (40-160 mm), plus equant microspar (Fig. 4.1A). Recognised variations in thickness are probably related to the direction of sediment transport along the length of these binding and trapping sediment-rich limestone layers (Hoffman, 1967; Gebelein and Hoffman, 1973). Abundant vertical burrows at the top of the limestone layers were initially filled with blocky spar which was subsequently replaced by microdolomite, and zoned mesodolomite at the base of the burrows (Fig. 4.1A). No burrows were observed in the microdolomite layers.

2. Wavy, irregular and crinkled stromatolites are common in the algal laminites of the Malaka Formation, Phetra Formation as well as within the uppermost part of the shallowing and thinning-upward sequence of the upper member of the La Nga Formation (Fig. 3.6D). In general, these rocks are the same as the flat stromatolites, although in places algal laminites are the alternation of the spar-rich and sediment-rich layers of micrites, dismicrites (micrite containing fenestral fabric) and fine grained pelsparites with more abundant small, rounded, micritic intraclasts (Fig. 4.1B) and a poor to well defined fenestral fabric.

   Occasionally, the wavy stromatolites can be traced upwards into irregular, small domed or laterally linked hemispheroid stromatolites (LLH-C). This microsubfacies is usually gradually developed on graded intrasparite microfacies (Fig. 4.1B). Microdolomite of this submicrofacies seems to be restricted to mud cracks and vertical burrows of the Malaka Formation and La Nga Formation. A siliceous tuff layer (450 mm thick) is present in this unit of the Phetra Formation at Ko Khao Yai.

4.2.1.2 Columnar Stromatolites

Although the well developed and densely crowded stromatolites in the Pa Nan Formation and Pa Kae Formation have formerly been classified, on the basis of their external features and morphology in the field, as either furcate or digitate stromatolites (Hoffman, 1969), they will actually be classified here on the basis of the arrangement of their basic hemispheroids as seen in vertical section (Logan *et al.*, 1964). These stromatolites comprise mainly laterally linked hemispheroids (LLH); discrete, vertically stacked hemispheroids (SH), and rare spheroidal structures (SS, oncolites) (Fig. 3.7B; 3.12B,D; 4.1C; 4.2A).

Pa Nan Formation: Most of the columnar stromatolites of the Pa Nan Formation are small scale (100-150 mm wide and 150-450 mm tall), discrete, vertically stacked hemispheroids with variable basal radii (SH-V). Convex laminations of 20-50 mm amplitude and 10-150 mm diameter are stacked to form vertically persistent columns which cross-cut bedding. Lateral linkage between these columns is intermittent due to only periodic sediment infilling of the intervening areas.

The laminae are fine (0.5-2mm thick), partly discontinuous, undulose bands composed of alternating layers of mostly dark grey micrite (3-5 mm) and microdolomite (45-75 μm) with a poorly developed tubular and laminoid fenestral fabric (Fig. 4.1D). Drusy cement within the fenestral porosity comprises blocky and equant spar (20-150 μm). Some limestone layers are pelsparite (20-40 mm peloids) with well developed laminoid fenestrae floored by vadose silts. Although the occurrence of bioclasts and intraclasts within the columns is rare, they are more abundant in the inter-column-areas. The vertical partitions between the columns have faintly concave-upward laminae which are partly or completely replaced by microdolomite. Micritic laminae contain approximately 1-2% very fine grained detrital quartz up to 75 μm in size, plus mica (60-100 μm) and authigenic quartz (20-60 μm). Stromatolite geometry within the Pa Nan Formation ranges from a vague, branching, stacked hemispheroid (SH-V) in the lower and intermediate parts of the sequence to a predominantly lateral-linked habit (LLH-C) at the top of the sequence. This vertical variation occurs at both Ko Pa Nan and Ao Dan (Fig. 3.7). In the second mode of occurrence the minor stromatolites (LLH- C-SH-V) are parasitic on the erosional surface at the top of the larger stromatolite (Fig. 4.1C).

Pa Kae Formation: In contrast to the Pa Nan Formation the digitate columnar stromatolites of the Pa Kae Formation are very small-scale domes with diameters ranging from 10-50 mm and heights from 40-150 mm. These domes are stacked

Fig. 4.2 Deeper water stromatolites showing :

A. An oncolitic stromatolite (LLH-C, 1) developing upwards to form pure oncolite (arrow 2). Note the rarity of bored erosional surfaces (arrow 3) encrusted with dark brownish-red ferromanganese crusts; and the inverted, stacked, hemispheroid oncolites (4). Thin section no. 389.15, the Pa Kae Formation.

B. A ferromanganese-mineral (arrow) coated around intraclasts (I). Note the abundant peloids, lumps, and trilobite fragments. Thin section no. 389.1, the Pa Kae Formation.

C. Stratiform deeper water stromatolites (1) with links between mesoclotted structures (2) within thrombolitic stromatolites.

D. SEM of slightly etched thin section showing well preserved microbial filaments (1), sheaths (2) and the possible remains of micro-organisms (3). Note the entrapment of micrites along stromatolite filaments(1).

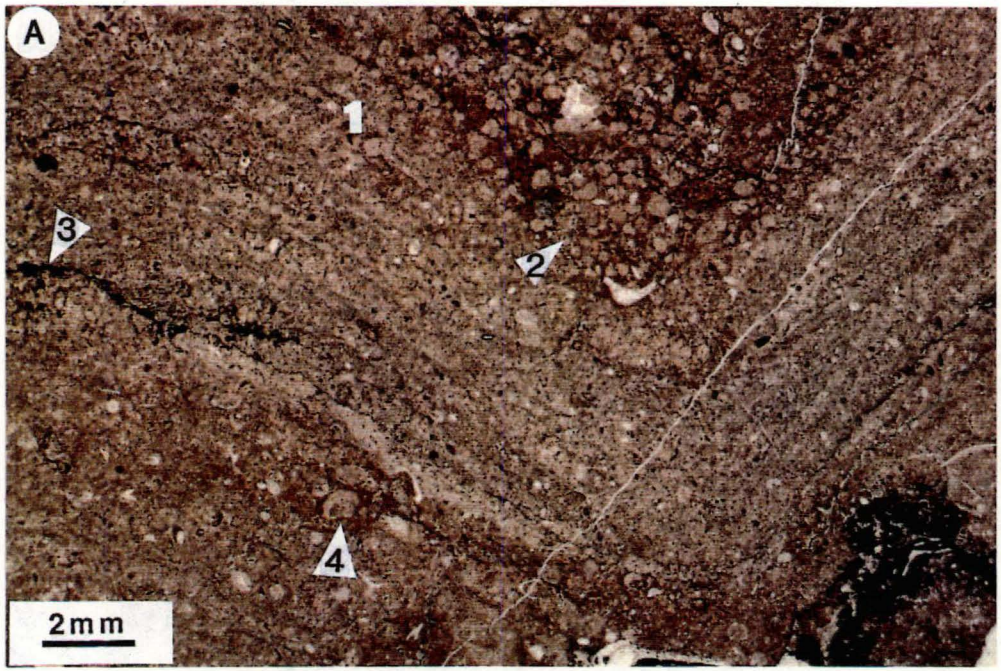
A
1
2
3
4
2mm

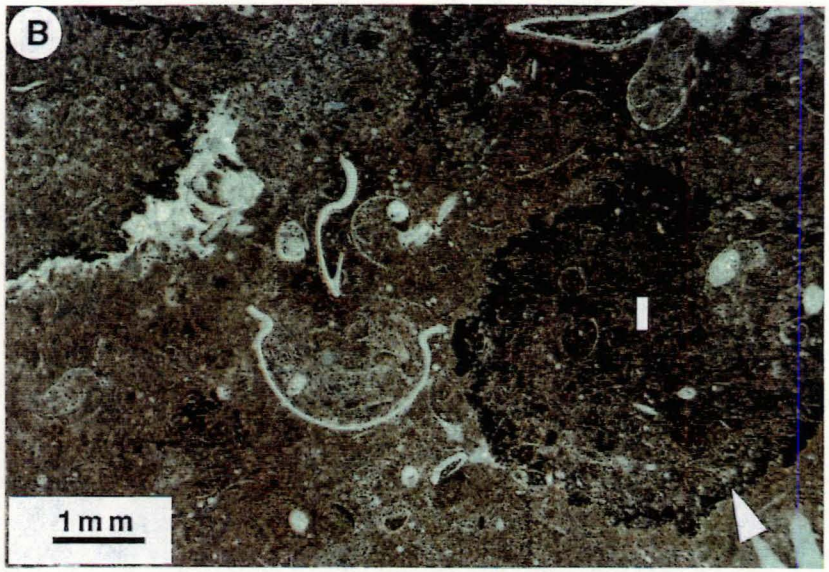
B
1
1mm


C
1
2
1cm

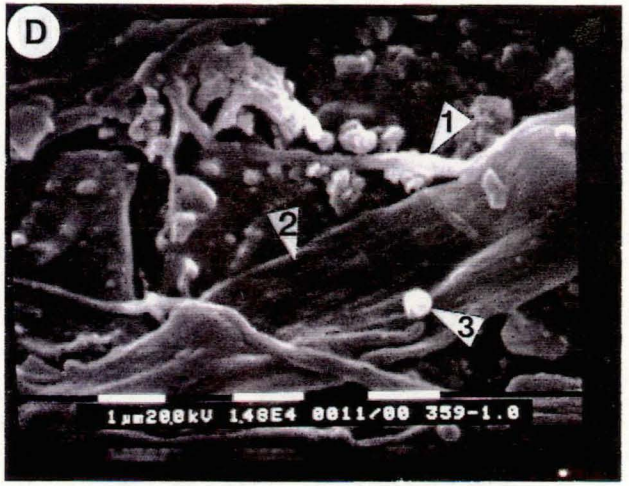
D
1
2
3
1µm20.0kV 1.48E4 0011/00 359-1.0

upwards across the bedding (Fig. 3.12D). Beds of this lithotype are thin, generally less than 150 mm thick, alternate with very thin beds of red calcareous silty mudstone containing red limestone nodules. Sparse thrombolites (Fig. 4.2C)are associated with columnar (LLH-C) and stratiform stromatolites in the lower member whereas they are absent or very rare in the upper member at type section. Oncolites (SS) are only observed in one horizon (150 mm thick). They have been trapped and bound within stromatolitic laminae (Fig. 4.2A). The typical characteristics of the Pa Kae Formation stromatolites are as follow:

1. The stromatolite forms within a single bed of the Pa Kae Formation are very variable in a vertical direction. In general there is an upward progression from stratiform stromatolites at the base of the bed to an intermediate lateral linked geometry (LLH-C, Fig. 3.12D, 4.2A) progressing still higher to the uppermost LLH-S hemispheroid (Fig. 4.2A) and recticulate stromatolites. Close stacked hemispheroid (SH) types are less common and usually develop above LLH-S types. The stromatolites are also laterally linked at some levels by laminae which can be traced across the partition from one column to another.

   The columns are mostly of a constant radius (LLH-C, LLH-S, SH-C) although some tend to gradually broaden upwards (SH-V). The columns have convex laminations of 10-50 mm diameters and amplitudes. Very narrow column interareas (2-5 mm wide) are filled with red silty mudstone. Erosional bored surfaces, coated with iron-rich mudstone (Fig. 4.2A), are only rarely observed in the columns. Vague coloured laminations within the columns are fine and continuous to partly discontinuous with a thickness of about 0.5-2.5 mm. Alteration of pale red spar-rich and dark red sediment-rich layers is common. They are composed of micrite and biomicrite with peloids, and lumps plus minor red and rare grey micritic intraclasts. The size of the rock components are as follows: 0.5-10 μm for detrital and precipitated micrite in the matrix, 2-4 μm for micrite in grey peloids and grey intraclasts, 10-150 μm for lumps and peloids, 100-200 μm for rounded grey intraclasts; 1-18 mm for regular red intraclasts coated by dark red, aphanitic iron-minerals and rounded grains; 5-35 μm for dark red separated iron-minerals in the matrix. The red intraclasts have the same lithology as the stromatolitic columns although the grey intraclasts have a different lithology and contain abundant calcareous tubes similar to the common calcareous algal fragments in the lower formation. The red intraclasts appear to have been torn out of the nearby columns and deposited in place, where they cross cut the stromatolitic laminations. The faunal assemblage includes ostracods, trilobites, calcispheres (60-450 μm) and echinoderms, as well as minor brachiopods, gastropods, sponge

spicules, cephalopods, calcareous algae, stromatoporoids, and conodonts. These faunal types are abundant but less diverse than in the lower formations.

Fenestral fabric is commonly absent or rare, but when present it is usually floored by an internal sediment (very small calcite crystals similar to vadose silts). Sparse shelter porosities under bioclasts and intraclasts are filled with blocky spar (Fig. 4.2B).

SEM studies reveal the presence of leaf-like microbial sheaths (0.5-2 μm wide, 15-30 μm long) and the probable remains of very small coccoid microorganisms (<0.5 μm) within the stromatolitic columns of the Pa Kae Formation (Fig. 4.2D). Rare isolated idiotopic microdolomite rhombs also occur locally.

2. Thrombolites are a minor microbial structure occurring within the lower member of the Pa Kae Formation. The external form of these thrombolites is similar to that of the stromatolites (digitate or laminate) and commonly occur together. The stromatolites form irregular laminations which bridge the clotted fabric (Fig. 4.2C). Irregular patches of mesoclots, up to 250 mm in diameter, are typically dark red and have a micritic, microcrystalline texture. The inter-clot sediments consist of pale red biomicrite with the same composition and texture as the stromatolites.This is classified as the thrombolitic stromatolite microsubfacies (Aitken, 1967).

4.2.1.3 Spheroidal Stromatolites (Oncolites)

Oncolites comprise the most minor component of the Pa Kae Formation. A single thin horizon of this submicrofacies has been observed in the lower member of the Pa Kae formation at the black shale quarry close to km 11 on the Thung Wa-La Ngu Road.

The oncolites have an irregular spheroidal to ellipsoidal shape. A cylindrical or elongated oncolite may occur when the nucleus is a long bioclast. According to the layer configuration terminology of Logan (1964), most of them are concentrically stacked hemispheroids (SS-C; Fig. 4.2A). Randomly stacked (SS-R) and inverted stacked hemispheroids (SS-I) are scarce (Fig. 4.2A). The vague concentric layering of oncolites is poorly developed around cores of ostracod valves and possible micritic nodules or peloids. Thick, slightly irregular, micritic laminae alternate with much thinner iron-stained laminae to form the oncoid coating whose outer layers usually show signs of physical erosion and boring. Some of the dense micritic oncolites look similar to oolites (Purdy pers. comm.). But over-all appearances and the existence of

SS-R and SS-I types and the mode of occurrence in relatively quiet water favours an oncolite interpretation.

This submicrofacies gradually progresses upwards from LLH-C stromatolites at the base of the beds to intermediate oncolitic stromatolites and then to pure oncolites within calcareous mudstone at the top of the columns and within the inter-column areas (Fig. 4.2A). This upward progression is also accompanied by an increase in the sphericity of the oncolites.

4.2.2 Microfacies II — Micrite and Fossiliferous Micrite

Lime mud or micrite is the most abundant calcium carbonate constituent of the Thung Song Group within the study area and its surrounds in the central peninsula of Thailand. It forms both distinct beds as well as interlaminations with other microfacies (Fig. 4.3A, B, C) in the Malaka Formation, La Nga Formation, and in the lower member of the Lae Tong Formation. Nodular micrite beds alternate with calcareous shale horizons (Fig. 4.3D) in the Talo Dang Formation, and in the upper member of the Lae Tong Formation. Micrite is the main component infilling interparticle porosities within the sparry limestone of the Rung Nok Formation and it also forms microbial laminae within the stromatolitic limestone of the Pa Nan Formation and Pa Kae Formation.

This microfacies is comprised of 90-100% lime mud, 0-10% allochems, 1-7.5% microdolomite, silt size detrital and authigenic quartz and feldspar, iron-minerals (mostly pyrite), and carbonaceous matter. The proportion of micrite and bioclasts in a single horizon is usually variable both vertically and horizontally and it usually grades upward into another microfacies (Fig. 4.3C, D). The lithotype which has a fossil content ranging from 1-10% is regarded as fossiliferous micrite while rocks containing 99% lime mud and 0-1% bioclasts are classified as micrite (Folk, 1959).

Micrites without bioclasts are widely distributed in the Malaka Formation at Malaka Creek and Ko Pa Nan, and within the lower member of the Lae Tong Formation at Ko Laen and Ao Ton Pung. In the Malaka Formation the micrite contains abundant brown microdolomite (40-80 μm) replacing burrows (Fig. 4.3A) and approximately 0-2.5% subangular to rounded detrital quartz silt. A distinctive characteristic of the micrite in the lower member of the Lae Tong Formation, especially at Ao Ton Pung, is very fine undulatory laminations and micro-hummocky cross laminations with extensively abundant subangular to rounded, detrital microdolomite, feldspar and quartz silt (up to 7.5%, 20-130 mm in size) along the foresets and alternating laminae (Fig. 4.3B). The detrital grains are very random and well sorted. Random, branching burrows, filled with brown microdolomite and equant spar, are

Fig. 4.3 A. Biomicrite interbedded with micrite (M). Note the burrow filled with microdolomite and subsequently bounded by stylolites (arrow). Thin section no. 435.16, the lower Lae Tong member

B. Micrite with detrital dolomite and some quartz silt (white spots) along hummocky cross-laminations (H). The upper part of the bedding was torn apart to form intramicrite. Thin section no. 4.1 F, the lower Lae Tong member

C. Normal graded bedding in biomicrite. Thin section no. 320.10D, the Malaka Formation.

D. Red nodular limestone (biomicrite, micrite), of the Lae Tong Formation, interbedded with red shale. Note the dewatering structure in the shale (1), and the plastic deformation feature (2) of the limestone. Thin section no. 401A, the Malaka Formation.

E. SEM of a broken slab showing a densely packed, interlocking mosaic of precipitated micrites within the La Nga Formation.

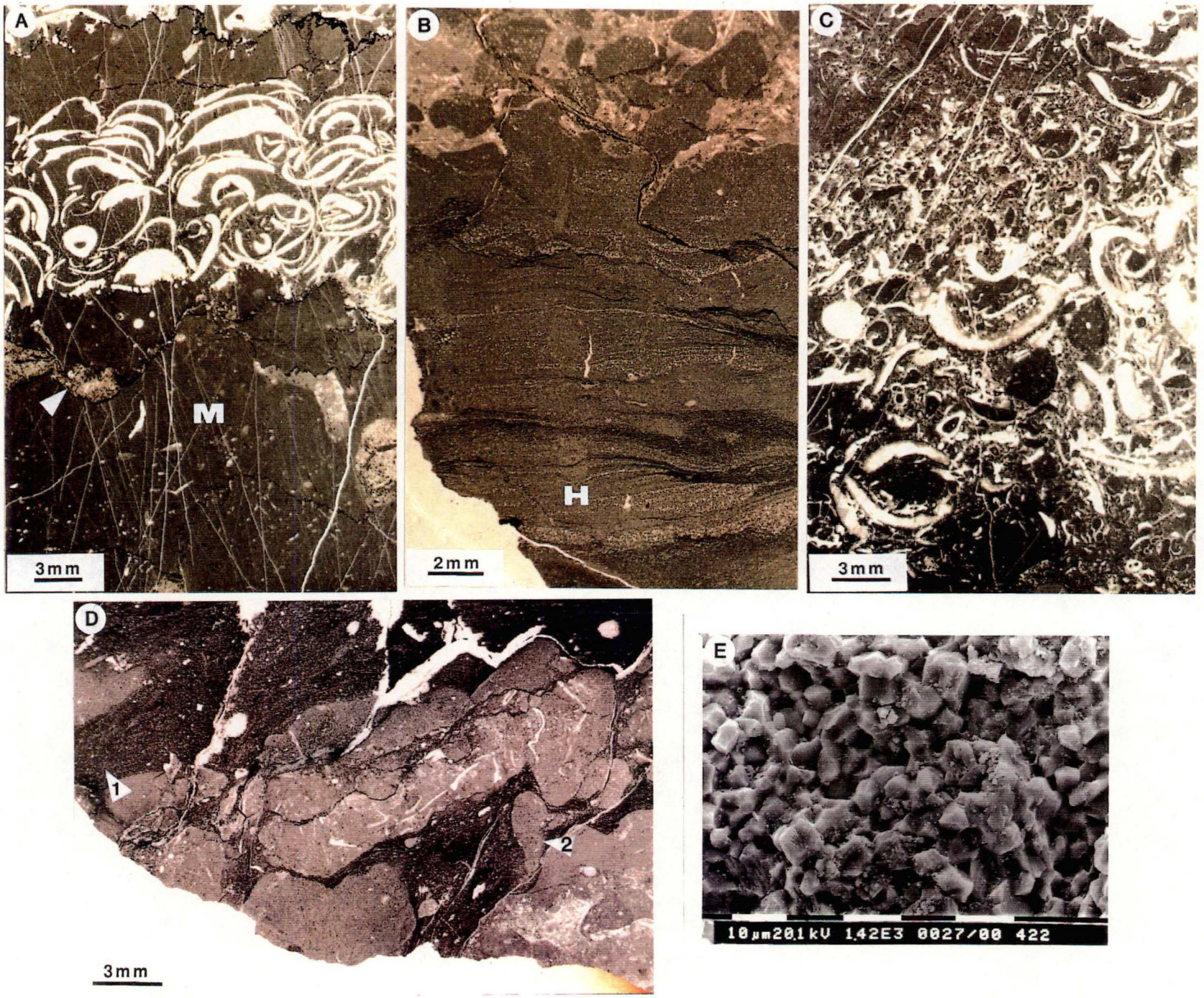
A
M
3mm
B
H
2mm
C
3mm
D
1
2
3mm
E
10µm20.1kV 1.42E3 0027/00 422

less extensive than the former one and they are usually confined to the top zone of some micrite beds. This upper zone has often been torn out to form the variously shaped intraclasts within successive intrasparite horizons (Fig. 4.3B). Wyatt (1983) and Mason (1986) observed escape burrows in this microfacies in the Langkawi Islands and on Ko Tarutao respectively. Although fossiliferous micrite is widely distributed in the La Nga Formation, and within both the lower and upper members of the Lae Tong Formation at Ko Lae Tong and Ko Laen, it is less abundant in the Malaka Formation and Talo Dang Formation. Some of these beds are graded. The fossiliferous micrite is composed of 90-95% micrite, 2-10% bioclasts including fragments of echinoderms, brachiopods, trilobites, pelecypods and gastropods, as well as rare bryozoans and primitive corals in the upper formations, 0-2% peloids and intraclasts, and 1-2.5% subangular detrital quartz, feldspar and pyrite.

The Thung Song Group micrite comprises an interlocking mosaic (Fig. 4.3E) of microcrystalline calcite crystals whose bimodal crystal size is larger than that of the modern standard micrite (1-4 μm in diameter), as defined by Folk (1959). Crystal size ranges in the micrite are as follows: 4-35 μm from the Malaka Formation, 5-35 μm from the Talo Dang Formation, 5-15 μm from the La Nga Formation (Fig. 4.3E), 3-60 μm from the Pa Nan Formation, 5-50 μm from the Lae Tong Formation, 5-10 μm from the Rung Nok Formation, and 0.5-10 μm from the Pa Kae Formation. Two textural types dominate: 1) fine grained micrite ranging from 3-7 mm, and 2) coarser grained (microspar?) micrite ranging from 4-60 μm. There is an overlap in the size ranges of these two types of micrites.

The grain size of the microcrystalline calcite from the Thung Song Group falls within the range of neomorphic microspar (5-30 μm) and pseudospar (>30 μm) as defined by Folk (1959, 1965). However, based on SEM studies of micrite from south Florida and the Bahamas, Lasemi and Sandberg (1984) took an opposite view whereby they used the term "micrite" as being inclusive of both micrite and microspar for lime mud ranging from 1 μm to 14 μm. SEM studies reveal that most of the micrites from shallow water carbonates including the Malaka Formation, La Nga Formation and Lae Tong Formation were mainly precipited from sea water. This is evidenced by their cryptocrystalline texture with polygonal crystals (Fig. 4.3E) whereas micrites from deeper water carbonates, the Pa Kae Formation, are made up of a combination of both detrital and precipitated micrites (Fig. 4.3E). This is possibly due to the supersaturation of shallow sea water with respect to calcite and the extensive maceration of carbonate grains in the deeper water deposits (as a description in chapter 7).

4.2.3 Microfacies III — Biomicrite

The biomicrites are ubiquitous and commonly interbedded or interlaminated with the other microfacies throughout the lower portion of the Thung Song Group, especially in the La Nga Formation and the Lae Tong Formation. The rock is composed of 10-45% bioclasts, 0-5% moderate to well rounded micritic intraclasts, 0-10% elliptical and oval peloids, 1-2.5% subangular to rounded quartz silt (20-39 μm), rare radial ooids and the calcareous algae *Nuia*, in a 50-80% micrite matrix (4-12 μm).

In general, the skeletal remains in the shallow water carbonates are diverse and fragmented (Fig. 4.3C). They include ostracods, trilobites, gastropods, echinoderms, calcareous algae, sponge spicules, brachiopods, polyplacophoran (Malaka Formation, Talo Dang Formation, and La Nga Formation); and rare receptaculitids, bryozoans, and primitive tabulate corals (Lae Tong Formation). As compared to the biosparite, microboring of the biomicrite bioclasts is less extensive. The gastropods and ostracods are mostly recrystallized. Echinoderm fragments are rimmed by syntaxial cement.

The micrite matrix of biomicrites in the lower member of the Lae Tong Formation yields a high proportion of argillaceous silt and clay. Pyrite is relatively abundant as both individual crystals and framboidal structures. Microdolomite is sparse and mostly occurs as vertical and random burrows. Birds-eye structures and shelter porosities occupied by blocky spar and calcite pseudomorphs after gypsum are found within the Malaka Formation and La Nga Formation.

The bioclasts are commonly poorly sorted with random orientations (Fig. 4.3C). There is also normal and reverse graded bedding roughly developed within the lower members of the Lae Tong Formation and the La Nga Formation (Fig. 9.3C, D). This texture is usually associated with biomicrites, containing rounded intraclasts, interbedded with intramicrite and micrite with cross laminations. Most of the mollusc shells are orientated with their convex sides facing upwards (Fig. 4.3A). The lower contact of the bedding or laminations is commonly erosional while the upper contact may be graded or sharp (Fig. 4.3A).

4.2.4 Microfacies IV — Intramicrite

Intramicrite is a carbonate rock containing at least 25% intraclasts within a micritic matrix (Folk, 1959). The Thung Song Group intramicrites are commonly interbedded or interlaminated with the scoured or erosional basal contact of the underlying microfacies in the Malaka Formation, Talo Dang Formation, La Nga Formation, and in the lower member of the Lae Tong Formation. Intramicrites are also present in the areas between the stromatolitic columns of the Pa Nan Formation. In both the Talo Dang Formation and the upper member of the Lae Tong Formation,

Fig. 4.4 A. Nodular limestone displaying the faint contact between intraclasts and matrix. Thin section no. 423.7, the Talo Dang Formation.

B. Intraclast with sharp contact and abundant sheltered cement (arrow) in the lower member of the Lae Tong Formation. Thin section no. 16.1

C. A poorly washed biosparite with geopetal fabric (1) and abundant syntaxial rim cement (2). Thin section no. 22.8, member 1, the Rung Nok Formation.

D. A majority of bioclasts within the biosparite are echinoderms and bryozoans (B) plus minor brachiopods and rare primitive corals. Rim cements postdate the micrite rims (arrow). Thin section no. 22.9, member 2, the Rung Nok Formation.

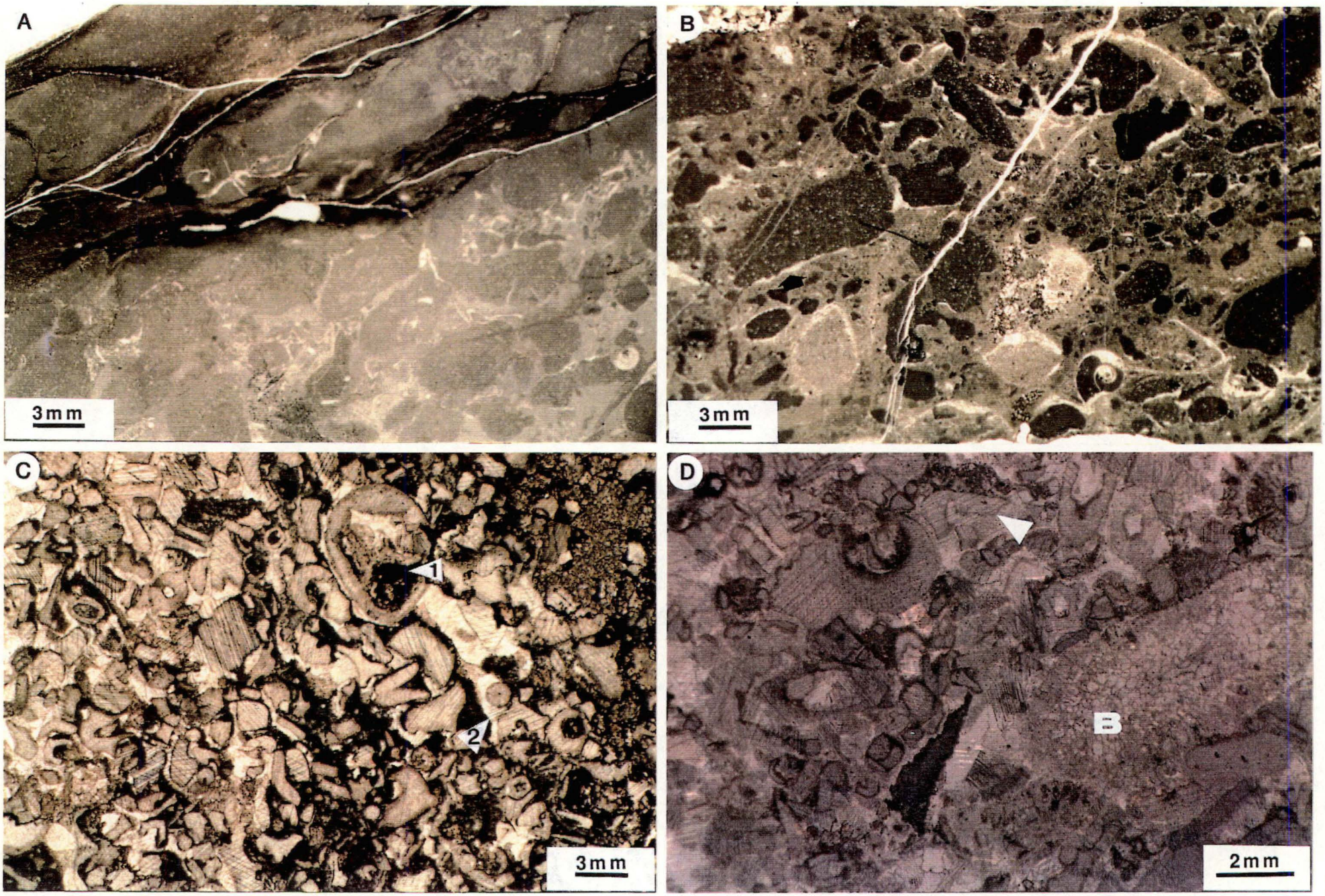
A
3mm
B
3mm
C
1
2
3mm
D
B
2mm

intramicrites are rare. Although intraclasts occur as limestone breccias in the third member of the Rung Nok Formation intramicrites are absent. Intraclasts are also found along the stromatolitic laminae of the Pa Kae Formation.

The rock is composed of 25-40% subangular to well rounded micritic intraclasts of various shapes with a bimodal size (Fig. 4.4B) range of 0.5 to 15 mm. The larger intraclasts are subrounded to well rounded, elongate to irregular in shape and occasionally greater than 15 mm. Smaller intraclasts tend to be well rounded or spherical. Intraclast imbrication is common. The boundary between intraclasts and the micritic matrix is generally sharp although an exception to this occurs in the lenticular layer of the Talo Dang Formation where the boundary is ill-defined (Fig. 4.4A). Microdolomite occurs in small burrows.

The intraclasts are composed of dark grey micrite with a high proportion of carbonaceous matter, abundant rounded quartz silt and rare bioclasts of limited diversity. Other allochems are absent from the intraclasts but usually exist (<10%) in the micritic matrix. The bioclasts in the matrix include *Chelodes*, gastropods and trilobites. These last are well preserved and much less fragmented than in the intrasparites. The relative proportions of intraclasts, bioclasts and peloids varies both vertically and horizontally within a single bed.

4.2.5 Microfacies V — Poorly Washed Biosparite

Coarse grained, white, grey and pink, sparry limestone or bioclastic calcirudite is found only in the lower two members of the Rung Nok Formation. The rock consists of 40-55% poorly sorted but well abraded bioclasts, 2-20% micrite, and 20-40% turbid syntaxial rim cement, fibrous cement and rare clear blocky cement. Detrital minerals are absent. Geopetal structures commonly have very small bioclasts and micrite as their internal sediments, plus some blocky spar infilling crinoid ossicles (Fig. 4.4C, D).

The bioclasts are primarily composed of fragmented and highly abraded crinoids (85%). Lesser components include globular bryozoans (5-10%), and rare inarticulated brachiopods, tabulate corals and trilobites (0-5%). The proportion of this latter group increases upwards to 5-15% in the second member of the Rung Nok Formation. Microboring and micritic envelopes are common. Average grain size varies between less than 1mm to 3mm; with a maximum of 10 mm.

This closely-packed rock is largely grain-supported, and some grains have irregular contacts (Fig. 4.4D). The primary porosity of the biosparite in the second member is almost completely destroyed by extensive syntaxial overgrowths on the crinoid debris (Fig. 4.4D). However, this turbid rim cement is less extensive in the

Fig. 4.5 A. Biopelsparite with brown chalcedony (C) replacing echinoderm ossicles (1), brachiopods (2) and matrix. Note the concentration of peloids on the upper side of bioclasts (3). Thin section no. 29.2, the lower Lae Tong member.

B. The pelbiosparite is poorly washed (1) and replaced by mesodolomite (2). Thin section no. 404 B, the lower Lae Tong member.

C. Pelsparite with intraclasts and microdolomite replaced blocky cements in a burrow (arrow, 1). Note the micrite envelopes around *Nuia* (arrow 2). Thin section no. 6.9, the Malaka Formation.

D. Abundant pellets cemented by equant calcite and blocky spar in the larger porosities. There are two types of peloids : 1) long irregular grains, and 2) oval-ellipsoidal grains. Note the microdolomite selectively replaced peloids (3). Thin section no. 70.3, the Malaka Formation.

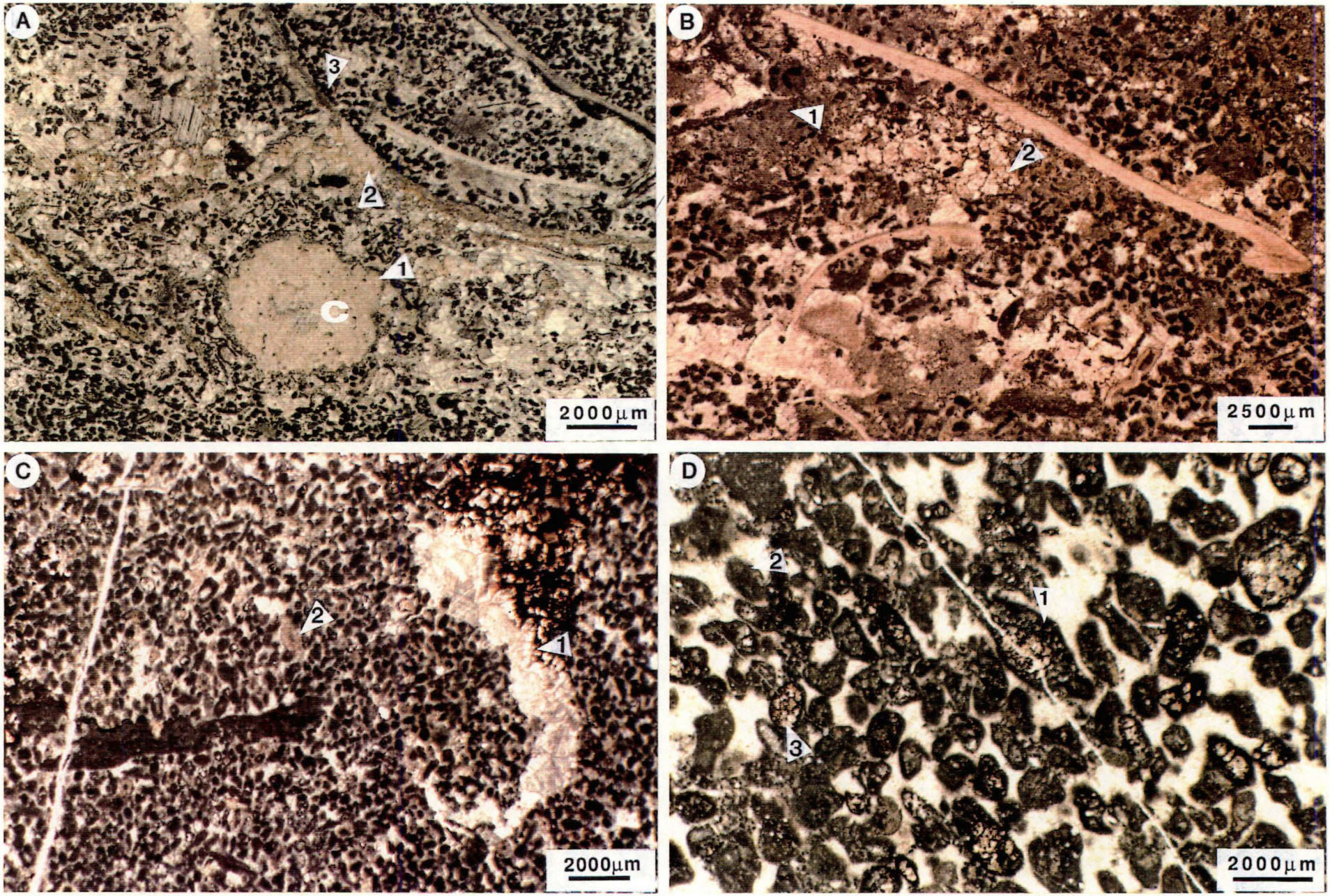
A
3
2
1
C
2000μm
B
1
2
2500μm
C
2
1
2000μm
D
2
1
3
2000μm

first member. Very dark grey micrite and very fine grained fragmented bioclast matrix has infilled the large inter- and intraparticle porosities after the formation of the cement rim, and before or after the formation of the blocky cement. The products of this infiltration are extremely poorly sorted (Fig. 4.4C). The micrite content of the rock decreases vertically upwards, resulting in the upper portion of the second member being almost completely devoid of micrite. Radial fibrous cement is rare at the bottom but increases toward the top of the sequence.

Dolomite is uncommon in the first member of the Rung Nok Formation where only a limited amount microdolomite has selectively replaced the micritic infiltrate. However, the dolomitization of the second member is very pervasive and most of the micrite has been selectively replaced by late diagenetic dolomite. This process imparts a pink colour to both the dolomitic limestone at Ko Lae Tong and the completely dolomitized rock at Ko Laen.

4.2.6 Microfacies VI — Pelbiosparite and Biopelsparite

The fine to coarse grained calcarenite considered here contains both fossils and peloids, amounting to greater than 10% of the rock volume, within a microsparry calcite cement (30-145 μm). If the volume ratio of peloids to bioclasts is greater than 3:1, the rock is a pelbiosparite. On the contrary, if this ratio is reversed, the rock can be classified as a biopelsparite (Folk, 1959). As the rocks of the study area are very variable in their relative proportions of peloids and bioclasts, even in a single layer, it is therefore difficult to assign an exact name to them. Although many of the rocks tend to be pelbiosparite, rather than biopelsparite, for convenience they will be grouped together under the same microfacies.

Pelbiosparite and biopelsparite are found predominantly along cross bedding and cross laminations in the Malaka Formation, lower and upper members of the La Nga Formation, and in the coarse grained layer (calcarenite) of the lower member of the Lae Tong Fm. These rocks consist of 10-30% bioclasts including ostracods, trilobites, brachiopods, calcareous algae (*Nuia*), and echinoderms, 10-40% well sorted, ovoid to ellipsoidal, fine grained peloids (39-98 μm), 1-7% radial and concentric oolites, rounded intraclasts, and grapestones, and <2.5% subangular to rounded quartz silts; within an equant, sparse radial fibrous and blocky cement (40-70%). The majority of the rocks are well washed (Fig. 4.5A) although some are poorly washed and contain up to 25% micrite (Fig. 4.5B). Pelmicrites and pelbiomicrites are rare but are visible as stromatolitic laminae within microfacies I.

Shelter porosities under large bioclasts and pseudo-fenestral porosities filled with small blocky spar (200-600 μm) are common and have been further replaced by later

diagenetic dolomite. The infiltration of peloids, which tend to accumulate on the large bioclasts, is probably a useful facing indicator (Fig. 4.5A). However, Purdy (pers. comm.) commented that this should be re-deposited after cementation. A few bioclasts, especially brachiopods and echinoderms, have been replaced by chalcedony (Fig. 4.5A). Some of the meso- to megadolomite, which often occur in burrows and vuggy porosities, appear to be pseudomorphs after gypsum and/or anhydrite (Fig. 4.5B). Microdolomite is sparse and confined to burrows.

4.2.7 Microfacies VII — Pelsparite

Pelsparite is a carbonate rock containing at least 10% peloids, as the major allochem, in a sparry calcite cement. This microfacies is a major rock unit in the La Nga Formation and it is usually associated with intrasparite along cross bedding in the Malaka Formation (Fig. 4.6A). Pelsparite also occurs along stromatolitic laminae within microfacies I in the Malaka Formation and Pa Nan Formation. This rock is made up of 25-40% well sorted micritic peloids cemented by microspar or small equant sparry cement. Some layers have a partly micritic matrix. Other allochems such as intraclasts, oolites, bioclasts and detrital quartz are sparse. Most of the bioclasts consist of a calcareous algae, *Nuia*, surrounded by a micritic envelope (Fig. 4.5C). The grains are in close contact.

The peloids have two dominant textural types: 1) fine grained peloids ranging in length from 16-40 μm, and 2) coarser grained peloids ranging from 120-400 μm. However, irregular peloids up to 800 μm in size are also present (Fig. 4.5D). The finer peloids (60-70%) are oval and elliptical shape while the larger ones tend to be irregular and elongate, with a sharp and smooth wall. Some of the large irregular peloids consist of very small calcite rods surrounded by micrite. The small peloids are virtually homogeneous dark grey micrite lacking any internal structure. These peloids are commonly well sorted and randomly orientated although some tend to be aligned parallel to laminations and cross bedding (Fig. 4.6A). Changes in pelloid grain size may sometimes define a faint grading or layering within these rocks.

Most peloids, especially the coarser grained types, are extensively replaced by iron-stained microdolomite (Fig. 4.5D). An equant spar within the interparticle porosities was the first cement followed by blocky and dolomite cement in the large voids or pseudo-fenestral porosities. The fenestral fabric in pelsparite is restricted to the stromatolitic laminae of microfacies I. Burrows, occupied by blocky calcite and calcite pseudomorphs after gypsum replaced by mesodolomite, are also observed but the majority are usually filled with microdolomite.

Fig. 4.6 A. Intramicrite (1) interbedded with intrasparite (I) and pelsparite (P) with cross-laminations. Note the possible erosional surface (black arrow) between the micrite and the other facies. The lowermost portion is cemented by Fe-cement (2). Thin section no. 5 B, the Malaka Formation.

B. Clotted micrite within large intraclasts of intrasparite (cross nicols). Thin section no. 4.2 D, the Malaka-La Nga Formation.

C. The long irregular flat-pebble conglomerate is cemented by fibrous calcite (1). Note *Nuia* enclosed by micrite envelopes (2) and Z-shaped pebbles (arrow). Thin section no. 403.2, the Malaka-La Nga Formation.

D. Well rounded, tabular or rod-shaped, composed of laminated pebbles. Both irregular and well rounded pebbles are clearly reworked carbonate sediments. Thin section no. 421.14, the La Nga Formation.

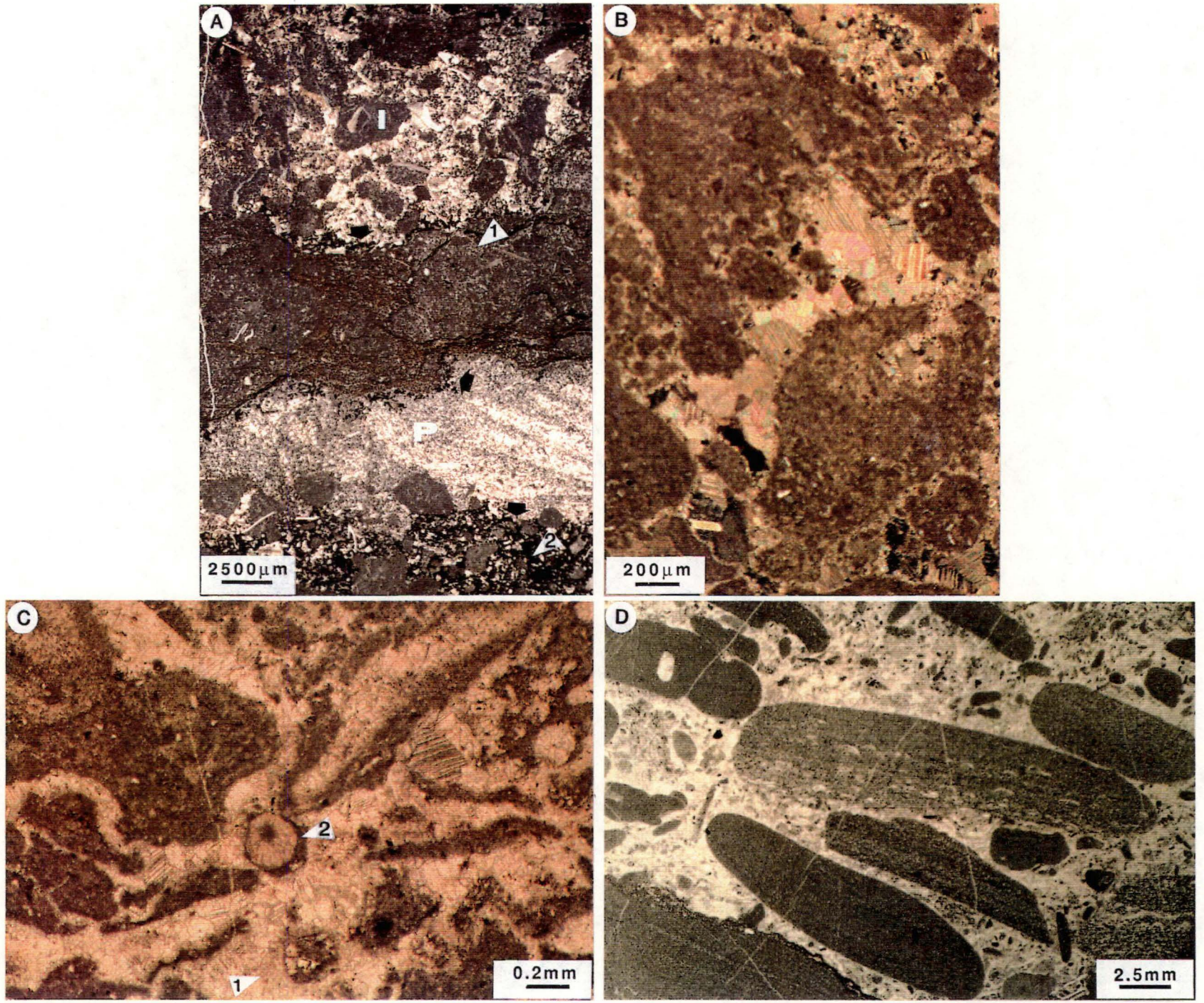
A
I
1
P
2
2500μm
B
200μm
C
2
1
0.2mm
D
2.5mm

4.2.8 Microfacies VIII — Intrasparite

Intrasparite is a carbonate rocks containing at least 25% intraclasts in a sparry calcite cement (Folk, 1959). This microfacies is common in the lower portion of the Thung Song Group in the study area. They are often interbedded or interlaminated with the scoured base or erosional contact of micrites and other microfacies within the Malaka Formation (Fig. 4.6A) and the lower member of the Lae Tong Formation. Intrasparite is also visible along cross bedding and cross laminations within the Malaka Formation and the La Nga Formation; as massive or thick beds intercalated with oosparite microfacies in the lower part of the shallowing-upward sequence of the La Nga Formation; and as a channel deposits in between the stromatolite columns of the Pa Nan Formation.

The rock consists of 25-50% subangular to well rounded micritic intraclasts ranging in size from 0.5-10 mm, 0-25% fragmented and abraded bioclasts including trilobites, echinoderms, *Chelodes*, ostracods, *Nuia* and other calcareous algae, 0-20% peloids, oolites and grapestones, and 0-5% detrital quartz silt. Intraclast shape varies considerably. The intraclasts along cross strata and thin beds are usually small and well rounded and they tend to be spherical, homogeneous or fossil-bearing micritic intraclasts. The larger intraclasts within massive beds are mostly irregular and some are broken, clotted micritic intraclasts or algal mats (Fig. 4.6B). The smaller intraclasts are better sorted than the large irregular ones. Within the massive limestone there are numerous fragments of trilobites, echinoderms and *Chelodes* with relatively thick rims of micrite.

The intraclasts are cemented by microspar (12-32 μm) or small equant sparry calcite (39-147 μm) in laminated to thinly bedded limestone, and by blocky spar (100-400 μm) in massive limestone. Rare hematite cement has been observed in the Malaka Formation. Calcite pseudomorphs after gypsum, and dolomite cement within the interparticle porosities are common.

4.2.9 Microfacies IX — Flat Pebble Conglomerate

This microfacies has been separated from the intrasparite microfacies because of its significance in environmental interpretation. It seems to have originated from more complex processes than the ordinary intrasparite. The flat pebble conglomerates are found within the lower and upper parts of the shallowing-upward sequence of the La Nga Formation and in the channel deposit of the Pa Nan Formation. Mason (1986) reported the occurrence of this microfacies 63 m above the base of the Malaka Formation.

The rock consists of about 25-55% tabular flat pebbles or intraclasts, 5-10% small intraclasts, oolites, peloids and abraded bioclasts, and 2.5-5% well rounded and well sorted detrital quartz silt (20-80 μm), within a sparry calcite cement (40-60%). The cement includes radial fibrous, short bladed, and blocky spar. The flat pebble conglomerates are poorly sorted, well washed and largely grain-supported. Imbrication of pebbles is common (Fig. 4.6C, D). Micritic envelopes around bioclasts within the massive limestones of the upper member of the La Nga Formation are thicker than those occurring within other microfacies.

There are two different types of flat pebbles. Firstly, the flat pebbles overlying the stratiform stromatolites above the shallowing- upward sequence comprise tabular, well rounded, laminated micrite and rare oosparite intraclasts with either smooth or bored surfaces (Fig. 4.6D). Most of them appear to have originated from the cemented stratiform stromatolites of microfacies I. The pebbles range in size from less than 5 mm to 600 mm long and less than 2 mm to 100 mm wide. The matrix comprises small intraclasts, peloids, and a few abraded bioclasts including *Chelodes*, *Nuia*, echinoderms, gastropods, ostrocods, and trilobites. The ooids in clast and matrix are relatively large concentric, radially concentric (1-2.2 mm) with a multiple cortex of up to 50 layers, and composite ooids. Most of these ooids have equidimensional nuclei of peloids and echinoderms. The pebbles within both the channel deposits and the interareas between the stromatolitic columns of the Pa Nan Formation are the same as above but smaller in size.

Secondly, the flat pebbles within the lower part of the shallowing-upward sequence of the La Nga Formation comprise irregular and partly broken micritic pebbles (Fig. 4.6D) similar to the intraclasts of microfacies VIII. Calcified algal filaments have been observed within clasts. Some pebbles are distorted to form Z–shapes (Fig. 4.6C) indicating the pliable nature of these clasts during deposition. These pebbles may have been eroded and transported from the columnar and stratiform stromatolites of microfacies I in a nearby area and/or they may be a product of *in situ* calcareous algal disintegration.

The flat pebbles and matrix were cemented firstly by radial fibrous and short bladed cement following by blocky spar and later dolomite cement within the interparticle porosities. Early diagenetic microdolomite selectively replaced ooids and peloids in the matrix. Calcite pseudomorphs after gypsum are present but not abundant.

4.2.10 Microfacies X — Oosparite

Fig. 4.7 A. Microdolomite selectively replaced radial concentric and composite ooids. Stained thin section no. 398.2 B, the Malaka Formation at Ko To sen.

B. Radial concentric ooids (a) and superficial ooids (b).

C. Irregular ooids with thick micritic layers (a), grapestones and compound ooids (b). Thin section no. 421.5, the Malaka-La Nga Formation.

D. Cup-shaped stromatoporoid (S) growing in place (arrow) on a nautiloid skeleton (C). Note the laminar stromatoporoids (L) which also encrust this nautiloid. Thin section no. 425.13, the third member of the Rung Nok Formation.

E. Blocky (B) and fibrous (F) cement on a stromatolite (1) with a micrite layer infilling above (2, crossed nicols). Thin section no. 400.9, the third member of the Rung Nok Formation.

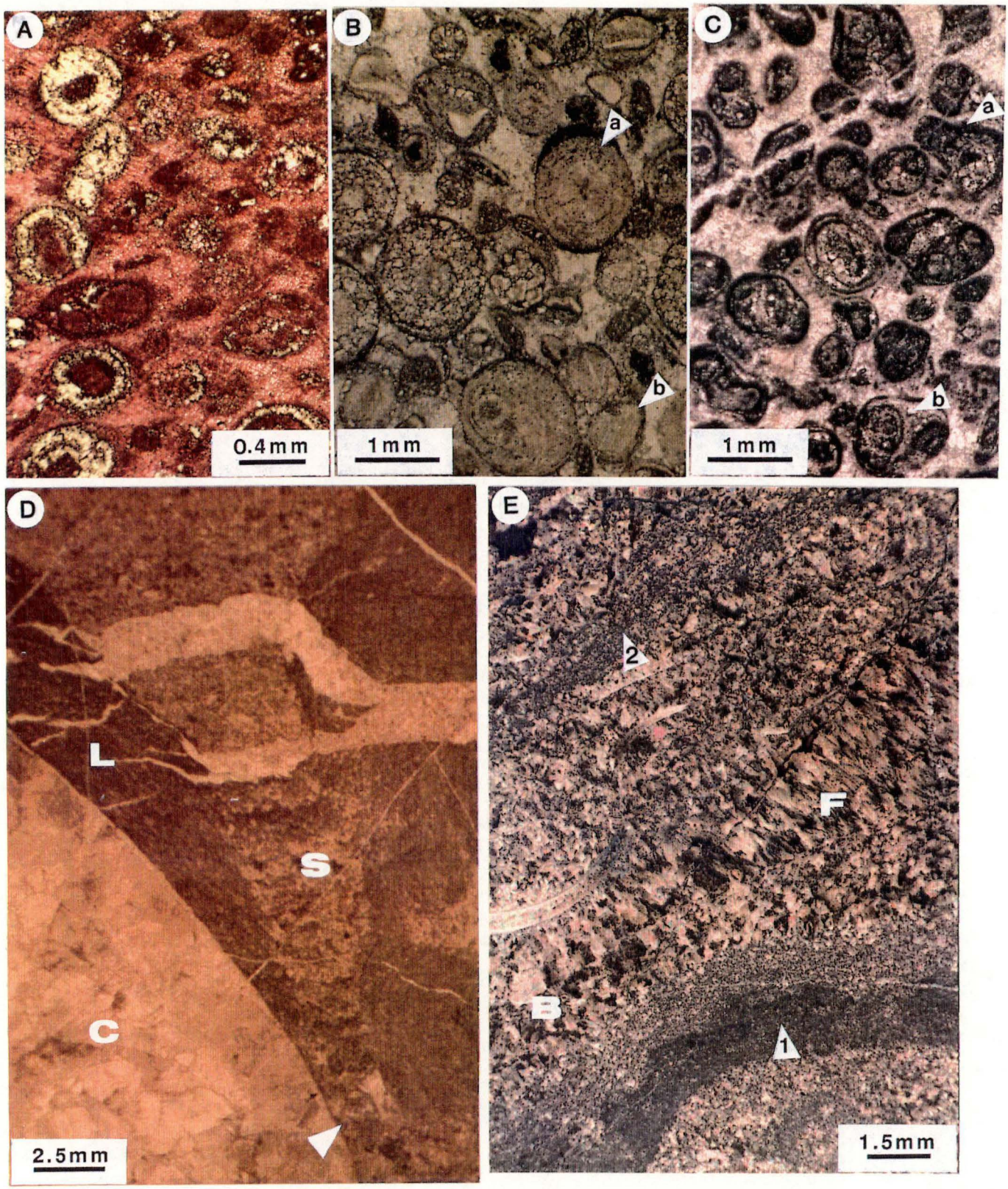
A
0.4mm
B
a
b
1mm
C
a
b
1mm
D
L
S
C
2.5mm
E
2
F
B
1
1.5mm

Oosparite is a carbonate rock containing at least 25% ooids, as the major allochem, within a sparry calcite cement (Folk, 1959). This microfacies is commonly associated with intrasparite and flat pebble conglomerates within cross bedding and some massive limestone units of the La Nga Formation, as well as thin cross strata and ripple beds intercalated with the stratiform stromatolites of the Malaka Formation. Oosparite is also occasionally associated with the extensively dolomitized, poorly washed biosparite of the second member of the Rung Nok Formation at Ko Laen. Individual ooids occur as a minor component within pelbiosparite and pelsparite of the Malaka Formation and the lower member of the Lae Tong Formation.

The rock is composed predominantly of 30-50% well layered subspherical to spherical ooids (0.6-1.6 mm) in cross beds and ripple beds, as well as in slightly irregular, matted surfaces in massive beds (Fig. 4.7A, B, C), 5-10% spherical to elliptical peloids and minor grapestones composed of peloids or small ooids in a micritic cement, less than 5% relatively less diverse, well abraded bioclasts including trilobites, *Chelodes*, echinoderms and *Nuia*. These components were cemented firstly by radial fibrous cement followed by blocky spar and dolomite cement in large intraparticle porosity. All oosparites are well washed and largely grain-supported with minor compactional effects.

Most of ooids are poorly defined because of extensive micritization (especially in the slightly irregular ooids) and selective dolomitization during early diagenesis. Broken ooids and polyooids are bound by algal layers with probable calcified filaments. In less altered ooids, the nuclei are commonly peloids, abraded bioclasts of echinoderms, trilobites and *Nuia*, plus broken and whole ooids. The ooids with trilobites as their nucleii are usually subspherical or even elongate as compared to the spherical ooids with pelloid or echinoderm nuclei.

There are four types of ooids in this microfacies: 1) radial, 2) radial- concentric, 3) composite, and 4) superficial ooids. The purely radial ooids are usually made up of a pelloid nucleus and a radial fibrous calcite (normal to the centre) cortex. Radial ooid is less abundant than the others and very difficult to differentiate from spherical *Nuias* cut perpendicular to their axis. The *radial-concentric ooids* are the main component of oosparites. The cortices of this type are composed of two distinct zones, an inner zone of radial fibrous calcite crystals similar to that of the purely radial ooids, with or without very faint concentric layers, plus an outer zone of radial calcite crystals arranged in concentric envelopes. The radial calcite envelopes of the outer zone alternate with thin micritic layers in the spherical well defined ooids but the micritic layers are much thicker in the slightly irregular ooids (Fig. 4.7B, C). The number of calcite layers in the outer cortex is variable but normally does not exceed seven.

The composite ooids are the second most abundant type, while the superficial ooids are relatively rare. Each *composite ooid* has two or three radial or radial-concentric ooids forming its nucleus, which is enclosed by one or two concentric layers of radial calcite crystals with micrite partings. The *superficial ooids* usually have large echinoderm nucleii enclosed by one or two concentric layers of fibrous calcite crystals (Fig. 4.7B). The alternating micritic layers within the concentric envelopes of these two ooids types are irregular in thickness and they are much thicker in the slightly irregular ooids than in the spherical ooids.

Based on the size and compositional correlation between the first three types of ooids, it seems likely that the largest composite ooids have gradually developed from the smallest purely radial ooids via the intermediate radial-concentric ooids. Similar types of ooids have been reported from many Cambrian rock units including the Warrior Formation, Pennsylvania (Heller *et al.*, 1980); the carbonate oolites of Carteret, France (Poncet, 1984), the Grand Cycle Formation of the northern Appalachian and the Port au Port Group in southwestern Newfoundland (Nancy and James, 1987).

4.2.11 Microfacies XI — Biolithite and Limestone Breccia

Biolithite is an autochthonous reef rock composed of organic structures which have grown in place to form a resistant mass (Folk, 1959, 1962). This rock type does not include any fragments that have broken off the organic structures. The biolithite of the Thung Song Group at Ko Tarutao is commonly surrounded by limestone breccias and coarse poorly washed biosparites which contain angular to subangular rubble made up of the remains of *in situ* organisms. The limestone breccia is composed of consolidated angular fragments of limestone, most of which are larger than 2 mm in diameter, plus matrix and cementing material (Bissell and Chillinger, 1967). Microfacies XI is the least abundant rock type of the Thung Song Group in southern Thailand. In the study area, the biolithites are present only within the third member of the Rung Nok Formation at Ko Lae Tong and Ko Sing Ha.

The biolithites, within thinly bedded grey calcarenites (15-20 cm thick) at the base of the third member of the Rung Nok Formation, are composed of both frame-building and sediment-binding organisms. The former are a cluster of simple tabulate corals and cup-shaped or bulbous stromatoporoids growing in place on the erosional surface of the former frame builder or poorly washed biosparite, as well as on megaskeletal remains such as nautiloids (Banks, pers. comm., Fig. 4.7D). Sediment binding organisms include long chained calcareous algae and possibly also stromatolites encrusted around or above the frame builders or megafossils (Fig. 4.8A,

Fig.4.8 A. Simple tabulate coral (1) bound by algal encrustation (2). Thin section no. 425.14, the lower part of member 3, the Rung Nok Formation.

B. Algal encrustation and simple tabulate coral from A.

C. Brecciated limestone with channel porosity (2) lined by radiaxial fibrous cement (3). Most of the breccia (1) is reworked algal encrustations. Thin section no. 400.8, the middle part of member 3, the Rung Nok Formation.

D. Laminar and low domical stromatoporoids (arrow) within biolithite at Ko Lae Tong. The upper part of member 3, the Rung Nok Formation.

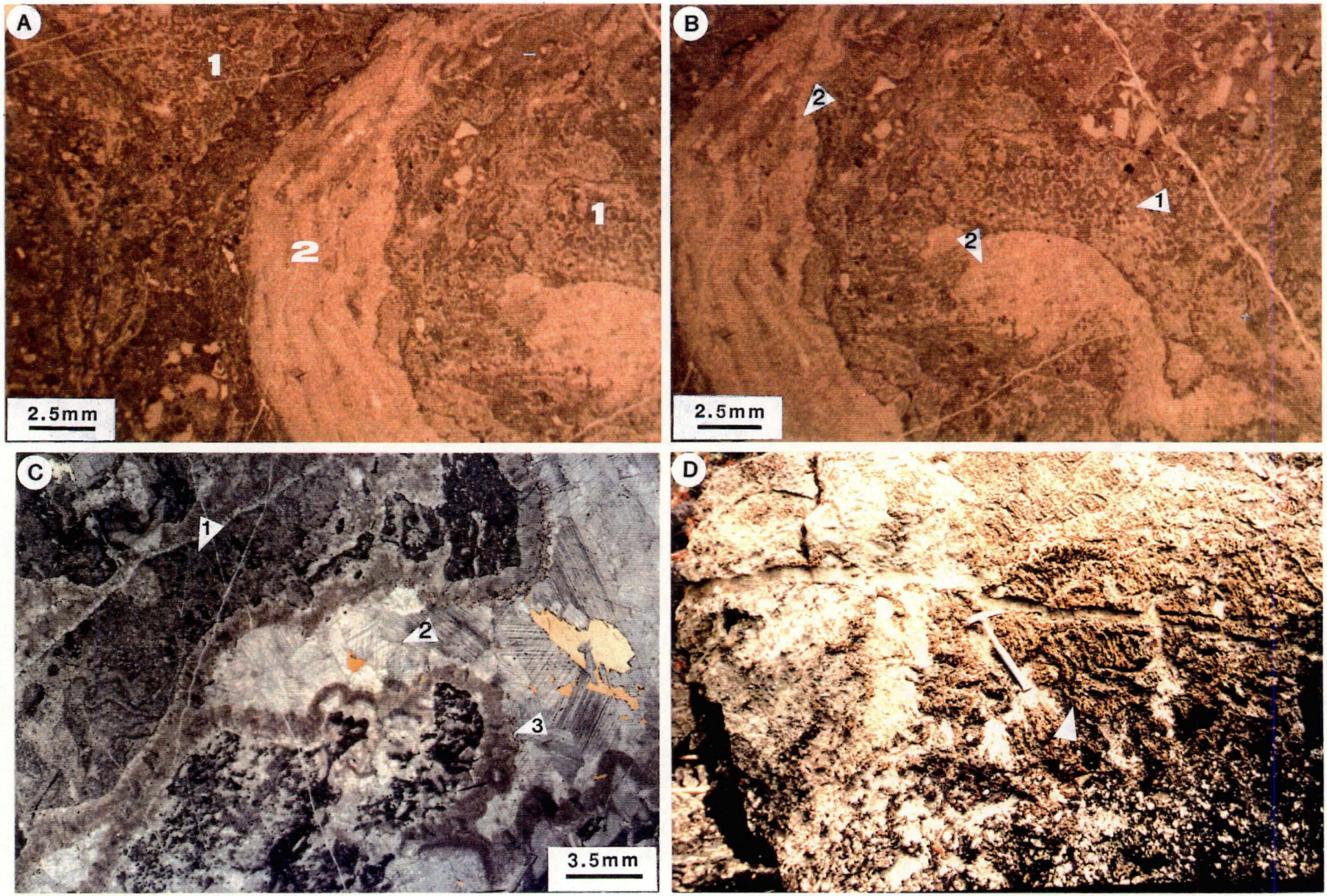
A
1
2
1
2.5mm
B
2
1
2
2.5mm
C
1
2
3
3.5mm
D

B). The alternating laminae of the stromatolites comprise faint irregular microspar and micrite layers. The sediments surrounding the stromatolites consist of predominantly coarse grained biosparites which contain bioclasts of crinoid ossicles and arm plates, globular bryozoans, trilobite debris, *Tetradium*, brachiopods with both valves together, occasional partially articulated brachiopods, and peloids (Banks and Burrett, pers. comm.). The boundary between the biolithites and their associated sediments is sharp. Cementation of the sediments between the frame-building organisms is more extensive than in the reefs themselves. The cementing material within the interparticle porosities of biomicrites is mostly cloudy, radial and radiaxial fibrous cement plus rare dolomite cement. Blocky cement is usually found infilling intraparticle porosities of frame-builders and megaskeletal remains (Fig. 4.7D). The primary porosity of these rocks increases upward where extensive cementation is interrupted by a micritic infilling layer (Fig. 4.7E).

The massive limestone in the middle part of the third member of the Rung Nok Formation is composed predominantly of limestone breccias (Fig. 4.7C) and minor poorly washed biosparites. The latter have abundant channel porosities infilled with cloudy radiaxial fibrous, (some) dolomite and blocky cement. The breccias comprise mostly angular to subrounded stromatolitic and sparse crinoidal biosparite intraclasts with a maximum size in thin section of 35 x 15 mm and up to 450 x 150 mm in outcrop. The pebbles are cemented by a limpid, stubby, bladed, cloudy radiaxial fibrous, and clear blocky cement within large interparticle porosities (Fig. 4.8C). The primary channel porosities (maximum size of 70 x 50 mm) are irregular and have commonly developed parallel to bedding. They cut through the rock and are concordant with the breccia boundaries over short distances. The cementing material is the same as above.

The upper part of the third member is a massive biolithite composed of laminar and low to high domical stromatoporoids (Fig. 4.8D) growing in place on an erosional surface of poorly washed biosparite. The latter rock type has an extensive array of conical sponges, nautiloids, gastropods, receptaculitids, and random burrows. The abundance of interbedded biomicrites as well as the degree of dolomitization increases upwards through this unit. Calcitic dolomite with relict stromatoporoids is the dominant rock type at the top of this member.

4.2.12 Microfacies XII — Dolosparite, Dolomicrite and Dolomite Breccia

Dolosparite is defined as a sparry dolomite rock containing more than 90% dolomite. Based on size analysis, there are four types of dolomite within the Thung Song Group in this area: 1) dolomicrite, 2) microdolomite (29-150 μm), 3)

Fig. 4.9 A. Dolomicrite (gray, 1) interbedded with lenticular limestone (red, 2) and very thin layers of gypsum pseudomorphs (white, 3). Stained thin section no. G, the Lae Tong Formation.

B. Equigranular, idiotopic-hypidiotopic microdolomites showing cloudy centers and clear rims (arrow). They are cross-cut by a dolomite veinlet.Thin section no. 498.1 B, the Malaka Formation.

C. Microdolomite layers (brown) intercalated with micrite layers (grayish green) Thin sectionno. 27.2 F, the Malaka Formation.

D. Microdolomite infilling burrows. Note the partial (1) and complete (2) replacement of mold-filling spar by microdolomite, and unreplaced micrite (dark brown) in between the burrows and molds.Thin section no. 399, the Pa Nan Formation.

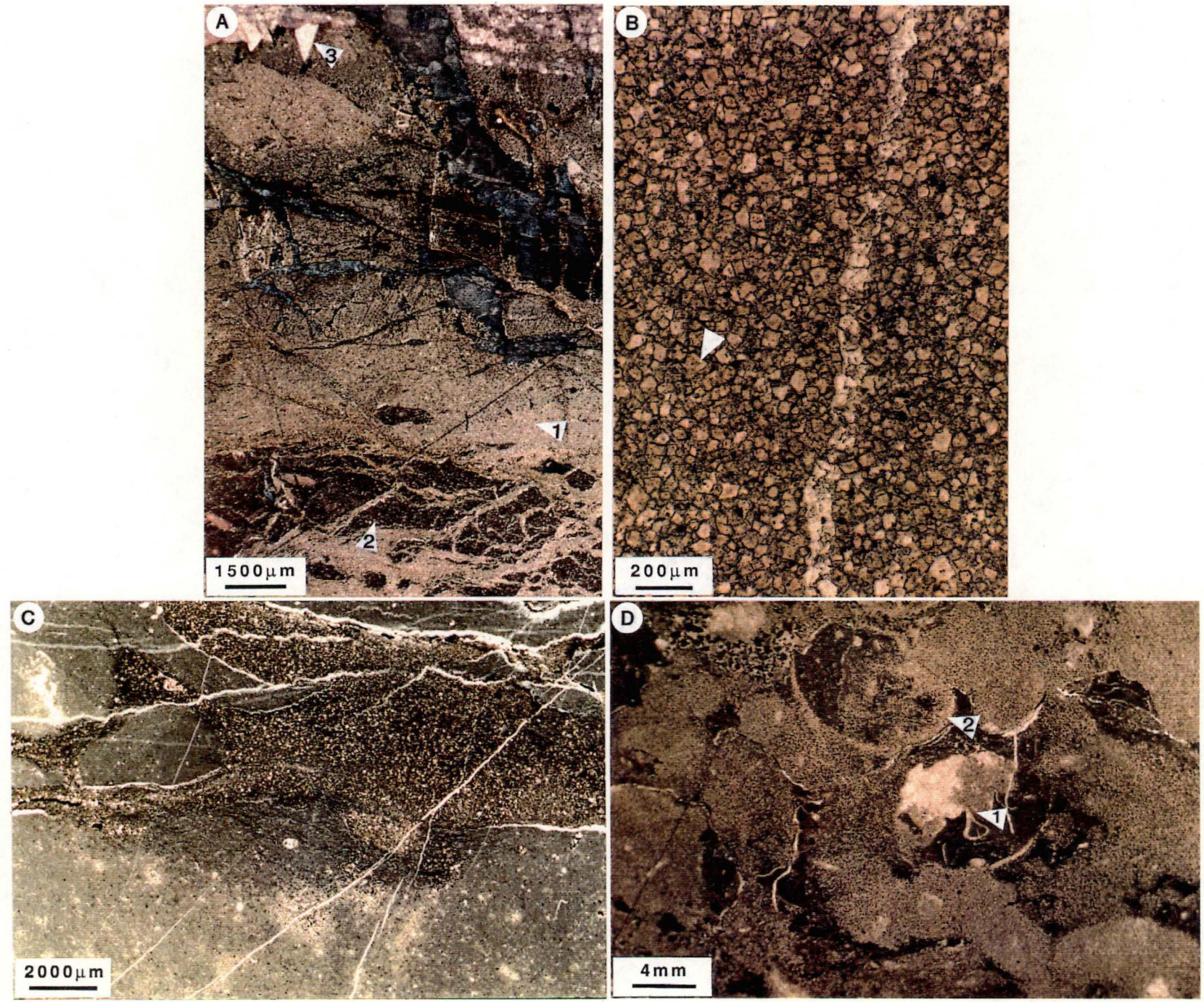
A
3
1
2
1500μm
B
200μm
C
2000μm
D
2
1
4mm

mesodolomite (147-400 μm) and 4) megadolomite (>400 μm). Dolomicrite is rare and has been found only at one locality within the upper member of the Lae Tong Formation at Ao Makham (Fig. 4.9A). At this location it is associated with a micro-tee pee structure and layers of calcite pseudomorphs after gypsum. The rock is 85-90% very fine microcrystalline dolomite (9-30 μm) and 5-10% clay minerals, interbedded with red micrite containing abundant pyrite nodules (7.5%).

Microdolomite is the most abundant dolomite type within the lower formation of the Thung Song Group. It occurs as interlaminations or interbeds within other rock types in the stromatolite facies of the Malaka Formation, La Nga Formation, and Pa Nan Formation; as ripple beds associated with the stratiform stromatolites and oosparite of the Malaka Formation; as a cross-lamination in the lower member of the Lae Tong Formation; and as burrow infill throughout the succession.

Most of the microdolomite in stromatolites and ripple beds are well defined rhombs, equigranular, idiotopic to hypidiotopic fabric, tightly to moderately interlocking crystals, with or without clay minerals in between rhombs (Fig. 4.9B, C). Organic matter is abundant and forms what appears to be a bituminous cap on the microdolomite layer at several outcrops. The majority of the microdolomite is brown and cloudy with some lightly coloured rims (Fig. 4.9B). The crystals with clear rims are usually coarser than the dark brown crystals. Microdolomite also replaces ooids within the oosparite microfacies (Fig. 4.7A, B, C).

The microdolomite found within burrows (Fig. 4.9D) is identical to that associated with the stromatolites, except that some display an increase in grain size plus the gradual development of zoned dolomite with iron staining towards the bottom of the burrows (Fig. 4.1A, 4.5C).

There are two types of dolomite within the fourth member of the Rung Nok Formation. The brown microdolomite (60-200 μm) is cloudy with some clear rim, equigranular, hypidiotopic to xenotopic fabric, tightly interlocking crystals without clay minerals and a low amount of carbonaceous matter. This dolomite has completely replaced the limestone at the top of the fourth member of the Rung Nok Formation. The ghosts of peloids, relict structures and dolomite breccia are also present (Fig.4.10A, C). In the middle part of the fourth member, microdolomite has partially replaced the cement and micrite of the poorly washed biosparite which has the same lithology as the third member. This lithotype is classified as calcitic dolomite. Secondly, in the lower part of the fourth member, the white mesodolomite (160-400 μm) has partly replaced all components of the poorly washed biosparite (Fig. 4.10B), except for the brown microdolomite. The white mesodolomite has a less equigranular, xenotopic fabric, and a partially poikilotopic fabric within the calcite spar.

Fig. 4.10 A. Brown, equigranular, micro- to mesodolomites with bryozoan relics (arrow). Thin section no. 400.3, the Rung Nok Formation.

B. Photomicrograph of a stained thin section showing white mesodolomite which has selectively replaced micrite in a poorly washed biosparite. Note the abundant algal chains (arrow) within the micrite relicts and/or intraclasts (C).Thin section no. 400.6, the Rung Nok Formation.

C. Dolomite breccia with ghosts of peloids (G) cemented and cut by blocky spar (B) in pores and veinlet. Thin section no. 400.6 B, the Rung Nok Formation.

D. Megadolomite at Ko Laen with saddle dolomite (S) growing in a pore. Note the cloudy centers and clear rims of both dolomites although the former one is more distinct. Thin section no. 13.1, the Rung Nok Formation.

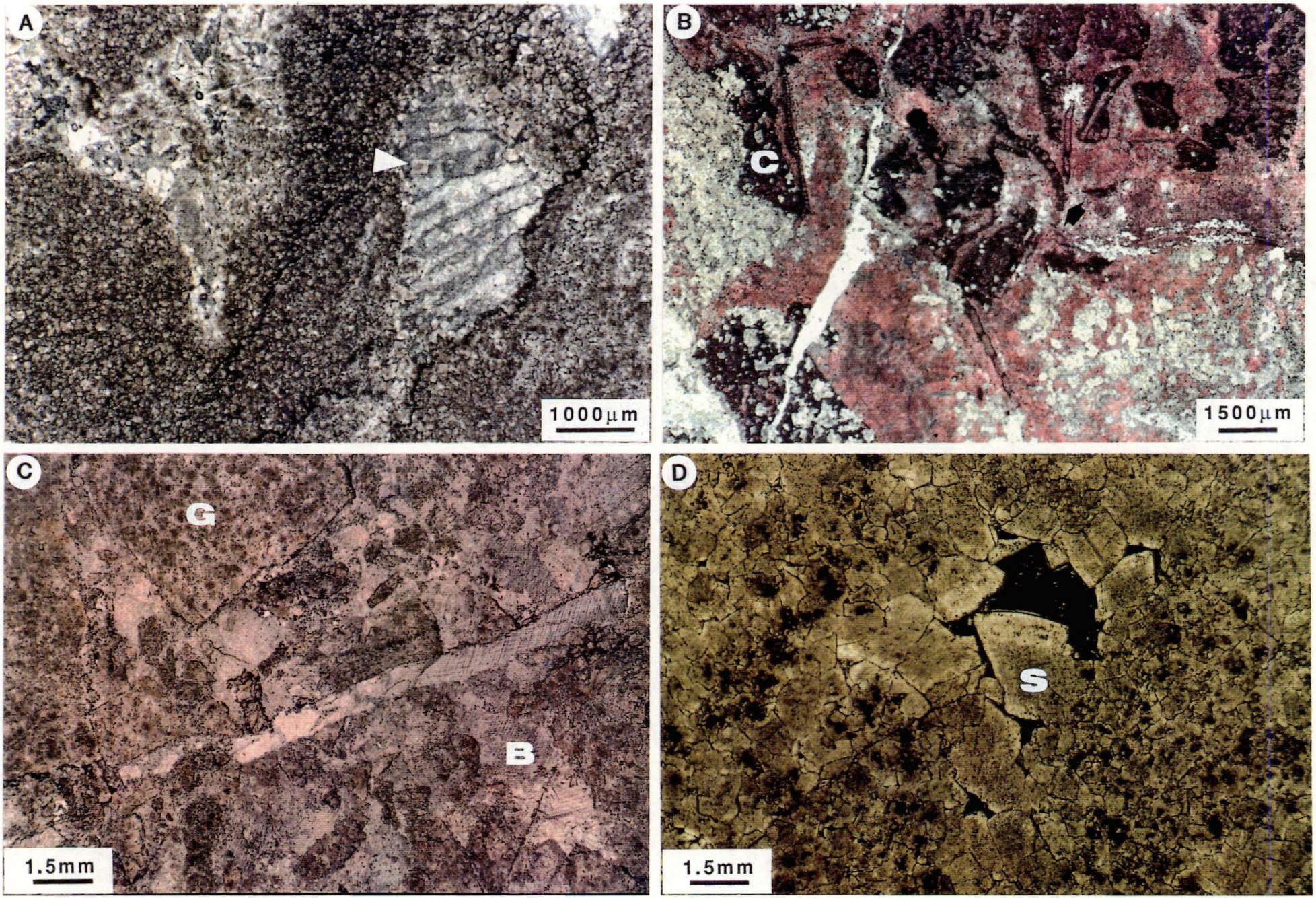
A
1000μm
B
C
1500μm
C
G
B
1.5mm
D
S
1.5mm

Dolomite breccias are composed of angular fragments of brown microdolomite cemented with large blocky spar. The proportion of breccia to cement is 50-60% and 40-50% respectively. Breccias are commonly rectangular with a maximum size of 59 x 110 mm (Fig. 4.10C).

Coarse-grained, pink megadolomite is interbedded with poorly washed biosparite within the second member of the Rung Nok Formation at Ko Lae Tong and Ko Laen. It has an equigranular, hypidiotopic to xenotopic fabric with sweeping extinction of saddle dolomite plus relict features of the biosparites. The carbonate rocks at eastern part of Ko Laen are completely dolomitized to saddle dolomites (Fig. 4.10D).

Chapter 5

DIAGENESIS

The present study of the diagenesis of the Ordovician Thung Song Group carbonates, is based mainly on conventional and cathodoluminescence micropetrography as well as on the isotope geochemistry of the carbonate components. This chapter is subdivided into cementation, calcite pseudomorphs after evaporites, compaction, and dolomitization.

5.1 Cementation

There are three types of cements in the Thung Song carbonates: mainly sparry calcite (Fig. 5.1A), rare hematite (Fig. 5.4B) and dolomite (Fig. 5.4A, 5.4C). The dolomite cement will be discussed later under dolomitization. The sparry calcite cement is the main pore filling type in interparticle, intraparticle, moldic and fenestral porosities. Three major types of the sparry calcite cementation are recognized: marine, meteoric and burial cementation.

5.1.1 Marine Cementation

The main cementation features formed under marine conditions in the Thung Song Group are as follows: 1) isopachous radial bladed and fibrous cement, 2) radiaxial fibrous cement, 3) epitaxial or syntaxial cement rims, and 4) blocky cement. These cements are considered to be marine because they are first generation cements (Davies, 1977; Grover and Read, 1983) which predate or alternate with internal sediments and micrite infilling. Furthermore, they have similar fabrics to Recent marine cement types and their isotopic composition falls within the field of the Ordovician marine cements from Nevada (Ross *et al.*, 1975; Rao and Wang, 1990).

Radial Bladed and Fibrous Cement: Isopachous radial bladed and fibrous cements (49-250 μm) are common as interparticle spars within oosparites from the cross stratified units of the Malaka Formation and the La Nga Formation (Fig. 5.1A). The crystals are non-ferroan calcite, elongate normal to the substrate with pyramidal or rhombic terminations. They form radial and isopachous fringes which usually infill interparticle porosities but may be followed by blocky spar within the larger pores. The bladed and fibrous crystals with rhombic terminations are commonly interpreted by many authors as being former Mg-calcites which have precipitated in the sea (James

Fig. 5.1 A. Photomicrograph of a stained oosparite with extensive radial isopachous bladed to fibrous cement. Note the pyramidal termination (arrow) of the bladed cement and the selective replacement of oolites by microdolomite (D). Thin section no. 396,the Malaka Formation.

B. Micritic crinoid ossicle and other allochems fringed by well developed fibrous cement (F). Zoned dolomite cement rhombs (black arrow) within crinoid cores are postdated by blocky spar. Bored brachiopod fragment is partly rimmed by micrite (1). Syntaxial rims predate the isopachous cement but postdate the micritic rims (2). Radiaxial fibrous cement (3). Thin section no. 400.10, the Rung Nok Formation.

C. Radiaxial fibrous cement (F) within the space chamber of a nautiloid increases in crystal size from the margin (1) toward the center. A nautiloid is encrusted by stromatolites (2). Thin section no. 425.11, the Rung Nok Formation.

D. Turbid radiaxial fibrous cement (F) infills an interparticle pore space (1) and occurs as isopachous lining channel porosity (2) , followed by brown dolomite cement (3) and blocky cement (4). This rock is representative of reef breccias with a large angular, reef fragments (B). Thin section no. 400.8, the Rung Nok Formation.

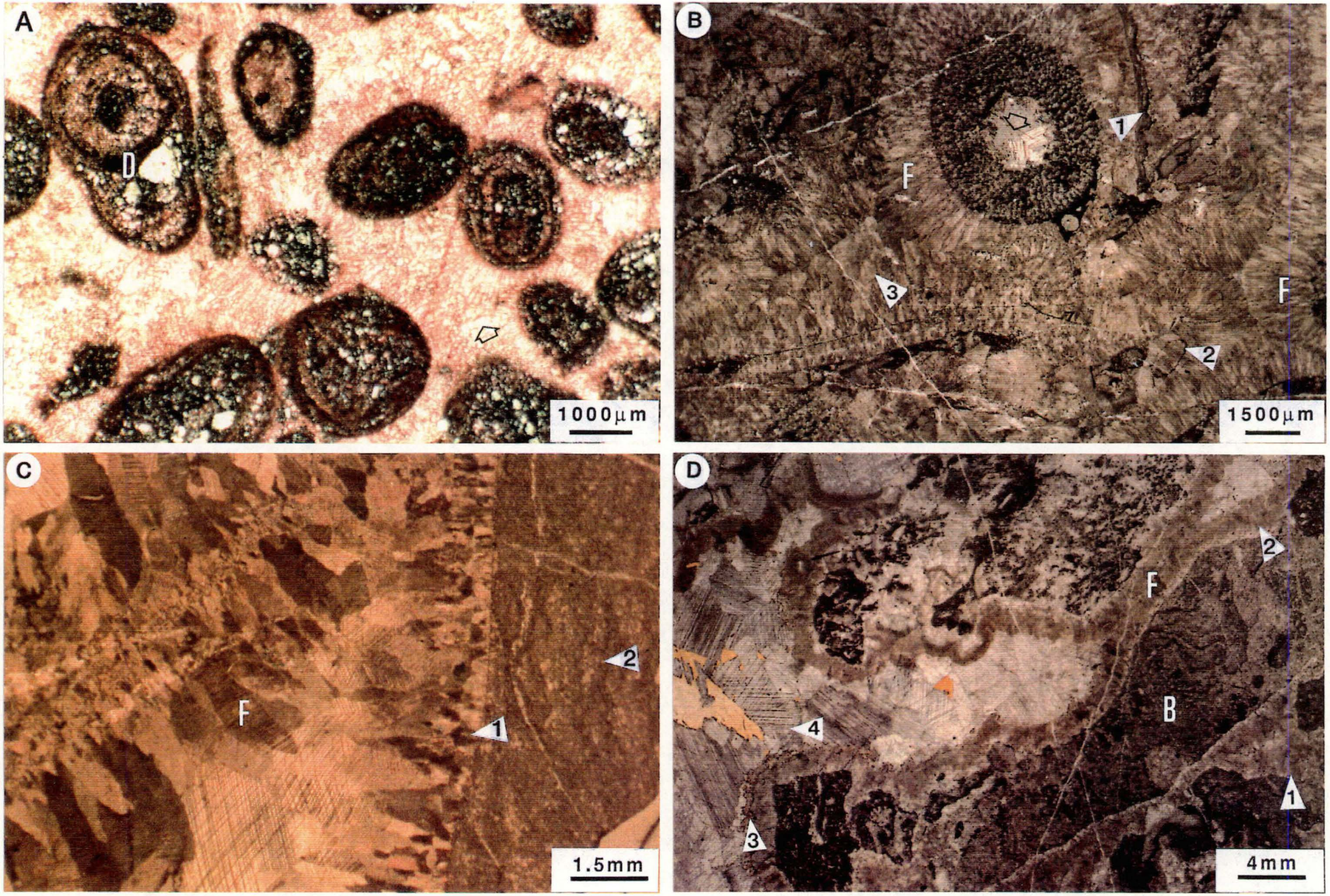
A
D
1000μm
B
F
1
2
3
F
1500μm
C
F
1
2
1.5mm
D
F
2
B
4
1
3
4mm

et al., 1976; James and Ginsburg, 1979; Scoffin, 1987; Wang and Rao, 1990). Under cathodoluminescence, radial bladed to fibrous calcite cements show brown dull-to non-luminescence (Fig. 5.6B) indicating the presence of oxidizing conditions within the formational pore fluid (Wang and Rao, 1990).

Well defined isopachous radial fibrous cements (2-4.5 mm) are found only within the moderately to poorly washed biosparites from the lower part of the third member of the Rung Nok Formation. Their precipitation predates micritic infilling but postdates micritized envelopes and syntaxial cement rims (Fig. 5.1B). Fibrous feature, isopachous geometry, polygonal boundaries between cement fringes, and the wide distribution of this cement suggest that deposition occurred in a very early marine diagenetic environment rather than a meteoric-phreatic zone (Longman, 1980). Isopachous fibrous cements are usually associated with radiaxial fibrous cements.

Radiaxial Fibrous Cements: Radiaxial fibrous cements (0.5-3 mm) are the dominant marine cement within the third member of the Rung Nok Formation. They are absent from the other lower formations of the Thung Song Group. These cements commonly fill interparticle, intraparticle and channel porosities of poorly washed biosparites and biolithites (Fig. 5.1C, D). Cement crystals are turbid and increase in size from the pore margin to the centre of the pore (Fig. 5.1C). Radiaxial fibrous cement are elongate, mostly normal to substrate and have rounded tips, curved cleavage, and wavy extinction (Fig. 5.1C). They radially dispose around limestone breccia and constitute isopachous fringes. These cements also occur as isopachous crusts within intraparticle porosities and channel porosities (Fig. 5.1C). This cement is characterized by converging optic axes and diverging suberystals away from the substrate.

Turbidity in radiaxial fibrous cement may be caused by dolomite microcrystals (Lohmann and Meyers, 1977), organic material and other solid impurities (Kendal and Tucker, 1973) or fluid-filled microcavities (Kendall, 1985; Saller, 1986). Based on the inclusion patterns within crystals, the radiaxial fibrous cements may be composed of low-magnesian calcite in inclusion-poor zones and high-magnesian calcite in inclusion-rich zones (Kendall, 1985). However, no inclusion zonation or inclusion-poor zones have been observed within the radiaxial fibrous cement of the Thung Song Group. It may therefore be concluded that most were originally composed of Mg-calcite.

Under cathodoluminescence, radiaxial fibrous cements display a zonation from non-luminescence to bright-luminescence within intergranular pore, and dark to light brown-dull luminescence in channel porosities (Fig. 5.2A, B). The non-to dull-luminescence of this cement is considered in this study as being indicative of a marine

Fig.5.2 A. Photomicrograph showing the sequence of cementation in a limestone breccia: 1) micritic rim, 2) syntaxial rim growing at the same time with interparticle radiaxial fibrous (2.1) and cavity-filled prismatic cement (2.2), 3) cavity-filled radiaxial cement predates the second generation syntaxial rim (3.1), 4) subsequent zoned dolomite cement, 5) and finally 6) blocky cement. Thin section no. 400.8, the Rung Nok Formation.

B. Photomicrograph under cathodoluminescence of A.

C. Photomicrograph of a poorly washed biosparite showing geopetal fabric (1), boring surface and micritic rims of echinoderms (2), and syntaxial rims (3). Micrite infills an interparticle pore after the rim cement (4). Thin section no. 23.8, the Rung Nok Formation.

D. Photomicrograph under cathodoluminescence of C., from a different angle, showing many generations of syntaxial rims and dolomite cement: 1) crinoid ossicles, 2) primary non-rim cement, 3) secondary bright and dull rim cement, 4) dolomite cement.

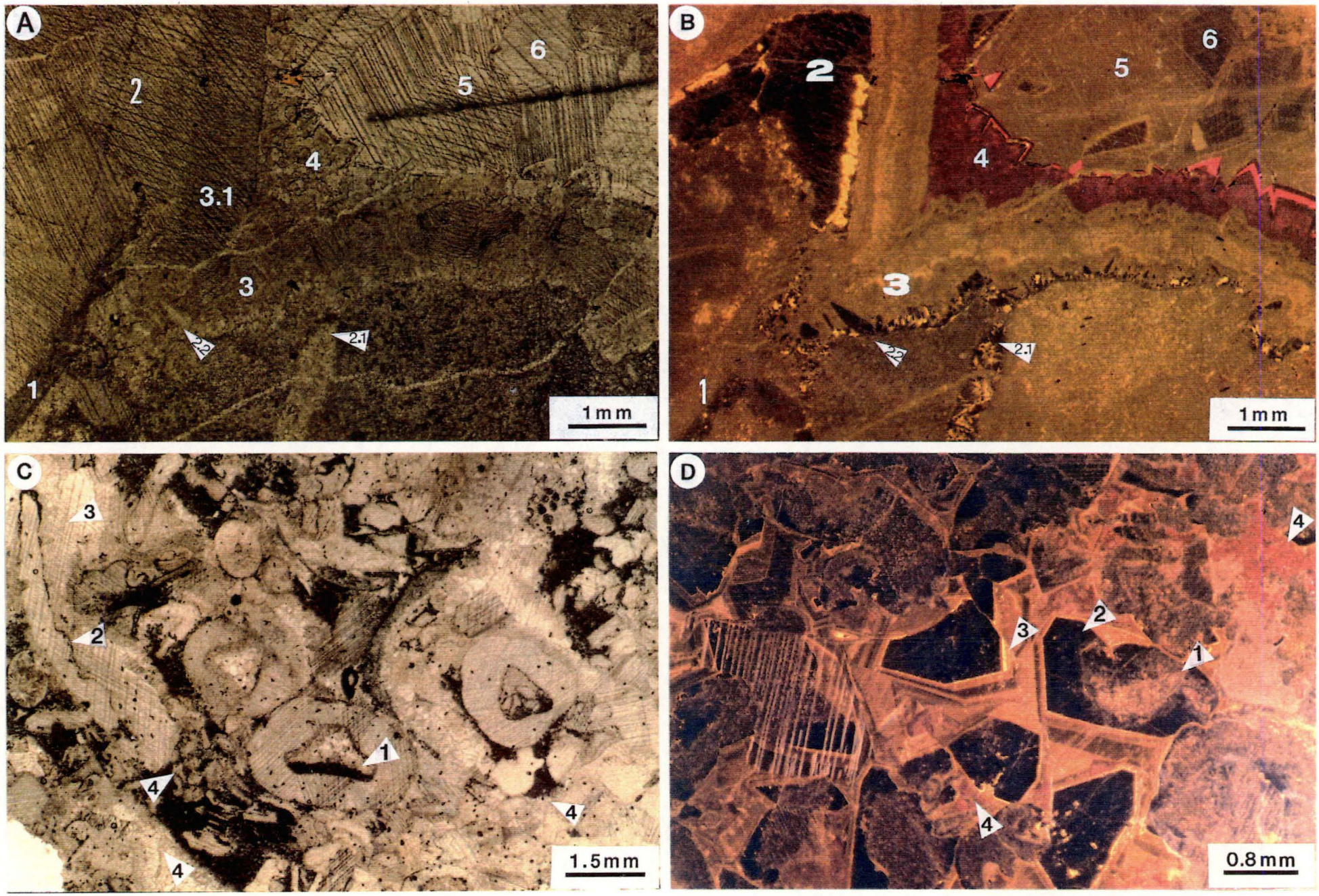
A
2
5
6
4
3.1
3
2.2
2.1
1
1mm
B
2
6
5
4
3
2.2
2.1
1
1mm
C
3
2
1
4
4
4
1.5mm
D
4
3
2
1
4
0.8mm

origin (Wang and Rao, 1989) and/or precipitation close to the depositional interface. Kendal (1985) and Wallace (1987) also proposed a marine origin for similar radiaxial fibrous cement of the Devonian reef limestone from the Canning Basin, Western Australia.

Epitaxial Cement: Epitaxial or syntaxial cement rims are very extensive and constitute more than 90% of the cement within the poorly to moderately washed biosparites from the first and second members of the Rung Nok Formation (Fig. 5.2C) . Sparry calcite overgrowths (0.1-1.5 mm) in lattice continuity with their host echinoderm fragments, extend outwards into the interparticle porosities. These overgrowths postdate the micrite envelopes and internal sediments within geopetal structures (Fig. 5.2C) and partly predate the micrite which infills the pore spaces. They are probably evidence of a marine origin (James and Choquette, 1983), and formation contemporaneous with carbonate build-up.

The single crystal nature of syntaxial rims (Fig. 5.2C), replacing the formerly Mg-calcite crinoidal skeletons reflects "host control" cementation (Glover and Pray, 1971). Therefore, the syntaxial rims must have consisted of an early Mg-calcite cement. James and Choquette (1983) also concluded that syntaxial overgrowths of Mg-calcite on echinoderm particles were common phenomena in the shallow marine environment of ancient rocks. In contrast, Purdy (personal communication) has observed that there is no syntaxial overgrowth on echinoderm fragments in the shallow, tropical Recent marine environments with which he is familiar.

However, some syntaxial rims around crinoids show an early non-ferroan stage and a late weakly ferroan stage within stained thin sections (Fig. 5.12A). Under cathodoluminescence, the early non-ferroan stage rim cements are non-luminescent (Fig. 5.2B, D, 5.12B) but the late weakly ferroan cements contain as many as four subzones of bright-to dull-luminescence (Fig. 5.2D, 5.12B). The non-luminescence of the first stage indicates precipitation of rim cements under oxidizing marine conditions. However, the compositional cement zones of the late stage favour the reducing environment of a late diagenetic stage after burial (Meyers, 1974, Grover and Read, 1983) with fluctuation of pore fluids.

Blocky Cement: Blocky cements (100-600 μm) are common as the products of both first and second stages of cementation within fenestral and shelter porosities of columnar stromatolites from the Pa Nan Formation and Pa Kae Formation (Fig. 5.3A, B, C; 5.7A). Cement crystals are clear and increase in size toward the centre of the pore spaces. As they formed contemporaneously with/or after infilling of internal

Fig. 5.3 A. Blocky spar (B) with internal sediments (I) in moldic and shelter porosities of the Pa Kae Formation. Calcite crystals increase in size from equant spar (arrow) at the pore margins to blocky spar in the centre of pore. Thin section no. 359.1/1, the Pa Kae Formation.

B. Cathodoluminescence photomicrigraph of A. showing non-luminescence of primary equant and blocky cement in intraskeleton, moldic and shelter porosities (white arrow) and showing zonation from non to bright of subsequent blocky spar at the centre of sheltered porosity.

C. Blocky cements infilling fenestral porosities of Pa Kae stromatolites postdate crystal silt (S) infilling. Thin section no. 359.1, the Pa Kae Formation.

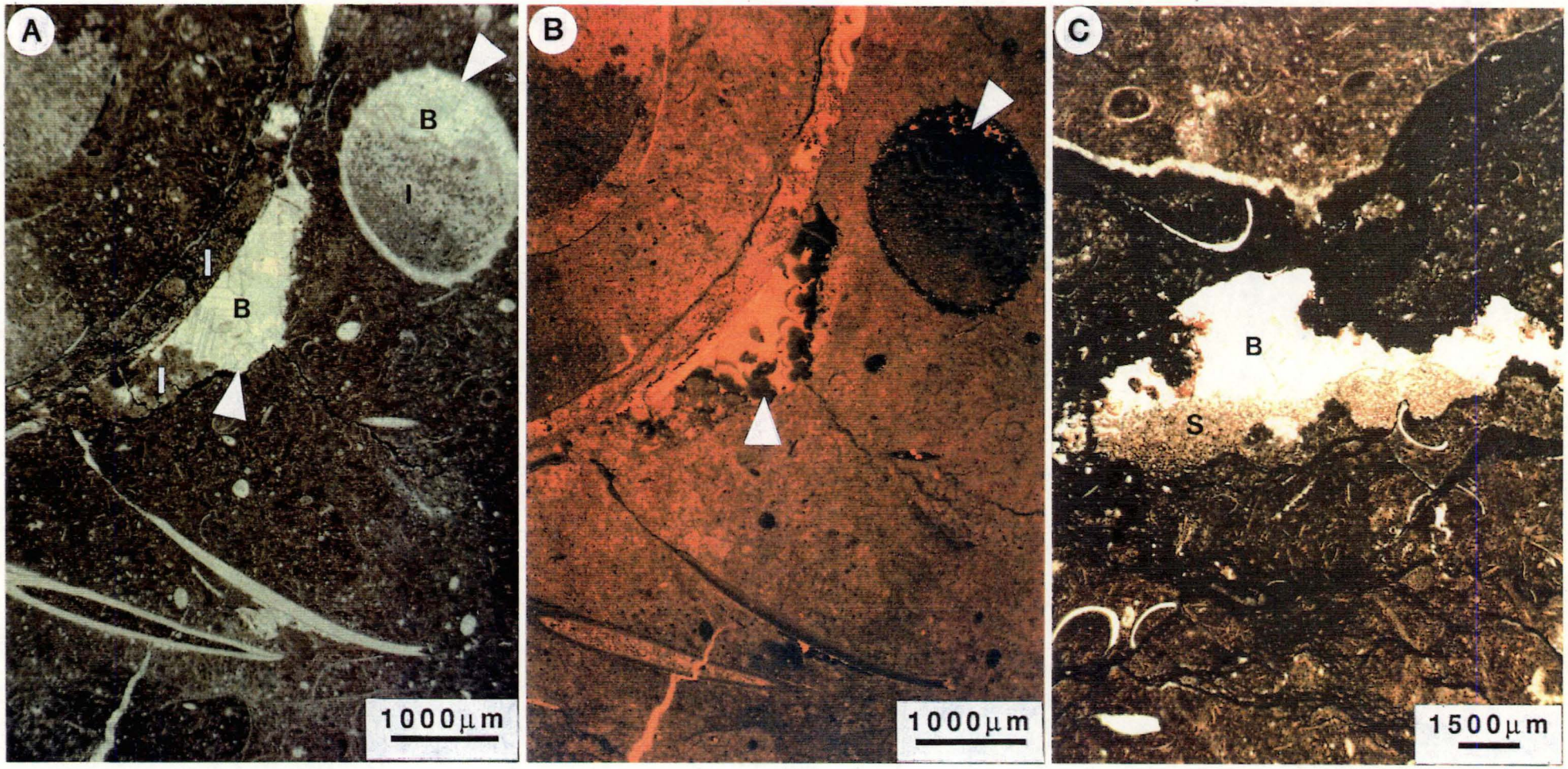
A
B
I
I
B
I
1000μm
B
1000μm
C
B
S
1500μm

sediments, and after equant spar, this indicates an early marine to burial origin for these cements.

So far, no petrographic evidence of the former mineralogy of these blocky cements has been observed within the stromatolitic limestones. By comparison, Recent carbonate sediments, display a close relationship between the mineralogy and the environment of deposition (Friedman, 1965). Under deep sea conditions, low-magnesian calcite is available whereas high-magnesian calcite is dominant in a shallow marine environment (Friedman, 1965; Schlager and James, 1978). Thus, it is possible that blocky calcite cements in shallow water stromatolites of the Pa Nan Formation were originally composed of high-magnesian calcite and those of the Pa Kae Formations' deeper water stromatolites were originally low-magnesian calcite.

Under the cathodoluminescope, most of the cements within small pores, including first equant and blocky spars, are non-luminescent. Distinctive cement growth zones are restricted to large shelter pores (Fig. 5.3B). These zones, from oldest to youngest, display non-luminescence, bright-luminescence with dull subzones, bright-luminescence, and finally dull-luminescence at the centre of the pore spaces. This sequence of cement zonation is largely related to the increasingly reducing conditions of pore fluids from the oxidation of non-luminescent cements in a marine environment to the reduction of dull-luminescent and normal bright luminescent cements after burial (Meyers, 1974; Grover and Read, 1983).

Stable Isotopes of Marine Cement: The stable isotope values of the cements, thought to be marine in origin, in the limestones analysed in this study range from -3.9 to -9.5‰ PDB for $\delta^{18}O$ and 3.3 to -0.4‰ PDB for $\delta^{13}C$. There is a close relationship between this wide range of stable isotope signatures and the environments of deposition. The deeper water marine cements of the Pa Kae Formation have $\delta^{18}O$ values ranging from -3.9 to -7.2‰ PDB and $\delta^{13}C$ values ranging from 3.3 to 1.9‰ PDB. The shallow water marine cements of the lower formation have $\delta^{18}O$ values ranging from -7.2 to -9.5‰ PDB and $\delta^{13}C$ values ranging from 0.1 to -0.4‰ PDB.

The isotopic signature of the deeper water marine cements is much heavier than for shallow water deposits suggesting relatively low temperatures of formation. This provides evidence of deposition in a deeper water environment for the red stromatolites of the Pa Kae Formation which appear to have been deposited in deeper waters than the rest of the Thung Song Group. The isotopic values of the shallow water carbonates fall within the range of marine cements from the Ordovician limestones of Nevada (Ross *et al.*, 1975) but the isotopic values are lighter than those of the Ordovician, Gordon Limestone of Tasmania (Rao, 1990; Rao and Wang, 1990).

5.1.2 Marine Vadose or Meteoric Cementation

Two common categories of meteoric calcite cement are 1) bladed, and 2) equant cements. Pendant cements are very rare. These cements are widely distributed in the peritidal limestones of the lower formation including the Malaka Formation, La Nga Formation and Pa Nan Formation.

Stubby Bladed Cement: The short stubbly bladed calcite cements are the primary cements of the peritidal limestones. They are very small (<40 μm) and fringe allochemical grains in most of the rocks (Fig. 5.4A). They nucleate on the surface of grains and grow outward to produce bladed isopachous calcite rinds. The length to width ratio of crystals is small, ranging from 1:1 to 3:1 with obtuse pyramid or flat pinacoid terminations. They are usually merged or associated with equant spars in small pore spaces. Pyramidal terminations indicate former Mg-calcites for these cements.

The mode of occurrence of stubby bladed cements is still not clear. They are one of two common varieties of Mg-calcite cement found in shallow marine Belize reef-limestone (James *et al.*, 1976; James and Ginsburg, 1979). Because of their association with meniscus equant cements, they are interpreted as having cemented Mg-calcite in meteoric or marine phreatic zones in a tidal flat prior to the precipitation of later meniscus cements during short-term sea-level fluctuations or regressions in the Lower Ordovician. However, some of them have well developed isopachous rims and could have been transported from subtidal areas to these tidal flats by wave action or storms. Land (1971) stated that "isopachous" morphology is also a common feature of beach rock cement.

Equant Cement: The second stage of calcite cementation involves the equant type which ranges in size from 12-150 μm. Equant cement is more common than the short stubby type and it usually occurs as *meniscus cement* between grain contacts and the corners of primary porosities (Fig. 5.4A, C). The equant spar increases in crystal size from the pore margin towards the centre of the pore and produces an interlocking mosaic (Fig. 5.4A). It also occludes fenestral fabrics within stromatolites (Fig. 5.5A) , some burrows, and moldic porosities. The solution enhanced moldic porosities, meniscus equant cements, and the coarsening of calcite crystals toward the pore centres are distinctive characteristics of early cementation in a fresh water phreatic environment (Loucks, 1977; Longman, 1980; Scoffin, 1987). The existence of fenestrae and well preserved peloids along stromatolite laminae also indicates early cementation of these rocks on tidal flat, especially in supratidal zone (Shinn, 1983). The original

Fig. 5.4 A. Meteoric calcite cement in intrasparite with peloids. The first-stage cement is small stubby bladed calcite (1) and the second cement is equant calcite occurring as menicus (2) and coarsening toward the pore centre (3). Blocky cement (4.1) and dolomite cement (4.2) are the last stages of cementation. Thin section no. 402 D, the upper La Nga member.

B. Hematite cement (black, H) with gypsum (1) and anhydrite (2) pseudomorphs covering the erosional surface (3). Thin section no. 5 B, the Malaka Formation.

C. Pelsparite with equant menicus spar (E), and blocky spar (B) within a large pore. Black minerals are pyrites (arrow). Thin section no. 402A, the upper La Nga member.

D. Luminescent light photograph of C. clearly reveals the meniscus habit (1) of the dull first equant spar, followed by the second bright blocky (2) and bright calcite pseudomorphs after gypsum (3) and subsequent very dull blocky spar (4) in the middle of a pore. Note the rounding of pore spaces left by meniscus cements, and the slightly bright and brown dull-luminescent very small stubby bladed cement (arrow).

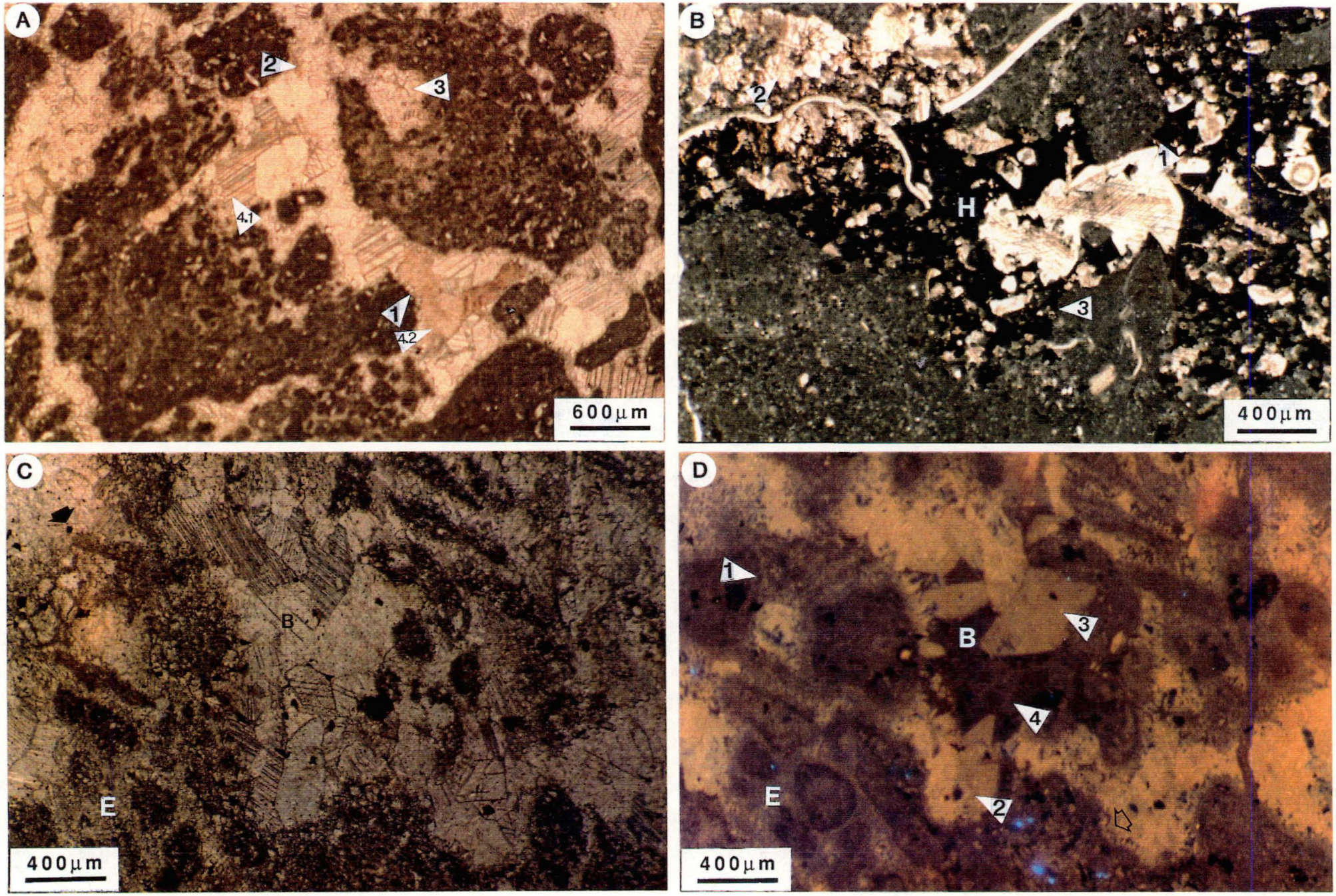
A
2
3
4.1
1
4.2
600μm
B
2
1
H
3
400μm
C
B
E
400μm
D
1
B
3
4
E
2
400μm

mineralogy of this equant cement, whose crystal size increases away from the substrate, was low-magnesian calcite (Land, 1971; Wilkinson and Janecke, 1982; Weiss and Wilkinson, 1988).

Using cathodoluminescence petrography, the stubby bladed and equant spars as well as the first blocky cement within a large moldic porosity (Fig. 5.5C, D) are observed to have dark-brown dull-luminescence (Fig. 5.4C, D). Some workers note that dull cement forms from reducing pore water with increasing burial (Grover and Read, 1983). On the other-hand, Wang and Rao (1990) demonstrated that the dull luminescence of the early equant to blocky cement of the Tasmanian Gordon Limestone is characteristic of an oxidizing meteoric environment in the phreatic zone.

Although most of the small intraparticle, fenestral and moldic porosities of the Malaka Formation, La Nga Formation and the Pa Nan Formation are filled with dull meteoric equant cement, there are some equant to blocky spars present in larger moldic porosities. These spars display cement zones ranging from very dull to non-luminescence at the pore margins to dull with zone and bright-luminescence at the centre of the pores (Fig. 5.5C, D). This may indicate either: 1) a change in composition of the formational water during early cementation, from oxidizing meteoric water to more reducing pore fluid, due to the decomposition of organic matter, with a high level of Mn shortly after burial (Wang and Rao, 1990), or 2) changes in fluid chemistry in response to sea-level fluctuation or rainfall (Longman, 1980; Wang and Rao, 1990). This may have been associated with the decomposition of organic matter on the tidal flats resulting in reducing conditions.

Pendant Cement: Pendant cements in the vadose zone are rarely observed and difficult to recognize under the conventional microscope as they are often overlapped by other type of sparry calcite cements. However, pendant cements, an excellent indicator of vadose meteoric water precipitation (Longman, 1980; James and Choquette, 1984), succeed fibrous, bladed, and stubby bladed marine cements (Fig. 5.6) with which they have erosional contacts (Fig. 5.6C, D) in large shelter porosities under bioclasts and micritic intraclasts of the Malaka Formation. This can be observed under either the conventional microscope or the cathodoluminescope. Using the latter, brownish-orange dull cement followed by subzones of dull and very dull cement are visible as pendant crystals growing downward from the roof of a shelter porosity (Fig. 5.6). The remaining pore space is filled with brown ,very dull-luminescent calcite cement and bright dolomite cement after burial. Some pendant cement crystals have been partly dissolved (Fig. 5.6A, B).

Under vadose conditions pendant crystals normally formed in peritidal Quaternary carbonates (Logan, 1974). They have been reported from peritidal Middle

Fig.5.5 A. Stromatolites consisting mainly of pelmicrosparite with equant spars within small laminoid fenestrae. Equant calcite crystals (1) coarsening toward a pore center of the larger fenestrae. Note the gypsum pseudomorph (2) and brown curved crystals of dolomite cement (D). Stained thin section no. 402 C, the upper La Nga member.

B. Pelbiosparite from the La Nga Formation showing abundant vadose silt (arrow) within interparticle porosities and blocky spar (B) within a possible trilobite mold and shelter porosity. Thin section no. 403.4 B

C. Blocky cement in moldic porosity showing the coarsening calcite crystals toward the center of the pore (plane light). Thin section no. TB, the Malaka Formation.

D. Cathodoluminescence of C. showing the cement zones from non to very dark brown (1) to dull light brown with bright subzones (2) and bright orange (3) luminescence in the middle of the mold.

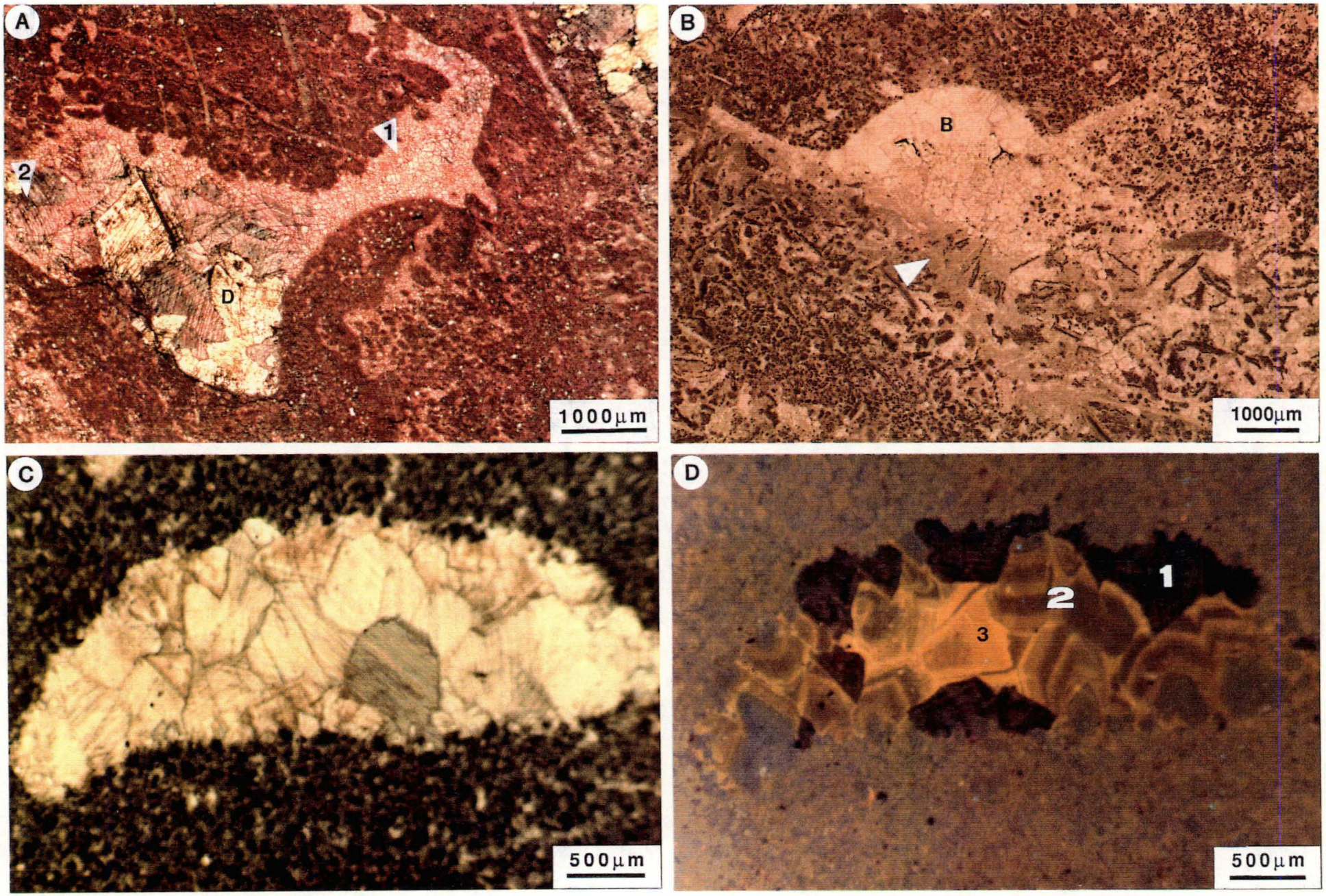
A
1
2
D
1000μm
B
B
1000μm
C
500μm
D
1
2
3
500μm

Fig. 5.6 A. Biopelsparite from the Malaka Formation showing an excellent pendant cement (P) and meniscus cement (M) under mollusc shells, postdating small stubby bladed cement (arrow) but predating blue stained equant cement. Stained thin section no. 421 B

B. Luminescent light photograph of A. showing dull luminescent stubby bladed cement (1), bright and dull subzone luminescent pendant cement (2) and meniscus cement (3), and very dull equant to blocky cement (4). Note the incomplete luminescent zonation nature of the pendant cement due to dissolution of calcite crystals within the vadose zone.Thin section no. 421 B

C. Pelintrasparite with radial isopachous fibrous fringes (1) around allochems and subsequent blocky calcite (2), iron-stained dolomite cement (3) in a slightly solution enlarged shelter porosity. Note the calcite pseudomorphs after gypsum (4) and the rafts of calcareous tubes in peloids (arrow). Thin section no. 396 C, the Malaka Formation.

D. Luminescent light photograph of A. Shelter porosity was filled by coarse bladed cement with brown dull orange to subzone dull luminescence (1). Note that cement zone occur as pendant crystals hanging from the shelter roof and the erosional surface on the base of the pore (2).

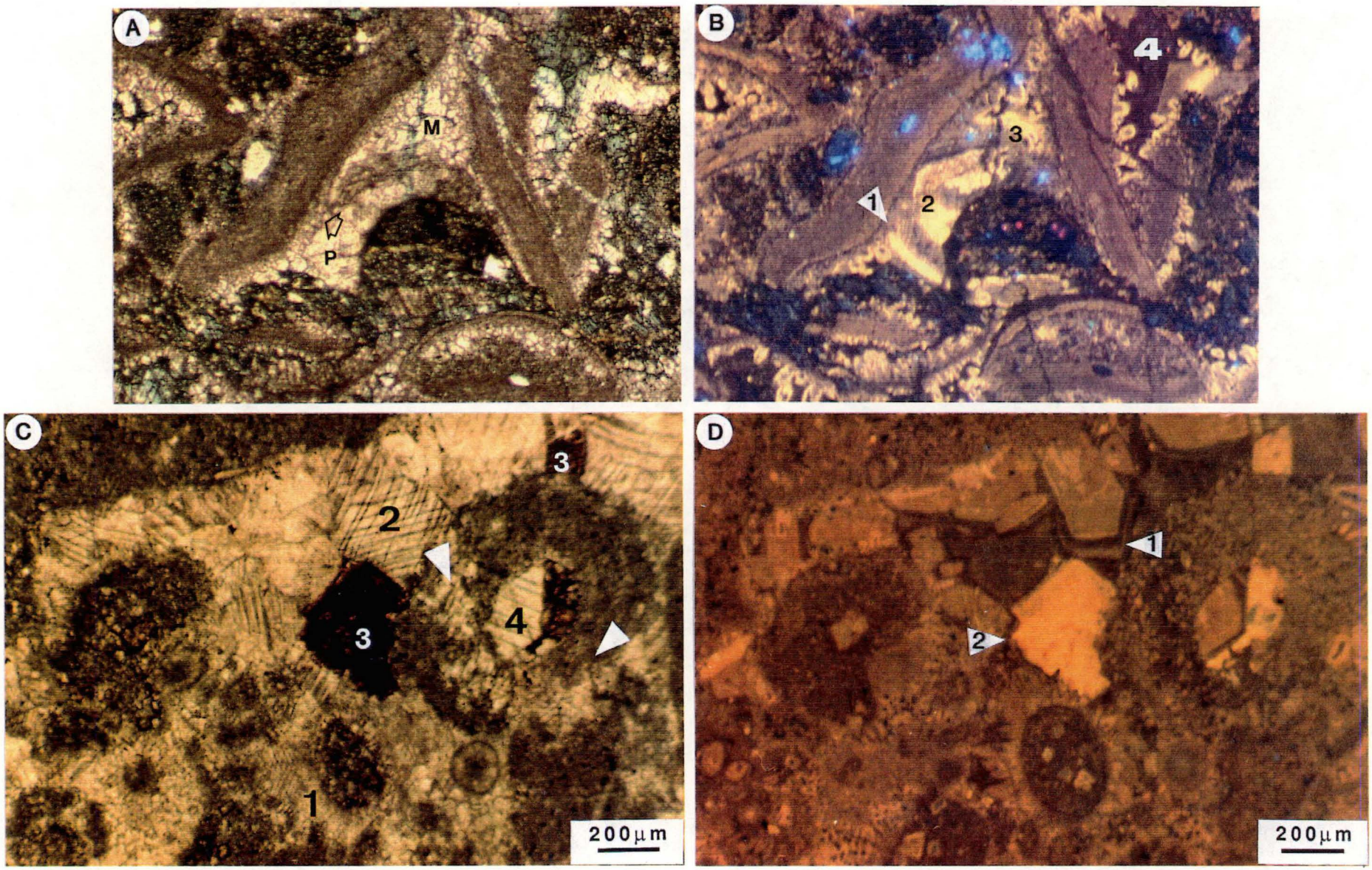
A
M
P
B
4
3
1
2
C
3
2
3
4
1
200μm
D
1
2
200μm

Ordovician carbonates in Virginia (Grover and Read, 1983) and in Tasmania (Rao and Wang, 1990). Within the Thung Song Group vadose cements are much less abundant than the other cement types. This is due to the fact that vadose deposits are very susceptible to erosion on tidal flats (Land, 1977). The original mineralogy of these cements was also low-magnesian calcite.

Crystal Silt: Crystal silt (20-49 μm) floors and fills many interparticle and moldic porosities of pelbiosparite from the upper part of the shallowing-upward sequence of the La Nga Formation (Fig. 5.5B). It results from internal erosion of host sediments and cement crystals under vadose conditions (Dunham, 1969).

In short, meteoric cementation of the lower formation of the Thung Song Group occurred mainly within the active meteoric-phreatic zone rather than in a vadose environment.

Stable Isotopes of Meteoric Cement: It is impossible to separate primary and secondary meteoric cements for isotope studies because of their very small interparticle pore spaces and very fine grain sizes. Therefore, only equant spars within large fenestral porosities have been used for whole-rock isotopic analyses.

The $\delta^{18}O$ and $\delta^{13}C$ values of these spars range from -11.2 to -11.8‰ PDB and +0.7 to +0.2‰ PDB respectively. The fact that these isotope values are lighter than those of marine calcite cements is due to isotopic fractionation within a meteoric water system with some influence from soil CO_2. The $\delta^{18}O$ values of meteoric calcites in the Thung Song Group are about 2‰ PDB less than those of marine cements. The $\delta^{13}C$ values of the meteoric calcites are heavier than normal marine cements but lighter than the $\delta^{13}C$ values of deeper water cements. Isotopic differences between meteoric and marine carbonates are largely due to differences in the original isotopic composition of formational waters plus isotopic alteration or post-depositional exchange with light water of marine sediments during early meteoric diagenesis (Anderson and Arthur, 1983).

5.1.3 Burial Cementation

Burial cements succeeding meteoric cements (Fig. 5.4A), marine cements (Fig. 5.1C, D; 5.2; 5.3; 5.7), and calcite pseudomorphs after gypsum (Fig. 5.4C, D) are common within the Thung Song Group. They form up to 30% of all interparticle cements and fill 80-100% of the secondary porosities such as moldic (Fig. 5.5C), channel (Fig. 5.1D), and fracture (veins) porosities (Fig. 5.7C).

The burial cements comprise two basic crystal types: clear blocky crystals (100-800 μm), and syntaxial rim cements (Fig. 45A, 46A,B, 43), which partially or

Fig. 5.7 A. Blocky cements (B) fill fenestral porosities and posdate internal sediment infilling (S). The internal sediments are micrites and peloids. Thin section no. 15, the Pa Nan Formation.

B. Photomicrograph of a limestone breccia (B) under cross palars. Note the blocky spars infilling the channel porosity after white saddle dolomite (1) and isopachous radiaxial fibrous cement (2). Thin section no. 400.8, the Rung Nok Formation.

C. Blocky spars (B) infill a veinlet and are subsequently cross cut by a stylolite. Thin section no. 401 B, the Pa Kae Formation.

D. Photomicrograph of A. under cathodoluminescence, showing zonation of blocky cements in a veinlet from dull-to-bright and non-luminescent cements from the margin to centre of the pore. Thin section no. 401 B

E. Photomicrograph of stained red nodular limestone showing blocky ferroan calcite cements (blue) in a vein which cuts through gypsum laminites (white, G) and dolomicrite (gray, D). Thin section no. G, the Lae Tong Formation.

F. Red nodular limestone (N) from the upper Lae Tong Formation showing physical breakage of limestone nodules (1) and dewatering laminations in a dark red calcareous shale (2). Thin section no. 401 A, the Lae Tong Formation.

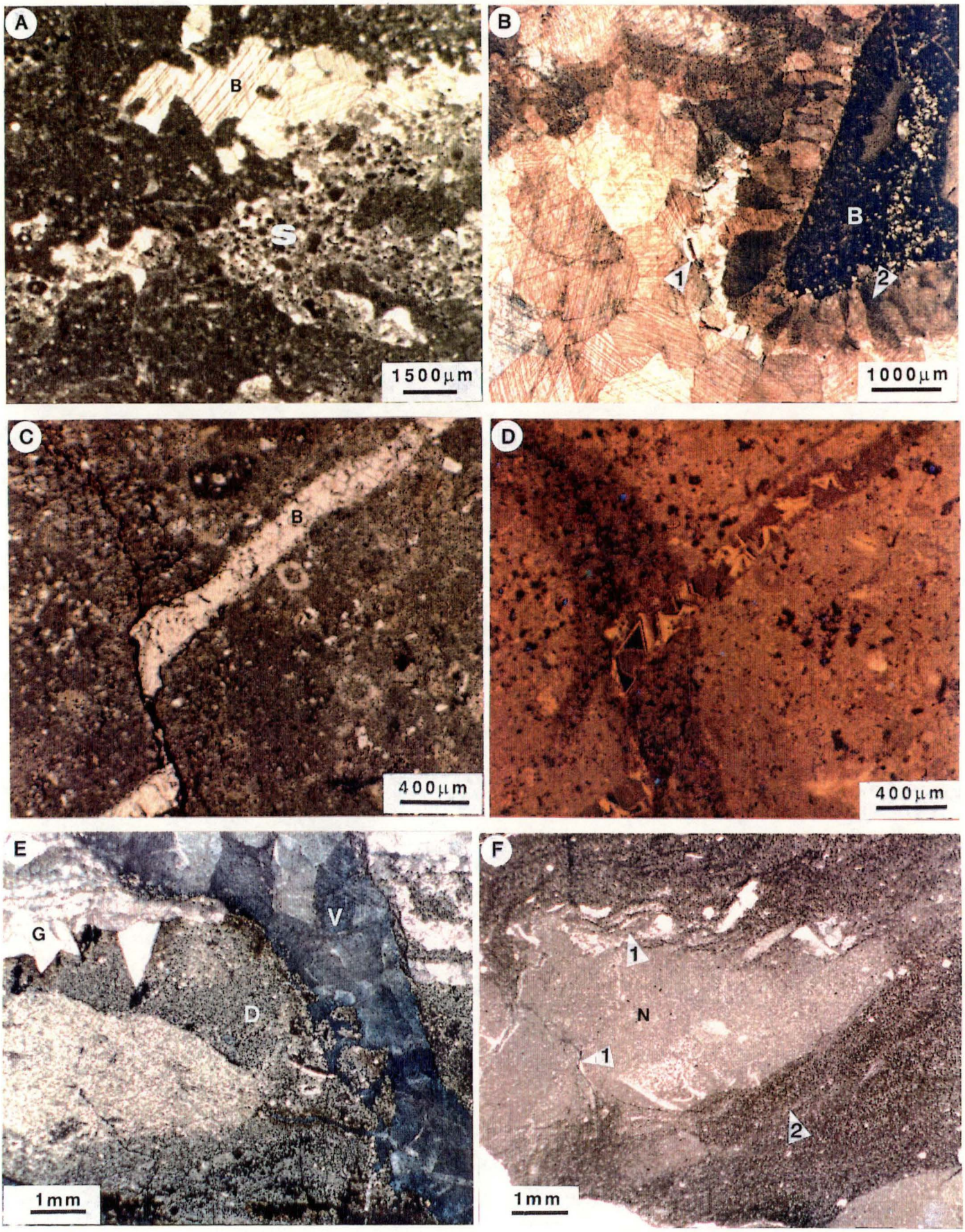
A
B
S
1500μm
B
B
1
2
1000μm
C
B
G
400μm
D
400μm
E
G
V
D
1mm
F
1
N
1
2
1mm

entirely fill single pore spaces and commonly predate both mechanical and chemical compaction. They consist of both ferroan and non-ferroan calcite. Although the non-ferroan stage is widely distributed, the ferroan stage is rare. Ferroan blocky calcite cements usually occur as late stage vein filling spars (Fig. 5.7C, E). Ferroan calcite also forms second generation rim cements within crinoidal limestones (Fig. 5.2A, B, C; 5.12A).

The non-ferroan blocky cements of the lower formation have dull luminescence (Fig. 5.4D) which is characteristic of deeper burial cements (Choquette and James, 1987; Rao and Wang, 1990). The non-ferroan and ferroan calcite rims of the Rung Nok Formation and the blocky cements of the Pa Kae stromatolites show compositional cement zones from non- to bright-luminescence, as mentioned earlier, (Fig. 5.2D, 5.3B) which indicates a transition of cementation from marine to shallow burial and then to a deeper burial environment (Meyers, 1974; Grover and Read, 1983)

On the other hand, the blocky spars which infill veins (Fig. 51A,B) consist of three generations of cement as observed by Wang and Rao (1989) in the Tasmanian Gordon Limestone. Zonation ranges from dull-luminescence to bright-luminescence with a dull subzone and non-luminescence in the middle part of the fracture porosities (Fig. 5.7C, D). This zonation indicates compositional changes in the pore fluid under reducing conditions during deep burial. There is also evidence of fracture formation at this stage.

Stable Isotopes of Burial Cement: The $\delta^{18}O$ and ^{13}C values of burial cements range from -9.3 to -27.4‰ PDB and +0.496 to -3.7‰ respectively. The isotopic compositions of these cements are much more varied than those of meteoric and marine calcite cements. The relatively wide range of $\delta^{18}O$ values from -9.3 to -27.4‰ PDB reflects the progressive diagenesis of the Thung Song Group carbonates during their burial history. The remarkable trend of $\delta^{18}O$ depletion without any significant change in $\delta^{13}C$ is also characteristic of burial cements (Choquette and James, 1987).

The $\delta^{18}O$ value of blocky cement from the Rung Nok Formation is -9.5‰ PDB. As this value is close to the isotopic composition of marine cement it tends to indicate that the blocky cement precipitated close to the sediment-water interface during shallow burial, from either formation water with a chemical composition similar to that of sea water or formation water that was originally sea water. However, the isotopic composition of calcite cement in veins or large voids is commonly depleted in ^{18}O, with values ranging from -10.2 to -27.3‰ PDB. This $\delta^{18}O$ depletion reflects temperature fractionation after deep burial.

5.2 Calcite Pseudomorphs After Evaporites

Calcite pseudomorphs after gypsum and minor anhydrite are common within the Malaka Formation, La Nga Formation, Pa Nan Formation, and in the lower member of the Lae Tong Formation. They comprise about 2-5% of the rock volume in thin section. These calcite pseudomorphs indicate that evaporitic minerals were formerly present within the Thung Song Group in the study area. They usually occur as either scattered single crystals or as clusters of crystals (Fig. 5.4B, 5.5A) but rarely occur as concentrations of crystals in very thin layers (Fig. 5.7E).

Gypsum crystals are prismatic to lenticular and grow both displacively within host sediments (Fig. 5.4B, D) and as infilling in fenestral porosities (Fig. 5.5A) similar to those observed in ancient peritidal carbonates (Lucia, 1972; Rao, 1990b). Some sparry calcite pseudomorphs after evaporites have straight sides and form rectangular crystals (Fig. 5.4B) similar to the calcitized anhydrite described by Lucia (1972).

Gypsum laminites, 0.4 to 0.9 mm thick, are found interbedded with dolomicrite within the upper member of the Lae Tong Formation (Fig. 5.7E). The laminae contain both prismatic and granular crystals. The latter have resulted from *in situ* breakage of the former during progressive crystal growth (Gunatilaka *et al.*, 1980). This feature was also reported from the laminites of abandoned tidal channels or evaporite pools in the supratidal zone of a Holocene carbonate Sabkha in southern Kuwait (Gunatilaka and Shearman, 1988), and from other shallow water sulphate laminites in Canada and Italy (Kendall, 1984).

The displacive growth, fenestral filling habit and corroded outlines of crystal surfaces provide evidence for the formation of evaporitic minerals during the early stages of diagenesis shortly after the deposition of host carbonate sediments in a tidal flat environment. Bright-luminescence of calcite pseudomorphs after evaporites (Fig. 5.4D) indicates that the evaporites were replaced by calcite after meteoric cementation but prior to the precipitation of blocky cements during later burial diagenesis and compaction.

Isotopic analysis was only performed on one sample from calcite pseudomorphs after gypsum laminite. It was found to have an $\delta^{18}O$ value -11.2‰ and a $\delta^{13}C$ value of -0.8‰ PDB. As the isotopic signatures of gypsum pseudomorphs fall within the range of meteoric isotopic compositions this confirms that the early replacement of gypsum by calcite occurred shortly after deposition. Scoffin (personal communication) also cited that if the gypsum was formed during the deposition of these limestones and the limestones suffered meteoric diagenesis it is surely almost certain that the evaporites will be lost at this stage.

5.3 Compaction

Compaction is defined by Meyers (1980) as any process which decreases the bulk volume of a rock. It includes mechanical processes that result in closer packing of grains, and chemical processes that decrease the volume of both grains and cement crystals.

The Thung Song carbonates were subjected to extensive meteoric and marine cementation. This phenomenon preserved most of the carbonates from physical burial compaction because of their early lithification (Meyers, 1980; Playford, 1980; Bathurst, 1987). Therefore, chemical compaction is more common than physical compaction in the Thung Song Group.

5.3.1 Physical Compaction

Appreciable physical compaction features, induced by overburden pressure, are common in the Lae Tong Formation. These rocks were deposited in a restricted lagoonal environment with only limited early diagenetic cementation. The physical compaction features in this alternating limestone and calcareous shale sequence consist of dewatering laminations within the calcareous shales (Fig. 5.7F), grain breakage and dislocation of fossils in the lenticular limestones of the lower member, and plastic deformation and breakage of the red nodular limestones in the upper member of the Lae Tong Formation.

Grain Breakage: Microscopic observations of lenticular limestones reveal breakage and displacement of some faunal skeletons (Fig. 5.8A). This post-dates their slightly bright cement rims but pre-dates later generation of this cement (dull to dull with zone doluminescent cements) as well as micro- to mesodolomite (Fig. 5.8A, B). The broken grains were healed by the second generation of rim cement (dull) and dolomite. Sutured intergranular contacts between bioclasts produce a fitted fabric (Fig. 5.8A) which is the result of a combination of physical compaction and pressure solution (Meyers, 1980; Meyers and Mill, 1983; Bathurst, 1987).

The breakage of grains and their very thin early cement rims suggests that physical compaction occurred shortly after burial. The healing of broken grains by later emplacement of secondary cement rims and micro- to mesodolomite rhombs confirmed this. Based on the experimental compaction of many modern shallow water and peritidal carbonate sediments, it appears that compaction features form easily in nature under as little as 100 m overburden and possibly even less (Shinn and Robbins,1983).

Fig. 5.8 A. Photomicrograph of a lenticular limestone from the lower member of the Lae Tong Formation, showing breakage of faunal fragments after the precipitation of the first cement rims (black arrow) and subsequent healing by second generation cement rims (1) and micro-to-mesodolomite (2). Note the suture between grain contacts (3). Thin section no. 401 D, the Lae Tong Formation.

B. Cathodoluminescence photomicrograph of A. showing compositional zonation of multigeneration cement rims (1) and micro- to mesodolomite (2).

C. Red nodular limestone showing preservation of burrow (1), plastic deformation (2), and stylolites (3) cross-cutting all components in red limestone nodules. Thin section no. 401 A, the Lae Tong Formation.

D. Poorly washed pelbiosparite showing calcite pseudomorphs after gypsum within a birds-eye structure (1), and irregular stylolites enclosing a microdolomite lens (2). Thin section no. 6, the Malaka Formation.

E. Photomicrograph showing the common style of stylolites in the Thung Song Group: swarms of irregular sutured seam stylolites cutting across all components including a veinlet (arrow). Thin section no. 17, the Malaka Formation.

F. Photomicrograph showing common style of stylolites in the Pa Kae Formation : a combination of low amplitude, peaked sutured stylolites (1) and non-sutured seams (2). Thin section no. 409.8, the Pa Kae Formation.

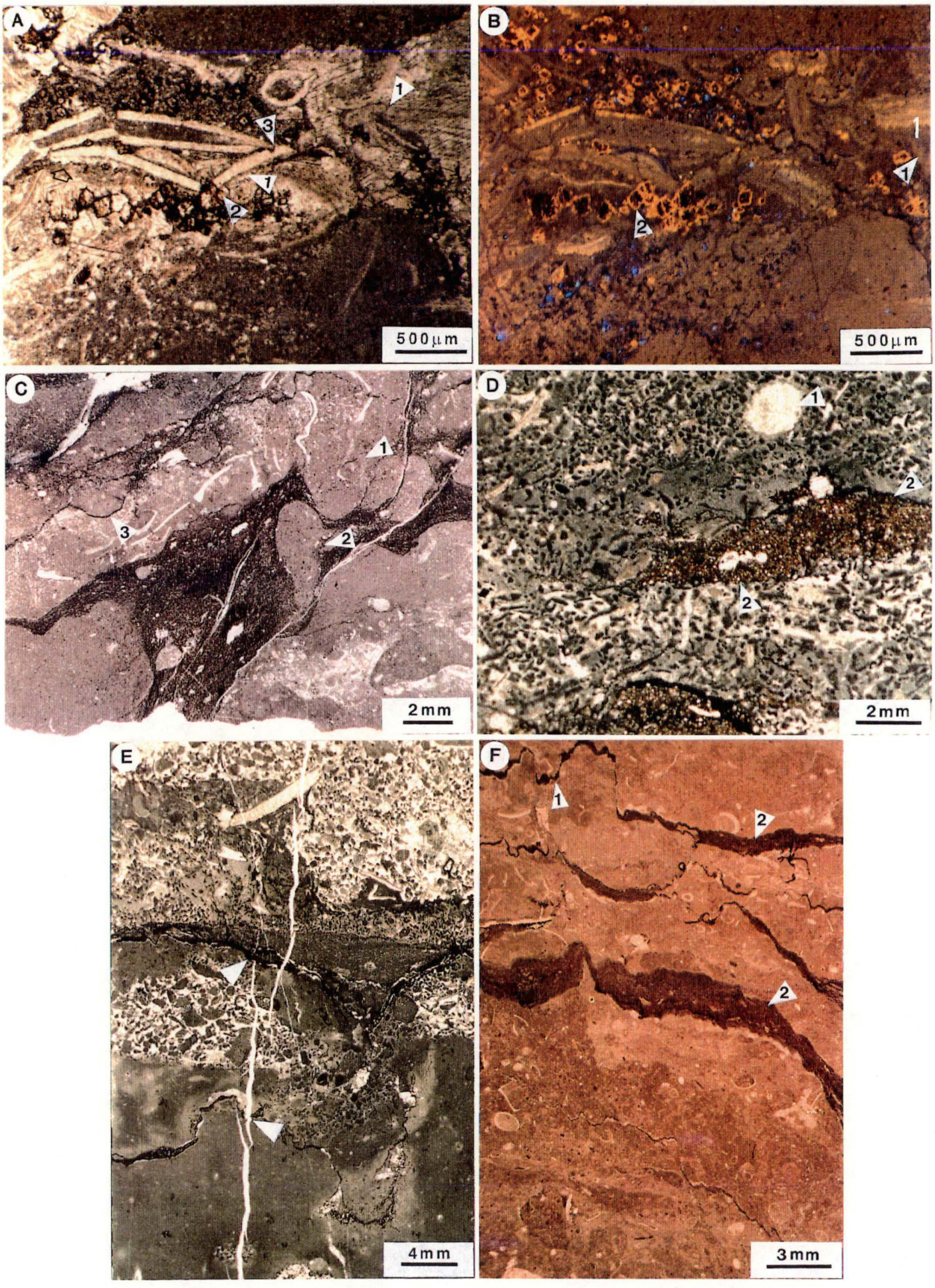
A
1
3
1
2
500μm
B
1
1
2
500μm
C
1
3
2
2mm
D
1
2
2
2mm
E
4mm
F
1
2
2
3mm

However, breakage and deformation of tubular siliceous spicules requires 12,000 m of overburden (Shinn and Robbin, 1983) whereas carbonate sands need an overburden of up to 1000 m in order to become compacted (Flugel, 1982). However,these figures do not seem to correspond well to the presence of micro- to mesodolomite in the Lae Tong Formation as microdolomite is usually only found in near surface modern environments. Therefore, it is possible that the breakage of grains within the Lae Tong Formation occurred at shallow burial as mentioned by Shinnand Robbins (1983).

Breakage and Plastic Deformation of Nodular Limestones: The physical compaction features of the red nodular limestones from the Talo Dang Formation and the upper member of the Lae Tong Formation are different from the features displayed in the lower member due to the fact that the limestone nodules are composed of micrite or fossil-bearing micrite. Fossil fragments in the nodules are too far apart to form either grain breakages or fitted fabrics as displayed in the other grainy or sparry rocks in the lower member. This does not mean, however, that there has been no physical compaction of the rock. On the contary, the present appearance of the nodular limestone itself is diagenetic in origin resulting from the local early cementation of the alternating limestone, the critical amount of detrital clay in shale layers and the extensive differential compaction during burial (Bathurst, 1987; Scoffin, 1987; Moller and Kvingan, 1988). The role of burrows (Eller, 1981; Scoffin, 1987) is less significant since the bioturbation is not common. However, biotubation in some layers of the Talo Dang Formation gives nodular appearance to bedding.

Evidence for early cementation of micritic nodules includes the breakage of nodules during compaction and the re-arrangement of some broken fragments along dewatering laminations; gradational contacts between nodules and calcareous shales with fossils crossing the boundaries; thinning and draping of sedimentary and/or dewatering laminations around nodules (Fig. 5.7F); and well preserved burrows within the nodules (Fig. 5.8C). However, there is also evidence for plastic deformation of the nodular limestones. This evidence is in the form of squeezing upward features of a micritic droplet which cross-cuts a dewatering lamination (Fig. 5.7F, 5.8C). This indicates that early cementation and lithification of rocks occurred locally, even within a single layer, as some parts of nodules remained semi-consolidated or unconsolidated during an early physical compaction stage. They were then deformed later by shear stress and dewatering processes prior to significant compaction (Mills, 1983) after deep burial. There is no evidence to determine where did the carbonate released during chemical compaction go to.

5.3.2 Chemical Compaction

Chemical compaction or pressure dissolution features are common in the Thung Song Group. There are two distinct types of chemical compaction features: sutured seam stylolites and non-sutured dissolution seams. Fitted fabric is very rare and less extensive.

The *sutured seam stylolites*, outlined by concentrations of black carbonaceous matter and clay along seams, are very common in every formation of the Thung Song Group. They are usually irregular to peaked stylolites with low amplitude and form bedding-parallel swarms (Fig. 5.8C, E, F). The amplitute of peak stylolites are up to 14 mm wide and 6 mm high. These stylolites normally cut through rock fabric, across allochems, cement, matrix and calcite veinlets but not cross micro- to mesodolomite layers. Instead, they tend to form selectively along contacts between limestone and microdolomite layers and/or around microdolomite lenses (Fig. 5.8D). This is because the non-hydrostatic stress at the boundary between the limestone and microdolomite units is at a maximum (Buxton and Sibly, 1981). The cross-cutting relationship between stylolites and rock fabric indicates that stylolites were formed in a late burial diagenetic environment (Bathurst, 1975).

Non-sutured dissolution seams occur in the upper Lae Tong member (Fig. 5.8C) and the Pa Kae Formation (Fig. 5.8F). In the Pa Kae Formation they form smooth, undulose seams of clay minerals and organic matter which lack the sutures of stylolites (Bathurst, 1987). It is difficult to determine whether the non-sutured dissolution seams of the upper Lae Tong member are actually non-sutured seams or physical compaction features. Due to the presence of broken nodules, gradational contacts and fossils cross-cutting boundaries, it is clear that some nodules or at least some parts of nodules are the products of physical compaction after early cementation (Fig. 5.7F). However, other nodules, with sharp boundaries that truncate fossil fragments (Fig. 5.7F, 5.8C) and microstylolites, are suggestive of chemical compaction during a later stage of burial.

5.4 Dolomitization

Dolomitization is generally recognised not only as a process of secondary replacement of calcium carbonate by dolomite from a solution supersaturated with respect to dolomite (McKenzie *et al.*, 1980; Morrow, 1982), but also as an early to late diagenetic dolomite cementation from various types of pore fluids including near normal marine, mixed meteoric-marine, and meteoric water (Kaldi and Gidman, 1982; Rosen and Holdren, 1986; Mirchell and Miser, 1987), plus warm migrating pore fluids (Beales, 1971; Choquette, 1971; Mattes and Mountjoy, 1980).

Throughout the Thung Song Group dolomite occurs as both a replacement phase and a cement phase. Based on the mode of occurrence, shape and size of its crystals, plus its stage of formation, dolomite can be subdivided into four categories: microcrystalline dolomite, medium crystalline sucrosic dolomite (mesodolomite), megadolomite and dolomite cement.

5.4.1 Microcrystalline Dolomite (Microdolomite)

Microcrystalline dolomite (6-150 μm) comprises brown, equigranular, hypidiotopic to idiotopic crystals scattered throughout unaltered limestone or occurring as mosaics of crystals. This type of dolomite forms layers or lenses in the lower members of the Thung Song Group. The three distinctive modes of occurrence of microdolomite are as 1) dolomite laminations within stromatolitic microfacies I, 2) microdolomite along cross-laminations, and 3) burrow-filling microdolomite.

Microdolomite laminations: Most of the rocks from the Malaka Formation, shallow-upward sequences of the La Nga Formation, and the Pa Nan Formation consist of microdolomites interlayered with limestones on a centimetre or millimetre scale (Fig. 4.1, 5.9A). These couplets commonly form as irregular to smooth laminites with minor mound shaped stromatolitic structures. Dolomite layers are composed of silt-sized microdolomite crystals in between which are variable amounts of clay and dark gray to black organic matter (Fig. 5.9C). Crystal sizes range from 6 to 60 μm in fine laminations and from 20-100 μm in coarse ones. Fairchild (1980) thought that the smallest crystals are closest to the original crystal size (6 μm).

Some layers display mudcrack patterns on bedding surfaces (Malaka laminites) which are usually associated with fenestral and gypsum pseudomorphs (Fig. 5.9B, C, D). Under cathodoluminescence, most of the microdolomite crystals display bright cores and non-luminescent rims (Fig. 5.9D). This is because the microdolomite formed initially in a reducing environment during the decomposition of organic matter within stromatolites-rich laminae (Gebelein and Hoffman, 1973), and was later exposed to an oxidizing environment. Many ancient peritidal and subtidal microdolomite laminations have been reported by a number of geoscientists (Davis, 1966; Kepper, 1966; Gebelein and Hoffman, 1973; Fairchild, 1980; Gasieviez, 1987; Rao and Wang, 1990). They concluded that microdolomite laminations result from either primary precipitation from sea water (Kepper, 1966) or penecontemporaneous replacement of aragonite and calcite in microbial-rich laminae by Mg-rich brines or mixed water after the deposition and decomposition of organic-rich stromatolitic layers. However, there is no modern analogue of microdolomite laminites.

Fig. 5.9 A. Brown micro dolomites (1) interlayer with micrite, intrasparite and pelmicrosparite. Note microdolomites (2) and blocky spar (3) filling in burrows. Thin section no. 396 C, the Malaka Formation.

B. Microdolomite in burrows (1) and interareas (2) of columnar stromatolites. Thin section no. PN, the Pa Nan Formation.

C. Photomicrograph of pelsparite (P) interlaminated with microdolomites (M) . Note the calcite pseudomorphs after gypsum (arrow). Thin section no. 403.3A, the Malaka-Pa Nan Formation.

D. Cathodoluminescence of C. showing bright cores (B) and non-luminescent cores (N) of microdolomite. Microdolomite crystals cross-cut gypsum pseudomorphs (arrow).

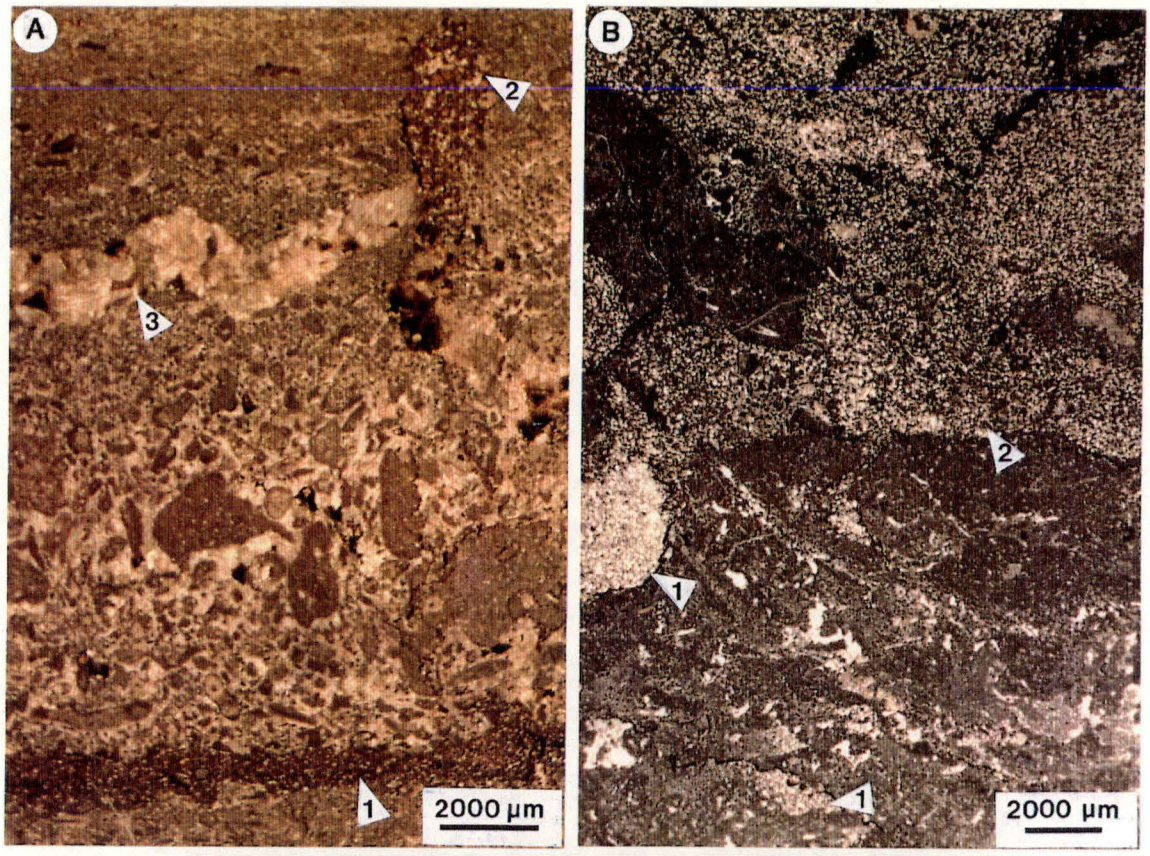
A
2
3
1
2000 µm
B
2
1
1
2000 µm

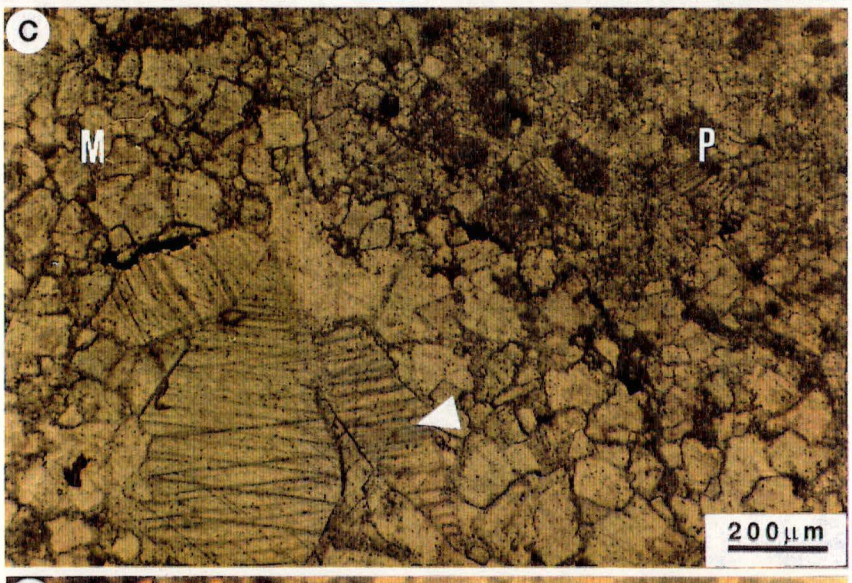
C
M
P
200µm

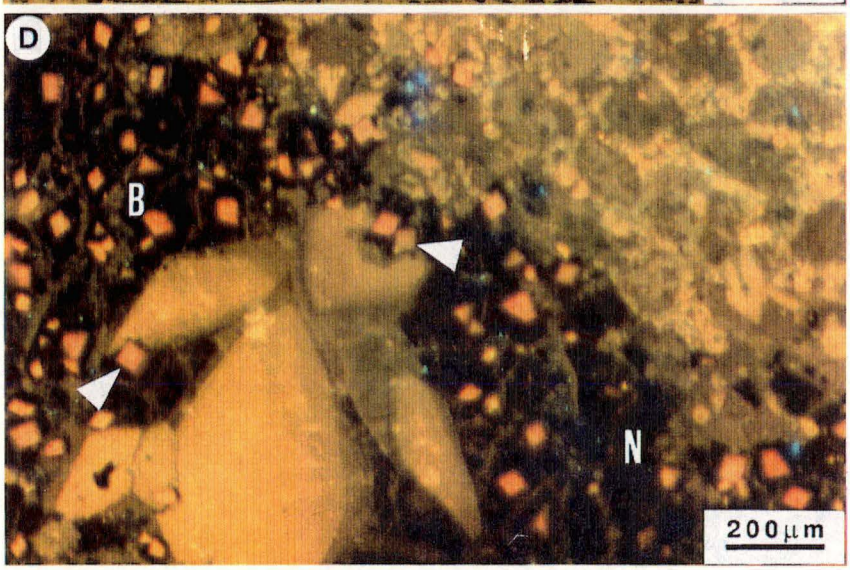
D
B
N
200µm

Several pieces of evidence, including small crystal size, bright- and non-luminescence, total dolomitization within sharply defined alternating layers of microdolomite and limestone, the association of fenestrae, mudcracks, and gypsum with the Thung Song's dolomite suggest a very early stage of dolomitization. Therefore, Thai Ordovician microdolomite laminites possibly originated from penecontemporaneous replacement of algal-rich layers within stromatolites during an early diagenetic stage after the deposition in an area between a supratidal and an upper intertidal environment where stratiform stromatolite is abundant as on modern tidal flats at Andros Island (Hardie and Ginsburg, 1977), the Persian Gulf (Shinn, 1983) and Shark Bay (Logan *et al.*, 1964). Some coarser microdolomite crystals have clear rims (Fig. 4.9B) indicating later replacement or partly neomorphism of original microdolomites after burial (Land, 1980).

The dolomitizing fluids in a tidal flat area covered by stratiform stromatolites should be either a mixture of fresh and marine water (Hanshaw *et al.*, 1971; Badiozamani, 1973; Land, 1973) or a hypersaline brine resulting from seepage refluction (Adams and Rhodes, 1960) and evaporative pumping (Hsu and Siegenthaler, 1969). Based on the isotopic compositions of dolomite, ranging from -7.1 to -13.8‰ for $\delta^{18}O$ and +2.1 to -0.4‰ for $\delta^{13}C$, the dolomitizing fluids which produced the microdolomite laminites are mixed waters because these isotopic compositions are lower than those of marine dolomites with carbonate buildup ($\delta^{18}O$ = -3.1 to -8.3‰ PDB, $\delta^{13}C$ = +1.5 to -0.7‰PDB) and they are also lower than the postulated Ordovician seawater value(-4.6‰, Rao and Wang, 1989). The extensive evaporation associated with the Sabkha model should result in increased oxygen isotope values for microdolomite above that of normal seawater (McKenzie, 1980; McKenzie *et al.*, 1980). However, the $\delta^{13}C$ values of microdolomite laminites was higher than those derived from soil gas or decaying organic material (range from -15 ‰PDB; Humphrey, 1988). This indicates the minor role of meteoric ground water in this mixing zone dolomitization. Stoessell *et al.* (1989) suggested that the mixing-zone model for dolomitization can be extended to a much higher salinity than the widely accepted "Dorag" model.

This interpretation of a mixed-water model seems to be contradicted by the presence of gypsum pseudomorphs in stromatolites and associated microfacies of the Thung Song Group. However, gypsum and other evaporitic minerals can occur and are partly preserved in Recent wet and dry climate of tropical and subtropical regions. The microdolomite lamination along columnar stromatolitic structures and intercolumn areas of the shallow subtidal, Pa Nan stromatolites, are possibly evidence of the transportation of mixed-water dolomitizing fluids offshore. The depletion of oxygen isotope values from -7.1‰ to -13.7‰ PDB is possibly the result of an elevation in

Fig. 5.10 A. Photomicrograph of a half stained thin section (left diagonal) showing detrital microdolomite (white spot) along hummocky cross-laminations. Note 1) synsedimentary microfault oblique cutting a lamination, 2) intraclasts of the same rock. Thin section no. 13.5, the lower Lae Tong member.

B. Photomicrograph of a stained thin section of the same rock as A. but taken from a different layer, showing a burrow (B) cut through a detrital dolomite layer and filled with clay, dolomite and micrite. Note the angularity of the microdolomite grains with partially preserved crystal faces (2), and pyrite (3). Thin section no. 404 F, the lower Lae Tong member.

C. This stained section shows selective replacement of micrite breccia by mesodolomite (white) leaving the fibrous and blocky spar (red) unaffected. Note the floating incipient dolomite (1), the complete dolomitization of some micrite grains (2), and the dolomite veinlet (3). Thin section no. 400.6, the Rung Nok Formation.

D. Photomicrograph (cross-polars) of a poorly washed biosparite shows extensive replacement of micrite infilling and void-filling spar (arrow) by mesodolomite. Note the minor bioclast relicts. Thin section no. 400.7, the Rung Nok Formation.

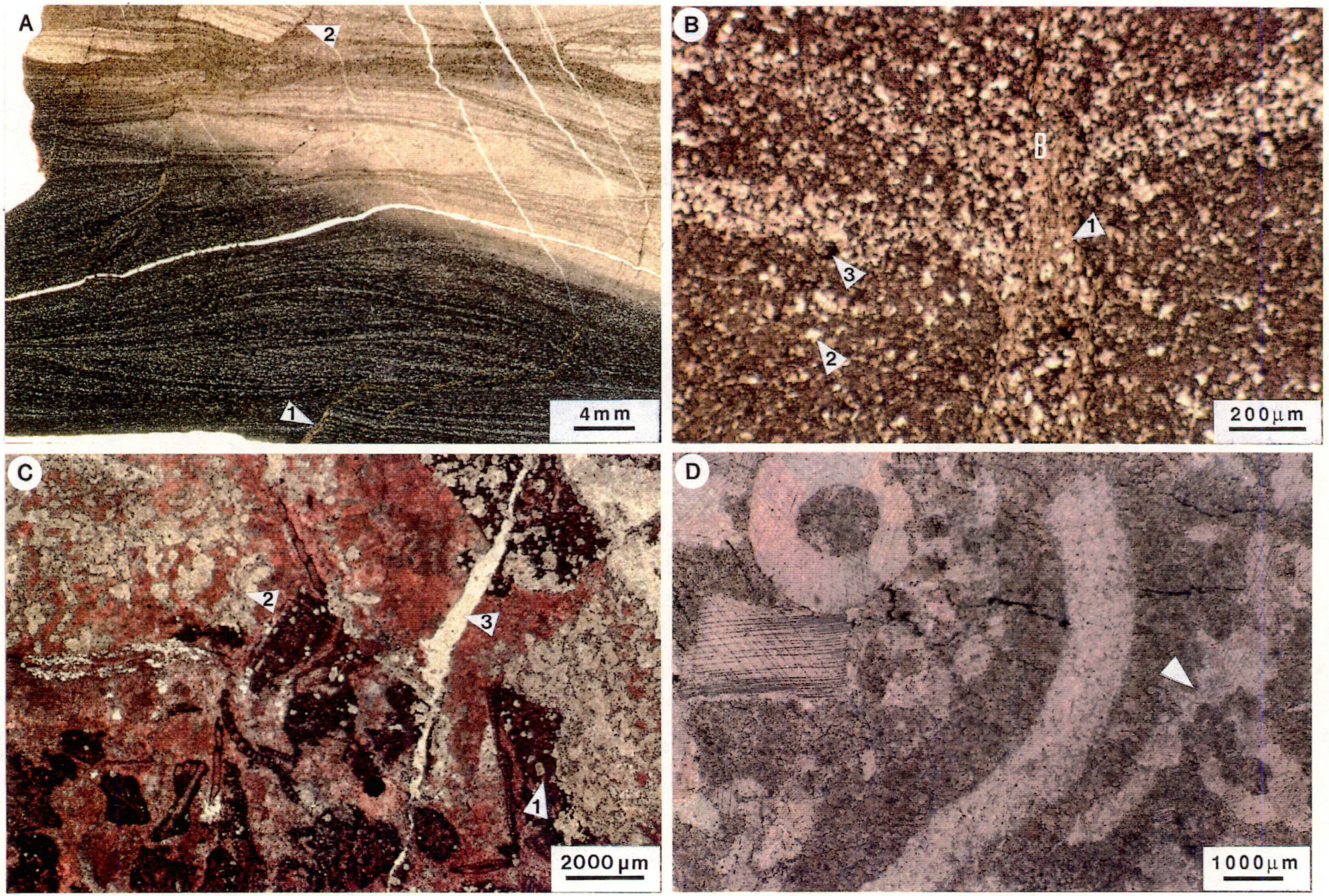
A
2
1
4mm
B
B
1
3
2
200µm
C
2
3
1
2000µm
D
1000µm

temperature and the re-equilibration of some microdolomite crystals with pore fluids during neomorphism after burial.

Microdolomite Along Cross-Laminations: This type of microdolomite is found interlayered with micrite along hummocky cross-laminations (Fig. 5.10A) in the lower member of the Lae Tong Formation. Wave ripples on top of bedding are common. Dolomite laminae consist mostly of angular to subrounded microdolomite grains (10-15 μm, Fig. 5.10B) plus subangular to rounded detrital quartz, feldspar (20-90 μm, <10%) and mica grains. Some microdolomite grains are polycrystalline and broken, displaying only partly preserved crystal faces and silica replacement.

Microdolomite laminae are cross cut by synsedimentary microfaults (Fig. 5.10A) and burrows (Fig. 5.10B) which are also infilled with angular microdolomite grains and clay minerals. The burrows are randomly orientated. Small pyrite crystals are abundant and usually lie along laminations. These features indicate penecontemporaneous deposit of microdolomite in a reducing lagoonal environment.

On the other hand, under cathodoluminescence microdolomite is non-luminescent suggesting that dolomitization involved oxidizing fluids. Due to the characteristic detrital features of the grains and their accumulation along hummocky cross-laminations, this type of microdolomite is possibly a detrital dolomite which was transported from an oxidizing environment by strong winds or storms and deposited within a restricted lagoon. Isotopic studies also support this hypothesis. Oxygen isotopic values of the Lae Tong detrital dolomites range from -7.6 to -11.3‰ PDB and carbon isotope values range from +0.1 to -1.1‰ PDB. The oxygen isotope values fall within the range of mixed-water microdolomite laminites but the carbon isotope values are lighter. This indicates that the detrital dolomite either originated in the mixing zone of a tidal flat environment, with only limited influence from the stromatolites, or underwent later re-equilibration with reducing fluids in a lagoon.

Burrow-replacing Microdolomites: Although this category of microdolomite has similar characteristics to the microdolomite laminites, it does differ however in its mode of occurrence and timing. Burrow-filling microdolomites commonly fill both vertical (Fig. 4.1A, 5.9A) and random burrows (Fig. 4.9B, 5.9B) in the lower formation of the Thung Song Group. In the Pa Nan Formation, this type of microdolomite also replaces both carbonate sediments within channels between stromatolitic columns (Fig. 5.9B) and calcite spar in molds of gypsum (Fig. 5.9D), and it may also partially or completely replace fauna (Fig. 4.9D). However, micrite in between burrows and molds is not dolomitized. There is therefore strong evidence for shallow burial replacement of calcite by microdolomite after recrystallization and/or

dissolution of skeletal grains followed by spar-filling mold in the meteoric phreatic zone. Kendal (1977) also suggested that dolomitization of dolomite mottling in Ordovician limestone from Canada is early shallow burial dolomitization of permeable solf sediments within burrows and moldic porosities posdating the early diagenetic cementation of host rocks. He proposed that the dissolution of magnesium calcites during stabilization stage is a source of magnesium.

Burrow-replacing microdolomites within the vertical burrows of the Malaka and La Nga Formations were localized by differences in sediment porosity and permeability during deposition (Morrow, 1987). Where vertical burrows penetrate from microdolomite laminar deep into limestone layers. There is a gradual increase in crystal size, which ranges from grains equal in size to those of the microdolomite laminar at the top of the burrows down to coarser iron-rich zoned micro- to mesodolomite grains at the bottom of the burrows, with relicts of calcite spar in between the micro-dolomite crystals (Fig. 4.1A, 5.9A). This should be the indicator of either long existence of dolomitizing fluids within burrows from penecontemporaneous stage in a peritidal environment to later diagenetic stage (Rao, pers. comm.) or those penecontemporaneous microdolomite crystal forming nuclei for the selective precipitation of late diagenetic dolomites from dilute subsurface solutions (Morrow, 1987).

Rao (1990b) pointed out that the dolomitizing fluids passing through the upper surface of peritidal carbonate sediments replace burrows and mudcracks, seep downwards to form mottle dolomite and extends into bottom-moving solutions to form laminar dolomite. This statement is confirmed by isotopic analyses of various microdolomites from the Thung Song Group. The fact that the isotopic compositions of burrow-filling microdolomite, -9.6 to -10.8‰ PDB for $\delta^{18}O$ and +1.9 to +0.5‰ for $\delta^{13}C$ fall within the ranges for microdolomite laminites suggest that there is a close relationship between the formational water of these dolomites, all three of which may possibly have formed from the same fluid.

In brief, microdolomite of the Thung Song Group resulted from either later-early diagenesis or the penecontemporaneous replacement of carbonate sediments within stromatolite laminae and burrows, by mixed-dolomitizing fluids shortly after deposition, followed by the neomorphism of some crystals in a later diagenetic stage after burial. Some of the dolomite was subjected to erosion and transportation during storms from a tidal flat environment to a nearby restricted lagoon where it was deposited as detrital dolomite.

5.4.2 Medium Crystalline Sucrosic Dolomite (Mesodolomite)

Some details of the petrography of this type of dolomite have been mentioned earlier under microfacies XII. The most significant features which allow interpretation of the diagenetic events involved in the formation of mesodolomite are as follows:

1. In general, mesodolomites are rather uniform in texture. They comprise brown, equigranular to bimodal, hypidiotopic to xenotopic (Fig. 5.10C, D; 5.11A, C), tightly interlocking mosaic, inclusion-rich crystals, commonly ranging from 60-200 μm and 160-400 μm. The crystals have compromise boundaries (Fig. 5.11A).

2. Mesodolomite crystals have cloudy centres surrounded by clear rims (Fig. 5.11A). The cloudiness of the crystal centres is due to the presence of very small red-staining calcite inclusions.

3. The bimodal grain size and white to brown colour, suggests that there has been more than one phase of dolomitization.

4. Based on relicts and ghost structures, it is clear that the precursors of mesodolomites are biosparites, pelsparites, limestone breccias (Fig. 5.10C, D) and minor biolithites.

5. The sucessive stages involved in the dolomitization process are visible within the fourth member of the Rung Nok Formation. These stages are represented by changes in the dolomite-calcite ratio from limestone at the bottom of sequence through partially altered limestone in the middle (Fig. 5.10C, D) to calcite-free pervasive dolomite (Fig. 5.11C) at the top of the sequence. The selective replacement of the micrite matrix and cement spar by mesodolomite in the lower part of this member usually leaves the bioclasts unaffected (Fig. 5.10C, D).

6. The common order of susceptibility to dolomitization from the most to the least susceptible is as follows: micrite matrix and micritic breccias, peloids, blocky spars and syntaxial rims, and skeletal components. Bullen and Sibley (1984), Malcolm (1987) and Rao (1990b) suggested that crystal size plays an important role in ordering dolomitization. This is confirmed by strongly fabric selective replacement of small incipient dolomites which float within micrite breccias (Fig. 5.10C), and crinoidal relicts within crinoidal dolomite (Fig. 5.10D) in the Rung Nok Formation.

7. Mesodolomites are usually re-replaced by low magnesian calcite (Fig. 5.11A, C) leaving irregular dedolomitized calcite patches of equant spars with some unusual sphere habits (Fig. 5.11A) in the upper part of the sequence.

Certain features, such as the replacement of blocky and syntaxial cements by mesodolomite; a pervasive dolomite sequence, and crystal size suggest that this rock type resulted from burial dolomitization. Based on the fact that mesodolomites (Fig. 5.10D) are cross-cut by stylolites, the dolomitization probably started early (small incipient dolomites) and was completed at a moderate depth following burial and lithification but before significant compaction of the carbonate sediments.

Fig. 5.11 A. Dedolomitization of mesodolomite from the fourth member of the Rung Nok Formation showing the unusual habit of rounded dedolomitized calcite crystals (1), calcite replaced dolomite (2), dissolution of calcite inclusions within dolomite rhombs (3), and crystal with cloudy centres and clear rims (4). Thin section no. 400.3, the Rung Nok Formation.

B. Cathodoluminescence photomicrograph of A. Note the dull centres and bright rims (1) of the dolomite crystals and dull with zone of dolomite (2) surrounding dedolomitized calcites.

C. Photomicrograph of a stained thin section showing complete dolomitization in the fourth member of the Rung Nok Formation, 1) dedolomitized calcite patches (red), 2) hypidiotopic to xenotopic crystals of mesodolomite, and 3) crystals with cloudy centers and clear rims. Thin section no. 400.3, the Rung Nok Formation.

D. Extensive replacement of poorly washed biosparite by cloudy, xenotopic megadolomite and which is subsequently cut by a dolomite veinlet (arrow). Thin section no. 23.7, the second member,the Rung Nok Formation.

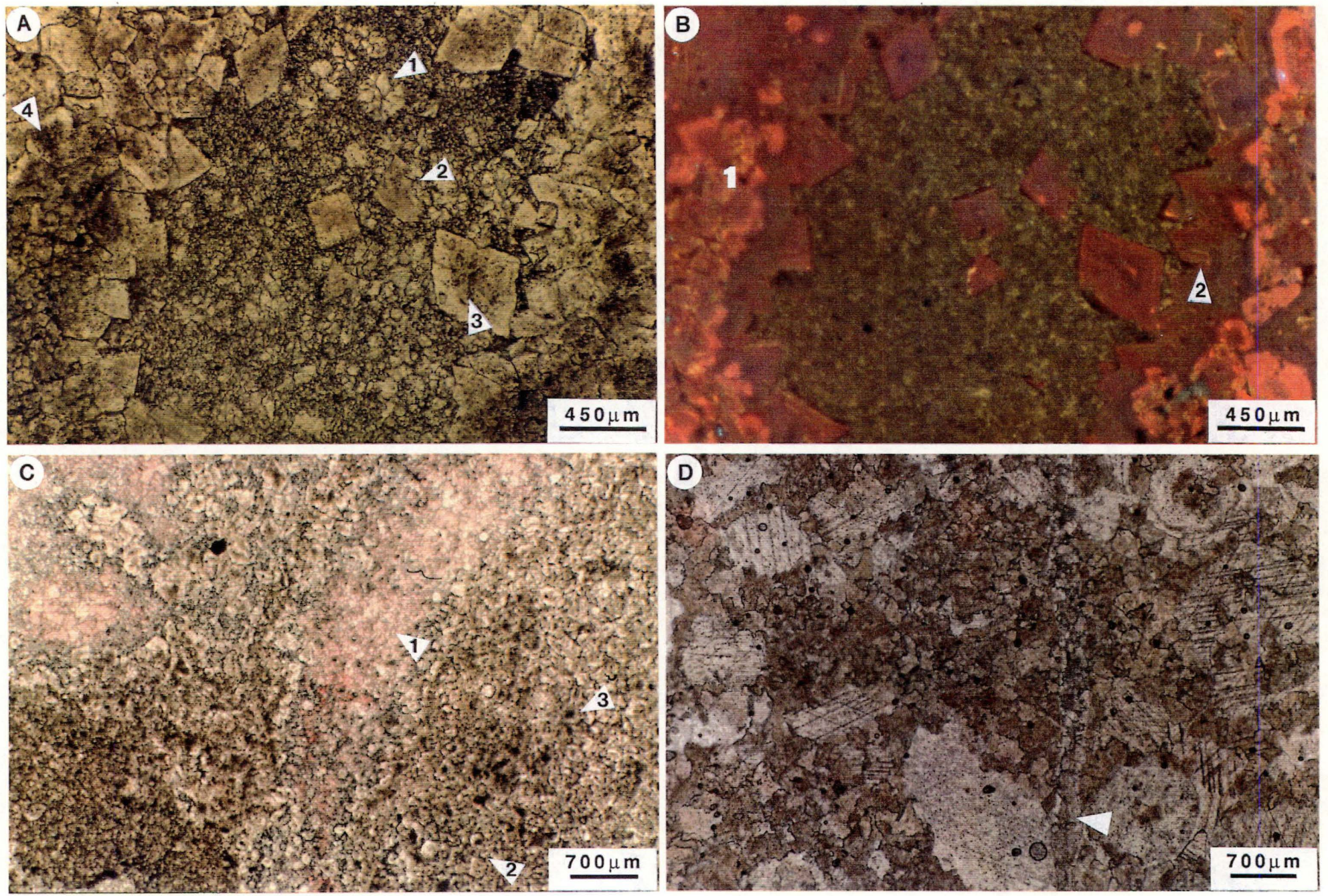
A
1
2
3
4
450μm
B
1
2
450μm
C
1
2
3
700μm
D
700μm

Under cathodoluminescence, mesodolomites show compositional zonation (Fig. 5.11B) suggesting a change in the composition of the dolomitizing fluids through time. The majority of small crystals with cloudy centres and clear rims have non-luminescent centres and bright rims whereas the larger crystals with less cloudy centres are dull with zoned rims and some have small brighter centres. This indicates a timing overlap between the first and second phases of dolomitization. The small bright cores of the larger mesodolomite crystals would have occurred penecontemporaneously with the bright rims of the small mesodolomite crystals during the later phase of dolomitization.

Sibly (1980) and Morrow (1982) suggested that the cloudy centre and clear rim phenomenon of dolomite crystals may be representative of the evolution of dolomitizing fluids from a near calcite saturation stage at the beginning to a later calcite under-saturation stage as grain growth continues under the influence of mixed-water diagenesis. However, isotopic analyses of Thung Song Group mesodolomites do not support the mixed-water model. Dolomite crystals have $\delta^{18}O$ values ranging between -3.1 to -8.3‰ PDB and $\delta^{13}C$ values ranging between +1.5 to -0.7‰ PDB. It is clear that the isotopic compositions of these mesodolomites within buildups (?) have much higher $\delta^{18}O$ values compared with other mixed water microdolomites of peritidal deposits (-7.1 to -13.8‰ PDB) as mentioned earlier.

This also indicates that the dolomitizing fluids of mesodolomite have a composition similar to sea water, probably with a subtidal or marine pore fluid origin. However, petrographic evidence suggests late diagenetic dolomitization involves the replacement of late calcite cements by mesodolomites. Furthermore, Land (1980) stated that as interstitial fluids alone are insufficient to produce the dolomitization of massive dolomites, active hydrologic transport of large amounts of magnesium is also required. Therefore, dolomitization of the fourth member of the Rung Nok Formation may have occurred during a shallow burial stage under the influence of sea water percolating through lithified sediments from the sediment and water interface as of subsurface dolomite from Enewetak Atoll (Saller, 1984). Cloudy centres and clear rims are a product of neomorphism during progressive stabilization of mesodolomite by the same fluids (Land, 1980), regardless of whether they are marine, hypersaline or mixed waters.

5.4.3 Megadolomite

Dolomitized biosparites interbedded with poorly-washed biosparites occur within the second member of the Rung Nok Formation. Fabric selective megadolomites

occur irregularly and are variably distributed (generally <40%) within dolomitized biosparites. However, some poorly-washed biosparites are also slightly dolomitic, containing less than 5% megadolomite on average. Permeability and porosity should play a major role in the dolomitization of these two rock types because both have the same lithology with just differing amounts of micrite and degrees of dolomitization.

Most of the megadolomites are uniform in texture and composed of 175-1600 μm dolomite crystals. They are cloudy, inequigranular, xenotopic dolomite crystals (Fig. 5.11D, 5.12A), which occur either individually or in clusters up to 3.75 mm in size. Crystal sizes vary widely. It appears that the coarser dolomite crystals grew by the replacement of micrite, in contrast to those crystals that developed on other grains such as bioclasts and calcite cements. Individual crystals contain submicroscopic inclusions, look like micrite, and have undulose to sweeping extinction under crossed polars. Megadolomite fabric selectively replaced the micrite matrix after precipitation or enlargement of the later deep burial syntaxial rims as indicated by the transection of rim cements and bioclasts by mesodolomites, and micrite ghost within dolomite crystals (Fig. 5.12A). Under cathodoluminescence, megadolomites show red mottled bright-luminescence which post-dates the orange, bright and dull compositional zonation of the second and later generations of syntaxial calcite rims (Fig. 5.12A, B). Cross-cutting relationships and cathodoluminescence indicate that megadolomites developed late after burial and lithification of the original carbonates under reducing conditions. In the rare completely dolomitized layers (massive dolomites) at Ko Laen, megadolomites have similar features to the mesodolomites but they have larger grains and form abundant void-filling saddle dolomites (Fig. 5.12C). Cathodoluminescence of this dolomite results in the same bright-luminescence for hypidiotopic to xenotopic megadolomites and a further non-luminescent zone at saddle dolomite rims (Fig. 5.12D).

The compositional zonation of saddle dolomites could be an indication of the fluctuation of oxidizing fluids into pore spaces during deep burial. The presence of saddle dolomites as void linings suggests that the development of megadolomite involves progressive neomorphism from smaller grains at shallow depth to larger megadolomites and saddle dolomites (both xenotopic and curved crystals) under deeper burial at temperatures greater than 60°C (Radke and Mathis, 1980; Gregg, 1983). However, Gregg and Sibly (1984) stated that at tempertures exceeding 50°C, carbonate texture is xenotopic whereas at lower temperature idiotopic texture is more common. The low $\delta^{18}O$ value of this dolomite also suggests relatively high temperatures of precipitation ($\delta^{18}O$ = -9.9‰, $\delta^{13}C$ = -0.6‰ PDB).

Based on assumptions about the effects of temperature fractionation upon the isotopic signature of xenotopic dolomites, the original signature of dolomitizing fluids

Fig. 5.12 A. Photomicrograph of a stained thin section of selectively dolomitized crinoidal, poorly washed biosparite showing the ferroan calcite zoned cement (blue) of syntaxial rims (1) : megadolomite replaced rim cement (2) micrite (3), and bioclasts (4). Thin section no. 22.8, the Rung Nok Formation.

B. Cathodoluminescence photomicrograph of the left part of A. showing the non to bright subzone luminescence of syntaxial rim cement and the red dull- to bright-luminescence of dolomite. Thin section no. 23.8, the Rung Nok Formation.

C. Photomicrograph of the completely dolomitized biosparite to megadolomites with a similar texture to other mesodolomites (Fig. 5.10 C). They have clearer bimodal grain size, darker cloudy centers (1), and more coarser crystals than the others. Note the void-lying saddle dolomites with rhombic terminal and curved faces projected into black carbonaceous matter within large voids. Thin section no. 13.1, the Rung Nok Formation at Ko Laen.

D. Cathodoluminescence photomicrograph of C. showing red dull to bright luminescent megadolomite and the non luminescent rim of saddle dolomite (arrow).

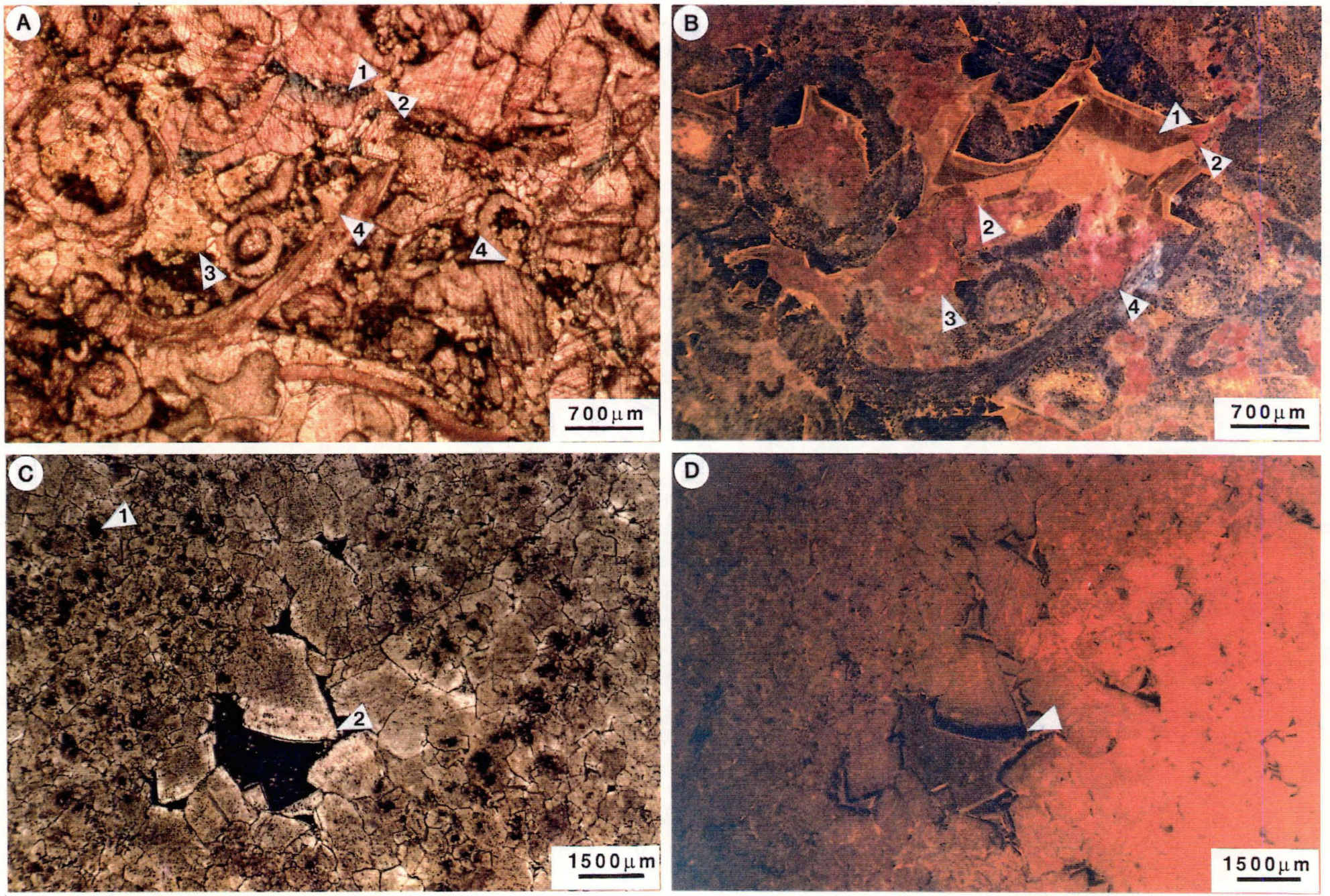
A
1
2
3
4
4
700μm
B
1
2
2
3
4
700μm
C
1
2
1500μm
D
1500μm

should be much heavier than this, therefore, the dolomitizing fluids are possibly marine in origin (?) as are those of the mesodolomites.

5.4.4 Dolomite Cement

The Thung Song Group displays two common categories of dolomite cements within the study area. These are xenotopic dolomite cements and saddle dolomite cements.

Xenotopic Dolomite Cement: Xenotopic dolomite cement (up to 250 μm) occurs rarely as an interparticle cement of peritidal limestone: oosparites, intrasparites and some stromatolites from the La Nga Formation, Malaka Formation, and Pa Nan Formation (Fig. 5.13A). It is commonly composed of non-ferroan dolomite with undulatory or sweeping extinction under crossed polars. Crystals may be cloudy or relatively clear with a white to brown colour in thin section.

Xenotopic dolomite cements usually form after the primary radial bladed and/or isopachous fibrous cements and the secondary blocky cements. In many thin sections, dolomite cements appeared to have occurred penecontemporaneously with large blocky spars. Boundaries between dolomite cement and former calcite cement are usually sharp although dolomite cement occasionally replaces the upper part of the calcite cement (Fig. 5.13A) before filling up the remaining pore space. Xenotopic dolomite cements post-date evaporite pseudomorphs.

Under cathodoluminescence, xenotopic dolomite cements display very dull-luminescence indicating strong reducing conditions for the dolomitizing fluids. Xenotopic dolomite cements must have formed after extensive lithification because they post-date all types of calcite cement including the burial blocky spars. There is no evidence that stylolites cross-cut xenotopic dolomite cements. This may provide evidence that dolomite cements form at a moderate depth in a late diagenetic environment. Beales (1971) reported the occurrence of a similar white sparry dolomite cement in the Middle Devonian Presquiile Dolostone at Pine Point Mine, Canada. He suggested that basinal, warm, saturated, saline fluids were responsible for this type of cement.

No isotopic analyses have been performed on this dolomite cement due to its very small crystal size plus the association of xenotopic dolomite cements with other microdolomites in peritidal limestones.

Saddle Dolomite Cement: Saddle dolomites are widespread within the second and fourth members of the Rung Nok Formation. The two common modes of occurrence

Fig. 5.13 A. Photomicrograph of a stained thin section showing the selective replacement of ooids by xenotopic microdolomite (1), and less cloudy xenotopic dolomite cement (2) within intergranular porosities. Dolomite cements fill pores after radial bladed (3) and blocky (4) calcite cements. Thin section no. 398.2 B, the Malaka Formation at Ko To Sen.

B. Photomicrograph of a stained thin section showing individual dolomite crystals and clusters of incipient dolomite crystals (1) within intraclasts whereas saddle dolomite (2) infill a veinlet. Note the dedolomitization of the saddle dolomite (3). Thin section no. 400.8, the Rung Nok Formation.

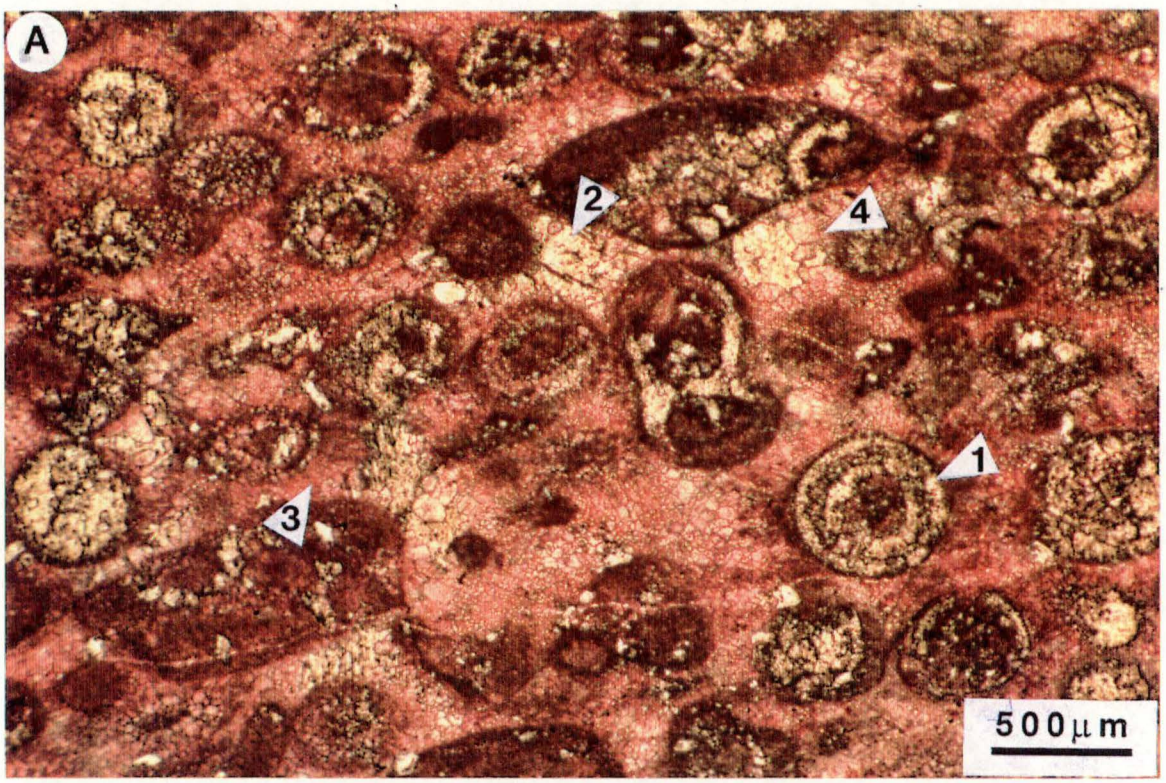
A
1
2
3
4
500μm

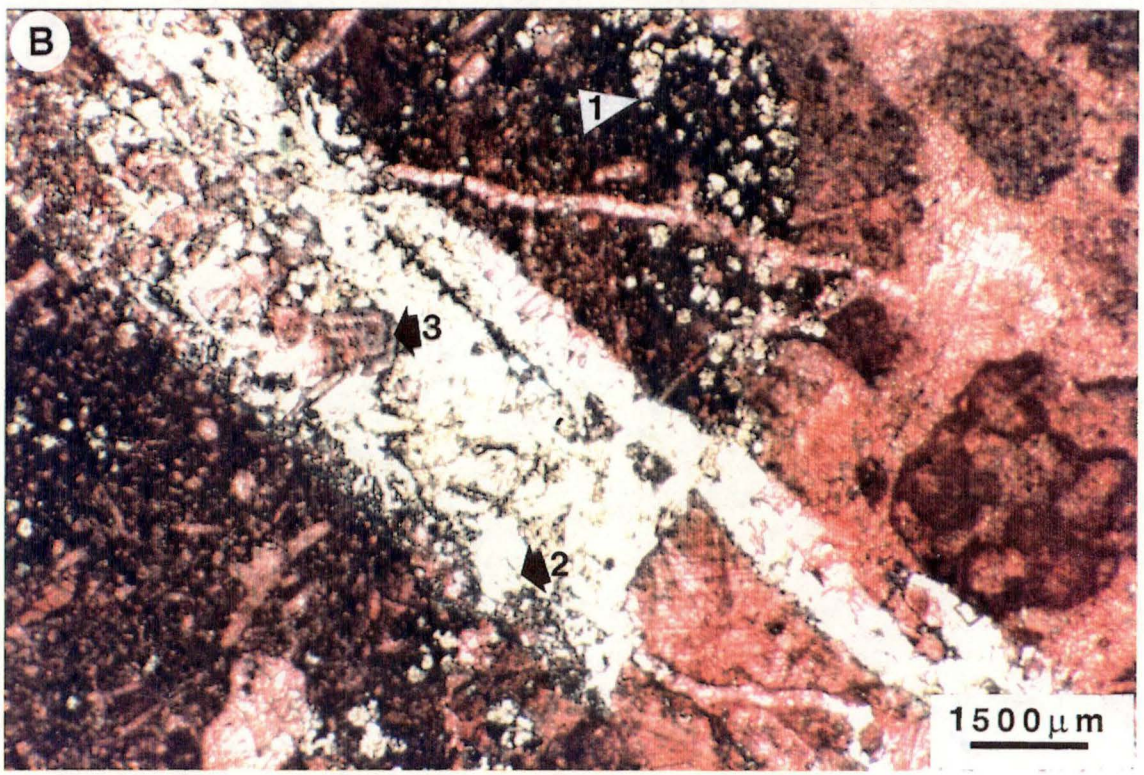
B
1
2
3
1500μm

of saddle dolomites are 1) void-filling, and 2) fracture-filling within dolomite or dolomitic limestones. Both share a common character but differ in colour and zonation.

Void-filling saddle dolomites are relatively coarsely crystalline (up to 5 mm), light brown to white in colour with slight inclusion bands. They are characterized by sweeping extinction, curved crystal faces, and well defined euhedral crystal boundaries (Fig. 5.12C). Saddle dolomites contain variable amounts of inclusion which may give crystals a zoned appearance. Contacts between saddle dolomite and its dolomite host are unclear. There is a gradual change from hypidiotopic or xenotopic meso- to megadolomites to larger saddle dolomites with the sharp termination of curved crystals toward the centre of vugs. Fracture-filling saddle dolomites have similar characteristics to the void-filling type but they have sharp zones and a milky white colour (Fig. 5.13B).

Under cathodoluminescence, saddle dolomite crystals have red bright cores with zones of bright- and non-luminescence at their rims. Based on petrographic studies, it is clear that saddle dolomites are epigenetic in origin occurring long after the lithification of the host rocks in a late burial diagenetic environment. Radke and Mathis (1980) suggested that saddle dolomites were precipitated from high pH and ionic concentrated fluid at elevated temperatures ranging from 60-150°C. Machel (1987) confirmed that saddle dolomites form at elevated temperatures from hypersaline brines. He also proposed that the dolomites were by-products of chemical compaction and thermochemical sulphate reduction in subsiding dolomitized rocks. Buchbinder, Magaritz and Goldberg (1984) demonstrated that saddle dolomite and host rocks have a similar isotopic pattern.

Both void and fracture filling saddle dolomites in the Thung Song Group have $\delta^{18}O$ values ranging between -11.9 and -20.8‰ PDB, and $\delta^{13}C$ values ranging between +0.4 and -0.6‰ PDB. Saddle dolomites have much lighter values than the other types of dolomites including the host rocks. This suggests that precipitation occurred at elevated temperatures during a deep burial diagenetic stage. The lightest $\delta^{18}O$ value indicates a precipitation temperature of around 142°C which lies within the range of Radke and Mathis's experimental data (1980). The bright cores (bright to dull) and zonal luminescent rims of the crystals document the fluctuation of the dolomitizing fluids from a deep burial diagenetic environment through fracture zones during subsidence of the basin of deposition.

Chapter 6

DEPOSITIONAL ENVIRONMENTS

Based on the lithostratigraphic, sedimentologic, and palaeontologic evidence (as discussed earier, Appendix 4,5); the depositional environments of the Thung Song carbonates are described in ascending stratigraphic order. The depositional environments of the Pa Kae Formation will be discussed later in chapter 7.

6.1 The Malaka Formation

The rocks of the Malaka Formation are mostly thin laminated stratiform stromatolites with some small domal structures (Fig. 3.4B, 4.1, 6.1A). They are made up of the interlamination of 3 distinct microfacies: pelmicrosparite, micrite, and microdolomite. Bioclasts within the bottom portion of the sequence are either absent or limited, with only a small amount of very fine and broken skeletal material. The occurrence of abundant vertical worm burrows (Fig. 3.4C), mudcracks (Fig. 3.4D, 6.1B), pendant and meniscus cement (Fig. 5.6) indicates intermitent flooding and subaerial exposure. The intercalation of occasional thin layers of minor biosparite, graded intrasparites (Fig. 6.1A) with erosional contact and small cross lamination (Fig. 4.6A) may be evidence of occasional storm deposition (Tucker and Wright, 1990). Mason (1986) reported the recovery of hummocky cross bedding associated with oolite rich carbonate sands and storm generated flat pebble conglomerates within this formation at Talo Topo Bay.

In the modern setting, stratiform stromatolites commonly accrete within the intertidal to supratidal zone at Andros Island (Hardie and Ginsburg, 1977), the Persian Gulf (Shinn, 1983) and Shark Bay (Logan *et al.*, 1964; Logan, 1974). The interlamination of microdolomites with limestones in stromatolitic laminites, some evaporitic pseudomorphs (Fig. 4.1A, 5.4), and mudcracks suggest a tidal flat environment, especially in the upper intertidal to supratidal zone. So far, there is no clear evidence of a modern analogue for this diagenetic microdolomite overprint on stromatolitic laminites. However, the similar ancient laminated unfossiliferous microdolomites interlayered or interlaminated with limestones have been also commonly interpreted as having tidal flat, upper intertidal-supratidal, origins including the Cambrian carbonates in Northwest Spain (Zamarreno, 1975), the Ordovician of Western Maryland (Matter, 1967), the Lower Devonian of New York State (Laporte, 1967), the Silurian of Ohio (Textoris and Carozzi, 1966), in the Visean of Canadian Maritime Province (Schenk, 1967) and those of Ireland (West *et al.*, 1967), and the Permian Platy Dolomite of North Poland (Gasiewicz *et al.*, 1987).

Fig. 6.1 Lithology and primary structures of the Malaka Formation.

A. Thin section photomicrograph of a stratiform stromatolite with small domal structures (A). Note the development of stromatolite on poorly graded intrasparite layers (G), microdolomite replacing sediment in vertical burrows and mudcracks (M). Thin section no. 396

B. Microdolomite (brown) in mudcrack on top of limestone bedding.

C. Stromatolitic laminites (A) occasionally intercalated with flat pebble conglomerate layer (B) with scoured base. Note the cross-bedding (C), a common feature in the upper part of the Malaka Formation at Malaka Creek.

D. Very thin bedded limestones interbedded with brown shales.

E. Flat pebble conglomerate (A) with scoured base lying upon a current ripple bed. Note the stratiform (B) and domical (D) stromatolites on top of conglomerate.

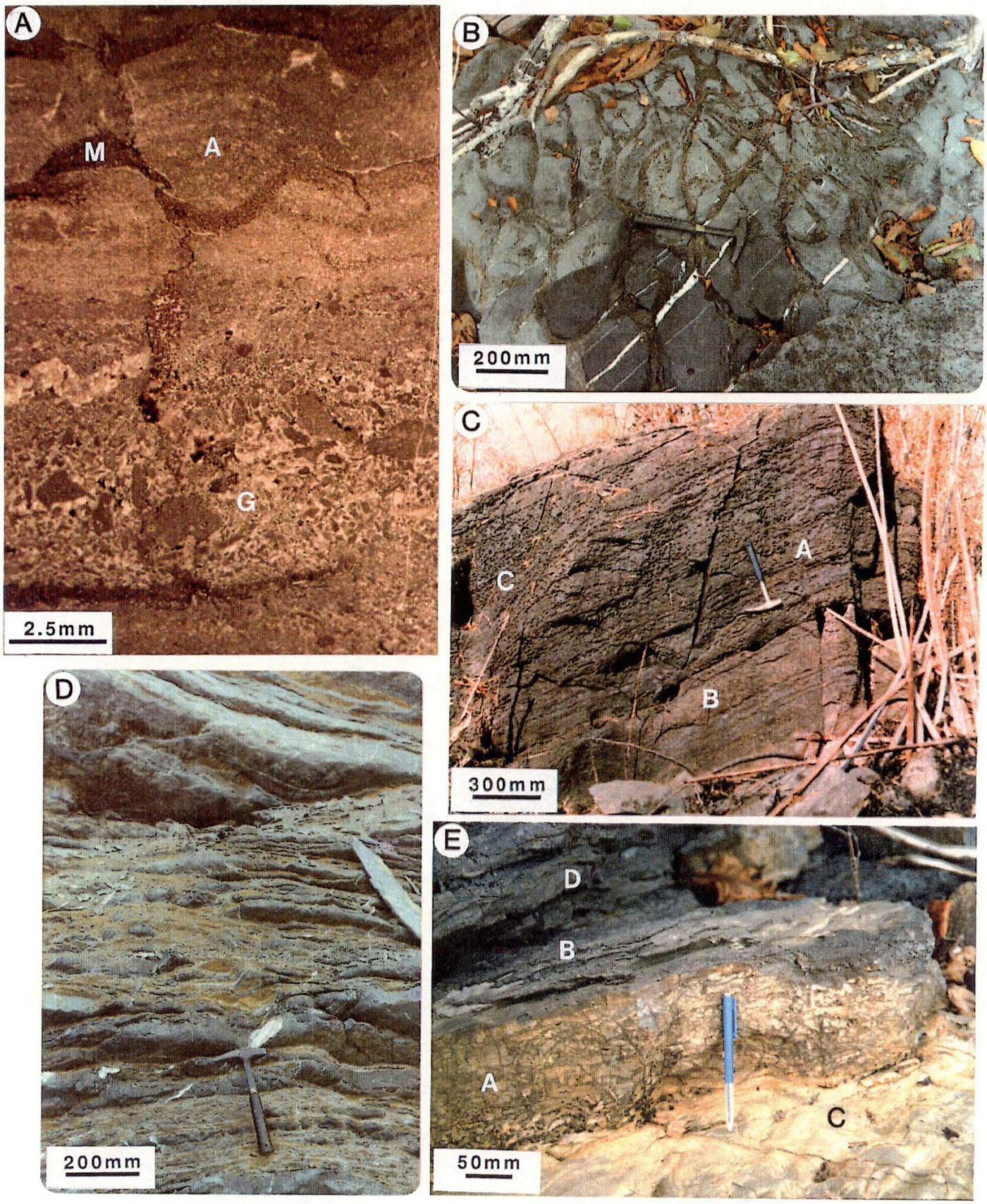
A
M
A
G
2.5mm
B
200mm
C
A
C
B
300mm
D
200mm
E
D
B
A
C
50mm

The sharp based limestone layers grading up to brown argillaceous limestone or shale (Fig. 6.1B) on top of bedding in some part of the sequence may be the evidence of the deposition in tidal ponds. The occasional association of the other grainy and sparry microfacies including intramicrite, pelbiosparite, intrasparite, few oosparite, and flat pebble conglomerate (Fig. 4.1B, 4.6B, D, 4.7) in the Malaka Formation increases to the top (Fig. 6.1C, D), with increased cross stratification, indicating increased energy of deposition as mentioned by Purser (1975) for changing from muddy to grainy cycle in the Bathonian carbonates of Burgundy, France. These microfacies usually lie interlayering on erosional surfaces or scoured bases with current ripple mark (Fig. 4.6A, 6.1A, C, E) within algal laminites and commonly show graded bedding or cross-bedding of intraclasts or imbricated flat pebble conglomerate. It represents a distinctive small tidal channel (Tucker and Wright, 1990) on the tidal flats. Some channels were large as demonstratated by large low angle tabular cross bedding (~ 1.5 m thick) at Malaka Creek. The graded flat pebble lag deposits and cross bedding also suggest the lateral migration of these tidal channels. The modern tidal channels are common in the lower part (intertidal) of transgressive tidal flats at Andros Island and relatively fewer in the regressive tidal flat of the Persian Gulf (Shinn, 1983)

.

At La Nga Bay, cross stratification, grainy or sparry microfacies, and fossil content increase upwards through the sequence and into the Malaka Formation and La Nga Formation (without the Talo Dang Formation which is here pinched out), whereas typical stratiform stromatolites decrease. However, stratiform stromatolites tend to develop along foresets of cross stratification since some of them consist of microdolomite in dark micrite and oosparite interlaminations. The increase of cross lamination units to the top of the Malaka Formation may indicate the change of environments from supratidal at the bottom to intertidal with tidal channels of the lower-energy littoral setting adjacent to lagoon (Fig. 6.6), and further to beach or foreshore environments (Inden and Moore, 1983) of the higher-energy littoral deposits on the top of the sequence especially where the barrier islands contact to the tidal flats. This is confirmed by the remarkable decrease or loss of the higher-energy setting (cross bedded setting, beach) in the south of Tarutao Island where there is a thick shalely sequence of lagoonal deposits, the Talo Dang Formation, sandwiched in between the Malaka Formation (tidal flats) and the La Nga Formation (Barrier Islands and spits) at Talo Dang Bay.

6.2 The Talo Dang Formation

The Talo Dang Formation consists of very thin bedded, variegated, micritic nodular limestones and fissile shale alternation (Fig. 3.5B, C, D). Based on the different arrangement and shapes of nodules, they were organized as a cycle (chapter 3). At least six repetitive cycles have been observed at the type locality. Many mechanisms have been proposed for the nodular bedding formation of limestones (see review by Flügel, 1982, p 226). They can originate by one or more of biological, chemical, and physical processes. These processes are the microbial decomposition of the organic matter (Grunder and Roster, 1963), marine subsolution (Hollman, 1962), submarine cementation (Garrison and Fisher, 1969), concretional growth (Jenkyns, 1974), compaction (Wanless, 1979; Logan and Seminiuk, 1976), the combination of early lithification and compaction (Tucker, 1974), and the combination of bottom currents enhancing submarine cementation and burrowing (Mullins *et al.*, 1980), etc.

There are many lines of evidence that support very early lithification prior to the compaction effects on this micritic nodular limestone (see earlier p.81). Micrites precipitated directly from sea water, possibly partly under photosynthetic control as evidenced by dense polygonal interlocking crystals of micrites which were subsequently bounded by stromatolite filaments (Fig. 6.2). However, stromatolites in the Talo Dang Formation are less extensive than those in the Malaka Formation and there are no clear stromatolitic structures showing on the rock surface. Even though the present appearance of bedding was largely induced by the early compaction, the alternation of micritic nodules and calcareous shale should partly record the environmental changes during their deposition.

Most of the Phanerozoic and Mesozoic red (originally) nodular limestones of Europe including the Devonian Griotte (France), Ammonitico Rosso (Alpine and Mediterranian region), the red Chalk of eastern England; and of the North Atlantic (off west Morocco coast) were deposited in deep water or basinal environments (Lancelot *et al.*, 1972; Jenkyns, 1974; Tucker, 1974; Eller, 1981). However, the similar red (weathering) nodular limestones in the Ordovician and Silurian of the Oslo Region deposited in a neritic environment below storm wave base and in lagoonal environments (Moller and Kvingan, 1988). Many lines of evidence suggest that the Talo Dang Formation was also deposited in lagoonal environments.

The nodular limestones of the Talo Dang Formation consist of mostly micrite with some bioclasts (micrite with fossils) and intraclasts (intramicrite) at the top of each cycle whereas the shale alternations decrease considerably. Pyrite and evaporite pseudomorphs are common. In general, skeletons including gastropods, brachiopods, trilobites, *Chelodes,* some straight and curve nautiloid are rare in limestone nodules and nearly absent from shale layers. This indicates the extremely high environmental stress during their deposition.

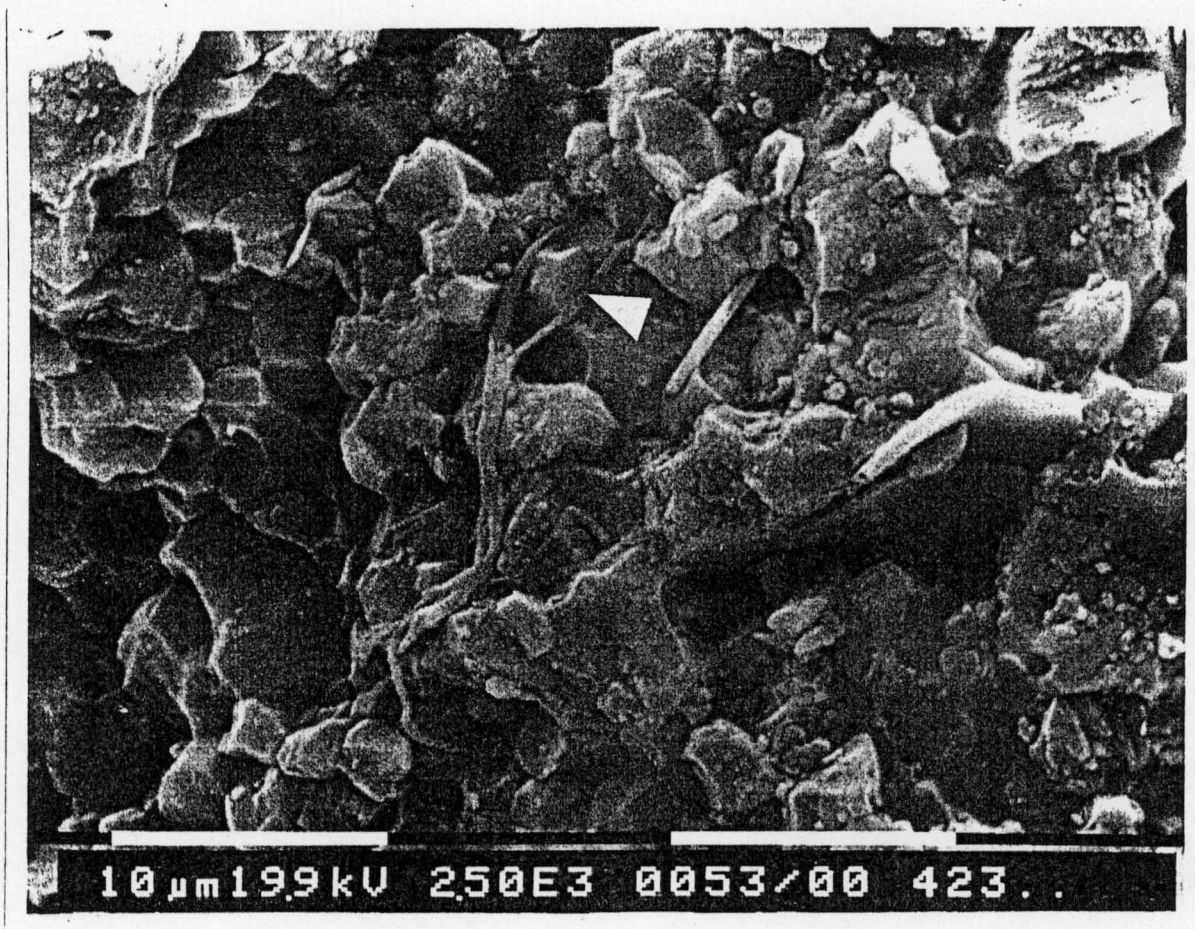

Fig. 6.2 SEM photomicrograph showing micrite with polygonal interlocking crystals of nodular limestone, the Talo Dang Formation. Note the stromatolitic filaments (arrow) within micrite. Broken slab no. 423

Based on the stratigraphic position of the Talo Dang Formation sandwiched in between the tidal flat carbonates (the Malaka Formation) and the oolite shoal (the La Nga Formation); the abundant micrite and clay minerals; and the rarity of fauna indicates the restricted lagoonal environments in between the large tidal flats and barrier islands (Fig.6.6). Pyrite and evaporites pseudomorphs suggest reducing and hypersaline condition in the lagoon. Wet and dry climates in tropical region are proposed for this setting and responsible for the alternation of limestone nodules and shales. In the wet season, surface water transported clay and small amounts of detrital quartz from a nearby area to the lagoon to deposit as shaly layers. The dilution of sea water in the lagoon during this time is evidenced by the near absence of marine fauna and the lack of evaporite pseudomorphs in shales. In the dry season, surface water influx decreases, coupled with the high degree of sea water evaporation raising the salinity and inducing stromatolite growth. Under this circumstance, micrites and evaporites precipitate in the lagoon. No subaerial exposure features have been observed whereas the horizontal worm burrows and marine fauna in limestone nodules which increase to the top of a cycle suggest subtidal conditions and more normal salinity of sea water.

The vertical development of a cycle from mainly calcareous shale horizons with sparse isolated limestone nodules at the bottom to strata-bound nodules in the middle and passing upward to continuous irregular or lenticular limestone with or without minor shale parting on the top of each cycle, and the increasing of biota activity represents the passage from restricted (lack of burrows and less marine skeletons, but more abundant evaporites pseudomorphs and pyrites) to more open lagoonal environments (more abundant marine bioclasts, horizontal burrows, but less evaporites and pyrites). The degree of depositional energy also increased in more opened lagoons as evidenced by the increase of intramicrite microfacies at the top of a cycle. The openess of this lagoon was possibly a result of a small-scale high sea level, which introduced a considerable amount of normal sea water to the lagoon, and decreased the environmental stress on marine organisms. Therefore, the repetition of the cycles (at least 6 times) should be the result of the eustatic sea level fluctuation in concert with the gradual subsidence of the basin during the Late Tremadoc. This Late Tremadoc transgressive events correspond to the conclusion reached by Barnes's (1984) analysis of the Early Ordovician eustatic events in Canada and is close to those of Fortey's (1984) transgression and regression analysis.

6.3 The La Nga Formation

The rocks of the La Nga Formation are mostly sparite with predominant oolites and can be subdivided into 2 members : 1) The lower La Nga member has a complex network of trough cross bedding (Fig. 3.6B, 6.3). The rocks are mainly oosparite (Fig. 4.7A) cross interlaminated with pelsparite, and subordinate intrasparite, flat pebble conglomerate. Oolites of the lower member are better sorted than in the upper member. Vertical, horizontal, and U-shape burrows are sparse. 2) The upper member is a cycle of the shallowing and fining upward sequence. At least 3 repetitive cycles have been observed in the type locality at La Nga Bay. The lower part of each cycle is massively bedded light gray intrasparite (irregular flat pebble conglomerate, Fig. 4.6C) with abundant bioclasts with thick micrite envelopes. The upper part of the cycle abruptly changes to thin bedded layers of gray pelsparite and pelbiosparite with some small intrasparites. Small scale tabular cross bedding, horizontal and vertical burrows are common (Fig. 3.6D). However, the third cycle on the top of the sequence grades further upward to stromatolite laminite with mud cracks and well rounded flat pebble conglomerate (Fig. 4.6D).

The Lower La Nga Member: The sparry nature and the lack of micrite, abundant well sorted oolites (mainly radial concentric type), and large flat pebble conglomerates of the Lower La Nga member indicate a high depositional energy (Folk, 1959, 1962). The diversified marine fauna including *Nuia*, and the extensive radial fibrous to bladed cement with rhomb-tip surrounding oolites (Fig. 4.7A, 5.1A) suggest a subtidal condition in an open marine environment where the sea water circulation is sufficient enough for HMC fibrous cement formation. Furthermore, oolites are usually regarded as an indicator of regularly agitated, shallow marine environments in tropical climates where sea water is saturated or supersaturated with respect to $CaCO_3$ (Lees, 1978; Heller *et al.*, 1980; Reijers and Ten Have, 1983; Lindstrom, 1984). The well sorted oolites within a complex trough cross bedding unit suggest deposition as free-rolling particles in a high energy environment with a current strong enough to sort oolites and create the cross bedding (Beukes, 1983). Ross *et al.* (1988) suggested the close relation between *Nuia* and shoal waters. In the modern tropical shallow marine setting, oolites commonly form as/or within a shoal complex, often in tidal channels, bars and deltas in the Bahamas and in the Persian Gulf where the salinity and water temperature are high (Illing, 1954; Loreau and Purser, 1973; Purser and Evans, 1973; Tucker and Wright, 1990).

In comparison with these modern marine settings and based on the stratigraphic position and on the evidence discussed earlier, the Lower La Nga member oolites are interpreted to have been deposited in an ooid shoal complex. The nearly-straight and narrow but long geometry covering a long distance of about 22 km (Fig. 3.2) and a

Fig. 6.3 Lithology and primary structures of the Lower La Nga Formation at type locality (A,B), and the stromatolite of the Pa Nan Formation (C,D). Photograph was taken by Roger Mason.

A. An extensive trough cross-bedding. Note the reactivation surface (1), and erosional surface and lag deposition (2). black lamination (B) of the cross-bedding is usually replaced by microdolomite.

B. Large flat pebbles of stromatolitic laminites within oosparite. Note the inbrication structures (A) and alignment of pebbles along the cross-bedding (b).

C. Stromatolite controls on the wavy bedding of the Pa Nan Formation. Dense columnar stromatolites (A) formed a persistent column across bedding. Note the inter-area between columns (B).

D. Alignment approximately in E-W direction of furcate columnar stromatolites (SH-V) on a top of bedding at Ko Pa Nan.

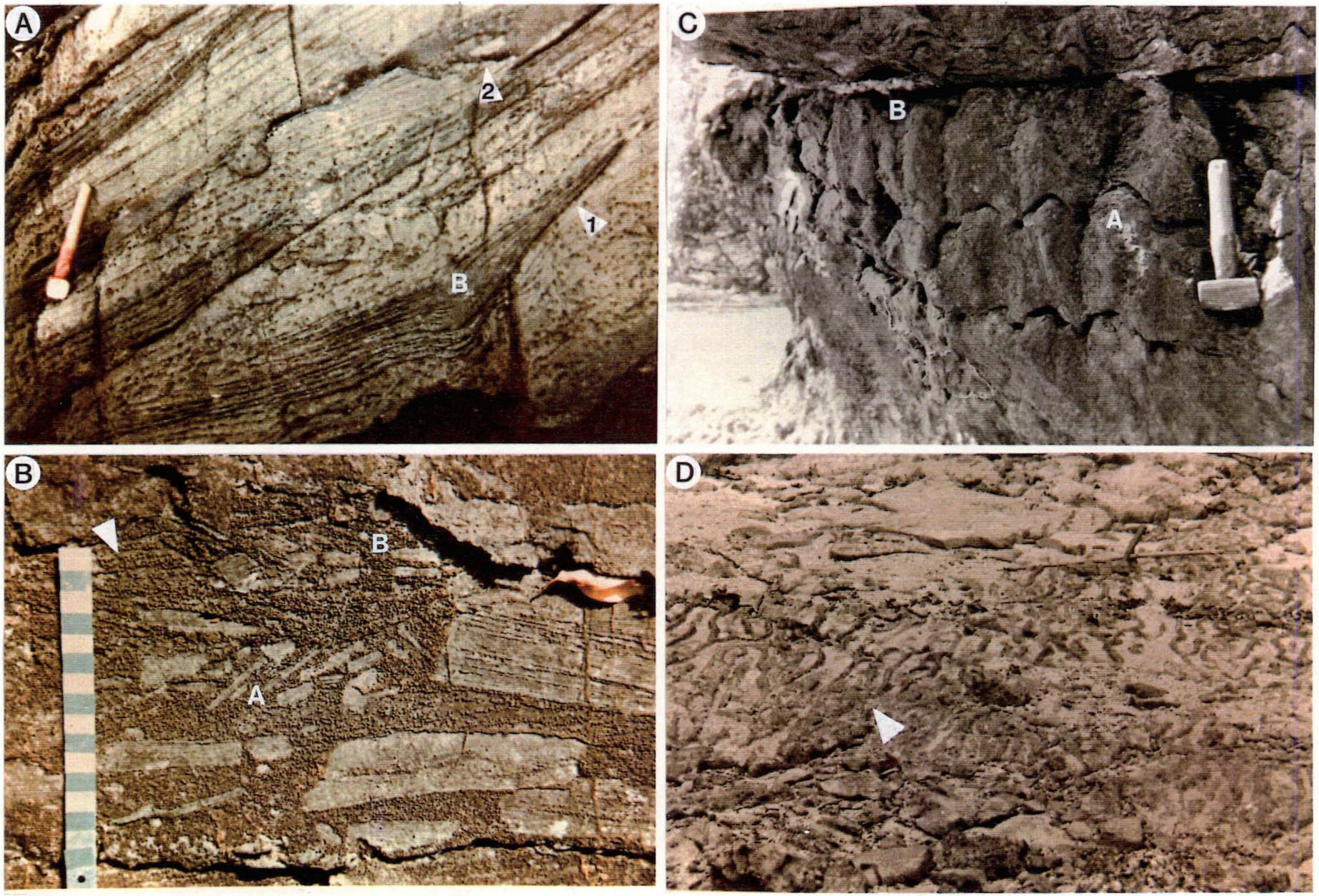
A
2
1
B
C
B
A
B
B
A
D

complex trough cross bedding of 27 m thick rock unit with the common reactivation surface suggest the long, migrating barrier islands complex environments, in response to tidal fluctuation and storms (Chow and James, 1987), for the lower La Nga member. The linear shape and straightness of the rock body was also used to distinguish a barrier island facies in the subsurface by Dickson *et al.*, (1972). The relatively low abundance of vertical worm burrows, and the lack of subaerial exposure features probably suggests submergence below sea level. The scoured bases with some flat pebble conglomerate lag deposits (Fig. 6.3A, B) and remarkable channel within channels structures, suggest that tidal channel systems were present. However, the microdolomite interlaminae with oosparite along black (carbonaceous) laminae of cross bedding (Fig. 6.3A) probably suggests the presence stromatolitic mats covering channel oolite sands in the upper intertidal to supratidal zone of the barrier islands. Where the barrier island complex is in contact with a large tidal flat (Malaka Formation) as at La Nga Bay, the spit morphology should be expected (Fig. 6.6). Perdy (personal communication) observed that it would not have worm burrows on a Recent migrating white shoal. However, the spit morphology of the rock body probably provided a stable substrate for some worm burrows.

The 27 m thick sequence of the extensive trough cross bedding at the bottom developing upward to the planar cross bedding on the top of the sequence probably represents a complete set of the barrier islands from the shoreface-foreshore up to the beach (Inden and Moore, 1983). Low abundant U-shaped burrows in the lower portion of this member and the lack of them in the upper part with vertical burrows is consistent with this interpretation. Dörjes and Hertweck (1975) suggested that in shallow marine environments U-shaped burrows of low-level suspension feeders or collectors are common from upper offshore to lower shoreface whereas vertical burrows are almost the only forms in shore zone between high tide level and wave base.Therefore, it is tempting to interpret that the thickness of the sequence probably represents the height of the islands. This is also confirmed by the lack of compaction features due to the extensive early marine cementation. Stylolites are not common in the La Nga formations. It implies that the depth of water at the buildup and the nearby lagoon (the Talo Dang Formation) is probably at least 27 m deep. However, Purdy (personal communication) noted that 3-4 m at most would be closer to the mark. As modern barrier islands commonly lie parallel to the shoreline, a nearly N-S directed palaeoshoreline (Fig. 3.2, 6.6) is proposed.

The Upper La Nga Member : The abundant bioclasts with thick micritic envelopes, marine radial bladed and fibrous cements of massive limestones (light gray, irregular flat pebble conglomerate, intrasparite with some pelsparite and pelbiosparite)

at the begining of the shallowing-upward sequences suggest either the marine phreatic diagenesis (Bathurst, 1975; Longman, 1980; Shukla and Friedman, 1983) or subtidal environment. Even though, the association of many oolites and *Nuias* and the abundant intraclasts and irregular flat pebbles of algal (stromatolites) origin (Fig. 4.6B, C) within these microfacies suggests an environment above the wave-base where the fragmentation or disintegration of stromatolitic mats is common, but the lack of hydraulic primary structure of the rocks favours subtidal environments below the wave-base. Therefore, the incorporation of oolites and *Nuias* into these rocks is probably evidence of the transportation of them by currents from the original areas above wave-base to lower subtidal depths. The water circulation or currents of the area was sufficient enough to form the extensive marine cement and sparry rocks, but it was still not strong enough to form the hydraulic structure as of the lower member.

The change from massively bedded rocks at the base of each cycle to thin bedded gray pelbiosparite and intrasparite with some oolites and planar cross bedding (Fig. 3.6D) in the upper part indicates the increased energy of deposition. Vertical burrows filled by microdolomites, and stromatolitic laminites have been observed. Based on this evidence, these rocks are interpreted as having been deposited in foreshore (beach) and lower intertidal environments, as in the Malaka Formation. However, no tidal channel structures have been observed. Some cycles developed from transitional facies to the extensive stromatolitic laminites with flat pebble conglomerate and mudcracks which represent the higher intertidal to supratidal environments. Tucker and Wright (1990) also stated that the gradual shoaling of a ramp results in relatively strong wave action in the shoreface-intertidal zone and this permits the formation of shoreline carbonate sand bodies. The general shoreward thinning of each cycle is common.

The shallowing-upward sequence is common in rock records throughout the geologic history. They are usually organized in form of cyclicity such as the shallowing-upward cycles of early Proterozoic age, the Rocknest Formation from Northwest Canada (Grotzinger, 1986); Middle and Upper Cambrian Waterfowl Formation, Alberta (Waters, *et al.*, 1989); Lower Ordovician Chepultepec interval, Virginia Appalachians (Bova and Read, 1987); Silurian Hunton Group, Oklahoma (Morgan, 1985), Jurassic ooid grainstone sequence of East Texas basin (Harwood and Moore, 1984); lower Tertiary limestone from the western Gulf of Suez, Egypt (Kuss and Lepping, 1989), etc. Three basic explanations have been commonly proposed for the repetition of the sequences including : eustatic, sedimentary or the rate of carbonate sedimentation, and tectonic (Tucker and Wright, 1990). James (1984) suggested that the *eustatic model* of Wilkinson (1982; the combination of subsidence rate and sea level change as the rate of carbonate sedimentation constant) and the alternative

autocyclic model of Ginsburg (1971; a combination of source area control and the change of mean sea level and subsidence) are suitable to explain small-scale shallowing-upward sequences whereas the combination of those factors and tectonic is responsible for the large-scale one. The sea-level fluctuations through changes in ocean volume in a response to tectonic or the rate of seafloor spreading are a long time scale and can not lead to rapid sea-level rises as required for many shallowing-upward cycles (Tucker and Wright, 1990) .

Based on the palaeobiographic and palaeogeographic study on the Shan-Thai terrane by Burrett *et al.* (1990), the southern part of Thailand was in close relationship with N.W. Australia during the Early Ordovician. Few volcanic rock associations have been observed. A small amount of detrital quartz and other clastic components, and the lack of deformed synsedimentary structure as well as turbidites also suggest a stable tectonic regime for this terrane during the Early Ordovician. Furthermore, apart from supratidal deposits, no significant change of faunal assemblage throughout the sequence has been observed. Therefore, the shallowing-upward sequences of the upper La Nga member started from lower subtidal and abruptly change upward to foreshore, intertidal, and end up with supratidal on the top of the sequence may be explained by the *Eustatic model* and reflects the fluctuation of mean sea-level during their deposition in Early Arenig. The subtidal interval of each cycle was initiated by rapid submergence due to sea-level rise of a few metres (Bova and Read, 1987) and subsidence of the basin. When the sea-level dropped abruptly, the rocks prograded to foreshore, intertidal, and supratidal interval. However, Purdy (personal communication) suggested relative sea-level changes as a control of this shallowing upward cycles.

6.4 The Pa Nan Formation

The rocks of the Pa Nan Formation are consist of densely , packed small-scale stromatolites. In contrast with the stratiform stromatolites of the Malaka Formation, they are completely made up of columnar stromatolites. Most of them are vertical stacked hemispheroids (SH-V, Fig. 6.3 C), elongated (Fig.6.3D), moderate branching, furcate columnar stromatolites. The branching digitate stromatolites with LLH-C structure are subordinate and commonly develop on top of the fucate one, at the top of the sequence at Ao Dan and Ko Pa Nan. Stromatolitic laminae are micrite and microdolomites (Fig. 4.1D) with abundant rounded intraclast (Fig. 4.1C) in some layers. The rounded intraclast and bioclasts are also abundant in inter-column area and channels on the top of the sequence. Tubular and laminoid fenestrae are poorly developed (Fig. 4.1D). Other microfacies such as pelsparite and biosparites are rare.

Most of the modern stromatolites at Shark Bay (Logan, *et al.*, 1964), Persian Gulf (Kendal and Skipwith, 1969), and Andros Island (Black, 1933) occur in intertidal and supratidal environments. However, subtidal stromatolites have been discovered at Burmuda (Gebelein, 1969); Hamelin Pool, Shark Bay (Playford and Cockbain, 1976; Burne and James, 1986; Walter and Bauld, 1986); in tidal channels of the eastern Bahama Banks (Dill *et al.*, 1986); in Crator Lake, Satonda Island, offshore Sumbawa/Indonesia (Kempe and Kazmierezak, 1990). The environmental significance of various stromatolite forms was proposed by Logan *et al.* (1964). They pointed out that the discrete, club-shaped head stromatolites (SH) with SH-V arrangement are common reef on an intertidal headland with moderate sea wave at Shark Bay. Recently, Burne and James (1986) described the subtidal (0-4 m depth) lithified platform covered by isolated club-shape stromatolites at Hamelin Pool, Shark Bay. They suggested that this type of stromatolites on the intertidal zone of Hamelin Pool headland are also subtidal origin but are exposed today because of a recent lowering of Holocene sea level.

Lack of subaerial features, scarcity of fenestral febric,*in situ* cup-shaped sponges growing on stromatolitic columns, and similarity in form of the Pa Nan stromatolites to Hamelin Pool stromatolites suggest shallow subtidal environments with moderate sea wave conditions. Walter and Bauld (1986) also reported the encrustation of sponges on subtidal stromatolites at Hamelin Pool. Additional evidence is that the Pa Nan stromatolites are overlain by lagoonal deposits, the Lae Tong Formation. The contradictory evidence for subtidal seems to be the occurrence of microdolomites along stromatolitic laminae and intercolumn areas but these microdolomites are formerly interpreted as early diagenetic dolomitization in a shallow subtidal area (chapter 5, p.85). The elongation of the Pa Nan stromatolites may reflect tidal current movement in intertidal environments as suggested by Logan *et al.* (1974) but this elongation could also be developed parallel with the direction of sediment transport in subtidal environments (Gebelein, 1969; Young and Long, 1976). Playford(1979) was pointed out that both environmental factors and biological factors control the external morphology of stromatolites at Hamelin Pool although environmental factors are dominant. He suggested that elongation of many subtidal to intertidal Hamelin Pool stromatolites are not only parallel to the wave-translation but also prevailing wind direction. The substrate also controls their shapes and trends. The Pa Nan stromatolites provide no strong evidence to evaluate the importance of these different factors.

Based on the stratigraphic position of the Pa Nan Formation which lies conformably on the barrier island deposits of the La Nga Formation and is conformably overlain by the lagoonal deposits of the Lae Tong Formation and coupled

with the vertically and laterally extensive mass of the Pa Nan columnar stromatolites (at least 50 m thick, 30 km long) it is suggest that the Pa Nan stromatolites formed as a reef, similar to those of Shark Bay. The elongation of the Pa Nan stromatolites possibly suggests the development of these stromatolites in high depositional energy such as strong or moderate current flow, and prevailing wind of a depositional area (Gebelein, 1969; Playford, 1979). Moreover, the development of parasitic columnar stromatolites upon an erosional surface of the former accreted stromatolites (Fig. 4.1C) possibly reflects the resistant property of this reef to wave and storm action within a shallow subtidal zone. In turn, the erosion surfaces may indicate early calcification and/or cementation of the Pa Nan stromatolites as of Hamelin Pool stromatolites (Burne and James, 1986). Playford (in Chivas *et al.*, 1990) reported the removal of several years of algal growth on subtidal Hamelin Pool stromatolites by a single storm. Therefore, it is most probable that the Pa Nan stromatolites were formed as a reef and occur as a part of barrier islands (Fig. 6.6).

Extensive stromatolitic buildups are common in the Proterozoic rocks of many continents such as Australia (Southgate, 1989), Africa (Trompette and Boudzoumou, 1988), and North America (Hoffman, 1974; Cecile and Campbell, 1978). They declined during the Palaeozoic, especially after the middle Ordovician, because of the rapid evolution of the metazoan grazers (Pratt, 1982) and the development of other shallow water encrusting skeletal organisms that could form reef (Monty, 1973). However, many Phanerozoic reefs have stromatolites as an important component such as the Devonian Canning Basin reefs (Playford *et al.*, 1976) and Late Mississippian Codry Group, reefs of western Newfoundland (Dix and James, 1987).

Although, there is no modern analogue for stromatolitic barrier islands or barrier reefs today, they do exist in the rock record as proposed by Trompette and Boudzoumou (1988) for the Late Proterozoic stromatolitic unit in the lower part of "Schisto-calcaire" (Shale-limestone) Group , in the west Congo Basin. They described the size (3-8 km wide, and 20 m thick) and morphology of the Congo Basin stromatolitic barrier reefs as being compatible to that of modern barrier reefs. Moreover, they proposed the modern coral barrier reef of Belize (James *et al.*, 1976) as a modern analogue for their stromatolitic barrier reefs. This statement seems to fit the Pa Nan stromatolites as well even though they are thicker than the Congo Basin stromatolites. The closest modern analogue for the Pa Nan stromatolitic barrier reef seems to be elongate lithified barrier made of lagoonal crustose coralline algae which consists of micro-ridge at Bahiret El BiBane, Tunisia (Thornton *et al.*, 1987).

The development from furcate columnar stromatolites (SH-V) to digitate (LLH-C) columnar stromatolites on top of the sequence at Ao Dan and Ko Pa Nan, and the occurrence of a small channel structures filled by intramicrite and some intrasparites

with bioclasts represent the development from shallow subtidal conditions to intertidal mud flat in protected areas, as suggested by Logan *et al.* (1964) for upper intertidal Hamelin Pool stromatolites. However, the lack of exposure features such as mud cracks may indicate the lower intertidal environment rather than the upper intertidal. Channel deposits are also associated with lower intertidal columnar stromatolitic biostormes (LLH) of the Dotsero Formation (upper Cambrian), western Colorado (Campbell, 1987) but he interpreted SH-V columnar stromatolites below these LLH columnar stromatolites as lower intertidal deposits based on Logan *et al.*(1964). Tucker (1977) took an opposite view and interpreted the channels within the subtidal stromatolitic biostromes of the Porsanger Dolomite Formation (Late Precambrian), Arctic Norway as an ancient analogue to channels dividing up modern coral reefs and connecting offshore areas with the back reef lagoon.

6.5 The Lae Tong Formation

The rocks of the Lae Tong Formation can be subdivided into two distinctive members :

1) The lower member is very thinly bedded, gray limestone alternating with gray to dark-gray shales. The limestones occur as sparse irregular nodules, and lenses, with lenticular beds (Fig. 6.4A, B). Bed geometries are developed from irregular and lenticular nodules at the bottom to more well-defined and regular beds with good continuity at the top of this unit (Fig. 6.4A, B). Irregular limestone layers at the bottom exhibit graded bedding with scoured bases and lag deposits. In the upper part, more regular limestone layers commonly have hummocky cross-laminated (Fig. 3.8D, 6.4B, F), and have a small interference ripple mark on top of bedding (Fig.3.8C).

The composition of limestones in the lower part and the upper part is also different. They change from intramicrite, poorly washed pelbiosparite and biomicrite (Fig. 6.4E) with round intraclasts and sparse detrital dolomites at the bottom to mainly micrite with abundant detrital microdolomite along hummocky cross-lamination (Fig. 6.4F) at the top of this unit. Clay minerals in limestones (Fig. 6.4E) are common and occur as both matrix and stringers. Shale partings are calcareous, organic rich and faintly laminated. Framboidal pyrites are more common in shales than in limestone layers. In general, fossils are rare including gastropods, echinoderms, but there are some fossiliferous limestone layers in the bottom part. Vertical and random burrows are moderately abundant in the upper part (Fig. 6.4F). The lower Lae Tong member grades into the upper member.

2) The rocks of the upper Lae Tong member are very similar to the rocks of the Talo Dang Formation but without cycles. They are very thinly bedded gray nodular

Fig. 6.4 Lithology and primary structures of the Lower Lae Tong Formation. Photographs of outcrops are shown on the left whereas their thin section photomicrographs are shown on the right.

A. Nodular to lenticular limestones interbedded with shales in the lower portion of the lower Lae Tong member. Limestone layers commonly show graded bedding and scoured bases (arrow).

B. Well developed limestone layers and shale partings in the upper portion of the lower Lae Tong member. Note the complex network of small-scale hummocky cross-lamination (B) within the limestone layers. Scoured bases are also common as A.

C. Sparse limestone nodules within calcareous shales dominating a portion in the lower part of the upper Lae Tong member.

D. In a middle portion of the upper Lae Tong member, stratabound limestone nodules were developed. Limestone nodules were broken as a result of physical compaction. Oblique arrangement of nodules may be controlled by later shear stress.

E. A stained thin section photomicrograph of the limestone in A. Pelmicrite (A) with calcite (C) and dolomite (D) pseudomorph after gypsum interlaminated with pelsparite (B) and argillaceous layers (E). Note the separation of small detrital dolomites (small white dots) within pelmicrite layer (A). Thin section no. 404B

F. Detrital microdolomite commonly occurs along hummocky cross-lamination (A) within micritic limestone layers in the upper part of the lower Lae Tong member. Note the lag deposition of detrital microdolomite on erosional surfaces (arrow), and vertical escaped burrows (B). Thin section no. 401F

G. Abundant subrounded to angular detrital dolomites in micrite of the upper portion of the lower Lae Tong member at Ao Ton Pung. Some grains still preserved original rhomb-shaped of microdolomites. Thin section no. 404C

H. Microteepee structure and calcite pseudomorph after gypsum laminites (C) within dolomicrite in nodular limestone (the upper Lae Tong member) at Ao Makham. Note the iron layer coated teepee structures (A) and the accumulation of framboidal pyrites (B) on that structure. Thin section no. G

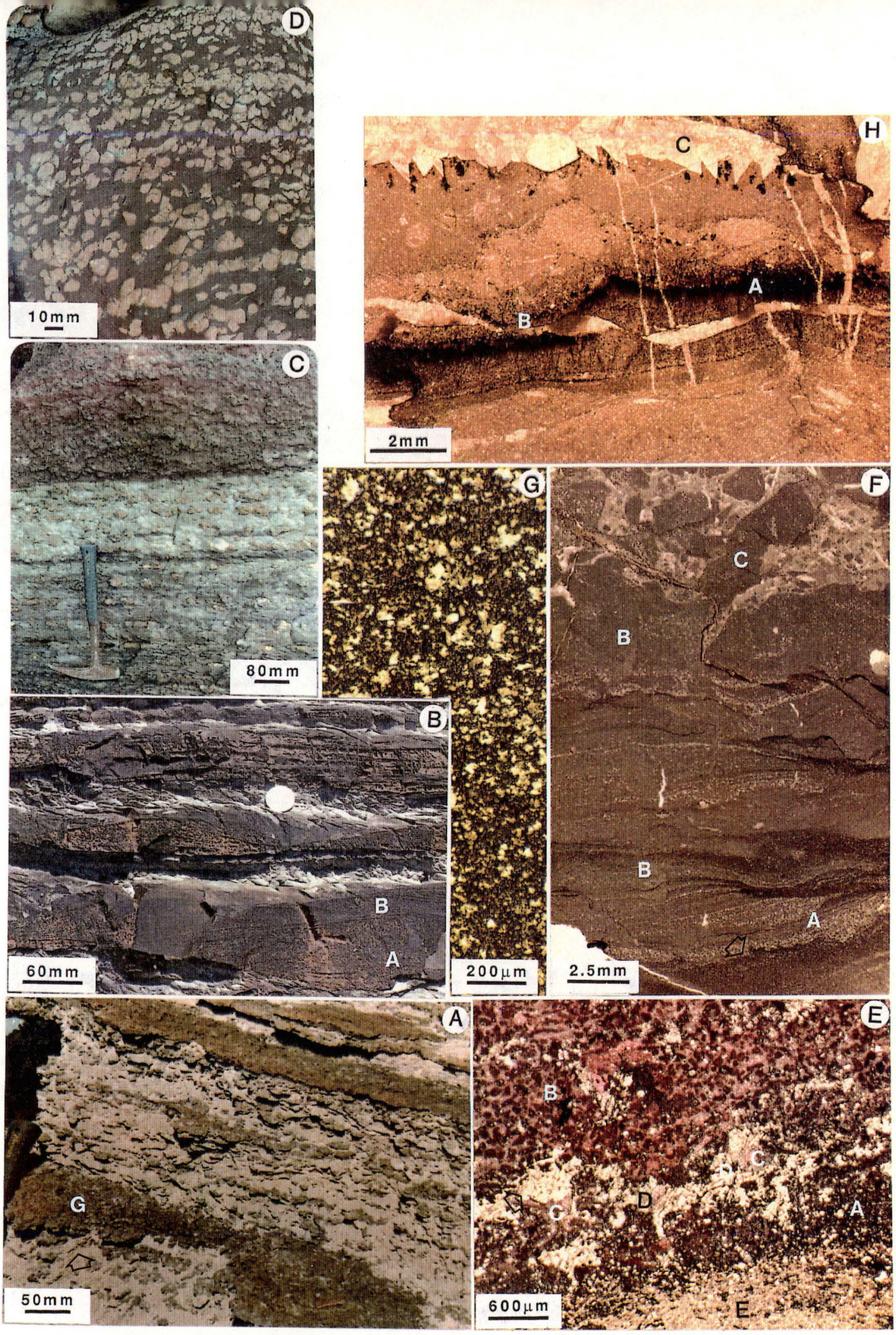
D
10mm
H
C
A
B
2mm
C
80mm
G
200μm
F
C
B
B
A
2.5mm
B
B
A
60mm
A
G
50mm
E
B
C
C
D
A
E
600μm

limestones interbedded with red weathering, greenish-gray shales. The bottom part of this unit is dominated by shales (Fig. 6.4C). Limestone nodules develop upward from sparse isolated micritic nodules to stratabound nodular limestones (Fig. 6.4C, D) in the middle to continuous lenticular to nodular limestone layers on the top of the sequence (Fig. 3.8A). Calcareous shale partings decrease considerably toward the top whereas fossils increase. Limestones are micrite and biomicrite (Fig. 4.3D).

The Lower Lae Tong Member : Based on many lines of evidence, the rhythmic sequence of nodular to lenticular limestones and calcareous shales alternation of this member are interpreted as restricted marine/lagoonal deposits (Fig. 6.6) similar to those of the Talo Dang Formation :

1) No evidence of subaerial exposure has been observed.
2) Thick micritic envelops around skeletons suggest a subtidal conditions.
3) Abundant micrite with clay mineral, and dark-gray shales with high organic matter contents suggest very low depositional energy within a closed to semiclosed basin.
4) Rare bioclasts but abundant framboidal pyrites are indicative of a restricted marine and euxinic basin.
5) Stratigraphically, the Lae Tong Formation is sandwiched in between the barrier island complex, of the La Nga Formation, and the carbonate buildups of the Rung Nok Formation.

The alternation of limestones and shales may represent a climatic change during their deposition. Carbonaceous shales were deposited during the wet season as mentioned for the Talo Dang Formation (p.100-102). Limestones were deposited in the dry season in the hypersaline part of lagoons as shown by prismatic crystals of calcite and dolomite pseudomorphs after gypsum (Fig. 6.4E) within limestones at the bottom part of a sequence. Abundant bioclasts with thick micritic envelops in this part suggest a shallow lagoonal stage. The later deeper lagoonal stage is indicated by the change of limestone compositions from grainy limestones at the bottom to micrite with minor biomicrite in the upper part of the lower Lae Tong member. Dolomite pseudomorphs may occur after burial.

The occurrence of graded bedding, scoured bases (Fig. 6.4A, B), and a common small-scale hummocky cross-lamination of limestone layers (Fig. 6.4B, F) represent episodic storm events during that time. These storms transported considerable amounts of angular to subrounded detrital dolomites from a tidal flat to be redeposited along hummocky cross-lamination in the upper part and as individual grains in the lower part. Although many features mentioned earlier favour a deep lagoonal environment for the upper part of the lower La Nga member; the abundant vertical and

random burrows (Fig. 6.4F), small-scale hummocky cross-lamination with sharp and scoured bases, and interference wave ripples on top of bedding suggest deposition above storm-base or in an area between the proximal to distal zone (Aigner, 1985, p.34-42). The Lae Tong hummocky cross-bedded micritic layers interbedded with calcareous shale are similar to the calcilutite interval of thin-bedded limestone/marlstone alternations in the more central parts of the upper Muschelkalk Basin. Aigner (1985, p. 85-91) regarded the Muschelkalk calcilutite interval as the most distal "fine tails" of storm flows in offshore deeper water. This is consistent with the interpretation of the upper part of the lower Lae Tong member as deeper lagoonal deposits.

The Upper Lae Tong Member : In contrast to the lower Lae Tong member, the upper Lae Tong has no evidence of hydraulic primary structure and burrowing within the lower part of a sequence (Fig. 6.4D). This indicates a deep lagoonal environment. The bioclast increase within stratabound nodular limestones in the middle of this member and suggests a shallower environment than the lower part but it was still presumably below storm-wave base. The more abundant fossils within lenticular-nodular limestone layers at the top of the sequence indicates the shallowest water conditions. Therefore, the development from sparse nodules at the bottom to lenticular bedding on the top of the upper Lae Tong member demonstrates the shallowing-upward sequence from deeper to shallow lagoon. However, the occurrence of rare micro teepee structure and calcite pseudomorph after gypsum laminites (Fig. 6.4H) at Ao Makham indicates that at least some parts of this lagoon experienced supratidal conditions.

Wet and dry climates are also envisaged as a control on limestone nodules and shale alternation. However, the absence of evaporite pseudomorphs in micrite nodules and shales implies that the upper Lae Tong member was possibly deposited in the central part of the more open lagoon where the salinity of sea water close to the normal marine or metahaline conditions such as that characterizing the outer part of Shark Bay lagoons (Logan *et al.*, 1974). The abundant framboidal pyrites in the nodular limestones and especially in shale partings further characterize the environment as reducing. However, Scoffin (personal communication) suggested that the pyrite famboids most likely are post depositional in origin and though requiring reducing conditions for formation do not imply reducing conditions during deposition.

6.6 The Rung Nok Formation

Because of outcrops limited to only 2 small steep seacliff islands, on the southeast of Ko Tarutao (Fig. 3), and extensive tufa covering and faulting ; it is not yet

possible to provide a detailed field study. However, the microfacies of the few accessible outcrops are distinctive.

The rocks of the Rung Nok Formation can be subdivided into 4 members. The rocks of member 1 and 2 are very similar but they are different in the degree of dolomitization. In term of palaeoenvironmental interpretation these two members will be discussed together. The rocks of these two members are rather consistent throughout the sequence. They are thinly bedded, poorly washed biomicrite (Fig. 14, 4.4C, D) with extremely abundant well abraded bioclasts of mainly crinoid debris with the lesser quantities globular bryozoans, rare brachiopods, tabular corals and trilobites. Cementing material is mainly syntaxial rim cements with minor fibrous cements. Rim cements decrease to the top of the second member but radial fibrous cement increase (Fig. 6.5B). Micritic envelopes and geopetal fabric are common in either intra or interskeletal porosities (fig. 4.4C,D). Micrite infilling in between bioclasts is abundant in the first member and decreases considerably toward the top of the second member. In contrast, xenotopic dolomites of selectively replaced micrite are more abundant in the second member than the first. In some parts of the second member at Ko Laen, the rocks were completely dolomitized to megadolomites with saddle dolomites filling in voids.

Member 3 is mainly coral-algal-stromatoporoid biolithite and limestone breccia with extensive early marine cementation (Fig. 4.7 D, E, 4.8). The lower part is thinly bedded limestone composed of sparse frame-building and sediment-binding organisms. Frame-builders are simple tabulate corals and cup-shaped stromatoporoids (Fig. 4.7D, 4.8A, B) growing on poorly washed biosparite and encrusted by long-chained calcareous algae (Fig. 6.5A, B). In the middle part, the rocks are mainly limestone breccia (Fig. 4.8C) and laminar stromatoporoids (Fig. 6.5C). Large stromatolitic breccias are firstly cemented by stubby bladed cement following by radiaxial calcite. Channel porosity (Fig. 4.8C) and stromatactis (Fig. 6.5D) are common. Laminar to domical stromatoporoids in this part increase toward the top. Stromatactis usually occurs either beneath domical stromatoporoids or parallel to the laminar ones. Erosion surfaces on top of stromatactis have been observed but internal sediments are rare. Then the rocks change to dense laminar and domical stromatoporoids (Fig. 6.5E) as a major frame builder with *in situ* conical sponges in the upper part. Stromatactis is more abundant. The massive biolithites of the upper part are conformably overlain by the bedded dolomitic biomicrite with random burrows.

Member 4 consists of dolomites and dolomite breccias. This member is excluded from this study because nearly all sedimentary structures and original components of the rocks were obliterated by extensive dolomitization.

Fig. 6.5 Lithology and primary structures of the Rung Nok Formation.

A. Photograph of the Rung Nok Formation at Ko Rung Nok showing the gradual contact in between the second and the third member. The rock changes upwards from thinly bedded in the lower part to thicker bedded biolithite in the middle part (C,D) and up to massively bedded biolithite (E) in the upper part of the third member. The rocks and thin sections from each position (B to E) are shown below.

B. Photomicrograph of biosparite at the contact zone between the second and third members. Note the extensive cementation of radial fibrous cement (F) surrounding the intraclast (C). Rim cement of micritic echinoderm ossicle (arrow) predates a fibrous cement.

C. Photomicrograph of biolithite and reef breccia in the middle part of the third member. Note the encrustation of possible stromatolite and calcareous (chained)algae (arrow) covered by reef breccia (B) and infilling bioclasts (C). An isopachous fibrous cement (F) is very extensive also postdating cement rim (S).

D. The occurrence of stromatactis (arrow) along the laminar and domical stromatoporoid layers in the middle portion of the third member.

E. Dense domical stromatoporoid biolithite in the massive limestone from the upper part of the third member.


A
B C
D
E

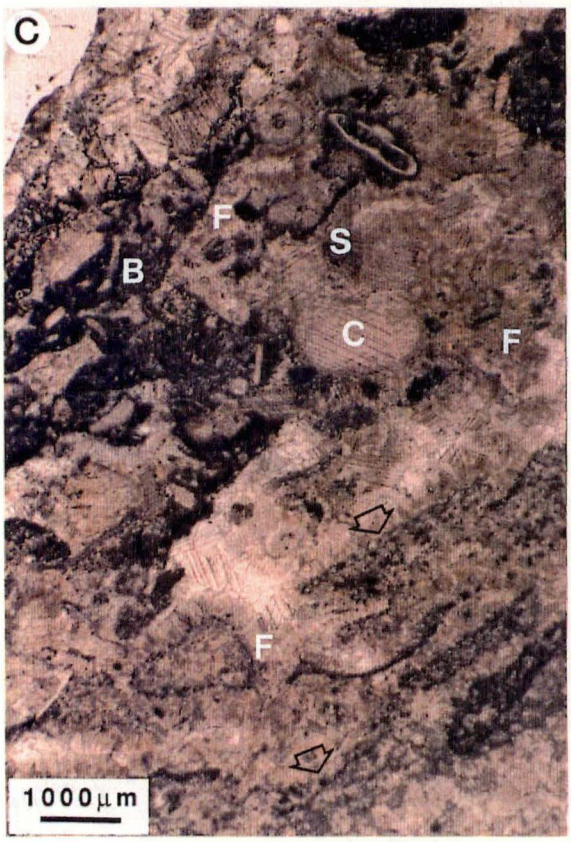
C
F
S
B
C
F
F
1000μm

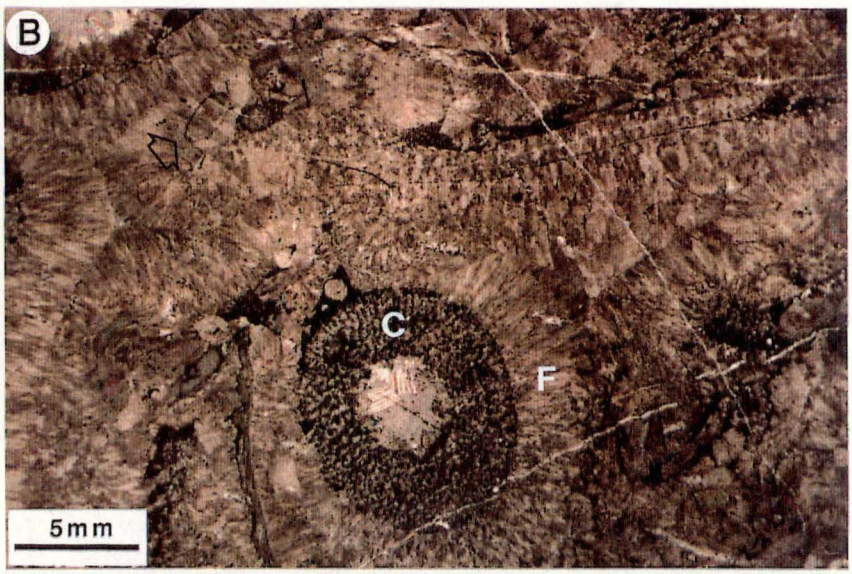
B
C
F
5mm


D

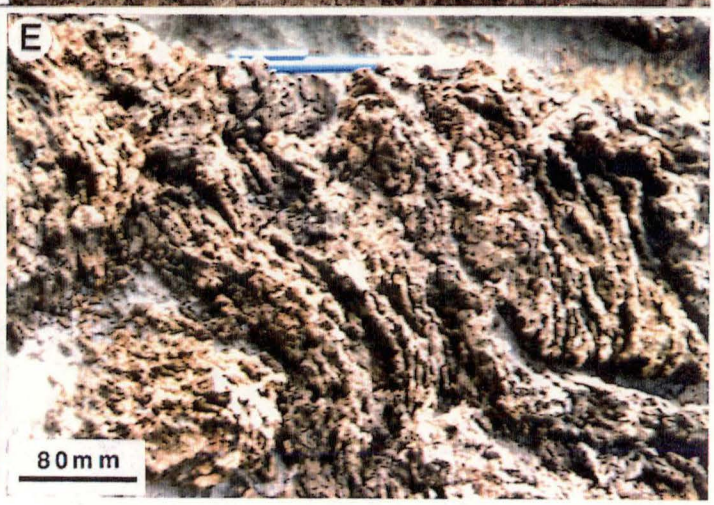
E
80mm

Member 1 and 2 : The poorly washed nature and presence of micrite in interskeletal porosities and in geopetal fabric of the Rung Nok crinoidal limestone may indicate low to moderate depositional energy (Folk, 1962). On the contrary, the well abraded, broken, and dissociated crinoid debris reflects higher energy conditions. Extensive syntaxial rim cements indicate early marine cementation which are common in the shallow marine environment of ancient rocks (James and Choquette, 1983). The nonluminescence of the first stage rim cements (Fig. 5.2C, D) in this rock also suggest early marine cementation in an oxidizing environment. In turn, the extensive early rim cements reflect well circulated, marine conditions. Therefore, cementation and micrite infilling in intra and interskeletal porosities should be considered chronologically separate events. In a study on the development of overgrowths from echinoderm fragments in the Ambléon Limestone of Bas-Bugey, southern French Jura, Evamy and Shearman (1965) pointed out that iron-free rim cements were an early phase whereas the micritic matrix was subsequently introduced from above.

Based on this evidence, the abundant well abraded crinoid debris and other minor skeletons including well preserved globular bryozoans and brachiopods, are interpreted as shoal water accumulations in the form of carbonate buildups or crinoidal sand shoals. In these early rim cements were precipitated in shallow marine environments. The micritic matrix infilling was deposited later and was followed by the iron-rich rim cements after burial.

The development of poorly washed biomicrites to cleaner deposits with abundant early rim cements as well as fibrous cements of member 2 suggest the transition to more current agitated conditions (Cain, 1968) above. The dolomitization of the Rung Nok crinoidal limestone occurred late after burial. Aigner (1985) interpreted dolomitic crinoidal limestone from the upper Muschelkalk basin (Middle Triassic) in SW-Germany, as a protected barrier-like belt, of ramp carbonates. However, the lack of hydraulic structures such as cross-bedding, graded bedding, etc, and abundant micrite suggest buildups below wave bases. The restriction of these buildups to only two small satellite islands of Ko Tarutao in southern Thai peninsula implies that they occurred locally. However, their stratigraphic position lying upon the Lae Tong lagoonal sediment suggests the barrier morphology.

Member 3 : The existence of well defined *in situ* coral-algal-stromatoporoid biolithites, stromatactis, and very extensive early marine fibrous cements in this member suggest reef deposition (Folk, 1959) in warm shallow marine environments (Linström, 1984; Webby, 1984). The Rung Nok reefs were initiated by the formation of early cemented crinoidal limestones (member 1 and 2) which provided a firm and hard substrates for reef colonization. Thinly bedded biolithites with sparse cup-shaped

stromatoporoids and tabulate corals encrusted by chain calcareous algae (Fig. 4.8) in the lower part of the third member reflect a reef colonization stage. The delicate structure of cup-shaped stromatoporoids and abundant biomicrite in between frame builder organisms suggest a low depositional energy below wave base environment. During an intermediate stage, bedding thickness as well as the number of frame builders such as laminar and small domical stromatoporoids, and encrusting stromatolites (?) increased considerably. Large stromatolite breccias (Fig. 6.5C) are common and early cementation is extensive. On the top of the sequence, the diversity of frame builders is low. Only dense domical stromatoporoids with abundant stromatactis (Fig. 6.5D, E) and *in situ* conical sponges have been observed in this end stage. Other reef associated faunas are crinoids brachiopods, cephalopods, and trilobites.

Coral-algal-stromatoporoid reefs of the Rung Nok are similar to those of the Middle Ordovician of Norway (Harland, 1981) and Canada (Harland *et al.*, 1987). But the difference is that the Rung Nok reefs have higher relief above wave base (or exposure) whereas the Norwegian and Canadian reefs are patch reefs. The interpretation is consistent with a stratigraphic position of the third member which lies conformably above the Lae Tong Formation. Although the third member is exposed at only 2 small islands at Ko Tarutao and is probably absent from the mainland Thai peninsula, it is interpreted as a local barrier reef (Fig. 6.6) because it lies above a lagoonal deposition. However, the limited exposures of the Rung Nok reef itself makes the interpreted occurrence of the barrier reef suspect (Purdy, personal communication)

6.7 Depositional Model

The vertical sequence of the Thung Song carbonates displays a change in depositional energy or a gradual change of depositional environments from shallow water to deeper water environments(Appendix4,5). Sediment gravity flow deposits such as turbidites and slumps have not been observed. These criteria suggest that there was not a pronounced break in depositional slope into deep water on the Thung Song carbonate platform. Even though, there is a reef breccia within the Rung Nok Formation, it occurs locally and is restricted to only two small islands. The lack of an extensive peri-platform talus and slope to basin deposition possibly rules out the rimmed carbonate shelf model (Ginsburg and James, 1974). Therefore, the Thung Song carbonates are interpreted as homoclinal ramp carbonates (Read, 1982). Purdy (personal communication) suggested the general term of shelfal and basinal carbonates.

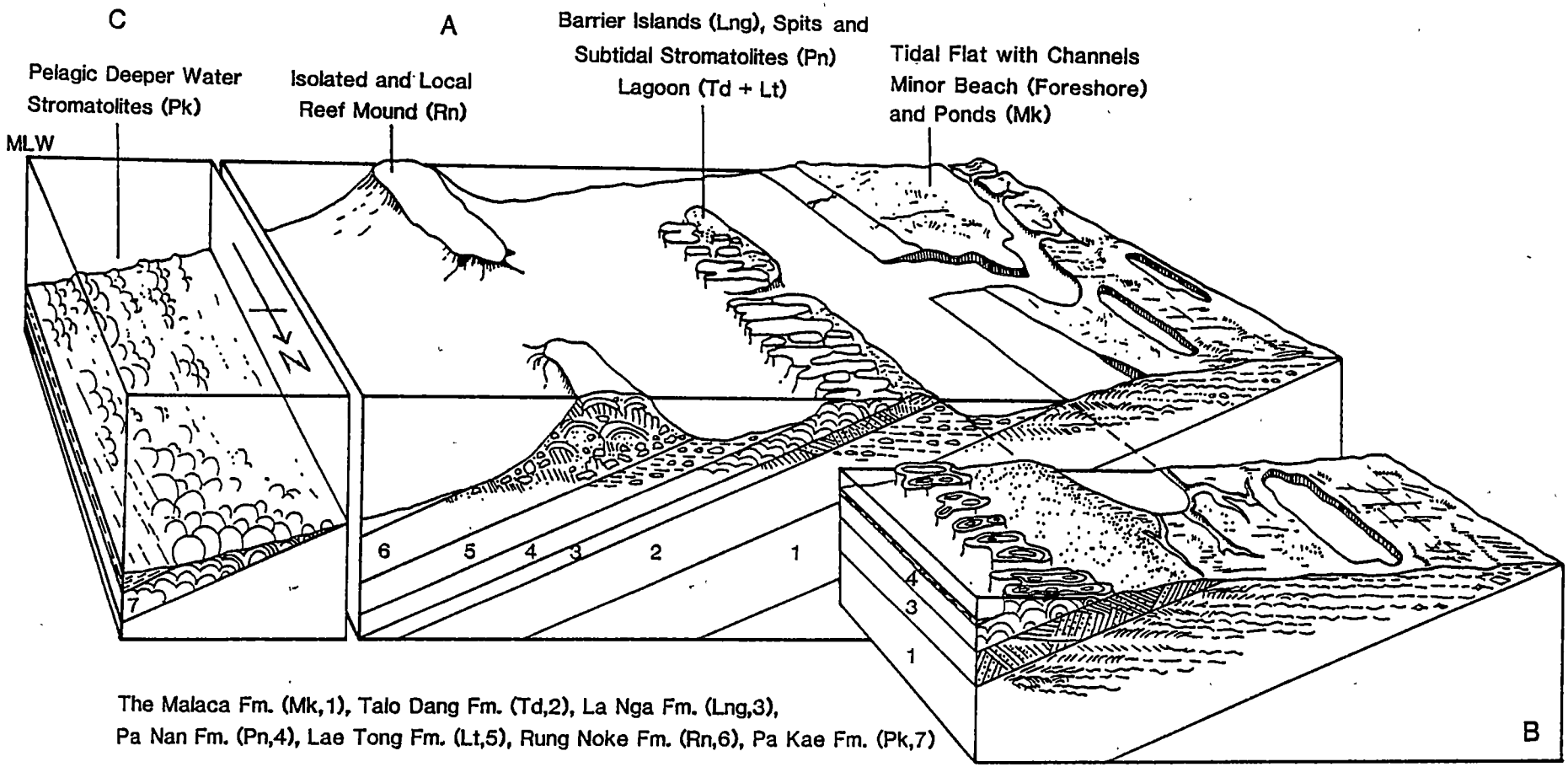

Fig.6.6 The diachronous depositional model for transgressive development of the Thung Song ramp carbonates showing environmental setting, distribution and relationship of common rock types. A) General environmental setting at Ko Tarutao. B) Spit morphology at La Nga Bay, NE Ko Tarutao, where the La Nga barrier island contacts with the Malaka tidal flat. C) Deeper water stromatolite, the Pa Kae Formation. Vertical and horizontal scales are exaggerated.

Six major facies in the study area at Ko Tarutao have been recognized. Their depositional relationships on a homoclinal ramp from intertidal-supratidal at the bottom of the sequence to shallow lagoon, oolitic shoal, subtidal stromatolitic reefs, deeper lagoon and terminating as local carbonate buildups and barrier reefs suggest the gradually deepening of a basin as a result of relative sea level rise. A long term transgression, with common minor eustatic sea level fluctuation, during the Tremadoc to late Arenig is postulated.

Based on a general concept that "vertical lithologic change at any point in a basin reflects the lateral migration of environments across it" (Walther's law in Horowitz and Potter, 1971,p. 17), a generalized depositional model has been reconstructed for the Thung Song carbonates in the study area (Fig. 6.6). The geometry and distribution of the barrier islands, of the lower La Nga member , suggest that the palaeoshoreline trended north-south. The westward movement of the Early Ordovician transgression reflects the existence of a continent to the west. A continental mass is indicated by the development of the Thung Song ramp carbonates on the thick sequence of the red siliciclastic Tarutao Group. The insignificant amount of terrigenous detrital grains within the Thung Song carbonates suggests a low relief for the nearby continent. Alternating wet and dry climates in a tropical region are indicated by sparse evaporite pseudomorphs in many formations. Storm events were common as evidenced by proximal and distal tempestites in the Lae Tong Formation. Because of no sharp break on slope but gradual increase in the water depth of the homoclinal ramp, extensive shallow water carbonates developed at a certain distance away from land to the east (Fig. 6.6A, B). Under this circumstance, carbonate production could be a maximum (Wilson, 1974).

The Thung Song carbonates on Ko Tarutao record a change in platform conditions through the Early Ordovician (Fig. 6.6A,B). Shallow subtidal to supratidal deposition with extensive stratiform stromatolites, tidal channel, minor beach and pond deposition is represented in the underlying Malaka Formation. Above the narrow gradational contact, the shallowing-upward cycles, of the Talo Dang Formation were deposited in a marine-shelf lagoon. Shoaling in the broad lagoon reached the littoral zone as evidenced by oolitic barrier islands, the La Nga Formation, and subtidal stromatolitic reefs, the Pa Nan Formation. The deeper lagoon deposits, of the Lae Tong Formation, were situated seaward in between the La Nga barrier islands and the Rung Nok carbonate barrier reefs buildups. No evidence of deposition deeper than the Rung Nok reefs have been observed at Ko Tarutao. However, the discovery of deeper water stromatolitic limestones in the Pa Kae Formation (Fig. 6.6C, see chapter 7) suggests existence of a deeper water deposition in this carbonate regime.

Chapter 7

THE RED, DEEPER WATER STROMATOLITIC LIMESTONE,THE PA KAE FORMATION (LATE ORDOVICIAN)

7.1 Introduction

The Pa Kae Formation contains a pelagic trilobite-conodont fauna quite different from that of normal tropical Ordovician carbonates such as those in the remainder of the Thung Song Group (chapter 6). In this chapter the association of stromatolitic structures in an apparently deep-water limestone will be discussed separately.

Since Kalkowsky (1908), stromatolites have been defined by numerous authors (e.g. Logan *et al.*,1964; Monty,1977; Buick *et al.*,1981; Krumbein,1983; Kennard and James,1986) as laminated organosedimentary structures built by microbial communities. These bodies that are formed from the interaction between benthic microbial communities and detrital or chemical sediments are also referred to as microbialites (Burne and Moore,1987). The term thrombolite was introduced for microbial structures without lamination and with a meso to macroscopic clotted fabric (Aitken,1967; Kennard and James,1986).

Most modern and ancient marine stromatolites occur in very shallow subtidal to supratidal environments (e.g. Black,1933; Ginsburg,1955,1960; Logan,1961; Bathurst,1967; Hofmann,1969; Kendal and Skipwith,1969; Neuman *et al.*,1970; Monty,1972; Zamarreno,1981; Walter *et al.*,1988; Beukes and Lowe,1989). However, there is clear evidence of modern shallow to deeper subtidal stromatolites at water depths of 0-4 m at Shark Bay (Playford and Cockbain,1976; Burne and James,1986; Walter and Bauld,1986),7-8 m on the eastern Bahama Bank (Dill *et al.*,1986),12.5 m at Bermuda (Gebelein,1969), 0-23 m at Satonda Island Crater Lake offshore Sumbawa/Indonesia (Kempe and Kazmierczak,1990). Oncolites at depths of 80-125m have been reported from the insular shelves of the Canary Islands (McMaster and Conover,1966). Because of the rarity of the modern analogues for ancient deep water stromatolites and light requirement for photosynthetic algae and bacteria, it is difficult to place stromatolites in the rock record below the euphotic zone. Monty (1977) argued that stromatolites need not necessarily be restricted to very shallow waters for photosynthetic purposes. He suggested that marine blue green algae can grow from 0 to at least 1,000 m by relying directly on the photosynthetic process not only in bright illuminated shallow waters but also by using a red pigment in shade to twilight condition and chemo-organotrophic metabolism in complete darkness below the photic zone. Indeed, living photosynthetic algae and organic mats are known from

depths of more than 200 m in modern seas (Le Campion- Alsumard *et al*,1982; Williams and Reimers,1982).

After the work of Playford and Cockbain (1969) on Devonian deeper water stromatolites(>45 m to ~100 m deep) from the Canning Basin, Western Australia, deeper water stromatolites have been reported from many continents including Australia (Southgate,1989), North America (Hoffman,1974; Cecile and Campbell,1978; Williams,1984), Europe (Jenkyn,1971; Peryt and Peryt,1975; Jozef,1980; Bridges and Chapman,1988), Africa (Berstrand-Sarfati and Moussine-Pouchkine,1983; Trompette and Boudzoumau,1988), and Asia (Monty *et al.*,1987; Beauvais *et al.*,1988; Wongwanich *et al.*,1990). Most of those stromatolites are associated with carbonate buildups and mud mounds (Playford *et al.*,1976; Pratt, 1982a,b) or even occur as reefs, especially in the Precambrian, due to the lack of competition from other marine organisms (Hoffman,1974; Monty *et al.*,1987). Some occurrences are thought to have been far beyond the shelf margin in an adjacent deep basin (Jenkyns,1971; Hoffman,1974). These deep, basinal stromatolites usually contain pelagic fossils and occur in stratigraphically condensed limestone sequences (Playford *et al.*,1976; Jozef,1980). A maximum depth of 200 m is commonly inferred to correspond to the photic zone in oder to fit the supposed light requirement of stromatolites. The Sicilian Middle Jurassic stromatolites, overlying a ferromanganese hardground (Jenkyn,1971), and many of the Devonian deep water stromatolites from the Canning Basin (Playford *et al.*,1976) occur in red pelagic limestones.

Although detailed stratigraphical, petrographical and morphological studies of deeper water stromatolites have been successfully carried out by the authors noted above, little is known about the diagenesis of the stromatolites and geochemistry of the rocks. Moreover, the paleodepths are still uncertain. The red stromatolitic limestones of the Pa Kae Formation are associated with a well-preserved pelagic fauna, and calcareous filamentous and coccal microbial sheaths so that this formation provides an excellent opportunity for examining Ordovician deeper water stromatolites. This study combines stratigraphical, morphological, sedimentological, diagenetic, and geochemical methods to interpret the depositional environment of that formation and further efforts have been made to establish a conceptual model in order to predict the paleodepth of the Pa Kae stromatolites.

7.2 Stratigraphic Setting

A 66-126 m thick rhythmically bedded sequence of red stromatolitic limestone and dark red calcareous mudstone, the Pa Kae Formation, is the uppermost rock unit of the Thai Ordovician ramp carbonates, the Thung Song Group, which is widely

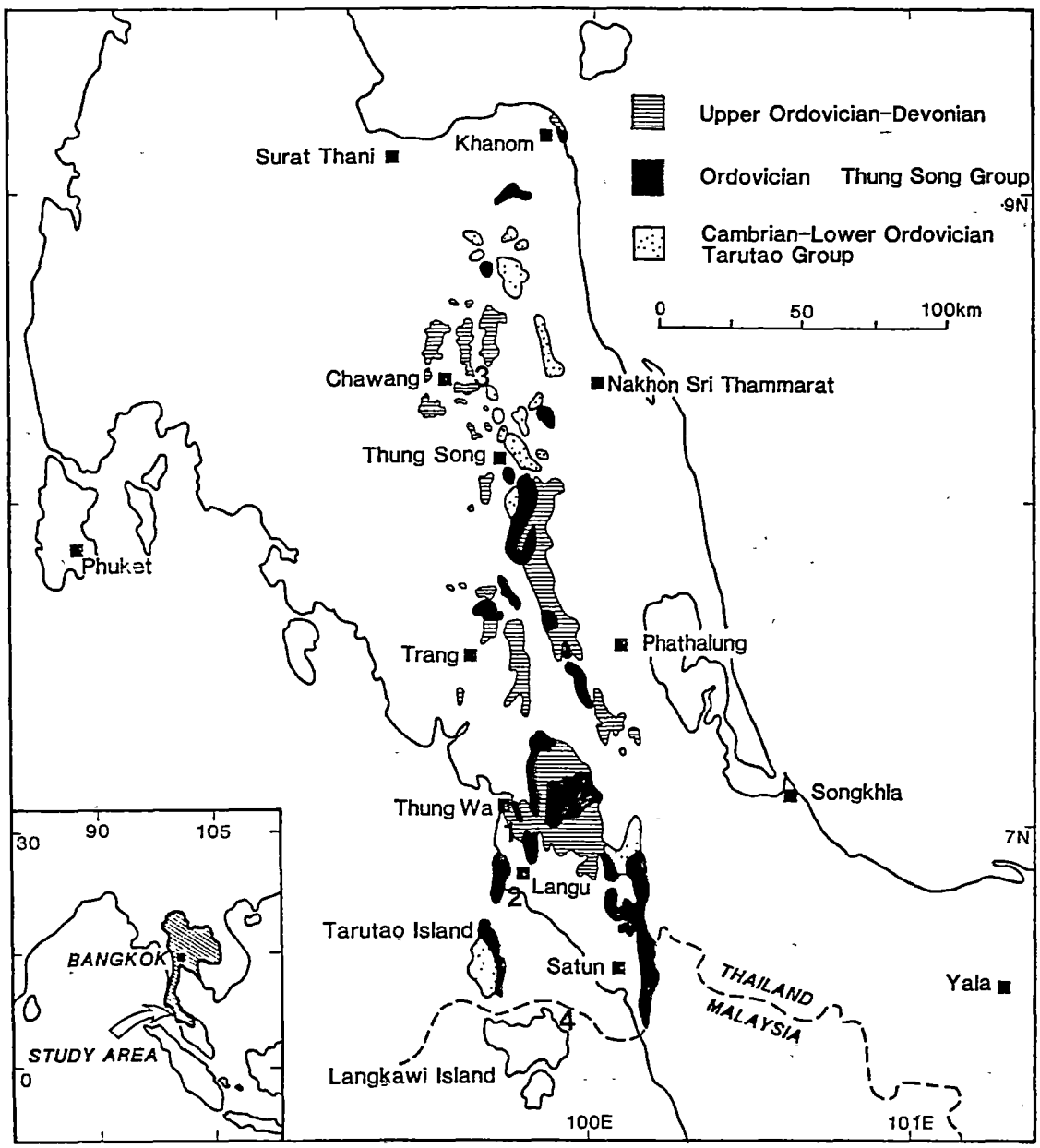

Fig. 7.1 Locality and geological map of the southern Thai peninsula, showing the Lower to Middle Palaeozoic rocks and the location of the Pa Kae Formation at 1) Ban Pa Kae, 2) Ao Nun, 3) Ban Na, and 4) Palau Langon, NE, Langkawi Islands. They extend in N-S direction covering a long distance of 230 km across Thai-Malay border.

distributed along the flanks of an irregular and discontinuous N-S mountain belt in central peninsular Thailand (Fig. 7.1, Wongwanich *et al.*,1990). It is well exposed as a lens about 1.5 km long at a type locality (1), Ban Pa Kae, Amphoe La Ngu, Satun Province (lat. 6°,58′,25″ N and long 99°,46′,42″E). Another 3 exposures are at Ao Nun (2); at Ban Na, Amphoe Chawang, Nakhon Sri Thammarat Province (3); and (a very similar rock unit) on the west coast of Palau Langon, Langkawi Islands, West Malaysia (4); covering a distance of about 230 km across the Thai-Malay border. The Pa Kae Formation lies conformably over the gray Thung Song shallow-water ramp carbonates with a thin graded contact zone and is abruptly but conformably overlain by the stratigraphically condensed sequence of black graptolitic shale and chert with some radiolarians, the Wang Tong Formation (Upper Ashgill-Upper Silurian).

The rocks are thin (50-200 mm) and wavy bedded red stromatolitic limestones with dark red poorly laminated mudstone partings (<20 mm) and stromatolitic polygons are on the top of the bedding (Fig. 7.2A,B). The small-scale, dense, columnar stromatolites give a characteristic wavy appearance to the bedding but stromatolitic laminae on the rock surface are vague. The stromatolitic limestone layers are predominant at the top of the sequence whereas the mudstone layers decrease in importance upwards. Well preserved fossils of Caradoc to Ashgill age (Fortey, personal communication) include very small pelagic trilobites and brachiopods, nautiloids, gastropods, crinoids, ostracods, calcareous algal fragments, and "North Atlantic Province" conodonts (Burrett, personal communication). Calcispheres are abundant in limestone layers but very rare in mudstone partings. Trilobites are either blind (no eyes) or have large eyes. Dark red iron or ferromanganese micronodules are common.

7.3 Petrography

7.3.1 Stromatolitic Facies

The limestone dominated layers are biomicrites with well developed and densely crowded stromatolites. Based on Logan *et al.* (1964), Hofmann (1969), and Kennard and James (1986)'s classification, the small-scale stromatolites are subdivided into 4 microfacies: stratiform stromatolites, columnar stromatolites, thrombolitic stromatolites, and oncolitic stromatolites (Fig. 7.2C,D,E). The former two categories are the most common whereas the latter are much less abundant and commonly confined to the lower part of the sequence. However, the stromatolite forms within a single bed are very variable in a vertical direction. In general, the stratiform stromatolites at the base of a bed gradually developed upward to the

Fig. 7.2 Lithologies, facies, and primary structures of the Pa Kae stromatolitic limestones.

A. Vertical sequence exposure of the rhythmically bedded red stromatolitic limestone and dark red mudstone parting. The wavy biogenic bedding is controlled by the dense columnar stromatolitic morphologies. Mudstone partings usually exhibit a mudstone-limestone couplet zone (arrow).

B. The typical small-scale stromatolitic polygons commonly observed on top of bedding. The dark red mudstone network represents the deposition of mudstone between the stromatolitic columns.

C. Etched slab illustrating a development series from flat laminites (1) at the bottom to columnar stromatolites LLH-C(2) at the top of bedding. The spar filling fenestrae (arrow) are rare. Note the amount of clay matrix increases toward the top whereas that of allochems decreases considerably resulting in less entrapment frameworks on the upper part of bedding. Sample no. 359.1/0.1

D. Etched slab of reticulate stromatolites (2) developing to thrombolites and trombolitic stromatolites (arrow) with clotted fabric (1) at the top of bedding. This is interpreted as a result of the stromatolites adaptation to the gradually decreasing current energy and attendant relative lack of sediment that could be trapped. Sample no. 389-10

E. Thin-section photomicrograph of oncolitic stromatolites microfacies (overlying LLH-C stromatolites). They are dense, concentric, with faintly micrite and spar-rich laminae (arrow). The cores are mostly faecal pellets and some bioclasts. Boring across outer and inner layers (arrow) is common suggesting a resting stage during their formation (microboring unconformity). Thin section no. 389.15

F. SEM of small well preserved, leaf-like calcified filamentous and round coccoid (black arrow) bacteria? exhibiting trapped allochems at the bottom and bound clay in between the sheaths (1,2). Some coccoids can be seen in the dividing stage (curve arrow). Thin section no. 359.1

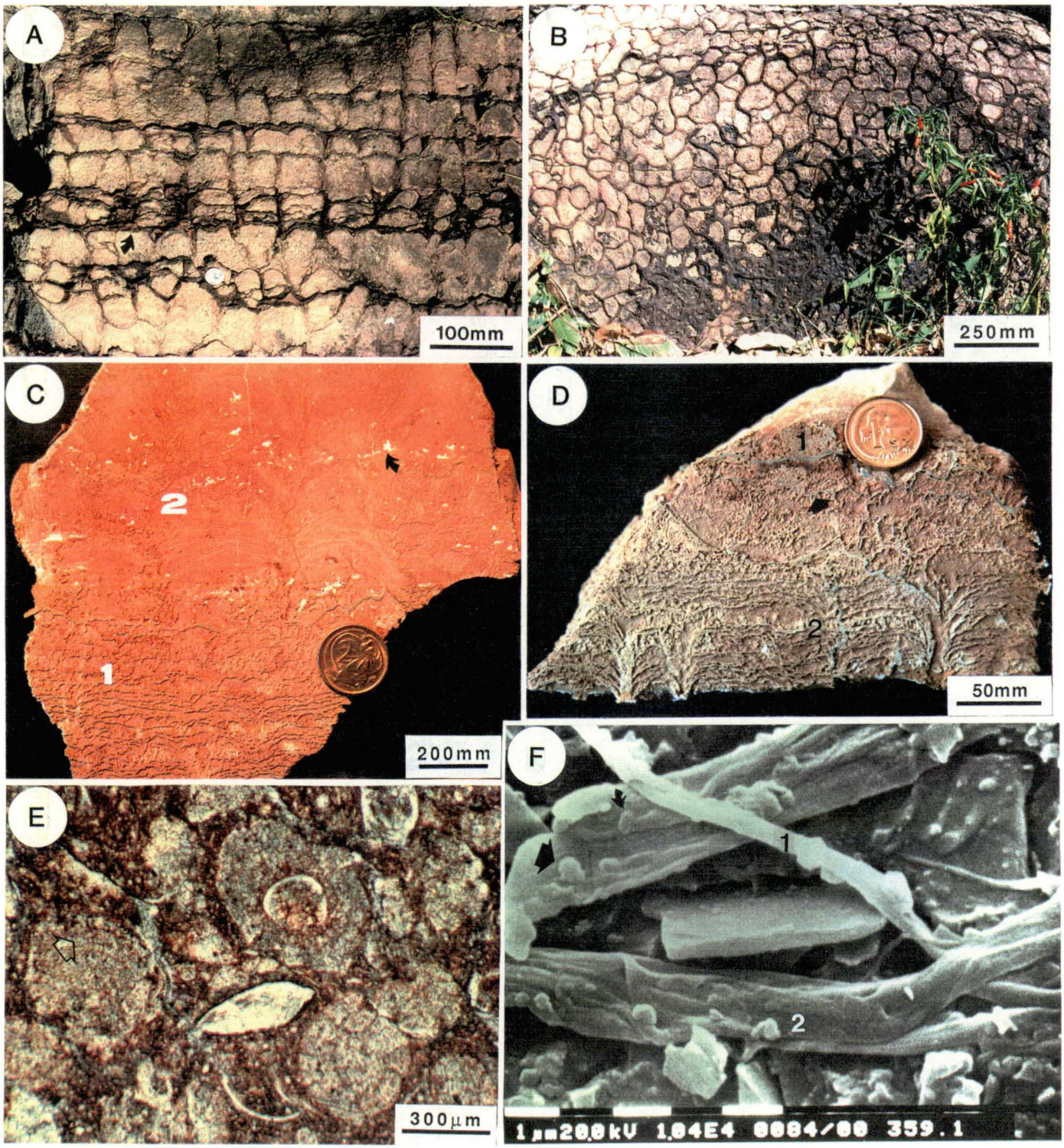
A
100mm
B
250mm
C
2
1
200mm
D
1
2
50mm
E
300µm
F
1
2
1µm20.0kV 1.04E4 0084/00 359.1

Fig. 7.3 Thin section photomicrograph showing lithologies, allochems, ferromanganese micronodules and hematite grains.

A. Allochemical rich layer with a genuine multilayering of ferromanganese (Fe-Mn) micronodules (C) in the smooth colloform structure and spar-rich laminae (B). There are abundant rounded pellets (white arrow) within allochem-rich layers. Lump structure (black arrow) usually occurred within ostracod carapaces. Thin section no. 409.1

B. The other 2 types of Fe-Mn micronodules: dark reddish brown Fe-Mn crust (1) surround red intraclasts (A), and bright red Fe-Mn impregnation in colloform structure around bioclasts (2). Dark reddish brown halo around type B micronodules suggests the diagenetic redistribution of Fe-Mn minerals. Thin section no. 409.11

C. Stained thin-section photomicrograph of a heavily bored echinoderm ossicle. The bored holes are commonly large and shallow. Large and deep ones (arrow) are rare. Thin section no. 409.3B

D. Bored glauconitic pellet (1), replacement glauconite at the rim of bioclast (black arrow), disseminated dark red to black hematite grain (white arrow), and dark red to black amorphous hematite filling in skeletal mould (2). The infiltration of this grain upon shelly skeleton is moderately common. Sample no. 435.5 (erratum: 500 μm is 250 μm).

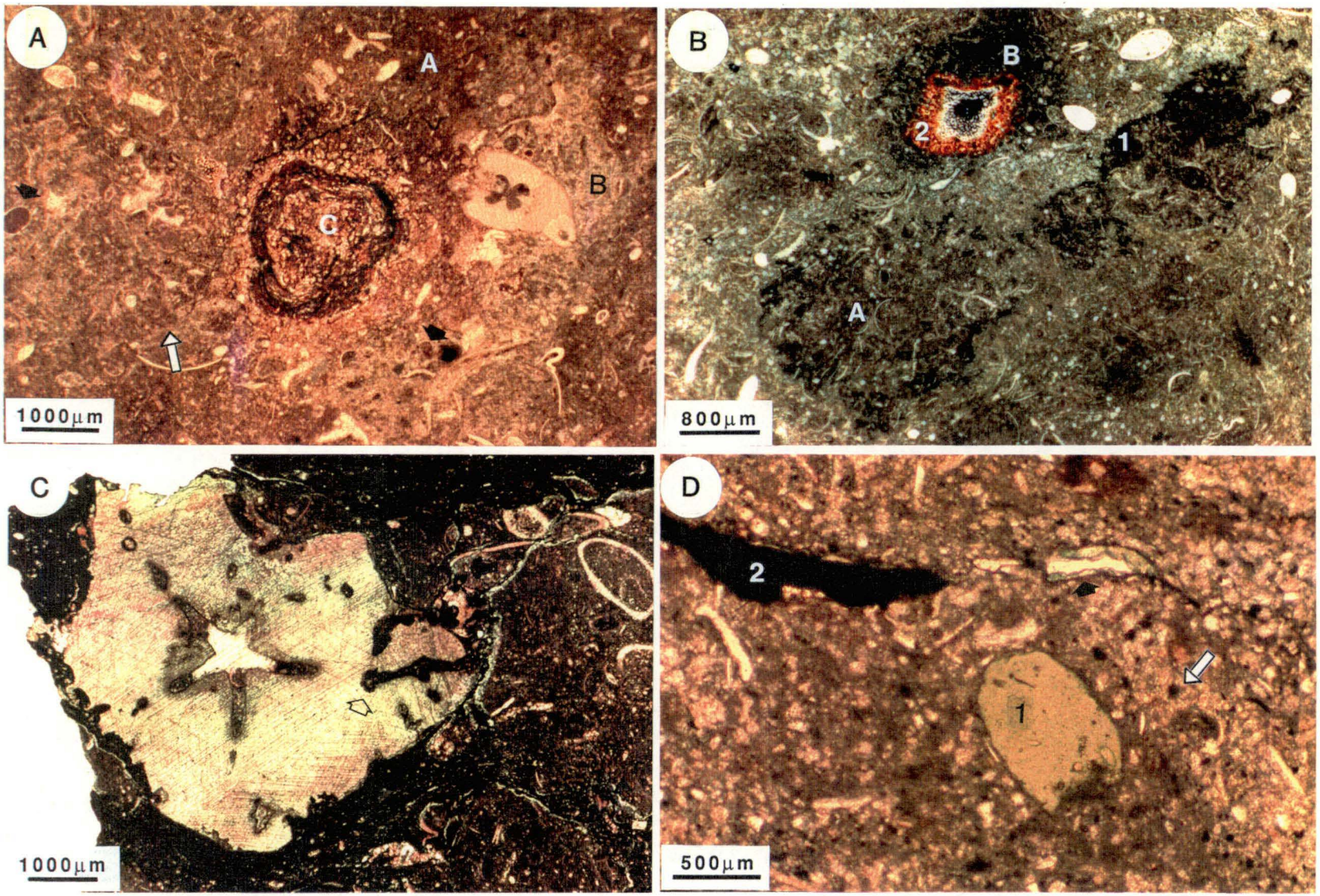
A
A
B
C
1000μm
B
B
2
1
A
800μm
C
1000μm
D
2
1
500μm

columnar stromatolites (Fig. 7.2C) but some also developed to thrombolitic or oncolitic stromatolites (Fig. 7.2D,E). The fenestral fabric is very rare (Fig. 7.2C) or normally missing. The SEM study reveals the presence of small, leaf-like microbial sheaths (0.5-2 μm wide,15-30 μm long) and possible small microbial remains (Fig. 7.2F), coccoid bacteria (0.2-0.5 μm).

Stratiform Stromatolites: They are irregular, wavy, and crinkly laminae composed of faintly spar-rich (0.5-2.5 mm thick) and sediment rich (1.2-5 mm thick) layers of biomicrites with abundant peloids, lumps, rounded intraclasts, and ferromanganese micronodules (Fig. 7.3A).

Columnar Stromatolites: This microfacies is the most common. Stromatolite structures are lateral linked hemispheroids developing from close link (LLH-C) to more space link (LLH-S) upward across bedding (Fig. 7.2C). The diameter of domes ranges from 10-50 mm and heights from 40-150 mm. Some are reticulate stromatolites (Fig. 7.2D, Playford *et al.*,1976). The composition of the reticulate stromatolites are similar to stratiform stromatolites with abundant peloids but the lateral linked stromatolites have much more abundant micrite and clay matrix. This observation supports the environmental controls on the development of stromatolites (Logan *et al.*,1969; Chafetz,1973; Celcile and Campbell,1978; Southgate,1989).

Thrombolitic Stromatolites: The external forms and internal compositions of this microfacies are similar to the other stromatolites but vague irregular patches of mesoclots (<30 mm) bridged by stromatolites are typical (Fig. 7.2D). They usually are associated with rectangular stromatolites.

Oncolitic Stromatolites: They are the least common component of the Pa Kae. Oncolites (150-600 μm) commonly have an irregular spheroidal and ellipsoidal shape. The faintly micritic and concentric layering of the coating are poorly visible around cores of ostracod carapaces and micritic nodules (Fig. 7.2E). Fenestral fabric is completely absent. The outer layers of oncolites have undergone erosion and boring as well as iron-staining. Microboring unconformities (Fig. 7.2E) within the coating are common. Oncolites were trapped and bound along stromatolitic laminae.

7.3.2 Allochems

Biochems (20-70%) and peloids (5-30%) are the major components (Fig. 7.3) of these densely packed biomicrites: intraclasts (<5%) are the minor components (Fig.

Fig. 7.4 Thin section photomicrograph exhibiting lithologies and early diagenetic fabrics.

A. Red intraclast (1) encrusted by dark red Fe-Mn crust (white arrow) following by stromatoporoid encrustation (2). Thin section no. 409.5

B. Dark brownish red Fe-Mn crust (1) lying upon erosional and bored surface (black arrow and 2). The large bored hole (2) filled by Fe-Mn minerals cut across submarine cements. Some bivalves bored and grew (white arrow) on this hardground. Thin section no. 389.15

C. Fe-Mn crusts interlayered with marine equant spars (2), resembling a stromatolitic structure. The boring across these layers suggests the submarine origin of Fe-Mn micronodules. Thin section no. 409.1

D. The maceration of micro and macrofaunal skeletons. A molluscan shell (1) shows partly maceration at skeletal rim and spines (white arrow). Some are completely macerated (2) into micrites but still retain the original shape of the grains. However, some grains were dissolved and then moulds filled by equant spars (3) after burial. Thin section no. 409.1

E. Extensive thick micrite envelopes around partly preserved ostracod carapaces (1,2). Some were macerated to micrites and seem to be cemented by amorphous hematite in some parts (white arrow). Geopetal fabric in ostracod carapaces (1) firstly filled by micrites and pellets (3) followed by synsedimentary submarine rhombic spars (4). The lower part of this fabric is heavily bored. Thin section no. 439

F. Thin-section photomicrograph of stained partly recrystallized bioclast (1) Original skeletal fabric is still preserved in the middle of the grain. The recrystallized outer layer is heavily bored (white arrow). Smaller skeletons have either disappeared through burial dissolution/ recrystallization process (2) or micritization (3). Thin section no. 439.5

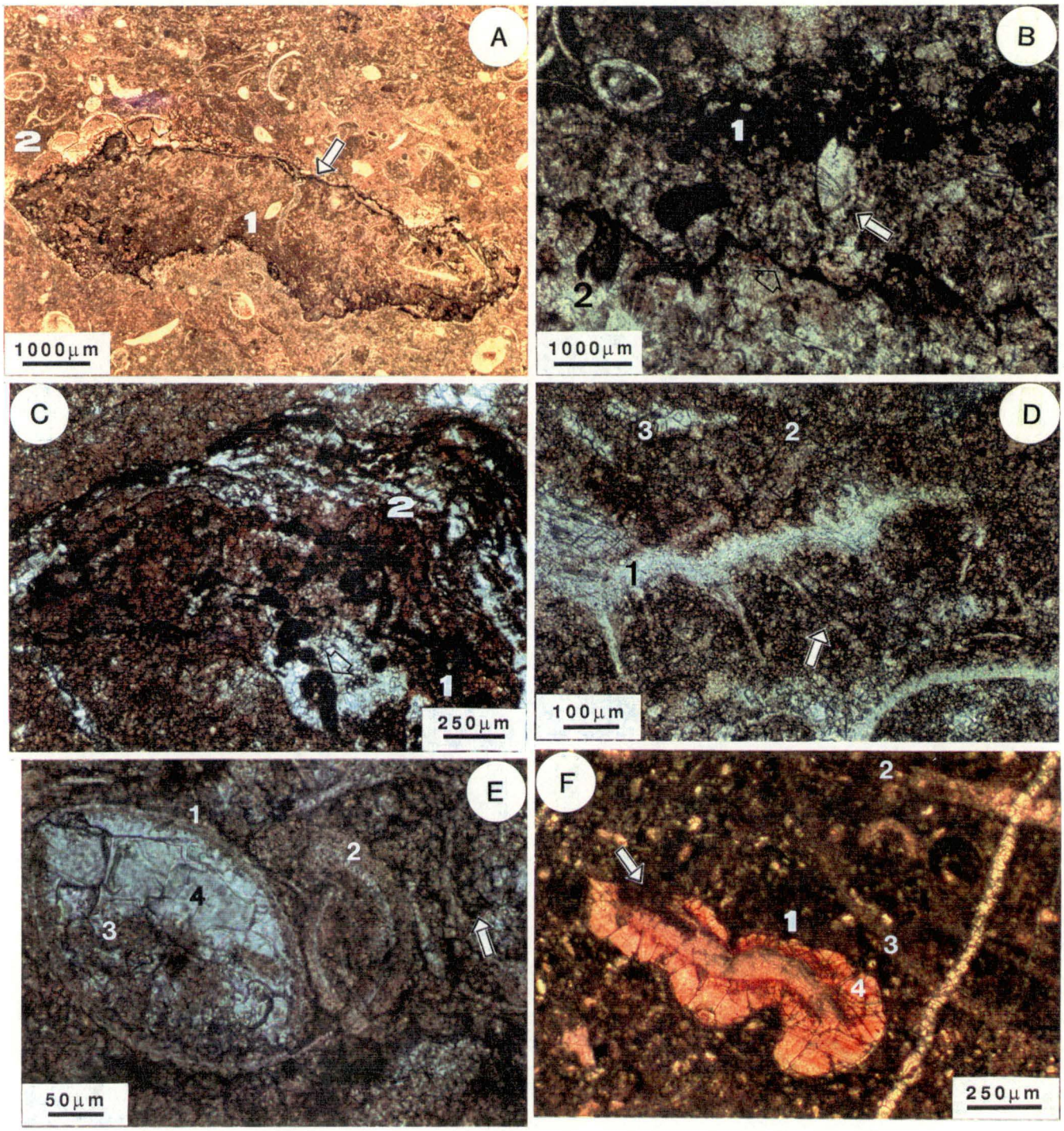
A
2
1
1000μm
B
1
2
1000μm
C
2
1
250μm
D
3
2
1
100μm
E
1
2
4
3
50μm
F
2
1
3
4
250μm

7.3A,B). Very small, rounded (5-35 μm) and rectangular (average 20x35 μm) disseminated hematite grains and ferromanganese micronodules are sparse (1-2.5%, Fig. 7.3D). Bored and eroded green glauconites (<450 μm, Fig. 7.3D) are rare and are confined to a transition zone between grey limestones and red limestones at the base of this rock unit. Very fine quartz shards and rounded aeolian quartz silt (40-100 μm) are also present (<1%). Small diagenetic pyrite crystals with square cross-section are rare.

Fauna: Ostracods (40-60%), crinoids (<10%), trilobites (<10%) and calcispheres(1-7.5%) are the dominant fauna with subordinate calcareous and a few siliceous sponges (spicules), brachiopods, bivalves, gastropods, calcareous algae, nautiloids, and conodonts. Stromatoporoids, corals and bryozoan are very rare. The skeletons usually show extensive biodegradation in the form of borings (Fig. 7.3C), micritized rims and maceration (Fig. 7.4E).

Peloids: Most peloids (10-150 μm) are spherical but some are ovoid. Under the conventional microscope, they consist of homogeneous micrites without the internal structure but some of them show a mixture of very fine bioclasts and micrites under the SEM. Therefore, these peloids may be the faecal pellets of detrital feeding organisms such as crustaceans and worms.

Intraclasts: There are two types of rounded intraclasts. The red, intraformational intraclasts (<18mm) have the same lithology as the stromatolites and are usually coated by a dark reddish brown ferromanganese crust (Fig. 7.3B,4A). The grey, well rounded intraclasts are different and contain abundant calcareous tubes within finer micrites similar to the common calcareous algal fragments in the older formations. They are interpreted as extraclasts transported from shallow areas up ramp. Coniglio and James (1985) also described the *Epiphyton* intraclasts from the Lower Palaeozoic limestone, Cow Head Group, western Newfoundland as the breakdown products from platform margin.

7.3.3 Ferromanganese Micronodules

Three forms of ferromanganese micronodules (2-18 mm) have been observed: reddish brown multilayered micronodules (Fig. 7.3A), brownish red encrustations and/or impregnations around fossil fragments (Fig. 7.3B), and thin dark reddish-brown encrustations around red intraclasts (Fig. 7.3B, 7.4A). Ferromanganese crusts of the first two categories show the developments of colloform structures simulating

stromatolite growth whereas the last commonly has no form but is thin and amorphous and forms very fine-grained ferromanganese crusts surrounding limestone clasts. The occurrence of ancient ferromanganese nodules in sublittoral to deep basin environments ranging from Precambrian to Miocene was discussed by Jenkyns (1977). Two major, purely inorganic, processes have been proposed for the formation of marine ferromanganese nodules. These are diagenetic growth processes (e.g. Tucker,1973; Calvert and Price,1977; Halbach,1986) and accretion in the form of precipitation directly from sea water (e.g. Jenkyns,1977; Halbach,1986). However, macro and micro-organisms have been implicated in the growth of these nodules (e.g. Hofmann,1969; Sorokin,1972; Dugolinsky *et al.*,1977; Monty,1977; McCave,1988). Many lines of evidence suggest that most of the Pa Kae micronodules formed during very early sea-floor diagenesis as indicated by the growth of stromatoporoids on red intraclasts after ferromanganese encrustation (Fig. 7.4A), by boring across recrystallization and iron impregnation zone at the rim of large skeletons (Fig. 7.4F), by boring across marine equant spar layers in between ferromanganese layers (Fig. 7.4C) of the nodules, and by the isopachous nature of marine equant spars surrounding many ferromanganese nodules.

Nevertheless, some micronodules with symmetrical, colloform structure surrounding skeletal grains do not show synsedimentary features. It is possible that some of these are genuine diagenetic micronodules formed during early diagenesis just below the sediment/water interface as are modern rough surface (type-r) nodules in the central to southern Central Pacific Basin (Usui , 1983/1984). Therefore, the Pa Kae ferromanganese micronodules are either the result of seafloor precipitation or early diagenetic growth. The former type is dominant. The role of stromatolites in the genesis of these micronodules is not clear.

7.3.4 Disseminated Haematite Grains

Dark red to black haematite grains (2.5%) are commonly round and oval (5-35 μm) with some having subround square, rhombic to hexagonal (5-12 μm) and rectangular (average 20-35 μm) cross section. The hexagonal shape is rare. They are haematitic with bright red internal reflection under the conventional microscope. Faint infiltration of grains on large skeletons has been observed (Fig. 7.3D). Patchy amorphous haematite is usually a cement between grains (Fig. 7.4E) resulting in intraskeletal porosities with a lump texture (Fig. 7.3A) after the dissolution of the host skeletons. This finely divided haematite and the amorphous haematite imparts the red coloration to the Pa Kae stromatolites as they do to those of the Canning Basin (Playford *et al.* , 1976).

Playford *et al.* (1976) proposed a bacterial origin for the iron of the Canning Basin stromatolites which probably precipitated originally as goethite (Playford *et al.*,1976). It is one of the most common iron minerals in modern marine sediments and in ferromanganese nodules. This hydrous iron oxide firstly deposits on the seafloor and transforms into haematite with time (Murray ,1979). Von der Borch (1972) also reported the primary precipitation of amorphous goethite mud from deep sea core sites 37 and 39, off the west coast of the USA. The Pa Kae haematite may have been precipitated direct from sea water in the form of goethite and subsequently transformed to haematite during early seafloor diagenesis. The weak infiltration of grains by haematite suggests the redistribution of some haematite particles by bottom currents. Even though the morphology of haematite grains is similar to that of magnetites produced by magnetotactic bacteria (McNeil,1990), the possibility of haematite forming from those magnetites is less probable because the grain sizes of the Pa Kae haematites are varied and much larger than those of ultrafine-grained (0.04-0.5 μm), single-domain biogenic magnetite (Kirschvink and Chang,1984; Stolz*et al.*,1990). A detrital mode of haematite is ruled out since other detrital grains within the rock are quite rare. The remobilization by diffusion of iron during early diagenesis did occur because there is a black halo surrounding ferromanganese micronodules, and a filling of haematite within skeletal molds (Fig. 7.3B,D).

The micritic matrix between allochems is either detrital, a maceration product or the result of marine precipitation as discussion later.

7.4 Diagenesis

The rate of sedimentation of the Pa Kae red stromatolitic limestones was very slow as shown by the occurrence of ferromanganese nodules (Ku,1977, Andreyev *et al.*,1987), green and yellowish green glauconite pellets (McRae,1972, Odin and Letolle,1980), extensive boring of carbonate grains and the formation of hardgrounds (Fig. 7.4B). Therefore, many early diagenetic events, either destructive or constructive, could occur on this well oxygenated seafloor, during the deposition of the Pa Kae, including the grain alteration leading to micrite formation and neomorphic spars prior to, during and after binding and trapping processes (Fig. 7.5E). Subsequently extensive cementation resulted in early marine lithification. Burial cements are subordinate and restricted to large pore spaces. The compaction effect is extensive at the contact between limestone and mudstone layers.

7.4.1 Grain Alteration

Fig. 7.5 Destructive and constructive diagenetic features.

A.Thin-section photomicrograph exhibiting the impregnation of red Fe-Mn crust in colloform structure (white arrow) into early marine recrystallized rim of a bioclast. Subsequently, this clast was bored (1) across the impregnated zone into the original grain inside (2). Then, the bored holes were filled by equant spars (short black arrow) and micrites (1). Thin section no. 389.15

B.Thin-section photomicrograph illustrating the paragenesis of the rock. After the Fe-Mn impregnation (white arrow) into the recrystallized zone around the bioclast, marine spars (1) precipitated from sea water and micritic and pelletal internal sediment was deposited in the sheltered porosity following by burial blocky spars (2). Then, the burial recrystallization of the remaining original bioclast took place through a dissolution /reprecipitation process leading to further burial blocky spars filling in the dissolution moldic porosity (3) and the remaining sheltered porosity. Thin section no. 389.15

C. Cathodoluminescent photomicrograph of B. The non luminescent equant spars (1) represent the early marine cementation on the oxygenated seafloor. Further dull luminescent blocky spars (2) suggests the precipitation occurred under strong reducing condition during the decomposition of stromatolites and other organic matter after burial. Subsequently, bright luminescent blocky spars (3) developed under moderate reducing condotion at deeper burial.

D. SEM of subrhombic micrite fringe around bored ostracod carapaces (top center). The systematic alignment of this micrite indicates that they precipitated from sea water as a cement, possibly under photosynthetic control. Thin section no.359.1

E. SEM showing the leaf-like, calcified stromatolitic sheath embedded by rhombic microspars (top left) and rhombic micritic cements (middle right) within a spar-rich laminae. Broken slab no. 433.4

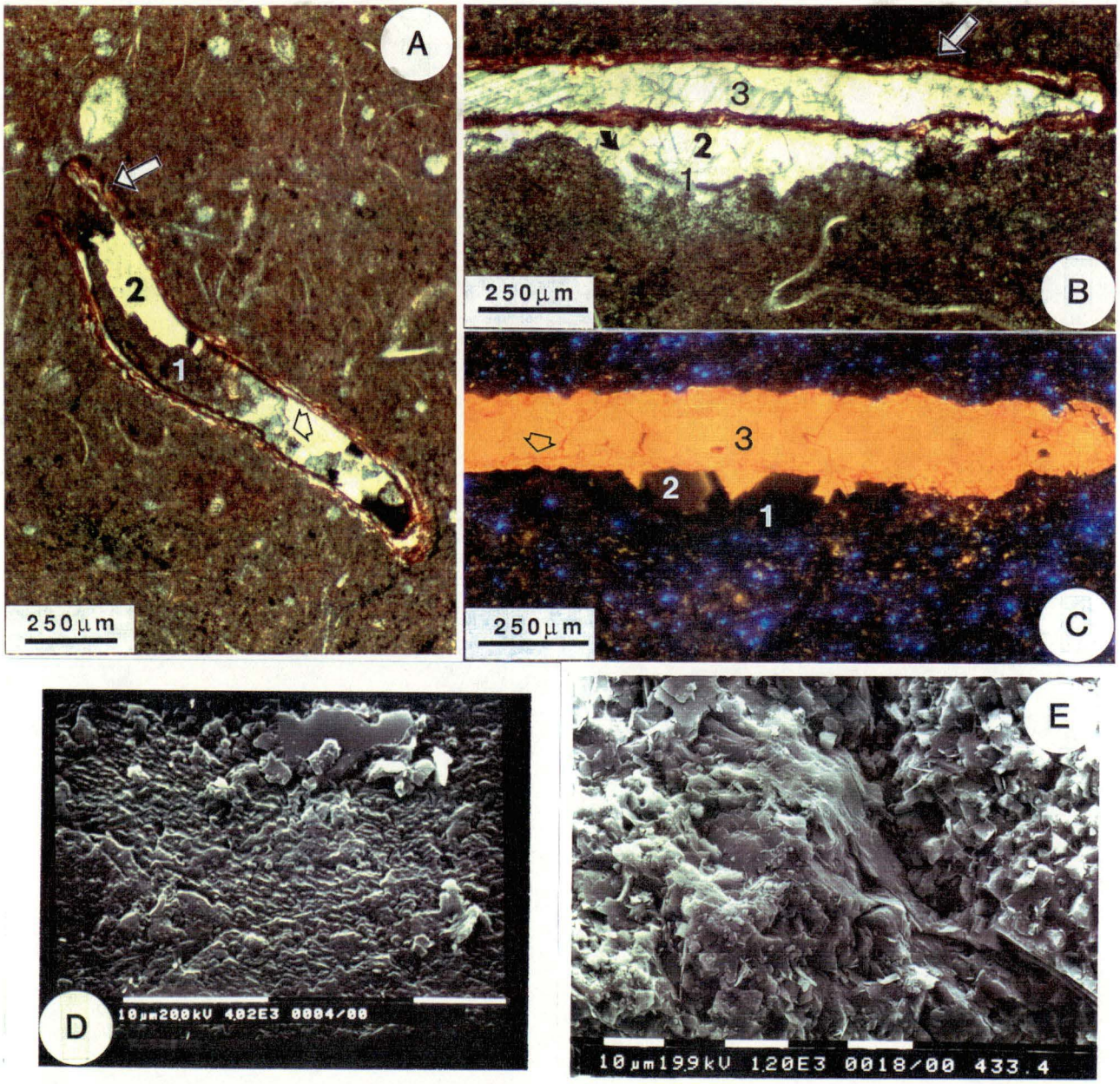
A
2
1
250µm
B
3
2
1
250µm
C
3
2
1
250µm
D
10µm20.0kV 4.02E3 0004/00
E
10µm19.9kV 1.20E3 0018/00 433.4

Abrasion and fragmentation of carbonate skeletons are not as important in this regime as bioerosion and chemical alteration, maceration and recrystallization. Maceration is a dominant process.

Bioerosion: Biological breakdown by borers has been recognized in many large skeletons including crinoids, trilobites, bivalves, brachiopods and dasyclades. However, crinoids, bivalves and trilobites are the preferred substrates for excavation (Fig. 7.3C). It is less obvious in the microfauna probably because they are usually modified by chemical alteration (Fig. 7.4D). Crustacea, molluscs, sponges, echinoids, worms, blue green algae, fungi and bacteria are listed as borers excavating present day unconsolidated particles (Milliman,1974). In the present case echinoids, blue green algae, worms, fungi and bacteria borers are less probable candidates or rare because of the absence of large but shallow, oval to circular cylindrical bore holes (30-500 μm in diameter) in random orientation within macrofauna shells (Neumann,1968; Coudray and Montaggioni,1986). Moreover crustaceans can be discounted because their holes are closely space and most common in intertidal environments. Therefore, the most likely borers are small molluscs and sponges. Indeed, mollusc shells have been observed in holes bored perpendicular to hardgrounds (Fig. 7.4B). However, thick micritic envelopes surrounding ostracod carapaces indicate the presence of microalgae and/or fungi (Bathurst,1975). The early cement and recrystallized spar as well as hardgrounds were also attacked by these boring organisms (Fig. 7.4B,C,E,F).

Maceration: All ostracod carapaces, other microfauna, and some large skeletons, especially brachiopods, show a gradual breakdown into various shapes of micrites after the decay of soft tissues on the seafloor (Fig. 7.4D,E,F). Micrite shapes depend on the mineralogy and structure of their original carbonate skeletons (Alexandersson,1979) and degree of disintegration. The most common shape is a granule with some rods and polygonal plates or irregular flakes. Fibrous grains are rare. Macerated micritic grains range from 0.5-10 μm. Due to the various degree of disintegration from partly altered grains (Fig. 7.4D) to loose individual micrite granules (Fig. 7.4E) preserved along binding and trapping stromatolite layers prior to cementation by micritic cements and rhombic microspar (Fig. 7.6B,C), the maceration process took place on the seafloor as in the case of the North Sea, Skagerrak carbonates (Alexandersson,1978,1979).

Recrystallization of Macrofauna Skeletons: The destruction of macrofauna by the selective recrystallization of the skeleton has been commonly observed in many molluscan shells (Fig. 7.4F, 7.5A, 7.5B), trilobites and echinoderm ossicles. It is

found that bivalves were readily affected by this process but echinoderms were less prone to alteration, because of ferromanganese staining or filling in the stereome, as with the haematization of crinoid ossicles from the Upper Devonian griotte of the Montagne Noire, France (Tucker,1973). Microfossils and shells such as those of brachiopods which suffered from extensive maceration and micrite encrustation show no recognizable recrystallization (Fig. 7.4D,F), even under the SEM (Fig. 7.6B). The alteration firstly occurred at the shell walls of trilobites and molluscs and progressed towards the middle part of skeletons where the original shell structures are sometimes preserved as relicts (Fig. 7.4F). But the alteration of brachiopod and echinoderm skeletals is selective and random. Completely recrystallized grains are rare. Recrystallized products, the neomorphic spars (LMC), are finely to coarsely granular and the small blocky (15-150 μm) mosaics have either irregular or some plane intercrystalline boundaries. Some crystals have a preferred elongation normal to the shell margin (Fig. 7.4F). The boundaries between the spars and the relicts as well as micritic matrix are sharp. The recrystallized grains still retain the original shape of the shells and in some cases evidence bored holes across the transformation zone into the relicts (Fig. 7.4F, 7.5A). Red ferromanganese impregnation in colloform structure (Fig. 7.5A) and/or staining within neomorphic spar layers is common.

The recrystallization of bioclasts is common in many ancient limestones including the Jurassic limestones of Britain (Hudson,1962,1965), limestones of Eniwetok and Guam (Schlanger,1964), Lower Miocene limestones of the Darai Complex of Papua (Banner and Wood,1969) and the British Dinantian limestones (Bathurst,1975). It is an *in situ* replacement of metastable grains by calcite through the migration of a solution film following the conversion of aragonite to calcite. in marine environment (Banner and Wood,1964) or following the framework stage (Benson,1974) when the only surviving porosity of the rock is 1-2% in the solution film of the intercrystalline boundaries (Bathurst,1975). It occurs in shallow phreatic meteoric diagenesis (Land,1971; Hudson,1962; Sandberg and Hudson,1983), at shallow depth below the seafloor (Baker *et al.*,1982) or late after burial (Bathurst,1983). Purdy (personal communication, 1991) has never found it in the recent marine environment.

The boring across the neomorphic spars surrounding skeletons (Fig. 7.4F, 7.5A) within the Pa Kae limestone suggests a very early diagenetic event prior to marine cementation. The first recrystallization of the Pa Kae bioclasts possibly occurred through a solution film in the reducing microenvironment shortly after the decomposition of organic matter within the shell wall and following the conversion of aragonite and HMC to calcite as evidenced by the relicts (LMC) of original grains, and the bright luminescence without zoning of the neomorphic spars (Fig. 7.7A,B). The

red ferromanganese impregnation as a colloform structure into the alteration zone (Fig. 7.5A) should be later in an oxidizing environment on the sea floor. However, some original grains and relicts could survive to completely transform by dissolution-reprecipitation process after burial. This indicates by the filling of bright luminescent blocky spars (50-300 μm) within the frame of bright luminescent subequant neomorphic spars and red ferromanganese colloform structure after non-and dull-luminescent spars in the shelter porosities under the former skeleton grain (Fig. 7.5B,C). Later neomorphic blocky spars extend across the skeletal frame to merge or epitaxial with bright luminescent blocky spars in shelter porosities.

7.4.2 Cementation

The significant role in forming the Pa Kae stromatolites was played not only by the destruction and production of grains by grain alteration processes and the binding and trapping of sediments mechanism but also by subsequent submarine and burial cementation. The role of the stromatolites in early submarine lithification will be discussed in detail. Evidence of meteoric diagenesis has not been observed in this rock.

7.4.2.1 Submarine Cements and Hardground

Micrite Cements: There are two forms of this extensive cement : micrite envelopes or fringe of micrite (Fig. 7.4E, 7.5D) and intergranular micrite cements (Fig. 7.5E). Micrite fringes up to 40 μm thick on microfaunal skeletons are nearly ubiquitous and mostly occur with well defined lineation surrounding ostracod carapaces (Fig. 7.5D) and irregular boundaries on other with bioclasts (Fig. 7.4E). Other micrite cements are usually associated with larger micro-rhombic spars within intergranular porosities along spar-rich stromatolitic laminae (Fig. 7.5E) and have a tendency to mix with or encrust the detritral micrites (Fig. 7.6B). These micrites are different in their form and size from grain alteration micrites. They are subrhombic to rhombic and their polyhedral crystals are smaller, ranging in size from 0.4-7 μm. Micrite envelopes are the result of micritization of the skeletons by either boring or encrusting algae (Bathurst,1975; Sibley and Murray,1972). Both micrite envelopes and intergranular micritic cements are here interpreted as largely biotically-induced precipitation (Kobluk and Risk,1977;Tsien,1985; Burne and Moore,1987) rather than inorganic precipitation or recrystallized lime mud (Moshier,1989). They are the earliest phase of cementation as envelopes or fringe and continued to precipitate during microspar formation as micrites in the cold water carbonates, of the Berriedale Limestone (Lower Permian) of

Fig. 7.6 Thin-section and electron photomicrograph (SEM) of early marine and burial cementation.

A. Nearly uniform fringe of LMC equant cements around red intraclast which were formerly impregnated or encrusted by dark red Fe-Mn minerals (1). Then isopachous cements themselves (2) were also impregnated by those minerals in colloform structure (white arrow).

B. SEM exhibiting a partly macerated ostracod carapace (1), detrital micrites including granule (2) and flake (3) shapes, partly dissolved rhombic microspars (4,5), zoned microdolomite (6), and subrhombic micritic cements (black arrow) embedded detrital micrites. Allochems and detritals micrites were trapped and bound by calcified filamentous cyanobacterial sheaths (white arrow). Subsequent rhombic microspars embedded a stromatolitic sheaths (above 4). The microdolomite also embedded the detrital micrites (6), calcified sheaths, and microspars. Broken slab no. 433.4

C. SEM showing well developed rhombic microspar crystals that nucleated on and grew away from a fenestral wall. Broken slab no. 433.4

D. Half stained (left) thin section illustrating multigeneration of early marine internal sediments and marine cements alteration within large cephalopod intraskeletal porosities. Two generations of mainly micrite internal sediments with an erosional contact between them lying on the bottom of pore chamber (1,2). Note the large intraclasts in the second generation layer. This was followed by the cloudy radiaxial fibrous calcite with botryoidal outline (3). Then the third generation of internal sediments 4, mainly pellets, deposited; and followed by the burial blocky spars (5). Stylolites modified the bottom part of this skeleton. All of those diagenetic features were cut through by ferroan fibrous calcite veinlets (6) and were subsequently replaced by locally deep-burial xenotopic dolomites (arrow). Thin section no.389.11

E. The micritic internal sediments (1) deposited within the upper cephalopod chamber while cloudy radiaxial calcite cements with botryoidal structure (2) dominated the lower one. Very rare irregular marine bladed cement (arrow< 3) grew from cephalopod into a sheltered porosity with increasing crystal sizes. Thin section no. 439.1

F. The red intraclast (1) bound by an ostracod carapace and erosional surface with Fe-Mn crust (white arrow), the outer rim of ostracod carapaces was cemented by a thin equant spar crust subsequently impregnated by Fe-Mn mineral (red, long arrow). Micritic internal sediments (2) deposited within a sheltered porosity following by equant spars which were bored (curve arrow) after the lithification of hardgrounds. Thin section no. 409/11

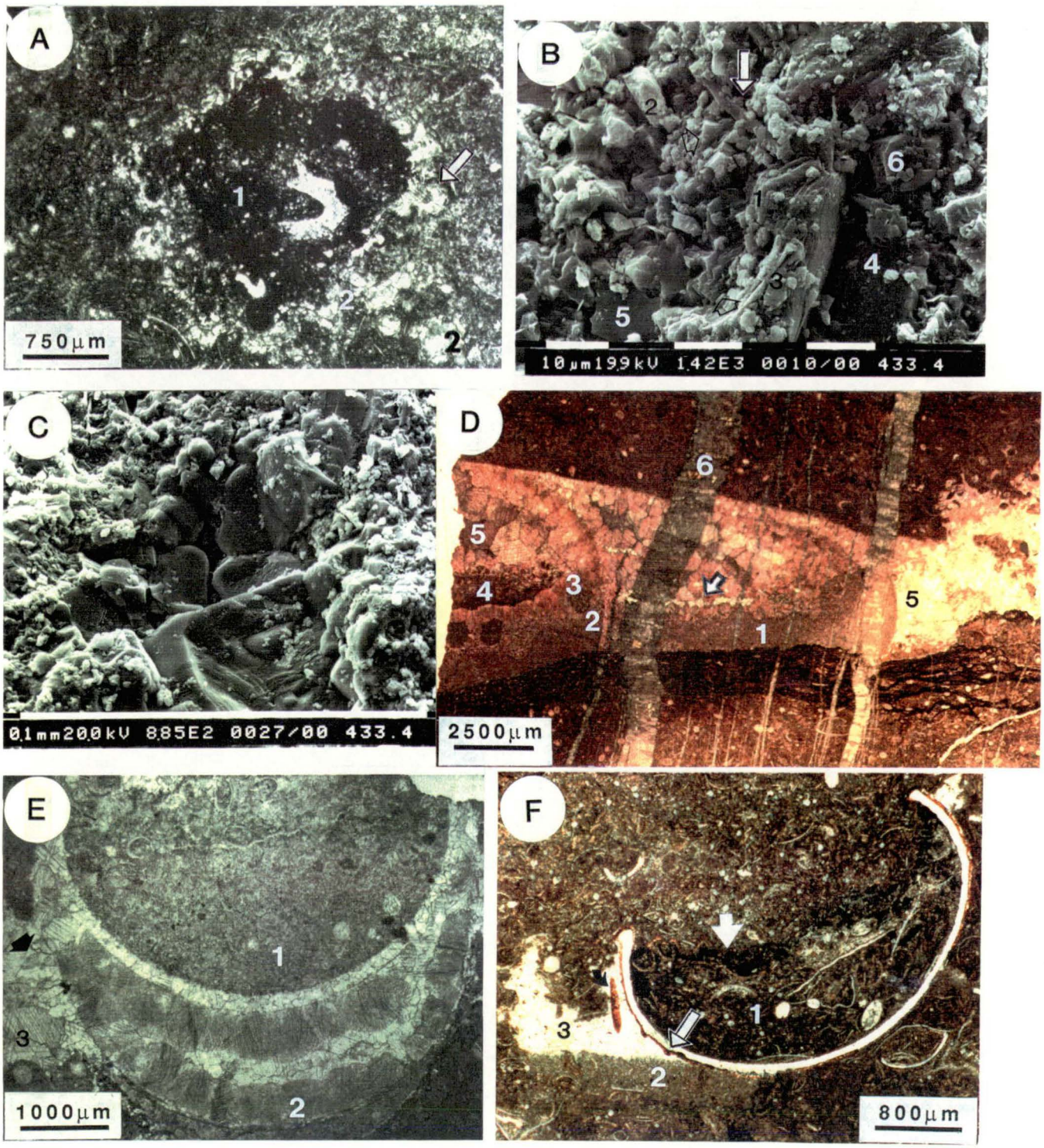
A
1
2
750µm
B
1
2
3
4
5
6
10µm19.9kV 1.42E3 0010/00 433.4
C
0.1mm20.0kV 8.85E2 0027/00 433.4
D
1
2
3
4
5
6
2500µm
E
1
2
3
1000µm
F
1
2
3
800µm

Tasmania (Rao,1981). In modern seas, the LMC rhombic and polyhedral calcite cements (2-4 μm) have been found forming vertical hardground on the deep-sea floor of Tongue of Ocean in the Bahamas (Schlager and James,1978). However, the dull luminescence of the Pa Kae micrites (Fig. 7.7A,B,C,D) suggests that they have gone through the recrystallization process to some degree. But the recrystallization of micrites should be slight because no strong alteration features have been observed, even on SEM (Fig. 7.5D,E; 7.6B,C) perhaps because of their original calcite mineralogy with rhombic crystals.

Isopachous Equant Cements: The cement fringes are present as a minor early diagenesis component. They usually form a thin (30-200 μm thick), irregular isopachous crust on intraclasts (Fig. 7.6A) and bioclasts (Fig. 7.6F) or as a discontinuous interlayer within ferromanganese nodules (Fig. 7.4C). The individual crystals are clear, and anhedral to subrhombic ranging from 10-210 μm. The fringe cements are usually impregnated by red ferromanganese mineral in colloform structure cross-cutting crystal boundaries. Spars within ferromanganese nodules are clean but heavily bored (Fig. 7.4C). The other type of isopachous equant cements is more common, larger (up to 250 μm), and usually occurs as an isopachous crust lying as the first cement in shelter and fenestral porosities (Fig. 7.7A) with increasing grain size toward a pore centre. They are nonluminescent cements. The bright orange luminescence of the isopachous equant cement fringes in the zone of ferromanganese impregnation and nonluminescence of equants spar outside that zone, and of spar laminae followed by non-luminescent, later equant spars within shelter porosities (Fig. 7.7A,B) suggest occasional reducing conditions of a generally well-oxygenated sea floor environment.

Microspar Cements: Under the SEM, microspars (5-100 μm) are either scattered individual rhombic crystals (Fig. 7.6B) or druse scalenohedral and rhombic crystals growing with increasing grain sizes from the substrates (Fig. 7.6C) into larger microporosities along stromatolite laminae, especially within spar-rich layers. They fill nearly all pores within the Pa Kae limestones, especially intergranular porosities, and usually embed the former micrites (Fig. 7.6B). Corroded margins are common in some layers. In large geopetal cavities within macrofaunas or shelter porosities (Fig. 7.6D, 7.7A), microspars usually occur as the first cement precipitating at the same time as the infiltration of the internal sediments including micrites, peloids, tiny skeletons, small intraclasts, microspars and equant crystal silts. But in small geopetal cavities within microfaunas, they are the only cements (Fig. 7.4E). With CL, these microspars nearly always exhibit no luminescence (Fig. 7.7D). In some instances,

Fig. 7.7 Thin-section (left) and cathodoluminescence photomicrograph (right) showing the diagenetic fabrics.

A. and B. The original skeletons including ostracodes and trilobites (white arrow), the first marine equant cements (1) Rhombic microspars within the ostracod carapaces are non-luminescent suggesting the oxidizing nature marine formational water

B. The zonation of burial blocky spars begin asdull to bright luminescence in the middle of the shelter porosity, suggesting the change from strong to moderate reducing conditions after burial. Recrystallized calcite with Fe-Mn impregnation around the trilobite skeleton (white arrow) and amorphous haematite patches or impregnation within micritic matrix show bright luminescence whereas micrites themselves are dull. Thin section no. 359.1/0.3

C. and D. Two generations of internal sediments : the first generation (1) is micrite with microspars within the ostracod carapaces and pellets in a sheltered porosity, the second is biomicrite within a moldic porosity (D) . The typically complete cathodoluminescent zonation of cement begins from non to dull and bright luminescence as B. Microspars, equant spars, and original skeletons are also nonluminescent. Thin section no. 359.1/1

E. and F. Multigenerations of internal sediments and cements within a cephalopod intraskeletal porosity show a different cathodoluminescent zonation than 7.7 B. Dull luminescence of micritic layer 1 and 2 as well as of marine radiaxial fibrous cement (3) is interpreted as forming in a reducing microenvironment on the sea floor . The bright luminescence of blocky spars (5) suggests precipitation in rather deeper burial whereas another dull luminescence of ferroan blocky calcite cement in the middle of pore and fibrous cements in veinlets indicate the formation of these cements long after burial. Blue luminescence of internal sediments (1) in F possibly suggests clay mineral contamination. Thin section no. 389.11

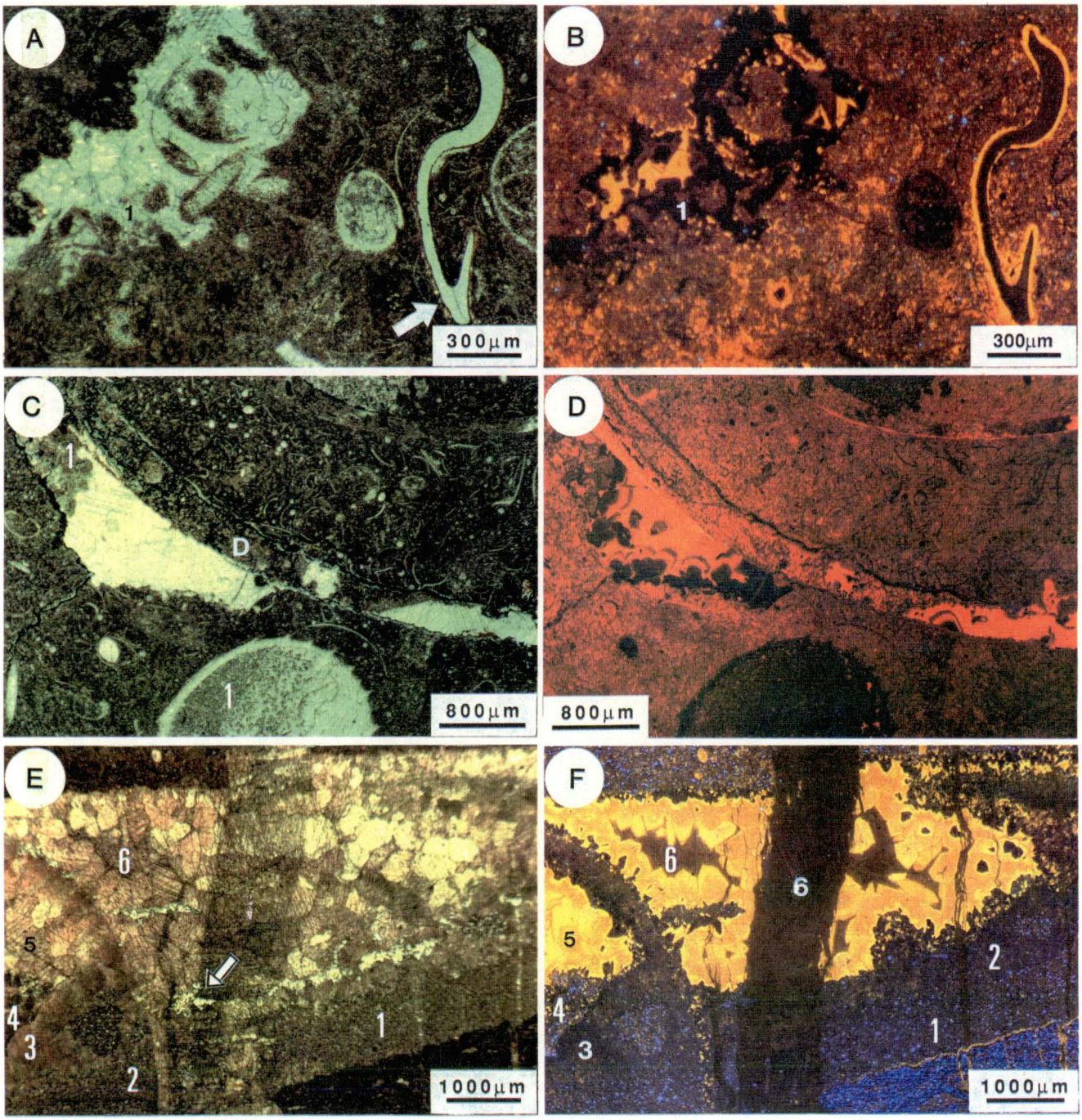
A
1
300μm
B
1
300μm
C
1
D
1
800μm
D
800μm
E
6
5
4
3
2
1
1000μm
F
6
6
5
4
3
2
1
1000μm

however, a very dark dull luminescence is observed in some microenvironments (Fig. 7.7F). Therefore, it seems likely that microspars are principally synsedimentary cements precipitating directly from oxidized sea water with some microspar forming later during the decomposition of organic matter or at the same time in specific reducing micro-environments.

Radiaxial Fibrous Cements: They are very scarce and confined to the intraskeletal porosities of nautiloids. The fibrous crystals have a very dark dull luminescence, and are cloudy, large, elongate crystals (up to 500 μm long) with vague subcrystal outlines (Fig. 7.6E), forming isopachous crusts in the form of a botryoidal structure. Radiaxial cements either alternate with internal sediments (Fig6D) or are overlain by blocky spars (Fig. 7.6E). They were also an early marine cement forming in reducing micro-environments within skeletons as shown by very dark dull luminescence.

Submarine Hardgrounds and the Role of Stromatolites: Extensive marine cementation lead to the early lithification of the Pa Kae stromatolites at the sediment/ water interface as demonstrated by many features including : (1) the excellent preservation of the stromatolite sheaths (Wright and Wright,1985), (2) the ferromanganese crusts lying upon some erosional and bored surfaces (Fig. 7.4B) which truncated shells, and (3) the marine organisms that grew on the lithified surfaces. Additional evidence are in the form of (1) intraformational intraclasts (Fig. 7.4A), (2) boring across marine cements (Fig. 7.4C,E), (3) multigeneration of internal sediments and marine spars (Fig. 7.6D,F), (4) nonluminescent equant cements forming as the first cements in many shelter porosities (Fig. 7.7), (5) fenestrae, and (6) neptunian dikes (Fig. 7.8E). The lithified stromatolites acted as hardgrounds and provided a source of red intraclasts, for the subsequently covered by later stromatolitic layers which grew upon the partly eroded surface. Both stromatolitic generations commonly have the same morphology. Erosional surfaces on these hardgrounds are probably rare or vague unless they were heavily bored by organisms and covered by thick ferromanganese crusts. The rarity is possibly the result of the rapidly upward growth of cyanobacteria covering the surface and protecting it from erosion and boring. Pratt (1982a) regarded this covering as a protective living algal mat cover.

It is clear that stromatolites play an important role on the accumulation and stabilization of allochthonous carbonate grains along stromatolitic laminae by the trapping and binding mechanism (Neumann *et al.*,1970; Scoffin,1970; Golubic and Focke,1978) but their role in synsedimentary submarine lithification events is not clear. Burne and Moore (1987) suggested that the lithification of the modern subtidal

stromatolites of Shark Bay (Burne and James,1986) may be partly the result of calcification of spherical microbial bodies whereas Logan *et al.* (1964) favoured entirely abiological cementation. It is still a matter of controversy. Based on the abundance of well-preserved aphanitic calcified stromatolite sheaths of filamentous and coccoid bacteria (Fig. 7.2F, 7.5E, 7.6B) within the Pa Kae stromatolites, the calcification of the stromatolitic microstructure had occurred early, preceding extensive cementation and the decomposition of organic matter. Calcified stromatolitic sheaths were engulfed by rhombic spars and micrites (Fig. 7.6B). The calcification of the stromatolitic elements themselves was possibly formed by the precipitation or impregnation (not encrustation) of amorphous calcite in and/or on the stromatolitic sheaths as suggested for modern micrite-walled tubes of *Girvanella* from Aldabra Atoll by Riding (1977). He stated that under biochemical control, micrite grade crystals can impregnate living *Girvanella* mucilaginous sheaths in meteoric environments but this photosynthetically induced $CaCO_3$ precipitation will be limited in normal marine environments because of the buffering capacity of sea water. However, in this case it possibly occurred in a deep sea condition. Scoffin (personal communication) stated that *Girvanella* is not a modern alga while *Plectonema* is the modern alga from Aldabra.

The calcification process of stromatolites is biologically controlled (Burne and Moore,1987) through the photosynthetical uptake of CO_2 from sea water by cyanobacteria. This results in amplifying supersaturation (Kempe and Kazmierczak,1990) or decreasing pCO_2 (Williams,1983) and elevating pH (Halley,1976) of sea water which in turn triggers the precipitation of fine-grained calcite and calcification of shells and faecal pellets (Kempe and Kazmierczak,1990). It is a bulk extracellular and/or intercellular biomineral formation (Lowenstam,1981) and its product has crystal habits similar to those of abiotic precipitation (Lowenstam,1981). The high $\partial^{13}C$ value (up to 3.5‰ PDB) of the Pa Kae (Table. 7.1) suggests that *in situ* photosynthesis induced the precipitation of calcite including micrites, and microspars. Therefore, the early submarine cementation of micrites and microspars during submarine lithification and the formation of the hardground following the calcification of stromatolites is wholely or at least partly biogenic but most spars within larger cavities such as shelter and intraskeletal porosities including burial cements are of abiotic origin. The other biogenic process, the bacterial decomposition of organic matter via anaerobic respiration inducing carbonate precipitation in some stromatolites (Purdy,1963; Lyons *et al.*,1984; Lanier,1988), seems to be less important during the calcification of the Pa Kae because of their sheaths, nonluminescent rhombic spars and heavy isotopic composition of the rocks.

This is the result of either early calcification of the Pa Kae on an oxygenated sea floor prior to organic decomposition or to the different kind of Pa Kae microbial communities.

7.4.2.2 Burial Dissolution and Cementation

The dissolution of many skeletons more stable than those which were recrystallized during destructive diagenesis occurs at shallow burial depths shortly after marine lithification leaving moldic porosities and partly providing $CaCO_3$ for further burial cementation. Dissolution of some corroded rhombic spars (Fig. 7.6B) should occur at this stage because of burial cementation inducing undersaturation with respect to calcite of pore fluids.

Blocky Cement: The moldic porosities and the other retentive primary porosities subsequently filled with clear, non to bright luminescent blocky spars (up to 300 μm, Fig. 7.7C,D). The zonation from non to dull and bright luminescence in shelter spars with CL suggests the gradual change of pore fluid chemistry from an oxidizing condition shortly after burial to strongly reducing fluids during the decomposition of stromatolites and other organic matter, and to moderate reducing conditions late after burial. This is also shown by the occurrence of dull ferroan calcite filling in veins, veinlets, as the last cement in some large voids (Fig. 7.7E).

7.4.3 Dolomitization

Microdolomites are the least abundant but nevertheless an important diagenetic component. They usually occur either within the stylolite seams (mudstone layers) and/or replacing various type of micrites, allochems and cements within biomicrites (Fig. 7.6B, 7.8A). Dolomite crystals (15-250 μm) are commonly hypidiotopic to idiotopic, cloudy with some clear rims. Some of them are broken and truncated by stylolites. Under SEM, some microdolomites exhibit zones, and embedded micrites and microspars (Fig. 7.6B). Micrites are the most susceptible to dolomitization whereas the faunal skeletons are the least. Based on this evidence, most of the Pa Kae microdolomites are considered to be of early burial dolomitization following submarine cementation and lithification but prior to compaction and the formation of neptunian dykes which are filled with laminated grey micrites and broken spar (Fig. 7.8E).

The $\partial^{18}O$ and $\partial^{13}C$ values of the Pa Kae dolomites range from -2.6‰ PDB to -10.7‰ PDB and -0.4 to +1.6‰ PDB respectively. The heaviest $\partial^{18}O$ isotopic

Fig. 7.8 Thin-section photomicrograph showing dolomitization and compaction fabrics.

A. Half stained thin-section Photomicrograph of thin section (half only stained) illustrating local dolomitization. Early burial dolomite has slightly cloudy centers and clear rims, hypidiotopic, and broken (black arrow). It replaced micrites (1), bioclasts (white arrow) and equant spar cements (2). Thin section no. 409.1

B. The compaction effect on lithology and bedding occurred during early shallow burial as evidenced by the plastic deformation of semilithified limestone layers (1), the collapse and penetration (structure) of limestone layers downward to break down some skeletal grains within a mudstone parting (2), and the dewatering lamination (3). The cross cutting and the relation between the blocky spars and stylolite (white arrow) indicate that some blocky cements occurred early during shallow burial. Thin section no. 409 A

C. Hummocky to smooth and low amplitude stylolites are common within limestone layers. Thin section no. 409.5 B

D. In contrast to C., stylolite seams are common within relative thinner limestone layers and thicker mudstone partings. They modified the original bedding to the nodular structure. Note the macrobioclast content in limestone within D. is much lower than that in C. and is nearly absent in mudstone layers. Thin section no. 409.4

E. Three generations of laminated internal sediments (1,2,3) filling in a neptunian dike which cut across the original bedding and stylolites. Subsequently, blocky calcite veinlet partly cut through all of those fabrics. Thin section no. 440.2

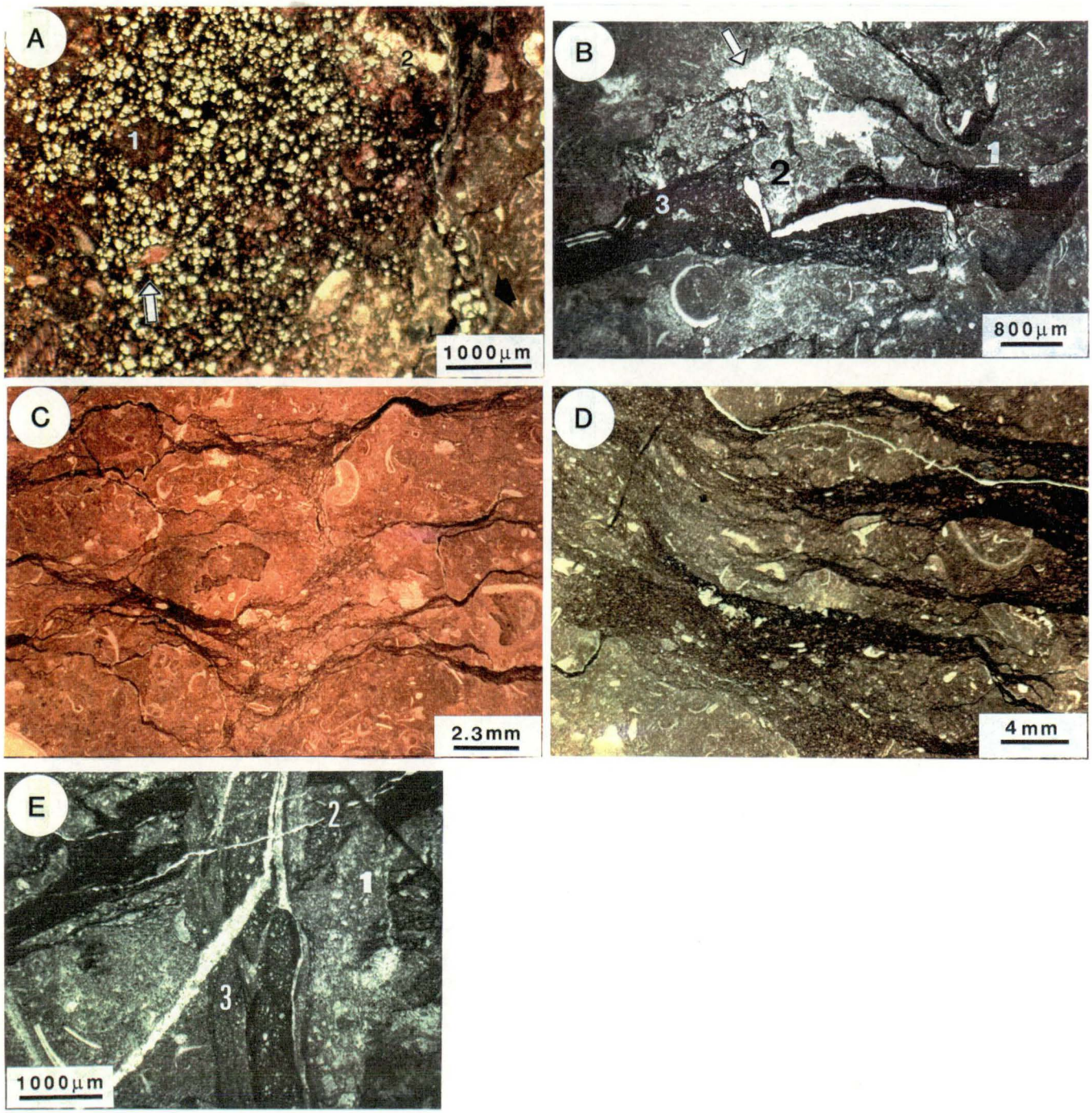
A
1
2
1000µm
B
1
2
3
800µm
C
2.3mm
D
4mm
E
1
2
3
1000µm

composition of -2.6‰ PDB and $\partial^{13}C$ isotopic composition of 1.6‰ PDB suggest that the dolomitizing fluids are similar to sea water of that age and the formational palaeotemperatures are probably close to those of normal sea water. Mg supply may partly come from the dissolution of Mg-calcite skeletons. The dull to bright luminescent zonation emphasizes the fluctuation of formational fluids from strong to moderate reducing conditions during the decomposition of organic matter, possibly by sulphate reducting bacteria. But the decomposition of organic matter by either aerobic bacteria in oxidizing environment in well oxygenated pore fluids close to rock/water interfaces or by sulphate- reducting bacteria within stagnant and anoxic pore fluids below the uppermost zone of the sea-bed produces isotopically light CO_2 and biocarbonate with depleted $\partial^{13}C$ (-25‰ PDB, Scoffin,1987). Therefore, another process must be involved and responsible for $\partial^{13}C$ isotopic enrichment up to 1.6‰ PDB. The other possibilities are that microdolomites occurred after the decomposition of organic matter in the normal reducing conditions of the burial environment or occurred below the sulphate reduction and organic fermentation zone. The last possibility is not so likely since much evidence favours shallow burial including the enrichment of $\partial^{18}O$ up to -2.6‰ PDB and most of organic matter was probably destroyed on the sea floor by oxidation.

If the Pa Kae dolomites had formed within the zone of methanogenesis, they would have had $\partial^{13}C$ values more than +20‰ PDB (Irwin *et al.*,1977). On the contrary, $\partial^{13}C$ values up to +1.6‰ PDB of the Pa Kae are close to the average value of 2.3‰ PDB of the Enewetak Atoll dolomites (Saller,1984) which formed from normal sea water. The slightly $\partial^{13}C$ depletion from those of the Pa Kae dolomites suggests that they formed from the slightly modified normal sea water by the decomposition of some remaining organic matter. However, some small xenotopic,very dull luminescent microdolomites (up to 200 μm) formed late after burial and replaced burial blocky spars and ferroan calcite in veinlets (Fig. 7.7E,F). Therefore, the localized replacement dolomitization may have developed throughout the burial history of the Pa Kae,but the most commonly was precompaction. This is confirmed by the $\partial^{18}O$ depletion of some dolomites to -10‰ PDB. The recrystallization or accretion of early diagenetic dolomites should be expected (Land,1980) since many of them show cloudy center and clear rim fabrics.

7.4.4 Compaction and Bedding

No significant physical compaction features have been observed within the limestone layers because of the extensive early cementation during sea floor diagenesis and the early phase of burial as mentioned earlier. However, the compaction can be

concentrated in the less cemented strata (Bathurst,1987) as evidence by plastic deformation in the thinner part of limestone layers enclosed by mudstones (Fig.7.8B). The differential lithification between limestones and mudstone partings also resulted in the formation of the physical compaction features when the compaction stress increased. These compaction features include the collapse and dislocation of the limestone layers which penetrated downward to break down or dislocate the skeleton grains within mudstones, and the dewatering laminae of mudstones (Fig. 7.8B). In contrast, chemical compaction is extensive within both limestones and mudstones leading to the formation of stylobreccia, hummocky to smooth and low amplitude stylolites, stylolite seams or dissolution seams (Fig. 7.8C), and even stylonodular-like bedding (Logan and Semeniuk,1976) within the zone of thinner limestone layer (<30 mm) with relatively thick mudstone partings (Fig. 7.8D). Clay minerals and some dolomites are commonly concentrated in the seams as stylocumulate .

Therefore, not only does the stromatolite morphology provide a wavy appearance (Fig. 7.2A) in the limestones (<3 cm thick) but compaction also induces the formation of nodular structure. These beddings are neither rhythmic diagenetic bedding,which originates by diagenetic carbonate dissolution and cementation in a closed carbonate system at several 100 m depth (Ricken,1986), nor diagenetically enhanced bedding (Bathurst,1987). But, they are partly an original marine rhythmic sequence or periodiates (Duff *et al.*,1967; Einsele,1982) and partly diagenetic modified bedding. As a whole, it is a rhythmic alternation of a wavy stromatolitic controlled-limestone-bedding, and very thin depositional mudstone-bedding on the upper part of the Pa Kae Formation whereas the diagenetic induced nodular bedding dominates the lower part of the sequence. They still record a periodically changing environment with a small break during their deposition (Einsele,1982).

Although, it is most likely that dissolution of limestones during the early stage of stylolitization provided $CaCO_3$ for burial cementation of this formation (Barrett,1964; Bathurst,1975; Hudson,1975; Nelson,1988; Finkel and Wilkinson, 1990); the cementation, lithification, and fluid-assisted fracturing ceased prior to the completion of stylolitization as shown by the cross-cutting of stylolites through blocky spars (Fig. 7.8B,C) and offsetting of short wedge-like veinlets. Stylolitization also finished prior to significant burial, shortly after most of pore spaces were obliterated by burial cementation (Nelson,1978,1988). This is suggested by the occurrence of neptunian dykes cutting across the stylolite seams (Fig. 7.8E). Physical compaction continued and created shear and tension fractures cutting through bedding and all former diagenetic elements, and subsequently filling by ferroan fibrous calcite (Fig. 7.6D). These fractures may occur at moderate to considerable depths. The partly translucent dark brown to dark gray, texturally unaltered conodonts with CAI of 3-4

Table 7.1—Major and minor elements and some isotopic compositions for the selected carbonates from the type section of the Pa Kae Formation

Sample no.	$\partial^{18}O$	$\partial^{13}C$	Ca%	Mg%	Ca/Mg	Sr(ppm)	Mn(ppm)	Fe(ppm)
A.Micrite (Biomicrite); red limestone at Ban Pa Kae								
1. 359.1/0	-6.7	3.3	34.5	0.4	90.8	255.1	1072.2	1407.5
2. 359.1Top	-9.2	2.4	35.0	0.4	100.0	193.1	673.6	1354.3
3. 359.1/0.3	-10.1	2.4	32.1	0.4	86.8	235.5	848.3	1881.6
4. 359.1/0.9	-10.0	2.3	35.6	0.4	101.7	216.9	667.9	1174.2
5. 359.1/1	-9.8	2.4	34.4	0.4	86.0	224.4	654.4	1104.7
6. 359.1/3	-9.9	2.5	35.3	0.4	95.4	194.9	702.4	1331.4
7. 359.1/7	-10.4	2.4	32.2	0.4	80.5	218.6	979.2	1962.7
8. 359.1/12B	-9.8	1.7	34.2	0.3	114.0	217.5	306.6	2233.9
9. 359.1/13	-8.3	1.3	34.2	0.4	97.7	209.4	670.1	1152.1
10. 359.1/24	-6.2	1.8	32.6	0.4	90.6	240.5	2030.7	1589.0
11. 359.1/26	-6.4	2.9	36.0	0.3	116.1	225.6	990.5	996.7
12. 359.1/46	-6.2	1.3	33.9	0.3	121.1	219.5	893.6	1191.7
13. 359.1/46C	-3.1	2.7	-	-	-	-	-	-
14. 359.1/46C2	-4.5	1.6	-	-	-	-	-	-
Mean	-7.9	2.2	34.2	0.4	98.4	220.9	874.1	1448.3
S.D.	2.4	0.6	1.3	0.0	12.9	17.6	418.5	389.0
B.Sparry calcite; Ban Pa Kae, Spar in Nautiloids(1-3), Spar in veins and voids (4-7)								
1. 359.1/0	-4.8	3.4	40.0	0.4	105.3	285.0	234.2	247.0
2. 359.1/1	-6.7	2.3	38.6	0.4	104.3	516.1	1118.5	1818.7
3. 359.1/1B	-7.0	2.4	-	-	-	-	-	-
4. 359.1/0.3	-9.3	2.2	-	-	-	-	-	-
5. 359.1/26	-6.6	2.4	38.2	0.3	119.4	546.6	1097.8	4916.2
6. 359.1/24	-4.0	1.9	39.5	0.2	197.5	106.3	648.2	185.3
7. 359.1/26B	-7.2	2.4	40.0	0.3	121.2	346.0	4145.0	254.0
Mean	-6.5	2.4	39.3	0.3	129.5	360.0	1448.7	1484.2
S.D.	1.7	0.5	0.8	0.1	38.8	179.8	1550.7	2038.5
C.Red Calcareous mudstone; Ban Pa Kae								
1. 359.1/0	-6.0	2.8	18.4	0.8	23.0	271.7	1460.6	10282.6
2. 359.1/Top	-9.6	2.1	14.9	0.9	16.4	316.8	1582.6	20295.3
3. 359.1/0.3	-10.6	2.0	10.3	0.8	13.2	236.9	1400.5	11650.5
4. 359.1/0.3B	-9.5	2.3	-	-	-	-	-	-
5. 359.1/0.9	-9.6	2.4	23.1	1.2	19.1	258.0	1597.8	14233.8
6. 359.1/1	-	-	15.1	0.6	26.0	241.1	1704.6	12397.4
7. 359.1/3	-9.7	2.1	9.7	1.1	8.9	251.3	1967.9	21689.0
8. 359.1/7	-9.0	2.4	20.9	0.5	45.4	252.6	1607.5	5741.6
9. 359.1/13	-8.3	1.7	12.2	0.9	14.4	288.5	1710.7	17573.8
10. 359.1/24	-5.9	1.9	20.3	0.5	41.4	252.2	3235.5	6285.7
11. 359.1/26	-6.7	2.5	12.1	0.7	16.6	300.8	1353.6	13983.5
12. 359.1/12B	-8.6	2.0	20.9	0.5	41.8	252.6	1984.5	11177.0
13. 359.1/46/11C	-	-	16.6	1.6	10.4	226.5	1572.3	7373.5
14. 359.1/5C	-	-	25.1	1.0	25.1	258.2	1633.9	12812.8
Mean	-8.5	2.2	16.9	0.8	23.2	262.1	1754.8	12730.5
S.D.	1.6	0.3	5.0	0.3	12.4	25.9	482.4	4945.8

(110-300°C; Epstein *et al.*,1977; Burrett personal communication) probably also suggest deep burial (Nicoll and Gorter,1984) for the Pa Kae Formation. Even though such CAI values still occur in a diagenetic regime (Rejebian *et al.*,1987), most of the Pa Kae diagenetic features were produced on the sea floor and at shallow burial level.

7.5 Geochemistry

7.5.1 Minor and Trace Elements

Because of the very fine nature of the biomicrites, the geochemical analyses have been performed mainly on whole biomicrites, calcareous mudstones, and cements within small shelter and intraskeletal porosities. The results are shown in Tables.1 and 2. In general, the Sr concentrations of 106-546 ppm are within the range of normal ancient marine carbonates but the Mn concentration of 648 - 4,145 ppm and Fe concentration of 1,448-12,750 ppm are higher than those of normal, shallow water limestones (Robinson,1980; Veizer,1983).

Strontium and Other Trace Elements: The relatively low Sr content with mean of 221, 262, and 360 ppm (Table. 7.1) in the early lithified marine limestone of the Pa Kae Formation with heavy $\partial^{18}O$ of -3.1‰ PDB reflects the low Sr content of their originally calcitic mineralogy because such $\partial^{18}O$ and Sr distribution (Fig. 7.13) does not favour the possibility of strong post-depositional alteration (Veizer,1977) of original aragonitic limestones. The high Mn content (up to 4,145 ppm) with low Mg concentration (0.2-0.4%) of sparry calcite (Table. 7.1) also points to original calcite (Rao,1979,1981b). Indeed, they contain mainly calcitic ostracod carapaces and low magnesian calcite (LMC) marine equant and rhombic spars (Rao,1981; Wilkinson *et al.*,1982), a common mineralogy and morphology of the deep sea cements LMC. Equant spars are also a common mineralogy and spar occurs in both a meteoric and burial environment (Perkins,1968; Bricker,1971; Benson,1974; Wanless,1983; James and Choquette,1984; Al-Aasmand and Veizer,1986; Moshier,1989), but this can be excluded for the Pa Kae Formation. Another possibility is the replacement of the original minerals by a Sr-depleted calcite in unmodified sea water of the Pa Kae early lithified limestone which was exposed on the sea floor (Schlager and James,1987; Land,1986). But the petrographic data available support the former possibility.

Brookfield (1988) suggested the close relation between water temperature and the distribution of marine organisms but proposed that geochemical values of limestones are more related to shell mineralogy than to the environmental and geographical setting. Moreover, Parker *et al.* (1985) did not find any correlation

between the trace elements and palaeoenvironments of the Ordovician Black River Group, New York, USA. However, several authors (e.g. Milliman *et al.*,1969; Folk,1974; Lees,1975; Rao,1981, 1990a,b; Nelson,1988) have emphasized the role of both an environment or a geographical setting on the original mineralogy, distribution and sedimentation of the carbonate rocks and their skeletal grains. In addition, the Sr content in calcite is dependent on the temperature of precipitation from formational water (Kinsman,1969; Rao,1981) which is low in this case as also shown by the low content of Mg (Füchtbauer and Hardie,1976; Rao,1986) as mention earlier.

The mean of 221, 262, and 360 ppm (Table. 7.1) of Sr is much higher than the average value of 91 ppm of the Indian Vindyan stromatolites (Kumar,1988). Furthermore, the maximum value of 546 ppm is also higher than 400 ppm of the other Late Precambrian intertidal to supratidal stromatolites from the Chattisgash Basin of India (Srivastava,1977).

The high Sr content of ancient limestones is usually due to either the absorption of Sr by clay during early diagenesis (Bausch,1968) or a function of facies types or environments (Veizer and Demovic,1973; Benson,1974). The Sr content of ancient basinal or deeper water limestone is commonly higher than those of shallow water ones (Veizer and Demovic,1974; Veizer,1978). The important role of strontium absorption by the clay fraction can be ruled out because there is not a significant difference in Sr content between the Pa Kae limestone and calcareous mudstone partings (Table. 7.1). Moreover, Baker *et al.* (1982) stated that the contamination from non-carbonates during laboratory leaching is usually unimportant because of the high concentration of Sr in carbonate rocks, the major sink for Sr in the marine environment. Therefore, in comparison with those ancient tidal stromatolites from Central India, the higher Sr content of the Pa Kae stromatolites should be the result of its deeper water origin as in the basinal facies of the Mesozoic carbonate sequence from the Central Western Carpathians of Europe (Veizer and Demovic,1974). It is confirmed by the positive correlation between P_2O_5 ,Ti, and Ba of the rock (Fig. 7.9A,B) and the high content of those elements which are much higher than that of the average carbonates (Veizer,1983) and the other Thung Song shallow water carbonates (Table. 7.2, Fig. 7.9). The leaching of Ti from clay fraction could be expected because of a high content of Ti (up to 2,390 ppm) in the calcareous mudstone partings. The leaching effect is probably responsible for the chemical separation between the deeper water, lagoonal and other shallow water limestones (Fig. 7.9). However, the concentration of these trace elements in deep sea clay tends to be higher than those in the shallow water setting (Veizer,1983). Eventhough, the area of the lagoonal limestones falls within the same region of the Pa Kae limestone, their P_2O_5, Ti and Ba content is much lower than many of the Pa Kae's.

Table 7.2—Barium, titanium and phosphorus concentration of the Thung Song limestones by X-ray fluorescence.

Sample no.	Ba (ppm)	Ti (ppm)	P_2O_5 (ppm)
1. 395.1	122	1075	195
2. 359.1/03	183	1540	197
3. 359.1/3	148	1590	246
4. 359.1	277	1270	210
5. 359.1/13	144	1270	175
6. 359.1/24	467	1185	260
7. 359.1/26	125	761	218
8. 359.1/46	113	1010	312
9. 409.7	139	1265	478
10. 439.1	044	441	445
11. 439.3	057	543	450
12. 439.5	158	1530	351
13. 439.7B	175	2390	233
14. 440.3B	115	1875	515
15. 423.7	088	1060	339
16. 401 B	283	765	333
17. 404 A	137	1380	345
18. 421.6	012	154	182
19. 401.8	005	089	113
20. 17	042	463	176
21. TB	008	188	043

: Deeper water, red stromatolitic limestones, the Pa Kae Formation (1-12 biomicrite ; calareous mudstone 13-14).

: Lagoonal limestones, Talo Dang and Lae Tong Formation (15-17).

: Subtidal limestones, La Nga Formation (18).

: Limestones with buildups, Rung Nok Formation (19).

: Intertidal stromatolitic limestones, Malaka Formation (20,21).

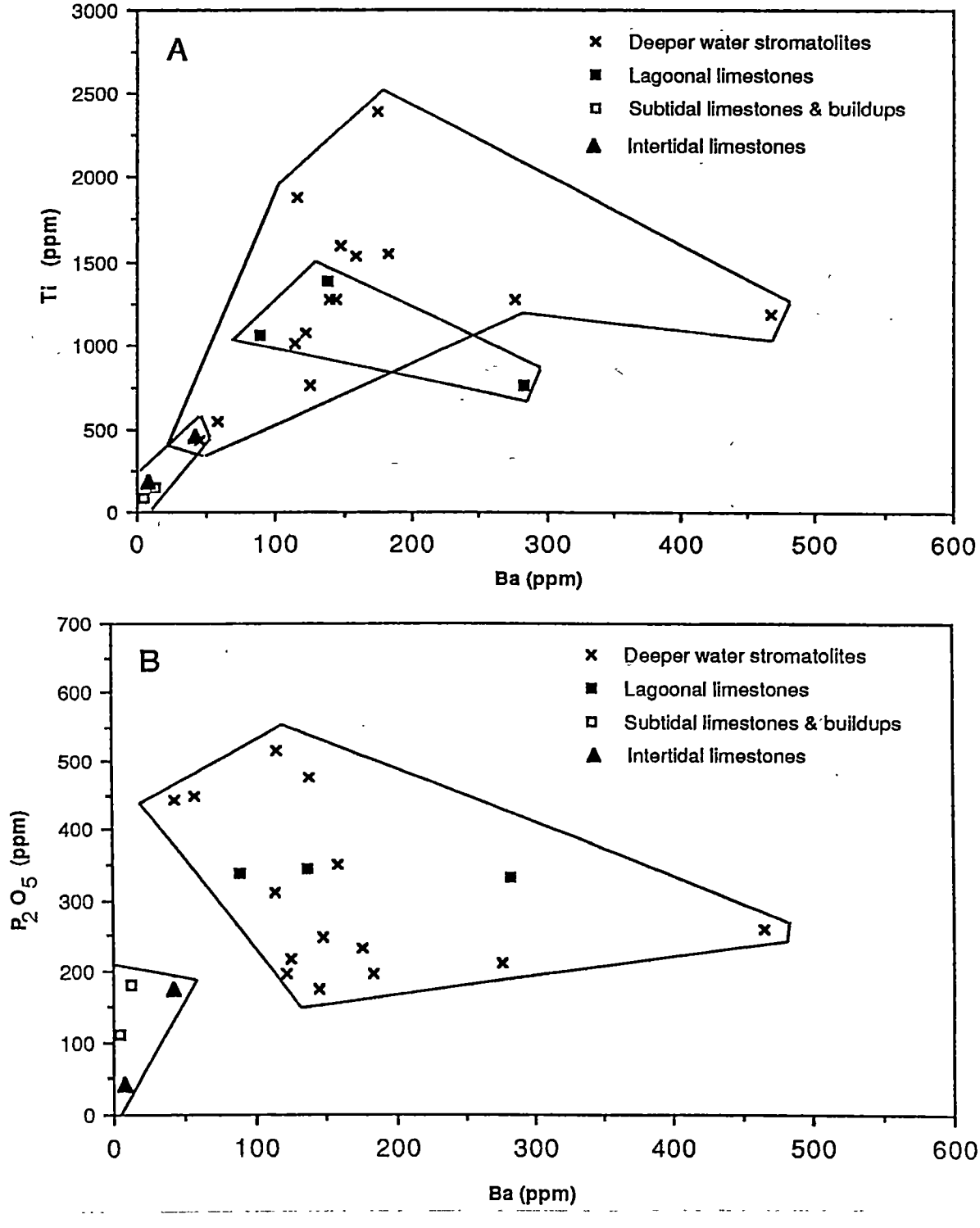

Fig. 7.9 Titanium (A) and phosphorous pentoxide (B) values for the Pa Kae Formation and the other shallow-water Thung Song carbonates plotted against barium values of those rocks. The covariance fields show gradual enrichment in Ti and P_2O_5 from intertidal and subtidal carbonates to lagoonal and basinal deeper-water stromatolitic limestones.

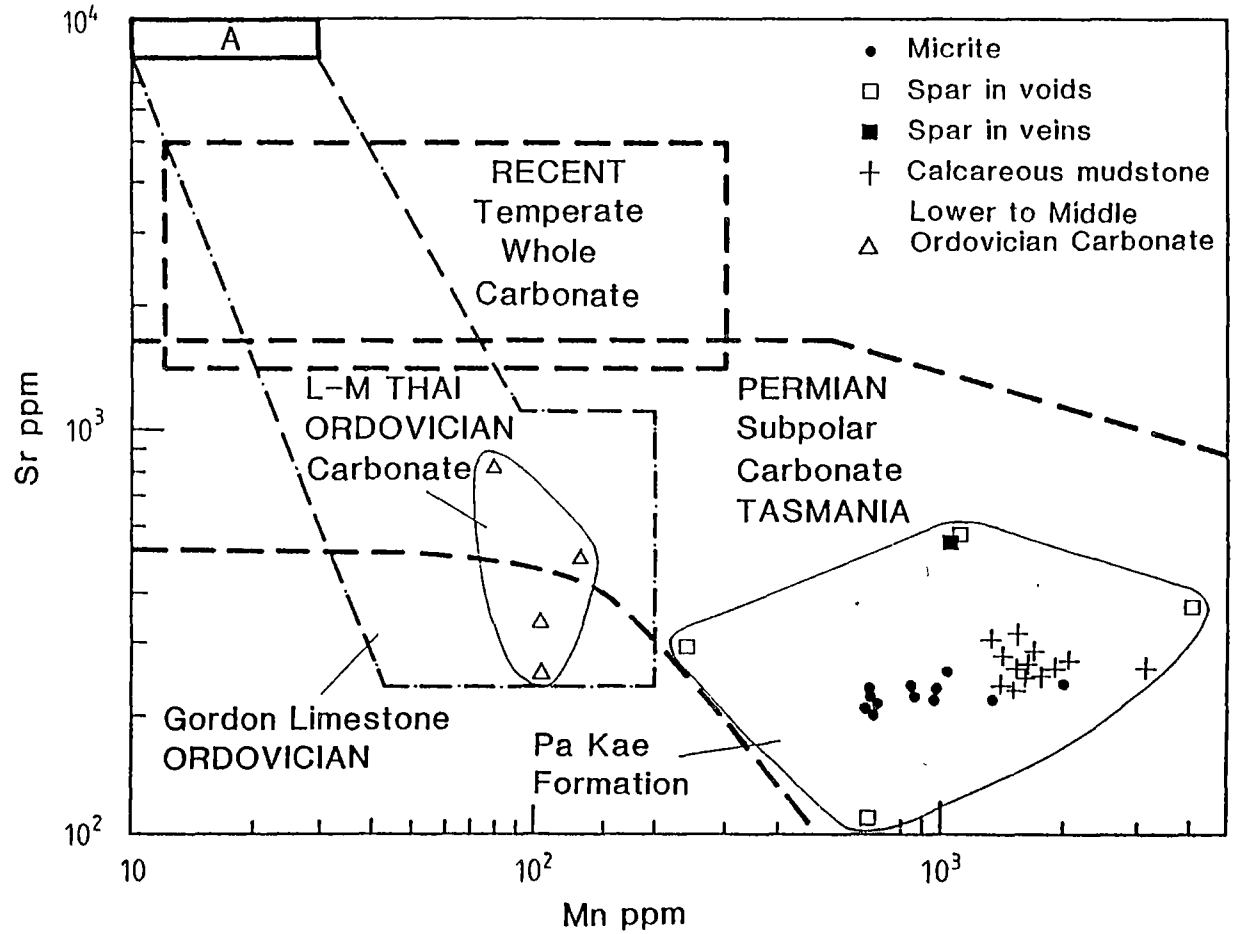

Fig. 7.10 Strontium and manganese variation in the Pa Kae deeper water stromatolites and the other Lower to Middle Ordovician Thai shallow water carbonates compared with the field of Recent temperate whole carbonates, Permian subpolar carbonates, and Ordovician subtropical Gordon limestone from Tasmania (Rao 1990a).

Manganese and Iron: The high concentrations of Mn (234 - 4145 ppm) with mean of 874, 1448, and 1755 ppm and Fe of 1448, 1484, and 12750 ppm are much higher than those (mean 33 - 41 ppm) of the Tertiary, warm shallow carbonates (Majid and Veizer,1987) and of modern temperate carbonates (Rao,1986). The high Mn concentrations of the Pa Kae are similar to those of the Permian cold water (subpolar) carbonates (150 - 3,800 ppm) from Mount Nassau and Douglas River areas,Tasmania (Rao,1990a) and the Middle Ordovician, lower slope to basinal carbonates (346 - 3,561 ppm) from Eastern Tennessee (Shanmugam and Benedict III,1983). The high Mn and Fe concentrations is due to the dominantly calcitic mineralogy (Shanmugam and Benedict III,1983), the slow rate of sedimentation, the submarine lithification (Rao,1986), and the occurrence of iron and ferromanganese minerals (for the whole rock analysis) as disseminated grain, crusts and micronodules within the Pa Kae. Shanmugam and Benedict III (1983) believed that the original difference in Mn content between shallow and deep marine carbonates has remained through time unaffected by late diagenesis.

The Sr versus Mn field falls with the trend of the Permian subpolar carbonates from Tasmania (Rao,1990a) but it is different from that of other Ordovician warm water carbonates from Tasmania and Thailand (Fig. 7.10). In comparison with Tasmanian cold water carbonates, the field of Sr and Mn covariance is consistent only with those of the second stage of stabilization of Tasmanian rocks that includes recrystallization of LMC and addition of calcite cements. But it is inconsistent with the first stage, the inversion of aragonite to calcite, or lack of it because of its calcitic original mineralogy. Recrystallization of the Pa Kae is not extensive. This is suggested by well-preserved micrites and bioclasts, and the heaviest value of $\partial^{18}O$ (-3.1‰ PDB) of biomicrite. The decrease of Sr with increasing Mn is probably related to the dissolution and precipitation of the Pa Kae carbonates during the open diagenetic system in their early diagenetic stage. The rate of dissolution and precipitation should be moderate to high since spars filling in moldic porosities is a common petrographic feature of this rock and there is a wide variation of Sr and Mn content of calcite cement.

The excess Fe and Mn for the precipitation of iron and ferromanganese minerals and their substitution in calcite may be transported to a depositional area by means of a periodic bottom current from either an organic-rich reducing environment further off-shore, where the oxidation and dissolution of biogenic material and minerals in the ocean increases during the formation of bottom water(Olausson,1985). Another possibility is from a distant active volcanic region as evidenced by the association of black shale and chert on the top of this Formation and the presence of

some small glass shards. The bottom current from deeper areas seems promising since there are abundant micro- and macro- pelagic fauna within these rocks, implying a high productivity of the area. The transportation from a volcanic region is probably less important because glass shards are rare and there are no volcanic rock associations within this formation. However, stream supply of iron and manganese from the nearby continental landmass (Elderfield,1976) cannot be ruled out.

Furthermore, the additional supply by the early diagenetic remobilization of Mn and Fe from a reducing interval to the upper surface for micronodules and ferromanganese crust formation on the oxygenated sea floor (Calvert and Price,1977; Malbach,1986) and for a diagenetic substitution of Mn and Fe in calcite cements (up to 4,145 ppm Mn and 1,916 ppm Fe) within bed rocks in that reducing condition itself is possible. This is suggested by the occurrence of a black halo surrounding many ferromanganese micronodules (Tucker,1973) and by the bright to dull luminescence of burial cements. Veizer (1977) stated that calcite precipitated in equilibrium with reducing sea water contains more Mn and Fe than normal sea water calcite. But this postulate cannot apply directly to this case because the Pa Kae Formation was deposited on a well oxygenated sea floor. It is probable that the pore water during an early shallow burial phase was similar to sea water. It was modified by organic decomposition which led to a reducing conditions below the sediment-water interface. This is consistent with the general cathodoluminescence zonation from non to dull and bright luminescence of calcite cement within large shelter and intraskeletal porosities, and also consistent with formational condition of the early diagenetic dolomites.

7.5.2 Oxygen and Carbon Isotopes

The isotopic composition of the various components from the Pa Kae carbonates and calcareous mudstone partings are demonstrated in Table. 7.1; Fig. 7.11 and 7.12. In general the $\partial^{18}O$ values range from -3.1 to -10.6 ‰ PDB and ∂^{13} C range from 3.5-0.5‰ PDB. The field of $\partial^{18}O$ and $\partial^{13}C$ covariance (Fig. 7.11) partially overlaps the field of warm modern shallow carbonates and its trend falls on the temperatures of equilibrium calcite line of warm surface-water, as defined by Rao and Green (1983), when moves the original $\partial^{18}O$ value of modern sea water from 0‰ PDB to the proposal original Late Ordovician sea water value of -3‰ PDB (Rao,1990a) with neglect ∂^{13} C value.

In comparison with the other worldwide Late Ordovician marine carbonates (Fig. 7.12), $\partial^{18}O$ of the Pa Kae shows a wider range than the others and its heaviest value is about 1‰ PDB heavier. The relatively narrow range with the highest value up to 3.4‰ PDB of $\partial^{13}C$, shows much more enrichment than the normal ancient

Fig. 7.11 $\partial^{18}O$ and $\partial^{13}C$ variation in the Pa Kae Formation in comparison with the field of modern warm shallow carbonates and cold water carbonates (Rao and Green 1983) when moved the original modern sea water oxygen isotopic value from 0‰ PDB in Rao and Green's model to the Ordovician sea water value of -3‰ PDB (Rao 1990a). Note the Pa Kae isotopic field falls about a line of equilibrium calcite in warm shallow water. The Pa Kae isotopic signature showes a bimodal distribution pattern. The heavier mode represents primary compositions, and the lighter mode with relatively lighter $\partial^{18}O$ values represents reset compositions during progressively burial.

Fig. 7.12 Comparison of the $\partial^{18}O$ and $\partial^{13}C$ marine calcite values of the Late Ordovician Pa Kae stromatolitic limestones and the Lower to Middle Ordovician shallow water Thai carbonates (dark stripe) with those of the other worldwide, Ordovician shallow water carbonates (light stripe, Rao and Wang 1990). Isotopic signature varies throughout the Ordovician and shows a considerable shift to more enrichment in Late Ordovician.

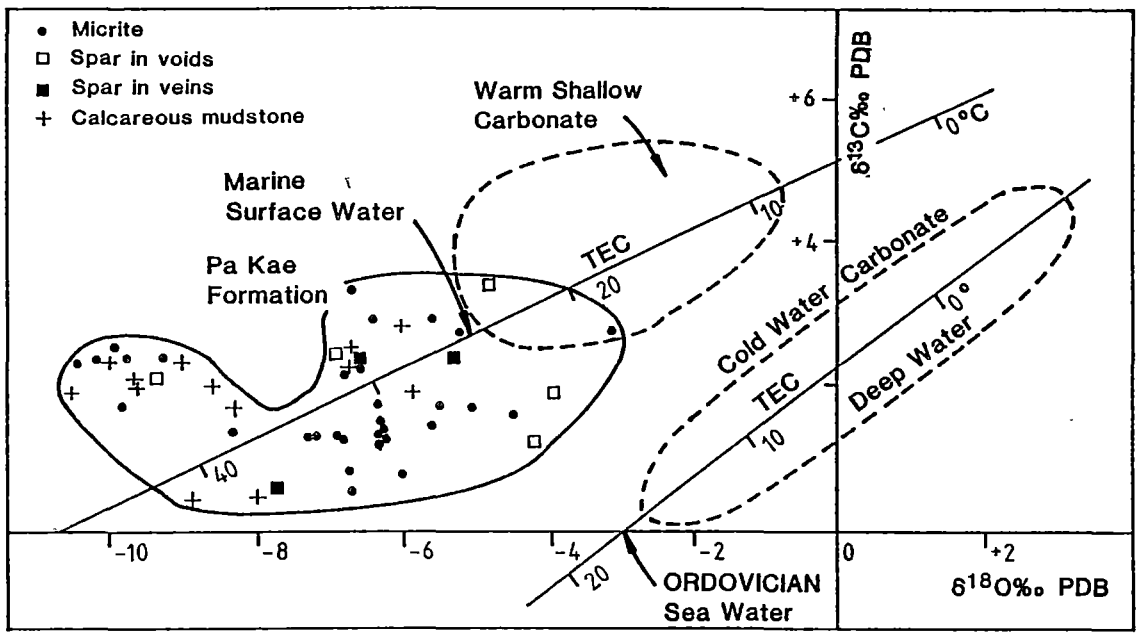
Micrite
Spar in voids
Spar in veins
Calcareous mudstone
Warm Shallow Carbonate
Marine Surface Water
Pa Kae Formation
TEC
Cold Water Carbonate
Deep Water
ORDOVICIAN Sea Water
δ13C‰ PDB
δ18O‰ PDB
0°C
10°
0°
+6
+4
0
+2
-10
-8
-6
-4
-2
40
20
10
20

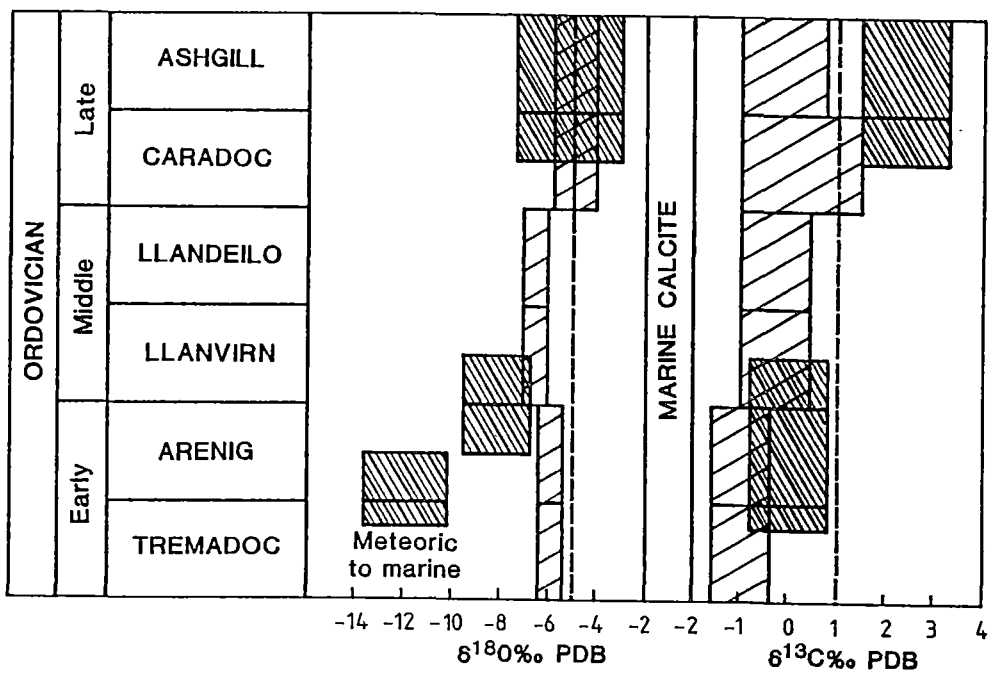
ORDOVICIAN
Late
Middle
Early
ASHGILL
CARADOC
LLANDEILO
LLANVIRN
ARENIG
TREMADOC
Meteoric to marine
MARINE CALCITE
-14 -12 -10 -8 -6 -4 -2
δ18O‰ PDB
-2 -1 0 1 2 3 4
δ13C‰ PDB

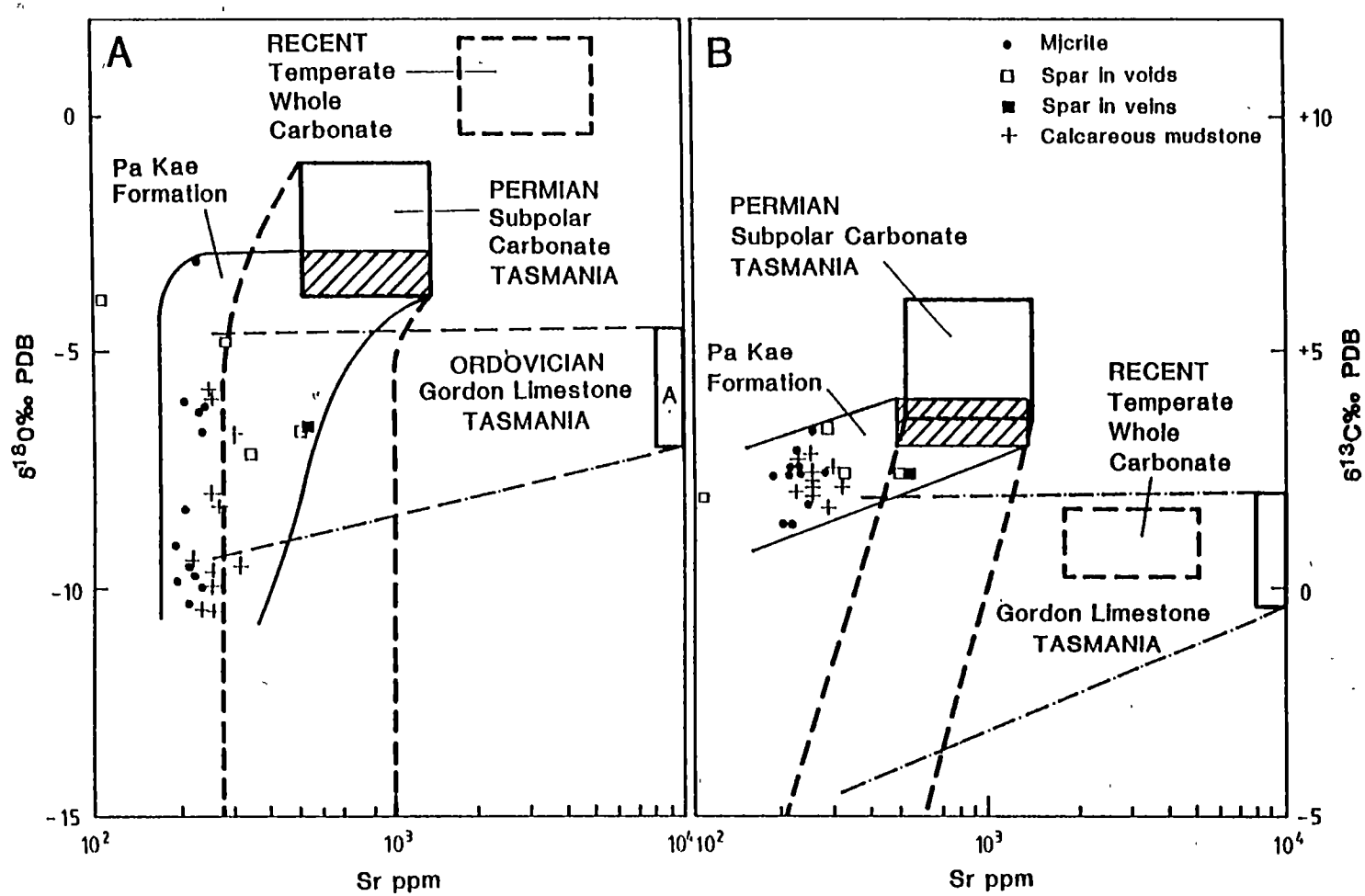

Fig. 7.13 A. Sr-$\partial^{18}O$ variation in the Pa Kae Formation compared with those of Recenttemperate whole carbonates; Permian subpolar carbonates, Berriedale Limestone; and Ordovician tropical carbonates, Gordon Limestone from Tasmania (Rao 1990a).

B. Sr-$\partial^{13}C$ variation in the Pa Kae Formation compared with those of Recent temperate whole carbonates; Permian subpolar carbonates, Berriedale Limestone; and Ordovician tropical carbonates, Gordon Limestone from Tasmania (Rao 1990a).

marine carbonates. This suggests neither the effect of burial fractionation (Hudson,1975), microbially oxidation of organic matter nor bacterial sulfate reduction (Irwin *et al.*, 1977) during a progressive diagenesis. But it is consistent with enrichment by carbon isotopic fractionation during photosynthesis (Berger,1986) by stromatolites (Burne and Moore,1987) on the sea floor.

However,there is no significant isotopic shift of $\partial^{18}O$ during photosynthesis (Burne and Moore,1987) and $\partial^{18}O$, produced in biocycle, still resembles the composition of sea water (Wagener,1975). Therefore, the wide range of $\partial^{18}O$ with bimodal distribution pattern (Fig. 7.11) was generated by the other sea floor and post-depositional phenomena. The bimodal character may due to a variable mixture of the original inhomogeneous marine carbonates and their differential diagenetic alteration and/or addition of burial cement (Dickson,1985). A general trend toward the lighter $\partial^{18}O$ value upto -10.6‰ PDB is clearly due to continuous re-equilibration with higher temperature pore fluids during progressive burial (Dickson,1985; Choquette and James,1987). The isotopical re-equilibration was finished early because the original bimodal character still dominates the trend and most of the primary porosities were occluded by the early shallow burial cements. Furthermore, the covariance of $\partial^{18}O$, $\partial^{13}C$ with Sr (Fig. 7.13) also confirms this contention. Since the relative small range of Sr (106-546 ppm) with slight depletion from their original values (500-1,400 ppm,LMC) suggests the low degree of the water-rock interaction within a semiclosed system and/or the early closure of these carbonate system. On the contrary, the wide range of $\partial^{18}O$ with large depletion from the original value while Sr remains relatively constant (Fig. 7.13A) suggests the further re-equilibration with the remnant pore fluids at elevated temperature during increasing burial. This trend is similar to those of the Permian subpolar carbonates of Tasmania (Rao,1990a) but with less $\partial^{18}O$ variation because of its normal marine origin (not like the mixed-marine origin, close to the pole, of Permian carbonates). As a whole, the degree of post-depositional alteration was low because of the relatively high Sr content, up to 546 ppm, (Kinsman,1969) for the original LMC dominated carbonate. The narrow range of $\partial^{13}C$ values with small depletion throughout the range of Sr values (Fig. 7.13B) is probably characteristic of early marine lithification.

Hence, the heavier mode ranging from -3.1 to -7.5 ‰ PDB represents the $\partial^{18}O$ of marine calcite values (Fig. 7.11, 7.12) whereas the higher mode ranging from -7.5 to -10.6 ‰ PDB represents the $\partial^{18}O$ of burial calcite values. The heaviest $\partial^{18}O$ values of -3.1‰ PDB is thought to be the original Late Ordovician marine calcite value of the Pa Kae carbonates because the heaviest $\partial^{18}O$ values is the least diagenetic alteration (Fig. 7.13A). This value is about 2‰ PDB heavier than the average $\partial 1^{8}O$ value (-5‰ PDB) of the worldwide tropical Late Ordovician shallow

marine carbonates (Fig. 7.12) and the proposed original Late Ordovician marine calcite value in Tasmania (-5±0.5‰ PDB, Rao,1990b). That two mil difference in $\partial^{18}O$ values indicates 10°C lower temperatures during the deposition of the Pa Kae Formation than normal warm water carbonates.

7.6 Environment of Deposition and Palaeobathymetry

Open Marine and Cold-Water Origin: Although Recent stromatolites are common in warm, low latitude shallow-water conditions (e.g. Ginsburg,1960; Logan,1961; Gebelein,1969; Monty,1972; Wray,1977; Dill *et al.*,1986) as indicated by lithostratigraphy, mineralogy, fauna, and geochemistry of the rock, the following evidence suggests an open marine and cold-water origin for the Pa Kae limestones:

1. The mainly original calcitic mineralogy of the stromatolite and other faunas, micrites, and sparry calcite (Rao,1981; Brookfield,1988).
2. The occurrence of some glauconitic pellets generally suggests an open marine environment far from the zones of active sedimentation at relatively low temperature ranging from 7°-15°C (Odin and Letolle,1980).
3. The occurrence of the "North Atlantic Province" conodonts, and of a normal marine fauna, suggests the free circulation of oceanic water at either a continental margin or in marginal cratonic basins(Barnes and Fahraeus,1975), and in cold water conditions (Burrett *et al.*,1983). The extensive north-south distribution of this rock unit in southern peninsular Thailand and their correlatives in Malaysia (Wongwanich *et al.*,1990) along the present-day eastern margin of the Shan-Thai Terrane, the similarity in lithology of the Pa Kae with the Chinese Late Ordovician Pagoda Formation which contains the same pelagic trilobite species (Chen Jun-Yuan,1985) in a possibly nearby terrane (S.China), and the diverse pelagic fauna of this rock favour the continental margin rather than the marginal cratonic basins. In this case the Pa Kae Formation possibly deposited on the deep ramp.
4. The Sr and Mn concentrations are similar to those of other cold-water carbonates and the Mg content is low.
5. The heaviest $\partial^{18}O$ value up to -3.1‰ PDB of the Pa Kae marine calcite when compared with low latitute worldwide tropical Late Ordovician marine calcite $\partial^{18}O$ values of -5‰ PDB indicates 10°C lower temperatures during deposition of the Pa Kae. There is no evidence of evaporation which could have been the cause of heavy $\partial^{18}O$.

Cycle and Sea Level Fluctuation: The rhythmically bedded sequence of red stromatolitic limestones and dark red calcareous mudstone partings were deposited during a period of intense Late Ordovician glaciation (e.g. Berry and Boucot,1973; Brenchley and Newall,1984; Caputo and Crowell,1985; Robardet and Dore,1988; Havlicek,1989; Scotese and McKerrow,1990), and could have resulted from glacio-eustatic changes in sea level. The abundant bioclasts in the limestone layers in contrast with near absence and highly corroded skeletons in the mudstones suggest differences in tsea surface productivity and/or dissolution of carbonate grains during the deposition of these couplets through the cold glacial and warm interglacial periods.

The limestone beds were deposited during regression phases (Rao,1981; Olausson,1985; King Jr.,1990) when the glaciers were growing at the south pole producing the exposure of a continental shelf, a preferred site for shallow water carbonate deposition, and inducing carbonate to deposit at the deeper zone or on the sea floor (Seibold and Berger,1982). The productivity during these times was very high as reviewed by Berger (1986) since there are abundant well preserved fossils within the limestone layers.

During interglacials following the deglaciation or during the long retreating stage of the ice cap, the high sea levels allowed only mudstone deposition on the sea floor with depletion in calcareous skeletons, probably due to dissolution and/or low productivity. The higher $\partial^{13}C$ value up to 3.4‰ PDB of limestones in comparison with 2.8‰ PDB of mudstones confirms the higher surface water productivity through photosynthesis during the limestone formation than those of the mudstone formation. But the enrichment of $\partial^{13}C$ by the photosynthesis of stromatolites has to be taken into account. However, the high $\partial^{13}C$ value up to 2.8‰ PDB of mudstones also implies higher productivity than normal condition (close to zero, Berger,1986) during mudstone formation.

Seibold and Berger (1982) stated that productivity variations play a secondary role in producing deep sea cycles. Einsele (1982) agreed with this but proposed a greater role for varying redox conditions and/or carbonate productivity for the genesis of the rhythms on the continental margins and epicontinental seas. The near absence of bioclasts with rare highly corroded skeletons at the time of higher productivity than normal and the much thinner layering of mudstones than limestone layers in this periodite probably suggest the major role of dissolution process for the mudstone genesis during the interglacial period. The other climatic forcing rhythm, the dilution model can be ruled out because of the rarity of the terrigenous detritus in both limestones and mudstones. Then, it is the combination of dissolution, due to the degree of the sea water saturation with respect to calcite and/or a fluctuating carbonate compensation depth, and the globally climatically controlled sea surface productivity

that are responsible for the genesis of the Pa Kae rhythms. Therefore, the very thin cycles of about 100-300 mm thick within the Pa Kae Formation possibly represent an active small-scale glacio-eustatic sea level fluctuation during the advancing and retreating of the Caradoc to Ashgill glaciation. So far, no strong sedimentological evidence of the fluctuation in response to the rate of sea floor spreading have been observed in this area.

Tropical Deep Setting Versus Shallow Temperate Origin: The cold water origin of the Pa Kae can be either as deeper, cold water carbonates at low latitudes or as shallow temperate carbonates at high latitudes. As mention by Brookfield (1988), it is difficult to distinguish them, since both may have some characteristics in common because of the strong control of fauna by thermal regime. Chivas *et al.* (1990) warned against using stromatolites as a possible palaeolatitude indicator. However, there is other evidence for and against both possibilities within these rocks (Wongwanich and Rao,1990). The light requirement for stromatolite growth, the absence of modern stromatolites in waters deeper than 23 m, the 7°-15° C range of glauconite formation, and the similarity between the geochemical signature of the Pa Kae and the Permian subpolar carbonates from Tasmania suggest either the shallow temperate origin at high latitudes or deeper environments in the upper temperate zone.

A deep environment in a tropical setting is indicated by :

1. the vertical gradation from the Pa Kae to black graptolitic shales and cherts with radiolaria on the top of the sequence,
2. the absence of shallow water and/or sub-aerial features such as oolites, mud cracks, and meteoric diagenetic features,
3. the slow rate of sedimentation (as noted earlier in the diagenetic section) and the typical red color of the rocks,
4. the abundant carbonate mud which is generally rare in modern temperate carbonates (Rao,1981; Brookfield,1988; Nelson,1988),
5. the diversified, blind and large eyed deeper water trilobites including *Microparia, Panarchaeogonus, Schoryia, Isobergia, and Panderia* ; and deeper water brachiopods such as *Foliomena,* and *Christiania* (Fortey personal communication),
6. the occurrence of ferromanganese micronodules, and glauconites which usually occur in water depths between 100-500 m on the present-day sea floor (Odin and Matter,1981) at the outermost shelf and upper slope (Weaver,1989),
7. the extensive low magnesian calcite cement occuring as equant and rhombic microspars (Schlager and James,1978; Rao,1981; Wilkinson *et al.*,1982),

8. the higher Sr, Ti, Ba, and P_2O_5 concentration than in the shallow water carbonates whereas the Mg concentrations are lower (Veizer,1978; Rao,1986).
9. The abundance of "North Atlantic" province conodonts as oppossed to the "Mid Continent" conodonts in the majority of the Thung Song Group.

The evidence for the tropical deeper water setting seems far more significant than that of a shallow temperate origin. The 10°C drop of temperature from that of the tropical sea surface points to a considerable paleo-depth. The light requirement at depth for stromatolite photosynthesis is still debated following the discovery of Devonian deep water stromatolites in the Canning Basin (Playford and Cockbain,1969). There is no doubt that modern stromatolites can occur in 0-23 m depths and can survive at least as deep as 80 m in the form of oncolites as mentioned earlier. But at depths below this, in the twilight zone and sub-photic zone there appears to be a limit the photosynthetic cyanobacterial activity.

Williams (1983) mentioned that cyanobacteria in mats are restricted to aqueous regimes within the photic zone while the living deeper water filamentous bacterial mats below the photic zone to 600 m depths are dominated by nonphotosynthetic sulfur-oxidizing bacteria as in the mats from Santa Barbara Basin off the California coast. They usually inhabit oxygen-deficient marine basins and coastal upwelling regimes and are associated with phosphate-rich zones. Based on the discovery of living deep water blue green algae (bacteria) from 0 to at least 1,000 m deep in modern sea, Monty (1977) took an opposite view. He proposed that through chromatic adaptation, the red pigment in twilight zone blue green algae can absorb the remaining blue radiation and transmit the energy to the chlorophyll while those in the complete darkness obtain the energy through chemo-organotrophic metabolism. Riding (1975) also warned about using Palaeozoic calcareous algae including blue green varieties (bacteria) as depth indicators since they can live far beyond the euphotic zone (0 - 100 or 150 m) in modern seas and are heterotrophic. He also mentioned that normal sunlight can penetrate to more than 800 m in very clear water whereas blue light can probably penetrate to 1,000 m.

Therefore, it is possible that the Pa Kae stromatolites are of the deep tropical or subtropical setting. The mode of occurrence in reducing environments as seen in the Californian deeper water sulfur-oxidizing bacterial mats should be ruled out because the Pa Kae sediments were deposited on the oxygenated sea floor under the photosynthetic control. Study on palaeobiogeography and palaeomagnetism by many authors also confirm these contentions. For example Burrett and Stait (1986) and Burrett *et al.* (1990) demonstrated that most of the Shan-Thai Terrane, especially Thailand, was situated in the southern tropical region during the Ordovician. Scotese and McKerrow (1990) had a similar idea but they put the Shan-Thai Terrane in the

tropical region of the northern hemisphere during the Late Ordovician. Both of them placed southern Thailand in a subtropical area close to the temperate zone.

Palaeobathymetry of the Pa Kae Stromatolites: The deep subtropical setting of the Pa Kae requires further comment on the palaeobathymetry of the rocks because it is one of the most important factors for their palaeoecological and palaeoenvironmental reconstruction. The abundant diverse open marine fauna and normal marine isotopic signature of the rocks suggest the Pa Kae stromatolites accreted in normal marine conditions. In comparison with normal modern seas, the palaeobathymetry of the rock should be a function of its formational temperature which decreases with depth. Other factors involved are palaeolatitude; types of currents during the Late Ordovician (warm, cold, or upwelling); and the local palaeogeographic and/or palaeoceanographic condition including the clarity of sea water, and the influence of the marine hydrothermal regimes.

The abundant and diverse normal marine fauna and high $\partial^{13}C$ of the rocks indicate high fertility and high productivity during the deposition of the Pa Kae. These phenomena commonly occur in the upwelling region but the low P_2O_5 content of the rocks which deposited on the oxygenated sea floor is not consistent with that. The sea water at that time is likely to have been clear as evidenced by the very slow rate of deposition noted earlier, the lack of turbidity current features, and the scarcity of terrigeneous sediments. Furthermore, no effect of deep sea hydrothermal circulation as well as high salinity imprint on the isotopic signature have been observed. No marine evaporites have been observed at either outcrops or in thin sections. The lack of deep sea hydrothermal circulation and high salinity are not consistent with the increased temperatures and salinity with depth in the salinity stratified ocean during the Ordovician (Caradoc) as Railsback *et al.* 's (1990) proposed but it is partly consistent with Marshall and Middleton's interpretation (1990). They interpreted the extremely heavy $\partial^{18}O$ (up to -1.4‰ PDB) and $\partial^{13}C$ (with marked shift up to 7‰ PDB) of the Late Ordovician Swedish mud mounds as a result of a change in the $\partial^{18}O$ of the Late Ordovician sea water, the decreasing in water temperatures, and the global cooling during the Late Ordovician glaciation. Scholle and Arthur (1976) interpreted the gradual increase in $\partial^{13}C$ values from +1‰ PDB from the base to the top of the Upper Cretaceous European chalk sequences and their marked jump to more than +4.5‰ PDB at the Cenomanian-Turonian boundary as the result of changed oceanic circulation in the Atlantic and the expansion of the oxygen minimum zones. The similar heavier isotopic signature than normal but smaller values ($\partial^{18}O$ up to -3.1‰ PDB and $\partial^{13}C$ up to 3.4‰ PDB) of the Pa Kae is also interpreted as a result of change in the $\partial^{18}O$ of sea water. But the heavier $\partial^{18}O$ and $\partial^{13}C$ values

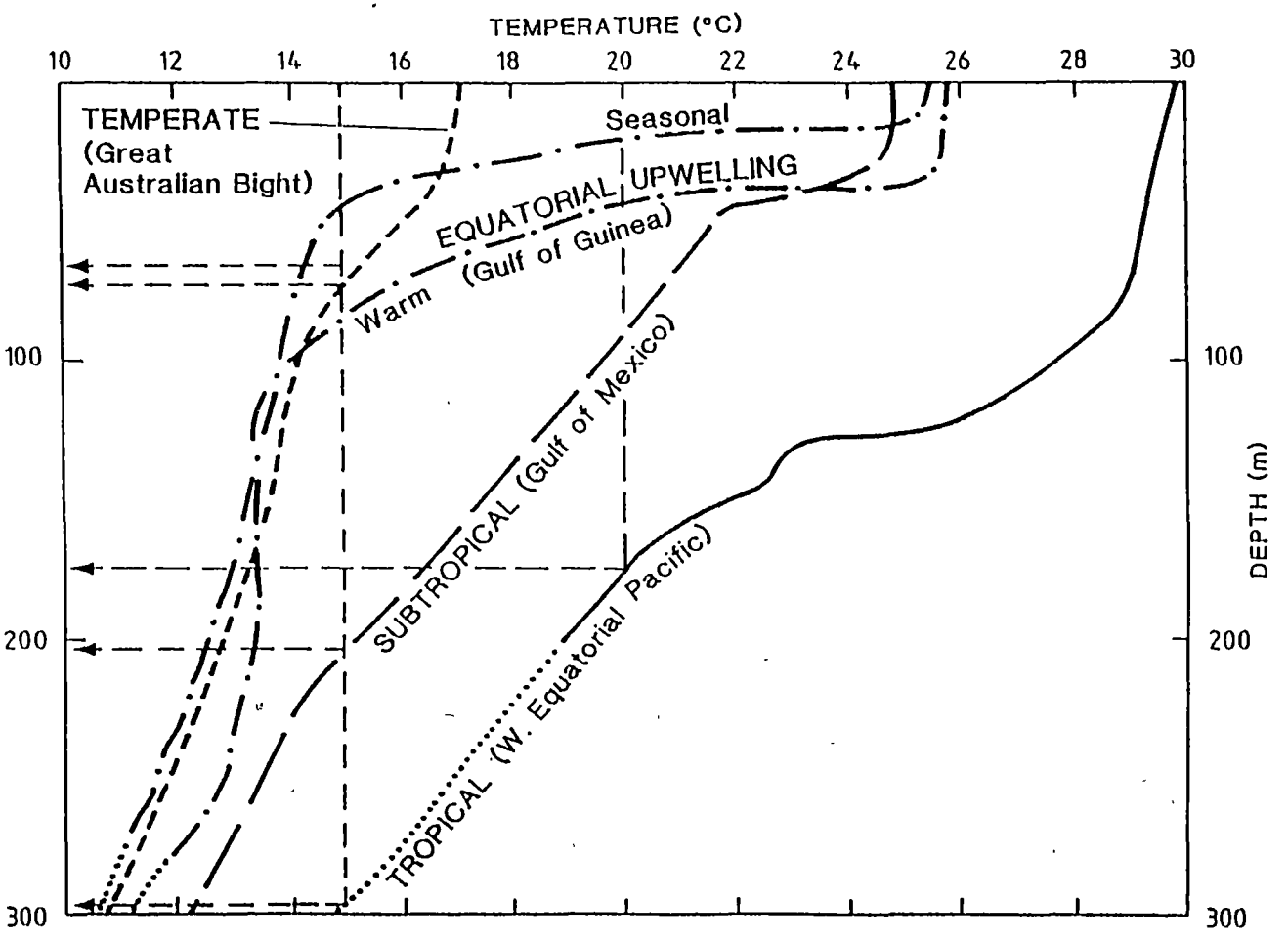

Fig. 7.14 Conceptual temperature-depth model for predicting the possible palaeobathymetry of tropical and temperate carbonates based on the drop of temperature from modern sea surface temperature (SST) in relation with the vertical thermal gradient profile in those climatic regions (see text). The vertical axis represents the depths from mean sea level. The horizontal axis represents either SST or the drop of temperatures from SST to the calculated or estimated palaeotemperatures (obtained from the heaviest $\partial^{18}O$ value of the rock) at a predicted depths. This model can be extrapolated to the depths of about 600 m from mean sea level. The arrows point out the water depths of each carbonate setting at specific temperatures.

of the Pa Kae more than those of the other Upper Ordovician shallow-water carbonates is a result of lower formational temperatures at depths in the subtropical region, the high sea surface productivity due to changed oceanic circulation (?), and of the photosynthesis control on the precipitation of the Pa Kae stromatolites during the Late Ordovician glaciation.

In an attempt to relate the palaeotemperature obtained from the heaviest $\partial^{18}O$ marine calcite value of the rocks to reconstruct a possible palaeobathymetry, a simple conceptual model (Fig. 7.14) has been developed based on the drop of the temperatures from the modern sea surface temperatures in relation to temperature gradient profiles (thermal gradient) from various modern climatic regions. These include the thermal gradient from the temperate climate at the Great Australian Bight (Gordon and Baker,1982); the subtropical climate at the Gulf of Mexico (Vukovich *et al.*,1978); the tropical climate of equatorial Western Pacific, the Melanesia, NE. of Pa Pua New Guinea (Godfrey and Lindstrom,1989); and the equatorial upwelling region at the Gulf of Guinea (Houghton,1986). In this case, it is assumed that palaeoceanographic conditions during Late Ordovician glaciation are similar to those of today. It is assumed that both periods are characterized by cold bottom water produced at high latitudes and transported to the tropical areas via deep oceans, that Late Ordovician sea surface temperatures were similar and that the ocean temperature decreased with depth. The heaviest $\partial^{18}O$ value of the Pa Kae stromatolites is about 2‰ PDB heavier than the average value of shallow Late Ordovician carbonates suggesting 10°C drop of their formational temperature from the sea surface temperature during that time.

Based on this model (Fig. 7.14), the 10°C drop of temperatures from the sea surface temperature in tropical region (30°C) gives a water depth of 175 m, 25°C in subtropical region to 15°C at depth gives a water depth of 206 m. The same method gives a depth of 62 m to the Pa Kae Formation in an equatorial upwelling regime (average), and 70 m in temperate region such as the Great Australian Bight. The formational temperature of 15°C (obtained from temperature of glauconite formation) in tropical region gives the palaeobathymetry of 290 m. Therefore, the Pa Kae stromatolites may have deposited in a water depth of 175-290 m in a subtropical or tropical climate. This model can be extrapolated to obtain the possible palaeobathymetry as deep as 600 m along the gentle thermocline in normal tropical region and about 500 m in normal upper temperate regions but beyond that the sea water temperatures tend to drop sharply. According to this model the Pa Kae stromatolites have a deeper water setting in either tropical or upper temperate regions.

Stromatolites, Palaeoenvironments, Palaeoecology, and Basin Analysis: From the above evidence previously mentioned, it is clear that the Pa Kae stromatolites originated in a deep subtropical setting within or not too far below the normal photic zone. They share several common features with the Canning Basin's deep water stromatolites (Playford *et al.*,1976) including fine lamination, rare or no fenestral fabric, evidence of iron and manganese precipitation, abundant pelagic faunas, possible markedly condensed sequences (60-126 m thick sequence covering a long time span from the Caradoc to Ashgill), commonly red color, but less diverse assemblage of forms. Additional features are the rather abundant ferromanganese micronodules, occurrence of some glauconite pellets, bored calcite cements, and abundant rhombic spars.

The Pa Kae stromatolites possibly grew on the very distal part of the Thung Song carbonate ramp or just beyond that on the edge of a basin. This implies that the Late Ordovician basin in southern Thailand was probably shallow (~300 m). Their lenticular geometry suggests that they built up as bioherms or reef mounds (400x1500 m at the type area) and experienced extensive synsedimentary submarine cementation.

Ancient subtidal to deep water stromatolites commonly occur as reef or bioherms (e.g. Hoffman,1974; Playford *et al.*,1976; Pratt and James,1982; Monty *et al.*,1987) and mud mounds (e.g. Pratt,1982a,b; Tsien,1985; Beauvais *et al.*,1988; Bridge and Chapman,1988). Pratt (1982b) pointed out that the subtidal stromatolite mounds were widespread in intracratonic shallow water carbonates during Cambrian to Lower Ordovician (Pratt and James,1982) and declined rapidly after Middle Ordovician because of the fast development of metazoan competitors. Losing their substrates in shallow areas during the successive lowering mean sea level (Middle Caradoc to Late Ashgill) during the Late Ordovician glaciation (Fortey,1984) and sea level regression coupled with increasing grazing pressure (Pratt,1982b) possibly forced this benthic microbial communities, which were widespread in the Thai Lower to Middle Ordovician shallow-water carbonates, to adapt to the less competitive areas in deeper water.

The Pa Kae stromatolites co-existed with small pelagic metazoans as shown by the abundant diverse pelagic faunas within these mounds. This association is similar to the widespread establishment of carbonate "mound" faunas in the Ashgill of Sweden, Kazakhstan, Salair, Ireland, and northern England (Fortey,1984, Webby,1984). Pelagic faunas provided a possible substrate on a muddy sea floor and foundation materials including bioclasts, faecal pellets, and mechanical micrites for stromatolites to colonize and build their frameworks by trapping and binding mechanisms in deep sea conditions. In turn, stromatolites gave back the primary food resources for some grazing faunas. The epifaunal metazoan activity on the Pa Kae

stromatolites was extensive as shown by the normal rearrangement of ostracod carapaces. In contrast with shallow water stromatolites, burrowing across stromatolitic layers by infaunal metazoans is scarce in deep sea stromatolites. Peryt and Peryt (1975) also proposed a similar symbiotic association for, and environmental control on the association of sessile tubular foraminifera with cyanophytic algae (bacteria) in algal and bryozoan carbonate mounds, and especially in the oncolitic basinal facies of the west Poland Late Permian.

Even though, the Pa Kae stromatolite mounds have abundant micrite in common with other Phanerozoic deep water mud mounds on carbonate shelf-to-basin slopes (Pratt,1982a), they are different in lacking radiaxial calcite spar-filling stromatactis but in having a densely stromatolitic framework. They deposited mainly by organic binding and trapping of the locally derived lime mud, faecal pellets, bioclasts, and by *in situ* marine spar precipitation under photosynthetic control.

The small-scale columnar stromatolites are the most extensive form of these mounds, but a series of sequence development (Fig. 7.2C,D) from flat laminites at the bottom to columnar stromatolites in the middle and some rare oncolitic stromatolites at the top of bedding have been observed. Vague thrombolitic fabrics commonly occur with the columnar stromatolites. The difference in stromatolitic morphologies have long been interpreted as the result of either a succession of environmental events (e.g. Logan *et al.*,1964; Aitken,1967; Cecile and Campbell,1978; Pratt and James, 1982; Campbell,1987; Ratcliffe,1988; Beukes and Lowe,1989) or control by biological factors (Gebelein,1974; Serebryakov and Semikhatov,1974; Golubic and Focke,1978). The combination of those two factors with environmental control dominant is also proposed for the control on the stromatolitic morphologies (Playford, 1979; Kennard and James,1986; Lanier,1988; Knoll *et al.*,1989). No palaeontological study on the Pa Kae benthic microbial communities has been done. However, there is sedimentological evidence to support the vital role of environmental control on these stromatolitic morphologies.

In general, observations on etched surfaces and thin sections under the microscope, demonstrates that the muddy (clays) matrix percentage increases from laminites through columnar stromatolites to oncolitic stromatolites whereas allochemical particles, especially faecal pellets, decrease toward the top of bedding. This possibly reflects the gradual decrease in energy of deposition and the productivity during the stromatolite accretion or building of limestone layers. Then, the rocks change to calcareous mudstone with a sharp contact. The repetition of limestones and mudstones have been interpreted as possible glacio-eustatic cycles. Therefore, the flat laminites at the bottom of limestone layers should accrete during the peak of bottom current activity due to strong sea surface thermal gradient between low and high

latitudes during the maximum glaciation. The thermal gradient gradually decreased during the retreat of ice cap resulting in less bottom current activity as well as productivity in the tropical region. This led to the columnar stromatolite, thrombolitic stromatolite and subsequent oncolitic stromatolite formation and increased the accumulation of clay minerals on the sea floor. The concentric nature of minor oncolites may suggest the continuous rolling of them under the higher energy condition (e.g. Logan *et al.*, 1964; Raticliffe,1988). However, because of insufficient bioclastic substrates and construction material on more muddy sea floor for forming laminites and columnar stromatolites possibly induced the oncolites to develop in more moderate currents. These currents were slow enough to keep the micritic oncolites at a depositional area but they were also strong enough to turn them around on this more muddy sea floor. During the resting stage, these oncolites were bored by the endolithic faunal metazoans (Fig. 7.2E). The decrease in energy of depositional environments also reflects the deepening of the basin because of the gradual rise in sea level (temporary transgression) during that time. There are no stromatolites preserved within the mudstone intervals because of the low productivity and high dissolution of carbonate grains on the sea floor during the high sea level of the interglacial period.

The altenation of the spar-rich and micrite-rich layers of stromatolitic laminae suggests the episodic but regular influx (Pratt and James,1982) of locally derived sediments to and winnowing of the unbound sediments out of the Pa Kae stromatolitic mounds. These episodic or periodic currents were strong enough to tear out semilithified stromatolites, as shown by the abundant red micritic intraclasts, and to promote the extensive early marine cementation of the rocks.

7.7 Discussion and Conclusion

The Late Ordovician, subtropical, cold and deeper water stromatolitic limestones, the Pa Kae Formation, are well exposed as reef mounds in southern Thailand. It is the uppermost rock unit of the Thung Song Group which conformably overlies the other peritidal Thung Song carbonates and is overlain conformably by the Silurian deep-water black graptolitic shales and chert with radiolarians. This rock unit is dominated by thinly and wavy bedded, red stromatolitic limestones rhythmically interbedded with very thin calcareous mudstone partings. It may be a glacio-eustatic cycle. The deeper water limestone layers were deposited during the regression phase when the glacier was growing at the South Pole on Gondwanaland resulting in high productivity and strong bottom current activity at low latitudes. Morever, this is probably a result of extensive terrigenous clastics dominating shallow sea during a glacial stage. The mudstone partings were deposited during the interglacial periods

when the sea level was high initiating the deposition of clay minerals and dissolution of the carbonate fractions.

The Pa Kae stromatolites, the frame builder of the limestone layers, formed as a reef mounds in or just below the photic zone, at about 175-290 m water depths, on the distal part of the Thung Song carbonate ramp. In the response to the fluctuation of the Late Ordovician glacio-eustatic sea level, they developed a series of morphologies from flat laminites at the base to columnar stromatolites with the thrombolitic fabric in the middle and subsequent oncolitic stromatolites at the top of bedding. The spar-rich and micrite-rich laminae suggest the available episodic or possibly periodic bottom current activity which transported sediment in and out the system.

Associated with the Pa Kae stromatolites is a very diverse small fauna of ostracods, crinoids, very small pelagic trilobites and brachiopods, calcispheres, cold water conodonts, sponge spicules; some bivalves, gastropods, calcareous algae, cephalopods; rare stromatoporoids, corals, and bryozoans. The community very abundant highly diversified faunas suggest optimum environmental conditions.

The Pa Kae stromatolites share many common features with the deep water stromatolites from the Canning Basin but they are different in the rather abundant ferromanganese micronodules, the occurrence of glauconitic pellets, bored calcite cements, and very abundant rhombic spars. The Pa Kae stromatolitic mounds were created by the accumulation of mainly micrites and bioclasts as were many other Phanerozoic deep water mud mounds but they possess the distinctive stromatolitic structure with excellent well preserved stromatolite sheaths of both filamentous and coccoid cyanobacteria. They lack the radiaxial calcite spar filling stromatactic lamination of European and North American mud mounds possibly because the Pa Kae mounds have a genuine rigid framework that is the result of rapid synsedimentary cementation. The existence of the Pa Kae deep water stromatolites mounds on the outer ramp of the Shan-Thai terrane during the Late Ordovician and the wide distribution of similar rocks across this microcontinent, and in the Pagoda Formation, of the South China terrane may suggest the close relationship between those two areas at that time. The deep-water similarity of faunas need not, however, reflect palaeogeographic proximity (Taylor and Forester,1979).

The diagenetic pathway of the Pa Kae under deep sea condition is similar to that of meteoric diagenesis as suggested by many authors. Both destructive and constructive diagenesis are important to the existence of these stromatolitic mounds. The bioerosion and maceration of the epifaunal skeletons provided micrites, the major foundation material in stromatolitic construction. The early marine cementation by micrite and microspar cements provided not only the rigid framework that protected the stromatolites from submarine erosion and later compaction but also provided a

substrate for epifaunal and some infaunal metazoans. Burial diagenesis, cementation also played a vital role in the good preservation of the Pa Kae stromatolite mounds. The geochemical signature of the rock provides the clues to investigate and interpret the depositional and diagenetic environments.

The diagenetic pathway of the Pa Kae began on the oxygenated sea floor during and shortly after the accumulation of sediments. Most of microfaunas including the ostracod carapaces and some macrofaunal skeletons were simply macerated to micrite under cold (~15°) deep water conditions. Many macrofaunal skeletons were partly recrystallised and subsequently impregnated by red ferromanganese mineral as colloform structure. These products were incorporated into stromatolitic laminae by bottom currents and the binding and trapping mechanism of stromatolites. At the same time, the calcification of stromatolite filaments and the extensive marine cementation took place under photosynthetic control. Goethite which subsequently transformed to haematite also occurred at this stage. This led to the formation of synsedimentary hardgrounds and ferromanganese micronodules. Calcium, iron, and manganese were transported to the system by means of periodic bottom currents. These currents also played a role in providing the sediments, winnowing the excess sediments out of the system, eroding the semilithified stromatolites and haematite crusts, and forming the ferromanganese micronodules. The decomposition of organic matter and stromatolites occurred either on the oxygenated sea floor or shortly after burial as evidenced by the cathodoluminescent zonation of cements within the large cavities from non to dull and bright luminescence.

After burial, the dissolution of unaltered macrofaunal skeletons took place followed by the compaction which provided the $CaCO_3$ for the subsequent burial cementation by blocky spars within the moldic and larger porosities. Physical compaction was predominantly active in mudstones whereas chemical compaction was common in limestone layers. Most of the thick limestone layers are less affected by physical compaction. They still retain the original wavy biogenic bedding inherited from the columnar stromatolitic morphology because of the synsedimentary submarine lithification. On the contrary, the thinner limestone layers with relatively thick mudstone partings at the bottom part of the sequence which are more prone to physical compaction and were modified to a nodular structure. Dolomitization in this rock occurred locally either during shallow burial under influence of the normal sea water and the decomposition of organic matter or late after deep burial under high temperature and reducing conditions.

The isotopic signature of the rocks is heavier than other Late Ordovician shallow water carbonates. The heavy oxygen isotopes indicate either a cold and deeper water origin of the rocks or the low degree of recrystallization after burial. This is also

confirmed by the distribution of trace elements. The heavy carbon isotopes suggest the photosynthetic control on the $CaCO_3$ precipitation during submarine diagenesis and high productivity of the sea surface waters at that time.

The possible palaeobathymetry (175-290 m) of the Pa Kae obtained from the newly proposed model, based on the relation between the drop of temperature from modern sea surface temperatures and the vertical thermal gradients seems to correspond to the depths of modern marine glauconite formation and falls within the possible range of modern ferromanganese nodule formation in the deep seas. This coupled with the abundant and diverse pelagic fauna including blind and trilobites, pelagic brachiopods and cold water conodonts imply that the temperature gradients of Late Ordovician oceans were similar to those of today. It is believed that the general thermal gradient of the Late Ordovician oceans decreased with depth and the ocean circulation system was similar to that of today. The cold bottom currents originated at high latitudes and subsequently traveled to replace the warm surface waters at low latitudes. The climate at that time was probably similar to the climate during the glacial and interglacial periods of the Cenozoic Era.

Chapter 8
STABLE ISOTOPES

The oxygen and carbon isotope composition of modern marine carbonates depends principally on temperature and salinity of sea water (Hudson, 1977), their mineralogy, and biochemical fractionation (Wagener, 1975; Rao, 1990). The original isotopic content is subsequently altered as the marine sediment undergoes meteoric and burial diagenesis. These changes depend on $d^{18}O$ of formation solution, latitude, altitude, seasonal variation of isotopic composition of meteoric water, temperature and salinity of precipitating solutions, nature and degree of diagenesis, and secular variations of sea water isotopic composition (Allan and Mathews, 1977; Brand and Veizer, 1980; Rao, 1989).

The present study on the oxygen and carbon isotope composition of the Thung Song Group deals with 1) isotopic composition of the individual components, 2) isotopic comparison between the Thung Song and worldwide modern and Ordovician carbonates, 3) isotopic composition of the Ordovician sea water, 4) calcite-dolomite fractionation. Furthermore, the relationship between isotopic composition of carbonates and environment of deposition is emphasized throughout this section.

8.1 Isotopic Compositions of the Individual Components

The range of isotopic compositions of the separate components (Fig. 8.1, Table. 8.1, 8.2, Appendix 6) from the Thung Song carbonates are as follows:

1. Allochemical components have $d^{18}O$ values from -10.8‰ to -14.7‰ PDB and $d^{13}C$ values from +1.3‰ to -0.4‰ PDB.

2. Micrites of shallow water limestones have $d^{18}O$ values from -9.3‰ to -15.1‰ PDB and $d^{13}C$ values from +1.3‰ to -0.9‰ PDB, as micrites from deeper water stromatolitic limestone have $d^{18}O$ values from -6.1‰ to -10.1‰ PDB and $d^{13}C$ values from 3.9‰ to 1.3‰ PDB.

3. Marine cements of shallow water limestones have $d^{18}O$ values from -7.2 to -9.5‰ PDB and $d^{13}C$ values from +0.1‰ to -0.4‰ PDB. Deep water cements have $d^{18}O$ values from -3.9‰ to -7.2‰ PDB and $d^{13}C$ values from +3.3‰ to +1.9‰ PDB. Meteoric or fenestral spars have $d^{18}O$ values from -11.2‰ to -11.7‰ PDB and $d^{13}C$ values from +0.6‰ to +0.2‰ PDB. Early and later diagenetic cements in voids and veins of shallow water limestones have $d^{18}O$ values from -10.2‰ to -13.5‰ PDB and $d^{13}C$ values from +0.4‰ to -1.2‰ PDB, as cements from deeper water limestones have $d^{18}O$ values from -6.6‰ to -9.3‰ PDB and d13C values from +2.3

Table 8.1— Oxygen and carbon isotopic compositions of the separated components from the Thung Song shallow water carbonates.

Sample No.	$\partial^{13}C‰$ PDB	$\partial^{18}O‰$ PDB
A. Marine cements		
1. 400.8/3	-0.452	-9.500
2. 400.8/5	-0.188	-9.356
3. 400.10/C1	-0.003	-9.173
4. 100.10/C2	-0.013	-9.289
5. 400.10/C3	0.191	-7.281
B. Early diagenetic cements in voids & veins		
1. G	-0.849	-11.251
2. 13.1	-0.980	-10.375
3. 399.1	0.183	-10.265
4. 400A	-0.681	-15.778
5. 400.2	-0.089	-15.879
6. 400.8	-1.264	-14.734
7. 398.1A	0.123	-13.566
8. 402A	0.496	-12.598
C. Late diagenetic cements in veins		
1. 396B	0.165	-23.509
2. 399.2	-3.736	-20.968
3. 400.8	-0.584	-18.213
4. 398A	-0.210	-27.376
D. Micrite		
1. 6	-0.255	-15.153
2. 396C	1.326	-12.384
3. 402A/2	0.498	-13.564
4. 402A/0	0.663	-13.173
5. 399	0.624	-15.910
6. 401E	-0.915	-11.134
7. 401F	-0.750	-11.372
8. 401C	-0.519	-11.373
9. 401A	-0.430	-11.357
10. 401A/N	-0.462	-11.193
11. G	0.656	-10.874
12. 70.6	-0.246	-12.582
13. 70.6/S	1.045	-10.251
14. TB	0.778	-9.826
15. 404B	-0.386	-10.006
16. 404E/D	-0.251	- 9.317
17. 404E/W	-0.603	-10.251
18. 404D	-0.592	-9.886
19. 404F	-0.518	-9.896
20. PN	1.104	-10.848

Table 8.1 — cont.

Sample No.	$\partial^{13}C$‰ PDB	$\partial^{18}O$‰ PDB
E. Whole rocks		
1. $396B_2$	1.271	-16.507
2. 403.5	0.043	-9.663
3. PN	0.768	-12.038
4. 399.1	0.311	-15.295
5. 400.8	-0.495	-12.596
6. 395.2B	-0.040	-15.264
7. 398.2A	0.082	-15.130
8. 398.1	0.209	-14.688
9. 396C	0.906	-16.893
F. Allochems		
1. 396A	1.334	-13.966
2. 403	-0.133	-10.995
3. 403.5	-0.433	-10.667
4. 402C	0.583	-11.840
5. 402D	0.331	-13.206
6. 399.1B	0.167	-15.460
7. 401B	-0.193	-11.176
8. 400.7	-0.151	-11.301
9. 398A	0.310	-14.770
G. Fenestral spars		
1. 402C	0.681	-11.228
2. 402D	0.320	-12.382
3. 399.1B	0.402	-11.250
4. 5B	0.233	-11.790

Table 8.2— Oxygen and carbon isotopic compositions of deeper water stromatolitic limestone, the Pa Kae Formation.

Sample No.	$\partial^{13}C$‰ PDB	$\partial^{18}O$‰ PDB
A. Marine cements		
1. 359.1	3.360	-4.833
2. 359.1/2	2.261	-6.744
3. 359.1/1B	2.355	-6.983
B. Early diagenetic cements in voids & veins		
1. 359.1/2C	1.930	-3.957
2. 359.1/26B	2.366	-7.220
C. Late diagenetic cements in veins		
1. 359.1/03	2.156	-9.320
2. 359.1/26	2.353	-6.638
D. Micrite		
1. 359.1/0	3.937	-6.716
2. 359.1	2.390	-9.241
3. 359.1/0.3	2.400	-10.052
4. 359.1/0.9	2.285	-10.006
5. 359.1/1	2.407	-9.848
6. 359.1/3	2.451	-9.860
7. 359.1/7	2.380	-10.445
8. 359.1/13	1.308	-8.272
9. 359.1/24	1.824	-6.193
10.359.1/26	2.859	-6.366
11.359.1/46	1.324	-6.174
12.359.1/46C	2.687	-3.095
E.Calcareous mudstone		
1. 359.1/0	2.841	-6.001
2. 359.1	2.063	-9.615
3. 359.1/0.3	1.985	-10.551
4. 359.1/0.313	2.272	-9.546
5. 359.1/09	2.446	-9.649
6. 359.1/3	2.111	-9.663
7. 359.1/7	2.382	-9.032
8. 359.1/13	1.700	-8.326
9. 359.1/24	1.886	-5.876
10.359.1/26	2.541	-6.733

Table 8.3— Oxygen and carbon isotopic compositions of dolomites of various palaeoenvironments.

Sample no.	$\partial^{13}C‰$ PDB	$\partial^{18}O‰$ PDB
A.Dolomite with stromatolites		
1. $396B_2$	2.163	-10.095
2. 396C	0.146	-13.765
3. TB	1.658	-8.380
4. 403	0.129	-9.401
5. 403.2	0.631	-7.650
6. 403.5	0.099	-9.654
7. 402A	1.491	-9.691
8. PN-L	0.771	-10.246
9. PN-D	2.123	-7.147
10. PN_2-D	1.249	-10.564
11. 399-L	0.435	-12.568
12. 399-D	1.076	-10.649
B.Dolomite with buildups		
1. 400-D_1	0.969	-6.216
2. 400-D_2	0.277	-8.335
3. 400A-D_1	-0.281	-4.676
4. 400.1-D_1	0.748	-5.685
5. 400.4-D_1	-0.777	-4.262
6. 400.6B-D_1	-0.288	-6.429
7. 400.7-S	1.543	-3.155
C.Dolomite with Lagoon		
1. 401E-D	-1.041	-9.401
2. 401C-D	-0.201	-9.484
3. 401F-D	-1.171	-11.086
4. G-D	-0.379	-9.006
5. 70.6-D	0.271	-9.495
6. 404B	-0.275	-8.689
7. 404D-W	-0.587	-7.662
8. 404D-D	-0.231	-8.651
9. 404F	0.142	-11.386

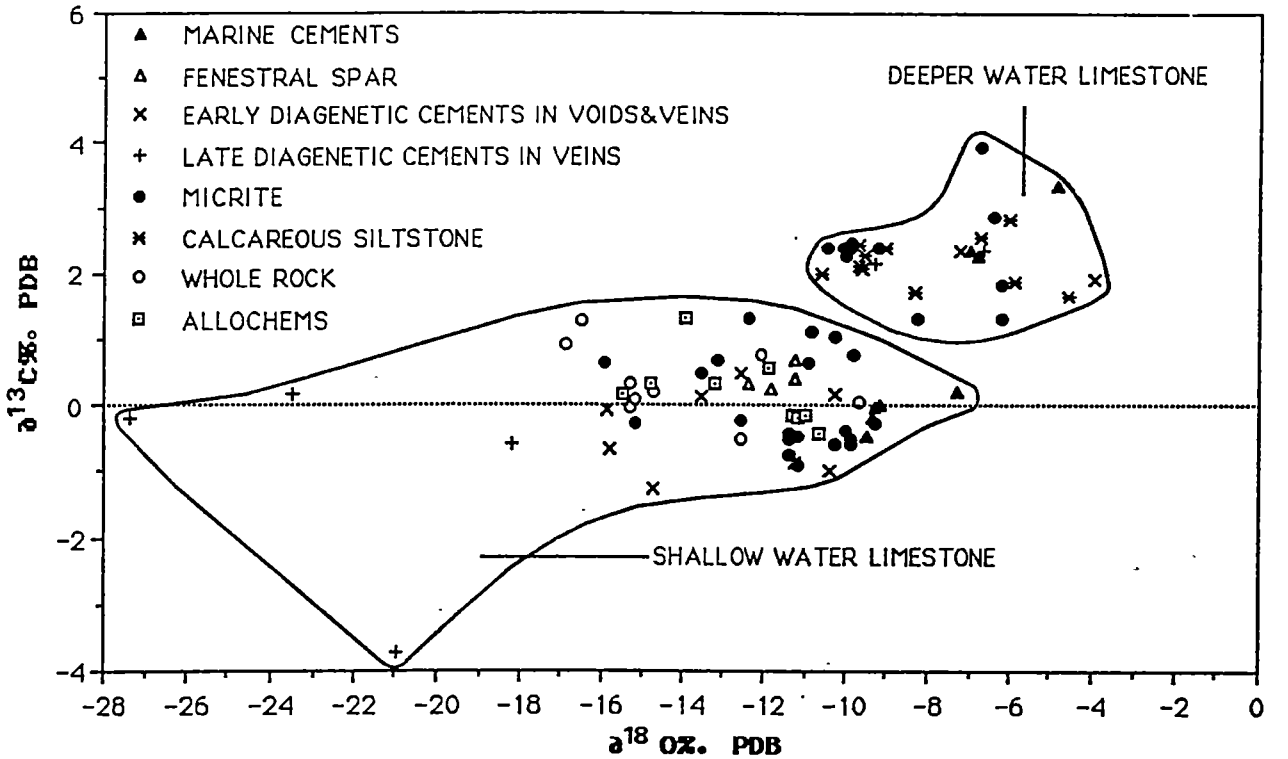

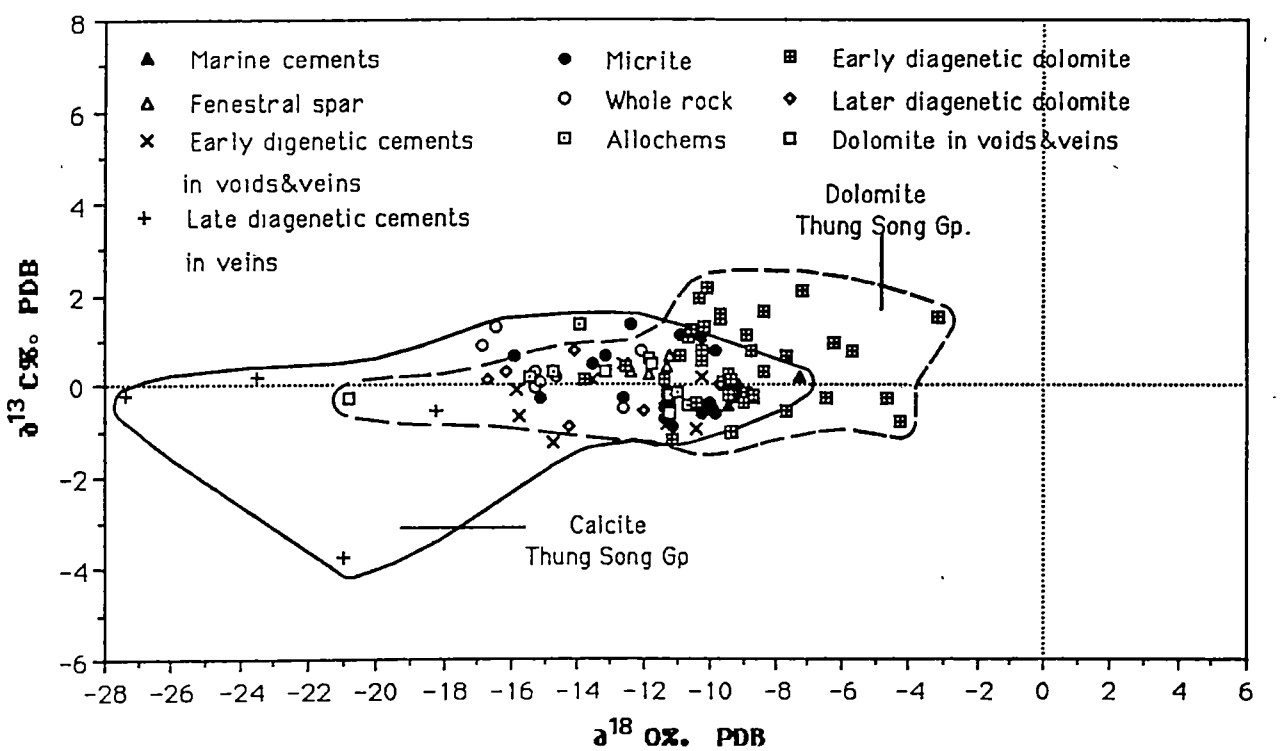

Fig. 8.1 A. Comparison of$\partial^{18}O$ and $\partial^{13}C$ of separate components from the shallow water limestones of the lower formation and deeper water limestones from the Pa Kae Formation, the Thung Song Group.

B. Comparison of$\partial^{18}O$ and $\partial^{13}C$ of shallow water limestones and dolomites.

‰ to +2.1‰ PDB. Late diagenetic cements in veins have $\delta^{18}O$ values from -18.2‰ to -27.3‰ PDB and $\delta^{13}C$ values from +0.1‰ to -3.7‰ PDB.

4. Microdolomites or early diagenetic dolomites have $\delta^{18}O$ values from -7.1‰ to -13.7‰ PDB and $\delta^{13}C$ values from +2.1‰ to -0.3‰ PDB. Microdolomites with lagoonal carbonates have $\delta^{18}O$ values -7.6‰ to -11.3‰ PDB and $\delta^{13}C$ values +0.1‰ to +0.5‰ PDB. Mesodolomites with buildup have $\delta^{18}O$ values from -3.1‰ to -8.3‰ PDB and $\delta^{13}C$ values from +1.5‰ to -0.7‰ PDB. Later diagenetic dolomites have $\delta^{18}O$ values from -11.9‰ to -16.7‰ PDB and $\delta^{13}C$ from +0.7‰ to -0.884‰ PDB as late diagenetic dolomites in veins have $\delta^{18}O$ values from -11.1‰ to -20.8‰ PDB and $\delta^{13}C$ values from +0.4‰ to -0.6‰ PDB.

The heaviest $\delta^{18}O$ composition of these separate marine components of the peritidal or shallow water limestones (Fig. 8.1A) from the Malaka Formation up to the Rung Nok Formation is about 3.3‰ PDB lighter than those of the deeper water stromatolitic limestones from the Pa Kae Formation, reflecting the temperature difference at the two main sites of deposition of the Thung Song Group. Formational temperature of the Pa Kae Formation is much lower than the lower formations. The heaviest $\delta^{13}C$ of the shallow water limestones is about 2.6‰ PDB lighter than the heaviest carbon isotope composition of deeper water limestones, indicating biochemical fractionation within the deeper water stromatolites from the Pa Kae Formation.

The photosynthesis process of micro-organisms preferentially uptakes light carbon (^{12}C) from the system as the heavy carbon (^{13}C) is retained in the surface reservoir as dissoluble bicarbonates in sea water (Schidlowski, 1988). Subsequently, the enrichment of heavy carbon in sea water results in precipitation of carbonates with heavy $\delta^{13}C$ as those of the Pa Kae Formation. The wide range of $\delta^{18}O$ of the shallow water limestones (Fig. 8.1) suggests gradual diagenetic alteration of the rocks with increasing temperature from an early diagenetic stage to deep burial.

The oxygen isotopic composition of microdolomites is about 4‰ heavier than oxygen isotopic composition of shallow water carbonate precursors (Fig. 8.1B). An O^{18} enrichment of 4‰ as observed in the Thung Song microdolomites is similar to $\Delta^{18}O$ of many ancient carbonates (Land, 1980).

8.2 Isotopic Comparison Between the Thung Song Group and Worldwide Ordovician Carbonates

The comparison between $\partial^{18}O$ and $\partial^{13}C$ values of Thai carbonates, the Thung Song Group, Thailand with worldwide and Gordon Limestone, Tasmania is illustrated in Fig. 8.2.

The wide range (-3.9 to -27.3‰ PDB) and mode (-9 to -11‰ PDB) of $\partial^{18}O$ in calcite of Thailand are much different from and lighter than those in the Tasmania calcite (Rao and Wang, 1989) and worldwide Ordovician calcite (Veizer and Hoefs, 1976). The $\delta^{13}C$ values of calcite from Thailand, Tasmania and worldwide are similar. The calcite from Thailand and worldwide have the same mode of $\delta^{13}C$ (0 to +2‰ PDB) but the mode of Tasmanian calcite (0 to -2‰ PDB) is lower. In addition, the $\delta^{13}C$ values in calcite from worldwide are the heaviest.

The range of $\delta^{18}O$ in Thai dolomite (-7.6‰ to -20.8‰ PDB) is also the widest. Those of Tasmania range from -3‰ to -6.8‰ and of worldwide dolomite is 0‰ to -11 ‰ PDB. The mode of $\delta^{18}O$ in Thai dolomite (-9‰ to -11‰ PDB) is lighter than mode of Tasmania dolomite (-3‰ to -5‰ PDB). On the contrary, the range of $\delta^{13}C$ in worldwide dolomite (-4‰ to -9‰ PDB) is the widest as the mode of Thai dolomite (0 ‰ to +2‰ PDB) is the heaviest.

The wide range of $\delta^{18}O$ in Thai calcite and dolomite are considered to undergo diagenetic alteration longer than Tasmanian and worldwide carbonates with more alteration from temperature fractionation. The calcite values lighter than -13‰ PDB and dolomite values lighter than -10.5‰ PDB might be due to deeper burial diagenesis.

Allochems: The $\delta^{13}C$ values of allochemical particles in the Thung Song Group (Fig. 8.3A) are at the lower end of the spectrum for values obtained from Recent marine sediments and skeletals in Recent shallow warm and cold water carbonates as well as Ordovician carbonates in Tasmania but are distinctively lower than those of ooids in eastern USA continental shelf.

In contrast, the $\delta^{18}O$ values of the limestone are remarkably lower than those of Recent sediments and Ordovician limestone (James and Choquette, 1983; Rao and Green, 1983; Rao and Wang, 1990) suggesting significant diagenetic alteration of the Thung Song's allochems.

Cements: In comparison (Fig. 8.3B) with the recent cements (Al-Aassam and Veizer, 1986), Ordovician spars in the Gordon Limestone, Tasmania (Wang and Rao, 1989), and Ordovician cements from Nevada (Ross *et al.*, 1975), the $\delta^{18}O$ values of marine cements in the Thung Song Group are lighter than those in Recent carbonates and the Gordon Limestone but fall within the same range as those of Middle Ordovician marine cements from Nevada. These variations probably resulted from a global "greenhouse mode" which caused the Ordovician atmosphere to be hotter than in the Recent (James and Choquette, 1983). Fenestral spar and spar in veins have $\delta^{18}O$

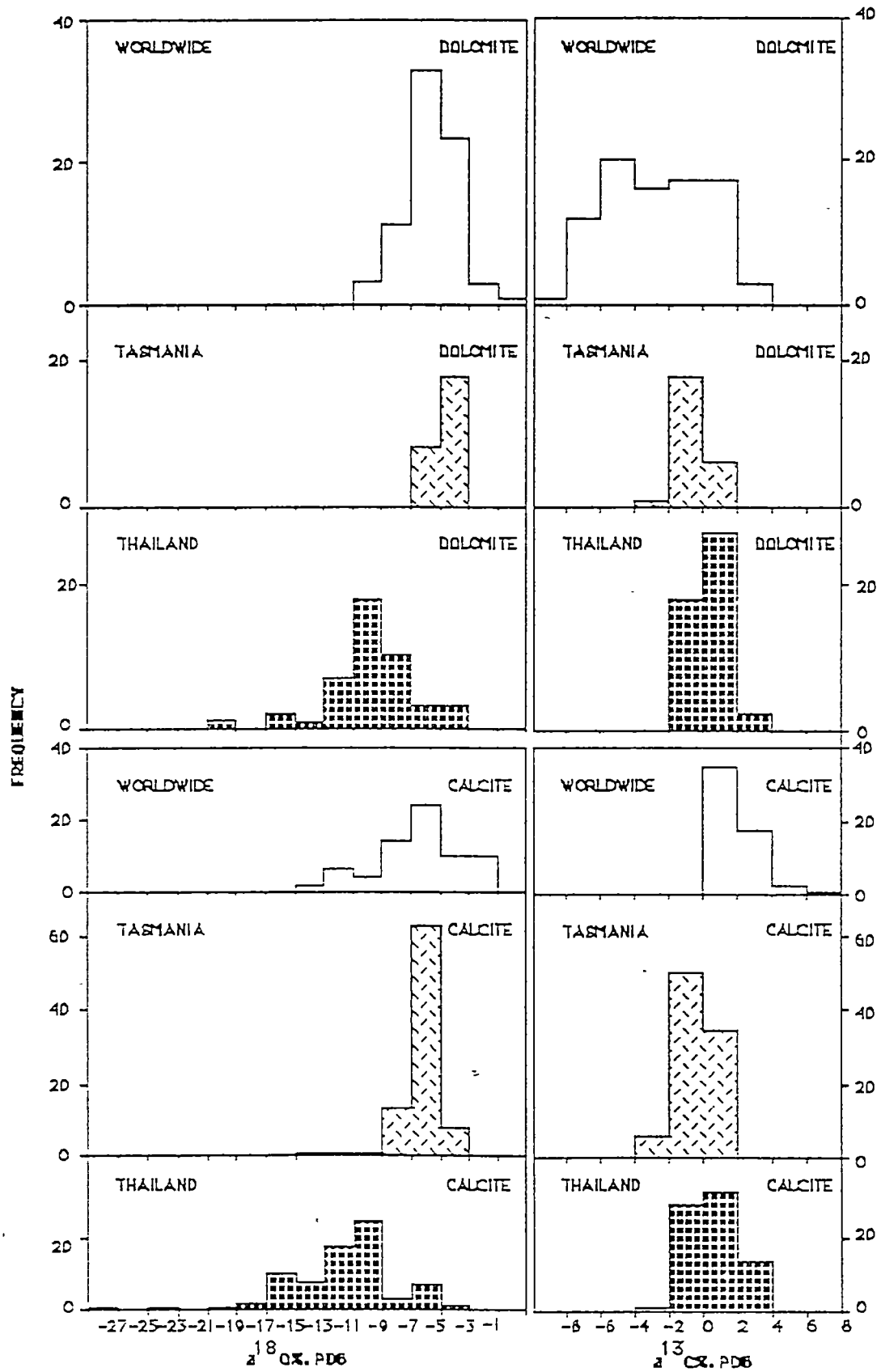

Fig. 8.2 Comparison histogram of dolomite and calcite from the Thung Song Group with those of worldwide Ordovician and Tasmanian calcite and dolomite (Veizer and Hoefs, 1976; Rao, 1989).

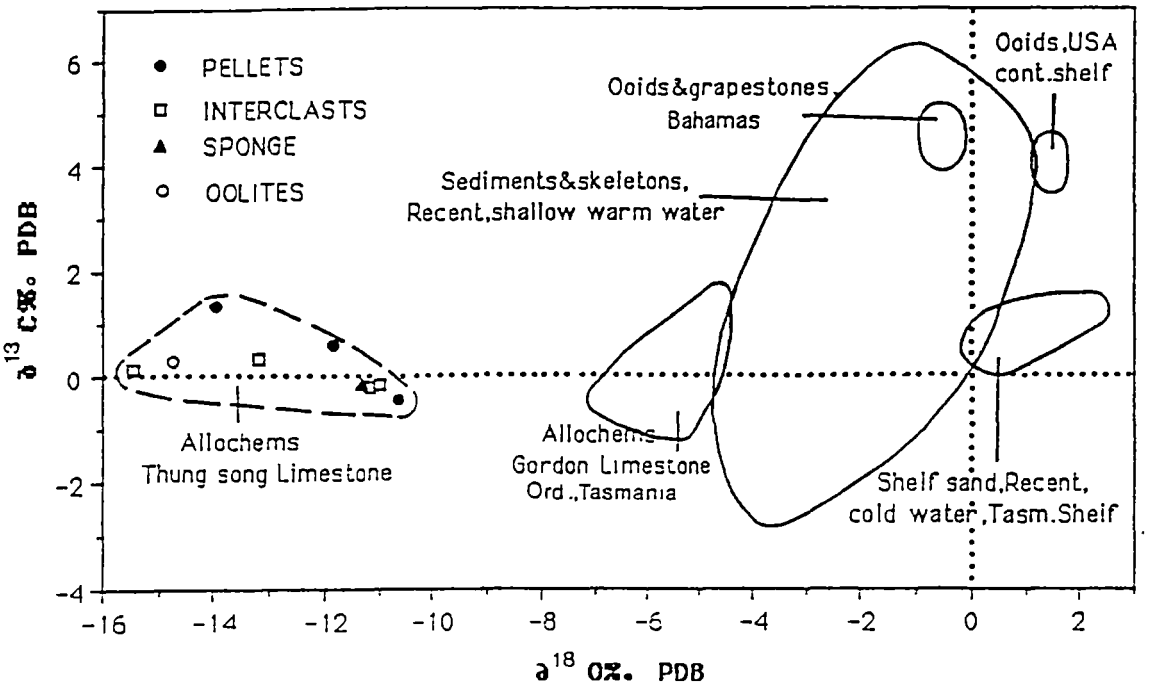

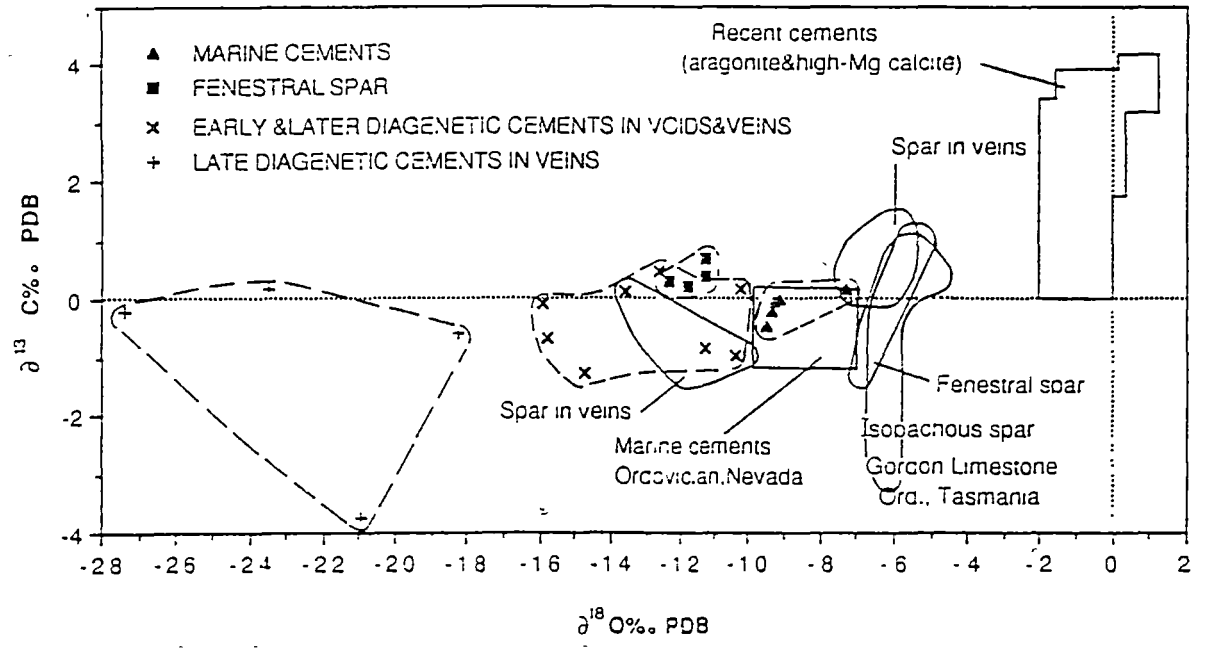

Fig. 8.3 A. Comparison of $\partial^{18}O$ and $\partial^{13}C$ of fauna, oolites within the Thung Song Group, Thailand, with those in Recent warm-marine (James and Choquette, 1983), cold-marine and Ordovician warm-marine (Rao and Green, 1983; Rao and Wang,1990).

B. Comparison of $\partial^{18}O$ and $\partial^{13}C$ of marine calcite cements, fenestral spars, early and late diagenetic cements, and late diagenetic cements, the Thung Song Group, with those in Recent aragonite and high-Mg calcite, Ordovician calcite cements from Tasmania (Rao and Wang, 1990) and Nevada (Ross *et al.*, 1975).

values much lighter than those from Tasmania and marine cements in the Gordon Limestone and Nevada Limestone.

However, the $\delta^{13}C$ values are similar to those of Nevada marine cements and are within the range of the Gordon Limestone but are slightly lighter than $\delta^{13}C$ values of Recent cements. The isotopic composition of late diagenetic cements in veins is distinctively depleted in both $\delta^{18}O$ and $\delta^{13}C$ because of burial before temperature fractionation.

Dolomites: In general, the oxygen and carbon isotopic signature of the Thung Song dolomites can be subdivided into three groups: dolomite with buildup, dolomite with lagoon, and dolomite with stromatolites (Fig. 8.4A, Table 8.3). All of them have $\delta^{18}O$ values much lighter than those of the Recent and Pleistocene dolomites. These variations can be explained as a result of diagenetic alteration and re-equilibrium (Dickson and Coleman, 1980).

The $\delta^{18}O$ values of dolomites with carbonate buildup from the fourth member of the Rung Nok Formation are the heaviest of the ranges studied and their field mostly overlaps with that of the Ordovician–Silurian Nevada dolomites (Dunham and Olson, 1980) and the Ordovician Tasmanian dolomites (Rao and Wang, 1990). The $\delta^{18}O$ values of dolomites with stromatolites from the Malaka Formation, La Nga Formation, and Pa Nan Formation and dolomites with lagoon from the lower member of the Lae Tong Formation are similar but lighter than those of dolomites with buildups suggesting dolomitization from different formational fluids with lighter isotopic composition than that of the Rung Nok Formation, possibly mixed-marine origin.

8.3 Isotopic Composition of the Ordovician Marine Value, Water Temperature and Possible Palaeolatitude

The isotopic composition of sea water is one of the most important original factors controlling the isotopic signature in sedimentary carbonates and provides a reference for isotopic assessment. It has long been observed that the $\delta^{18}O$ of marine carbonates tend to decrease with increasing geologic age (Veizer and Hoef, 1976; Anderson and Arthur, 1983). Two contrasting hypotheses have been developed to explain this isotopic variation with respect to sea water:

1. The $\delta^{18}O$ variation reflects meteoric or burial diagenesis, and sea water temperature of the past was higher than present (Degens and Epstein, 1962; Knauth and Epstein, 1976) and ∂_w value of sea water through time.
2. The $\delta^{18}O$ composition of ancient sea water is changed through time.

The latter is more acceptable (James and Choquette, 1983).

The isotopic composition of ancient sea water can only be inferred indirectly from evidence in the geologic record. It is estimated from the heaviest value of unaltered marine carbonate components. In the Thung Song carbonates, the heaviest $\delta^{18}O$ value of all components in shallow marine limestones is that of marine cements from carbonate buildups (-7.2‰ PDB, Fig. 8.1A, 8.3B). This -7.2‰ value is considered here as the $\delta^{18}O$ value of the Lower Ordovician original marine value of Thailand. It is about 2.6 ‰ lighter than the Late Ordovician marine value of Tasmania (-4.6‰, Rao and Wang, 1990) and only 0.4 ‰ lighter than the Middle Ordovician marine value of Nevada, USA (-6.9‰, Ross *et al.*, 1975).

The decreasing $\delta^{18}O$ Ordovician marine values from Tasmania to Nevada and Thailand should be reflected the difference in palaeogeographic position of those microcontinents since the temperature and latitude are the major factors controlling the oxygen isotopic composition. The greater the distance away from the Equator, the heavier the $\delta^{18}O$ values are.

The Tasmanian carbonates formed at a palaeolatitude of about 10°N (Embleton, 1973) indicating the tropical zone as well as the Nevada carbonates which formed at 10 °S (Rao and Wang, 1990). Thus, the Thung Song Group should have formed closer to the Equator than those carbonates at the time of carbonate buildups (the Rung Nok Formation) deposition during the Middle to Late Arenig. Moreover, the lighter $\delta^{18}O$ of the Thailand Ordovician marine carbonates by 0.4‰ compared to those of the Nevada marine value may suggest that the Thung Song carbonates formed in marine temperature about 2°C higher than the Ordovician limestone of Nevada.

8.4 Calcite–Dolomite Fractionation

The $\delta^{18}O$ and $\delta^{13}C$ values of the co-existing calcites and dolomites obtained from a sequential analysis are plotted in Fig. 8.4B to understand calcite–dolomite fractionation. For almost all samples, dolomites are enriched in $\delta^{18}O$ and $\delta^{13}C$ relative to calcite. The higher the isotopic values of associated calcites, the heavier the dolomite isotope values are observed. Rao and Wang (1990) interpreted this phenomenon as the inheritance of isotopes from the original calcites. The similarity of slopes of the connecting line between calcite and dolomite pairs also indicate both isotopic inheritance from calcite precursors and variable composition of dolomitizing fluids. In addition, the co-existing calcites vary widely in $\delta^{18}O$ (-10 to -18.6‰) and $\delta^{13}C$ (+1.3 to -0.9‰) suggesting that the calcium carbonate precursors had variable original values of isotopic composition (Rao and Wang, 1990).

On average, the dolomites from Thailand are enriched in $\delta^{18}O$ by about 3.0‰ ($\Delta^{18}O$) and 0.3‰ in $\delta^{13}C$ ($\Delta^{13}C$). The $\Delta^{13}O$ values of the Thai dolomites are lower

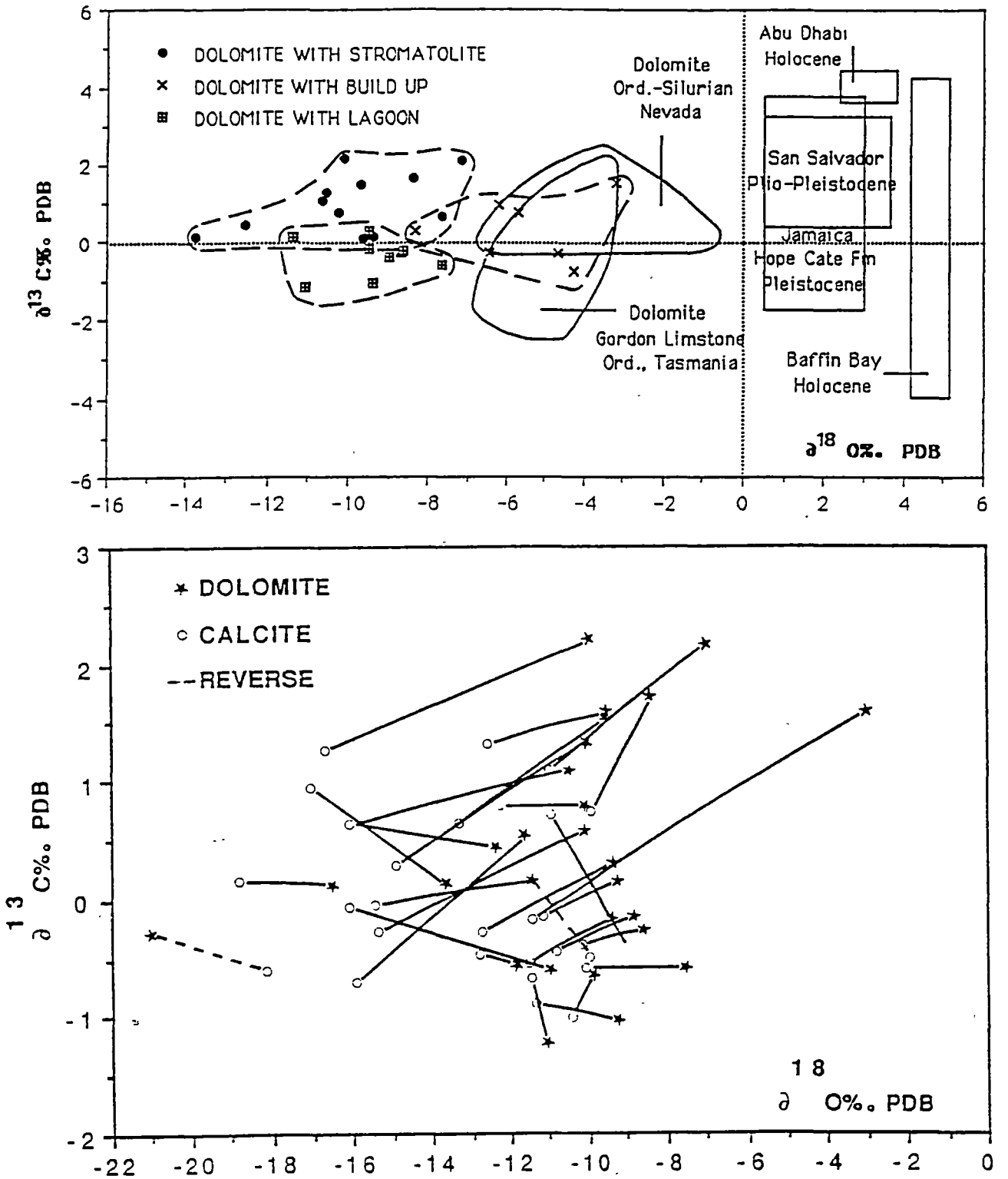

Fig. 8.4 A. Comparison of $\partial^{18}O$ and $\partial^{13}C$ of dolomites, the Thung Song Group, Thailand, with those in Holocene and Pleistocene dolomite (Choquette and Steinen, 1980), Ordovician dolomites from Tasmania (Rao and Wang, 1990) and Ordovician-Silurian dolomites of Nevada (Dunham and Olson, 1980).

B. Sequential analyses of $\partial^{18}O$ and $\partial^{13}C$ in calcite and dolomite, the Thung Song Group, Thailand. The line joining calcite and dolomite are isotopic values obtained for these minerals in the same samples.

than those from the experimental data extrapolated from high temperatures to 25°C by Sheppard and Schwarcz (1970). However, they are very close to the values of the Holocene marine dolomites from Baffin Bay and hypersaline dolomites from Persian Gulf which are enriched in $\delta^{18}O$ from +2 to +3‰ relative to their carbonate precursors (Land, 1980). The $\delta^{18}O$ fractionation between dolomite and solution bicarbonate ion is normally as small as 0.8‰ (Wigley *et al.*, 1978; Rao, 1990).

The Thai dolomites with $\delta^{18}O$ values heavier than -4‰ are regarded as marine dolomites and those falling within the range of -4.1 to -6.1‰ are interpreted as mixed-marine to burial dolomites. The dolomites with $\delta^{18}O$ values lighter than -6.1‰ are interpreted as later to late diagenetic dolomites. Most of $\delta^{18}O$ values from sequential analyses are in the range of the latter (Fig. 8.4B). In addition, similar trends of decreasing $\delta^{18}O$ and $\delta^{13}C$ values in the majority of the Thai dolomites possibly indicates that the original carbonates had undergone marine to meteoric and burial diagenesis while the dolomitization proceeded.

Chapter 9
CONCLUSION

The Thung Song Group in Satun Province, southern Thailand, is a 1,400 m thick sequence of tropical carbonates and minor shales. The sequence ranges from Late Tremadoc to Ashgill. This group can be subdivided into at least 7 conformable rock units as follows: the Malaka Formation, Talo Dang Formation, La Nga Formation, Pa Nan Formation, Lae Tong Formation , Rung Nok Formation,and Pa Kae Formation. The Pa Kae formation has been proposed as the uppermost rock unit of the Thung Song Group in southern Thailand (Wongwanich *et al.*, 1990). These formations conformably overlie the red siliciclastic, Tarutao Group (Upper Cambrian–Tremadoc) on Ko Tarutao, and is conformably overlain by a sequence of chert, black shale and siltstone of the Wang Tong Formation (Lower to Upper Silurian) on mainland Satun Province. The Ordovician-Silurian boundary has been placed in the lower part of the Wang Tong Formation 20 m above the Pa Kae Formation.

Based on the absence of extensive carbonate buildups and reef complexes, the Thung Song carbonates are proposed as a homoclinal ramp carbonate complex with marine-shelf and lagoonal deposition resembling the modern Persian Gulf. As a result of a long term transgression during the Late Tremadoc to Late Arenig, deepening-upward sequence is a general characteristic of the Thung Song carbonates. The sequence starts from shallow subtidal to supratidal deposits of the Malaka Formation to restricted shallow lagoonal deposits of the Talo Dang Formation, migrating barrier island deposits of the La Nga Formation, shallow subtidal stromatolitic reefs of the Pa Nan Formation, deeper-water lagoonal deposits of the Lae Tong Formation, carbonate buildups and barrier reefs of the Rung Nok Formation, and end up with the deep water stromatolites of the Pa Kae Formation. The rocks pass upwards to the black graptolitic shales and cherts of the Wang Tong Formation.

The extensive tidal flat facies of the Malaka Formation are represented by the extensive deposition of stromatolitic laminites with mud cracks, flat pebble conglomerates as lag deposits, and cross bedded oolites in tidal-channel subfacies. Microdolomite is very extensive occurring as laminites, thin bedding, and replacing sediments in mud cracks. The intercalation of nodular limestone and variegated shale in the Talo Dang Formation and Lae Tong Formation represents lagoonal deposition. These two formations were deposited in lagoons behind barrier islands and outer ramp buildups. Shoaling in a broad lagoon and migrating barrier islands are suggested by abundant oolites, a complex network of trough cross-bedding with common reactivation surfaces, scoured bases, and escape burrows in the lower La Nga Formation. The development of carbonate buildups on the outer ramp is represented by

a thick sequence of poorly washed to unsorted biosparites of the first and second members in the Rung Nok Formation. Coral-algal-stromatoporoid biolithite and breccias of the third member represents local barrier reefs. The distribution of these microfacies is localized to only three small islands, SW. Ko Tarutao. Reef growth was initiated by increasing rate of the carbonate production of frame-builder organisms including simple tabulate corals, globular bryozoans, and stromatoporoids ; and a deposition of these faunal skeletons (Read, 1980) and other encrusting organisms such as stromatolites, calcareous algae on the gradually submerging carbonate ramp. The development of buildups on the outer ramp during the Ordovician transgression resulted in the formation of restricted lagoons (the Lae Tong Formation) landward and deeper water stromatolites (the Pa Kae Formation) seaward.

Common small-scale shallowing-upward sequences within the Thung Song Group, such as those of the upper La Nga member and the Talo Dang Formation, resulted from a combination of gentle subsidence and sea level fluctuation (Ginsburg, 1971; James, 1984). Wet and dry palaeoclimates are envisaged since evaporite pseudomorphs occur in nearly all formations except the Rung Nok and Pa Kae Formations. Evaporites are not abundant enough to suggest long term arid climates such as those of the modern Persian Gulf. Storm events were common as suggested by abundant marine tempestites in the Lae Tong Formation

The Thung Song Group has experienced many stages of diagenesis including early marine, early to late meteoric, burial diagenesis, and dolomitization.

Early marine diagenesis in peritidal carbonates is not clear, especially in the supratidal to intertidal zone. In the subtidal, high-Mg calcites (HMC) reduced much of the primary porosities within the stromatolites of the Pa Nan Formation, whereas their fenestral porosities subsequently filled by internal sediments and blocky cements. Some small radial stubby bladed cement (HMC) in intertidal sediments of the Malaka Formation and La Nga Formation are probably of marine origin and were later redeposited on a tidal flat by wave action. Marine cementation in lagoon carbonates is rare because of the restricted nature of lagoonal water circulation. However, early cementation of micritic nodular limestones has been presented. In contrast, intense marine cementation occurred in carbonate buildups and this filled up nearly all interparticle and intraparticle porosities by HMC bladed to fibrous isopachous cements and syntaxial rims. Radiaxial cements are also common and usually occurred as a first cement within channel porosities. Marine cementation in deeper water stromatolites is relatively less extensive than those of carbonate buildups because of low porosity and weaker circulation. However, micrite and microspar cements are extensive.

The early to late meteoric cementation is common in intertidal sediments. Equant cements (LMC) are present in all primary pore types and microfacies. Meniscus

cements are common but pendant cements are rare indicating poor preservation of the vadose meteoric zone in the Thung Song Group. Mixed-marine microdolomites and gypsum pseudomorphs are also widely distributed in this intertidal deposit. Dissolution and reprecipitation of semistable minerals occurred mainly in a meteoric phreatic zone as shown by blocky spars infilling moldic porosities and the preservation of micritic rims.

Burial diagenesis in intertidal, shallow and deeper marine carbonates are very similar. All of the remaining porosities and fracture porosities were destroyed by blocky calcite, xenotopic dolomite cements, and the second generation of syntaxial rims. Physical compaction has been observed mostly in lagoonal carbonates. Extensive dolomitization in the upper portion of the Rung Nok Formation predated stylolitization. Stylolites are abundant in the Thung Song Group and include both tectostylolites and diagenetic stylolites. Dedolomitization may have occurred late after uplift of the carbonate ramp.

Under cathodoluminescence, marine cements from carbonate buildups and from deeper water stromatolites generally display a compositional zonation from early non-luminescent cement to bright-luminescent cement and dull-luminescent cement indicating the change of pore fluids from oxidizing marine waters to more reducing fluids after burial. However, many of the intertidal and lagoonal cements have a zonation from bright- to dull-luminescence or reversed order suggesting that most of them formed under reducing marine or mixed marine water. This possibly resulted from restriction in a lagoon and the decomposition of organic matter in these areas. The abundant pyrite crystals in intertidal and lagoonal carbonates and the widespread stromatolites in intertidal deposits also support this interpretation.

The oxygen isotopic composition of the Thung Song carbonates can be subdivided into four groups. The $\partial^{18}O$ values of marine limestone in deeper water stromatolites and carbonate buildups are heavier than those of intertidal limestones and burial cement respectively. The $\partial^{18}O$ values of deeper water stromatolites are the heaviest and the $\partial^{18}O$ values of burial cement, the lightest. The progressive decrease in isotopic composition of the Thung Song Group compared to modern tropical carbonates primarily reflects increasing temperature of the pore fluids as diagenesis proceeded.

The $\partial^{18}O$ values of the Thung Song dolomites in buildups are heavier than those of the intertidal stromatolites and lagoonal sediments but $\partial^{13}C$ values fall within the same range. The $\partial^{13}C$ values of dolomites with stromatolites are heavier than $\partial^{13}C$ values of lagoonal dolomites. The Thung Song dolomites formed in marine and mixed-waters as the $\partial^{18}O$ and $\partial^{13}C$ field of dolomite overlap the marine calcite diagenetic

field and extend up to the meteoric calcite diagenetic field. However, they were altered after burial by temperature fractionation or diagenetic alteration and re-equilibration.

The oxygen isotopic compositions of the Thung Song Group are much lighter than those of modern and Pleistocene dolomites as well as that of the Late Ordovician limestone from Tasmania and the Middle Ordovician of Nevada probably because of the "greenhouse depositional mode" and the lighter Ordovician $\partial^{18}O$ marine value. The $\partial^{18}O$ of the Early-Middle (?) Ordovician marine value (from buildup marine cements) of Thailand is -7.2‰ which is lighter by 0.4‰ than $\partial^{18}O$ of the Middle Ordovician marine value of Nevada. This indicates that the Ordovician marine water in Thailand was about 2°C warmer than Nevada. Therefore Thai Ordovician carbonates formed in a tropical climate probably at a lower latitude than Nevada limestones.

The further research should be concentrated on the Phetra Formation to fulfill the gap between the lower and the upper formation.

REFERENCES

Adam, J.E., and Rhodes, G.M., 1960, Dolomitization by seepage refluxion: Am. Ass. Petrol. Geol. Bull., v.44, p.1912–1920.

Aigner, T., 1985, Storm Depositional Systems: Berlin, Springer-Verlag, 147 p.

Aitken, J.D., 1967, Classification and environmental significance of cryptalgal limestones and dolomites, with illustration from the Cambrian and Ordovician of Southwestern Alberta: Jour. Sed. Petrology, v.37, p.1163–1178.

Al-Aasam, I.S., and Veizer, J., 1986, Diagenetic stabilization of aragonite and low-Mg calcite, I. Trace elements in Rudists: Jour. Sed. Petrology, v.56, p.138-152.

Al-Aasam, I.S., and Veizer, J., 1986, Diagenetic stabilization of aragonite and low-Mg calcite, II. Stable isotopes in Rudists: Jour. Sed. Petrology, v. 56, p.763–770.

Alexandersson, E.T., 1978, Destructive diagenesis of carbonate sediments in the eastern Skagerrak, North Sea: Geology, v.6, p.326-327.

Alexandersson, E.T., 1979, Marine maceration of skeleton carbonates in Skagerrak, North Sea: Sedimentology, v.26, p.845-852.

Anderson, T.F., and Arthur, M.A., 1983, Stable isotopes of oxygen and carbon and their application to sedimentology and paleoenvironmental problems: Soc. Econ. Palaeont. Mineral., Short Course No.10, p. 1-1 to 1-151.

Andreyev, S.I., Kulikov, A.N., and Anikeyeva, L.I., 1987, Sedimentation rates in areas of nodule formation in the Pacific Ocean: Int. Geol. Review, v.29, p.1093-1099.

Badiozamani, K., 1973, The dorag dolomitization model — application to the Middle Ordovician of Wisconsin: Jour. Sed. Petrology, v.43, p. 965–984.

Baker, P.A., Gieskes, J.M., and Elderfield, H., 1982, Diagenesis of carbonate in deep-sea sediments - evidence from Sr/Ca ratio and interstitial dissolved Sr^{2+} data: Jour. Sed. Petrology, v.52, p.71-82.

Banner, F.T., and Wood, G.V., 1964, Recrystallization in microfossiliferous limestones: Geol. Journal, v.4, p.21-34.

Barnes, C.R., 1984, Early Ordovician eustatic events in Canada, *in* Bruton, D.L., ed., Aspects of the Ordovician System , Palaeontological Contributions from the University of Oslo no. 295: Oslo, Universitets forlaget, p. 51-63.

Barnes, C.R., and Fahraeus, L.E., 1975, Provinces, communities, and the proposed nektobenthic habit of Ordovician conodontophorids: Lethaia, v.8, p.133-149.

Barrett, P.J., 1964, Residual seams and cementation in Oligocene calcarenites: Jour. Sed. Petrology, v.34, p.524-531.

Bathurst, R.G.C., 1967, Subtidal gelatinous mat, sand stabilizer and food, Great Bahama Bank: Jour. Geology, v.75, p.736-738.

Bathurst, R.G.C., 1975, Carbonate sediments and their diagenesis: 2nd ed., Amsterdam, Elsevier, 658p.

Bathurst, R.G.C., 1983, Neomorphic spar versus cement in some Jurassic grainstones: significance for evaluation of porosity evolution and compaction: Jour. Geol. Soc.London, v.140, p.229-237.

Bathurst, R.G.C., 1987, Diagenetically enhanced bedding in argillaceous platform limestones: stratified cementation and selective compaction: Sedimentology, v.34, p. 749–778.

Bausch, W.M., 1968, Outlines of distribution of strontium in marine limestones, *in* Muller, G., and Friedman,G.M., eds., Recent Developments in Carbonate Sedimentology in Central Europe: Berlin, Springer-Verlag, p.105-115.

Beales, F.W., 1971, Cementation by white sparry dolomites, *in* Bricker, O.P., ed., Carbonate Cements: Baltimore, Johns Hopkins Press, p.330–338.

Beauvais, L., Blanc, P.H., Bernet-Rollande, M.C., and Maurin, A.F., 1988, Sedimentology of Upper Jurassic deposits in the Tembesi River Area, Central Sumatra: Geol. Soc. Malaysia Bull., v.22, p.45-64.

Benson, L.V., 1974, Transformation of a polyphase sedimentary assemblage into a single phase rock: a chemical approach: Jour. Sed. Petrology, v.44, p.123-135.

Berger, W.H., 1986, Deep-sea carbonates: reading the carbon-isotope signal: Geol. Rund., v.75, p.249-269.

Berry, W.B., and Boucot, A.J., 1973, Glacio-eustatic control of Late Ordovician-Early Silurian platform sedimentation and faunal changes: Geol. Soc. Am. Bull., v.84, p.275-284.

Berstrand-Sarfati, J., and Moussine-Pouchkine, A., 1983, Platform to basin facies evolution: the carbonate of Late Proterozoic (Vendian) Gourma (West Africa): Jour. Sed. Petrology, v.53, p.275-293.

Beukes, N.J., 1983, Ooids and oolites of the Proterophytic Boomplaas Formation, Transvaal Supergroup, Griqual and West, South Africa, *in* Peryt, T.M., ed., Coated Grains: Berlin, Springer-Verlag, p. 199-214.

Beukes, N.J., and Lowe, D.R., 1989, Environmental control on diverse stromatolite morphologies in the 3000 Myr. Pongola Supergroup, South Africa: Sedimentology, v.36, p.383-397.

Bissell, H.J., and Chillingar, G.V., 1967, Classification of sedimentary carbonate rocks, *in* Chillingar, G.V., Bissell, H.J., and Fairbridge, R.W., eds, Carbonate Rocks, Developments in Sedimentology 9A: Amsterdam, Elsevier, p. 87–169.

Black, M.,1933, The algal sediments of Andros Island, Bahamas: Philos.Trans. Ser.B 222, p.165-192.

Bova, J.A., and Read, J.F., 1987, Incipiently drowned facies within a cyclic peritidal ramp sequence, Early Ordovician Chepultepec interval: Geol. Soc. Am. Bull., v. 98, p. 714-727.

Brand, U., and Veizer, J., 1980, Chemical diagenesis of a multicomponent carbonate system – 2: stable isotopes: Jour. Sed. Petrology, v. 51, p. 0987–0997.

Brenchley, P.J., and Newall, G., 1984, Late Ordovician environmental changes and their effect on faunas, *in* Bruton,D.L., ed., Aspects of the Ordovician System, Palaeontological Contribution: Oslo, University of Oslo, Universitets forlaget no.295, p.65-79.

Bricker, O.P., ed., 1971, Carbonate Cements: Baltimore, John Hopkins Press, 376p.

Bridges, P.H., and Chapman, A.J., 1988, The anatomy of a deep water mud-mound complex to the southwest of the Dinantian platform in Derbyshire, U.K.: Sedimentology, v.35, p.139-162.

Brookfield, M.E., 1988, A mid-Ordovician temperate carbonate shelf-the Black River and Trenton Limestone Group of southern Ontario, Canada: Sed. Geology, v.60, p.137-153.

Brown, G.F., Buravas, S., Javanaphet, J.C., Chalichada, N., Johnston, W.D., Sresthaputra, V., and Taylor, G.C., 1951, Geological reconnaissance of the mineral deposits of Thailand. Geological Investigation in Asia: U.S. Geol. Surv. Bull., · 984 ·p.

Buchbinder, L.G., Magaritz, M., and Goldberg, M., 1984, Stable isotope study of karstic-related dolomitization:Jurassic rocks from the coastal plain, Israel: Jour. Sed. Petrology, v. 54, p. 0236-0256.

Buick, R., Dunlop, J.S.R., and Groves, D.I., 1981, Stromatolite recognition in ancient rocks: an appraisal of irregularly laminated structures in an Early Archaen chert-barite from North Pole, Western Australia: Alcheringa, v.5, p.160–181.

Bullen, S.B., and Sibley, D.F., 1984, Dolomite selectively and mimic replacement: Geology, v.12, p. 655–658.

Bunopas, S., 1974, On the Lower Palaeozoic rocks in Thailand: Geol. Surv. Thailand Newsletter, v. 4, p. 17–40.

Bunopas, S., 1976, Stratigraphy succession in Thailand — a preliminary summary: Jour. Geol. Surv. Thailand, v. 2(1-2), p. 31–58.

Bunopas, S., 1983, Palaeozoic succession in Thailand, *in* Nutalaya, P., ed., Stratigraphic Correlation of Thailand and Malaysia: Geol. Soc. Thailand, Bangkok, p. 39–76.

Bunopas, S., Muenlek, S., and Tansuwan, W., 1980, On the geology of Tarutao Island, South Peninsular, Thailand, *in* Mantajit, N., ed., Geological Excursion to the Lower Palaeozoic Geology, Tarutao Island, Southern Thailand: Geol. Exc. Guidebook No.5. Geol. Soc. Thailand, Bangkok, p. 13–29.

Buravas, S., 1957, Stratigraphy of Thailand: Mimeogr. distributed at IX Pacific Sci. Congr., Bangkok.

Burne, R.V., and James, N.P., 1986, Subtidal origin of club-shapes stromatolites, Shark Bay (abst.): Inter. Assoc. Sed. Congress Canberra, p.49.

Burne, R.V., and Moore, L.S., 1987, Microbialites: Organosedimentary deposits of Benthic microbial communities: Palaios, v.2, p.241-254.

Burrett, C., and Stait, B., 1985, Southeast Asia as a part of an Ordovician Gondwanaland — a palaeobiographic test of a tectonic hypothesis: Earth Planet. Sci. Letters, v.75, p.184-190.

Burrett, C., and Stait, B., 1986, China and southeast Asia as part of the Tethyan margin of Cambro-Ordovician Gondwanaland, *in* McKenzie, K., ed., Shallow Tethys 2: Rotterdam, Balkema, p.65-77.

Burrett, C., Long, J., and Stait, B., 1990, Early-Middle Palaeozoic biogeography of Asian terranes derived from Gondwana, *in* McKerro, W.S., and Scottese, C.R., eds., Palaeogeography and Biogeography: Geological Society Memoir no.12, p.163-174.

Burrett, C., Stait, B., Laurie, J., 1983, Trilobites and microfossils from the Middle Ordovician of Surprise Bay southern Tasmania, Australia: Memoirs of the Australasian Association of Paleontologists, v.1, p.177-193.

Burton, C.K., 1974, The Satun Group (Nai Tak Formation and Thung Song Limestone) of Peninsular Thailand: Sians Malaysiana, v.3, p.15-34.

Buxton, T.M., and Sibley, D.F., 1981, Pressure solution features in a shallow buried limestone: Jour. Sed. Petrology, v.51, p.19–26.

Cain, J.D., 1968, Aspects of depositional environment and palaeoecology of crinoidal limestones: Scottish Jour. Geol., v.4, p.191-208.

Calvert, S.E., and Price, N.B., 1977, Shallow water, continental margin and lacustrine nodule: distribution and geochemistry, *in* Glasby, G.P., ed., Marine Manganese Deposits: New York, Elsevier Sci. Publ. Co., p.45-86.

Campbell, J.A., 1987, Upper Cambrian stromatolitic biostrome, Clinetop Member of the Dotsero Formation, western Colorado: Geol. Soc. Am. Bull., v.87, p.1331-1335.

Caputo, M.V., and Crowell, J.C., 1985, Migration of glacial centers across Gondwana during Palaeozoic Era: Geol. Soc. Am., v.96, p.1020-1036.

Cecile, M.P., and Campbell, F.H.A., 1978, Regressive stromatolite reefs and associated facies, Middle Goulbum Group (Lower Proterozoic) in Kilohigok Basin, N.W.T.: an example of environmental control of stromatolite form: Can. Petrol. Geol. Bull., v.26, p.237-267.

Chafetz, H.S., 1973, Morphological evolution of Cambrian algal mounds in response to a change in depositional environment: Jour. Sed. Petrology, v.43, p.435-440.

Chen Jun-Yuan, 1985, Ordovician changes of sea level: New Mexico Bureau of Mines and Mineral Resources Memoir 44, p.387-404.

Chivas, A.R., Torgersen, T., and Palach, H.A., 1990, Growth rate and Holocene development of stromatolites from Shark Bay, Western Australia: Aust. Jour. Earth Science, v.37, p.113-121.

Choquette, P.W., 1971, Late Ferroan dolomite cement, Mississippian carbonates, Illinois Basin, U.S.A., *in* Bricker, O.P., ed., Carbonate Cements: Baltimore, John Hopkins Press, p. 339–346.

Choquette, P.W., and Pray, L.C., 1970, Geologic nomenclature and classification of porosity in sedimentary carbonates: Am. Assoc. Petrol. Geol. Bull., v.54, p.207–250.

Choquette, P.W., and Steiner, R.P., 1980, Mississippian non-supratidal dolomite, Ste Genevieve Limestone, Illinois Basin: Evidence for mixed-water dolomitization, *in* Zenger, D.H., Dunham, J.B., and Ethington, R.L., eds, Concepts and Models of Dolomitization: Soc. Econ. Geol. Mineral. Spec. Pub. No.28, p.163–196.

Choquette, P.W., and James, N.P., 1987, Diagenesis in Limestone-3, the deep burial environment: Geosci. Canada, v.14, p.3–35.

Coniglio, M., and James, N.P., 1985, Calcified algal as sediment contributors to early Palaeozoic limestones: Evidence from deep-water sediments of the Cow Head Group, western Newfoundland: Jour. Sed. Petrology, v.55, p.746-754.

Chow, N., and James, N.P., 1987, Cambrian Grand Cycles: A Northern Appalachian perspective: Geol. Soc. Am. Bull., v.98, p.418-429.

Craig, H., 1957, Isotopic standards for carbon and oxygen and correction factors for mass spectrometric analysis of carbon dioxide: Geochim. Cosmochim. Acta, v.12, p.133–149.

Coudray, J., and Montaggioni, L., 1986, The diagenetic products of marine carbonates as sea-level indicators, *in* Plassche, O., ed., Sea-level Research: Norwich, Geo Books, p.311-360.

Dansgaard, W., 1964, Stable isotopes in precipitation: Tellus, v.16, p.436–468.

Davies, G.R., 1970, Algal laminated sediments, Gladstone embayment, Shark Bay, Western Australia: Am. Assoc. Petrol. Geol. Mem., v.13, p.169–205.

Davies, G.R., 1977, Former magnesium calcite and aragonite submarine cements in upper Palaeozoic reefs of the Canadian Arctic: A summary: Geology, v.5, p.1175.

Davies, Jr., R.A., 1966, Willow River Dolomite: Ordovician analogue of modern algal stromatolite environments, J. Geol., v.74, p.908–923.

Degen, E.T., and Epstein, S., 1962, Relationship between O^{18}/O^{16} ratios in coexisting carbonates, chert and diatomites: Am. Assoc. Petrol. Geol. Bull., v.46, p.534–542.

De Lange, G.J., Middleburg, J.J., and Pruysers, P.A., 1989, Middle and Late Quaternary depositional sequences and cycles in the eastern Mediterranean: Discussion: Sedimentology, v.36, p.151-158.

Dickson, J.A.D., 1966, Carbonate identification and genesis as revealed by staining: Jour. Sed. Petrology, v.36, p.491–505.

Dickson, J.A.D., 1985, Diagenesis of shallow-marine carbonates, *in* Brenchley, P.J., and Williams, B.P.J.,eds., Sedimentology: Recent Developments and Applied Aspects: Geol. Soc. Spec. Publ. 18, p.173-188.

Dickson, J.A.O., and Coleman, M.L., 1980, Change in carbon and oxygen isotope composition during limestone diagenesis: Sedimentology, v.27, p.107–118.

Dill, R.F., Shinn, E.A., Jones, A.T., Kelly, K., and Steinen, R.P., 1986, Giant subtidal stromatolites forming in normal salinity waters: Nature, v.324, p.55–58.

Dix, G.R., and James, N.P., 1987, Late Mississippian bryozoan/microbial buildups on a drowned Kryst terrane : Port and Port Peninsula, western Newfoundland: Sedimentology, v.34, p.729-793.

Dörjes, J., and Hertweck, G., 1975, Recent biocoenoses and ichnocoenose in shallow-water marine environments, *in* Frey, R.W., ed., The study of trace fossils: New York, Springer-Verlag, p.459-491.

Duff, P.Mel.O., Hallam, A., Walton, E.K., eds., 1967, Cyclic Sedimentation. Developments in Sedimentology 10: Amsterdam, Elsevier, 280p.

Dugolinsky, B.K., Margolis, S.V., and Dudley, W.C., 1977, Biogenic influence on growth of manganese nodules: Jour. Sed. Petrology, v.47, p.428-445.

Dunham, J.B., and Olson, E.R., 1980, Shallow subsurface dolomitization of subtidally deposited carbonate sediments in the Hanson Creek Formation (Ordovician-Silurian) of central Nevada, *in* Zenger, D.H., Dunham, J.B., and Etrhington, R.L., eds, Concepts and Models of Dolomitization: Soc. Econ. Palaeont. Mineral. Spec. Pub. No.28, p.139–161.

Dunham, R.J., 1969, Early vadose silt in Townsend mound (reef), New Mexico, *in* Friedman, G.M., ed., Depositional Environments in Carbonate Rocks, A Symposium: Tulsa, Okla. Soc. Econ. Palaeont. Mineral., Spec. Pub. No.14, p.139–181.

Einsele, G., 1982, General remarks about the nature, occurrence, and recognition of cyclic sequences (Periodites), *in* Einsele, G., and Seilacher, A., eds., Cyclic and Event Stratification: Berlin, Springer, p.5-7.

Elderfield, H., 1976, Manganese fluxes to the Oceans: Marine Chemistry, v.4, p.103-132.

Eller, M.G., 1981, The Red Chalk of Eastern England : a Cretaceous of Rosso Ammonitico, *in* Farrinacci, A., and Elmi, S., eds, Rosso Ammonitico Symposium: Rome,Tecnoscienza, p.207-231.

Embleton, B.J.J., 1973, The palaeolatitude of Australia through Phanerozoic time: Jour. Geol. Soc. Aust., v.19, p.475–482.

Epstein, S., Graf, D.L., and Degens, E.T., 1964, Oxygen isotope studies on the origin of dolomites, *in* Craig, H., Miller, S.L., and Wasserburg, G.R., eds, Isotopic and Cosmic Chemistry: Amsterdam, North Holland, p.169–180.

Epstein, A.G., Epstein, J.B., and Harris, L.D., 1977, Conodont color alteration-an index to organic metamorphism: U.S. Geol. Sur. Prof. paper. 995, p.1-27.

Evamy, B.D., and Shearman, D.J., 1965, The development of overgrowths from echinoderm fragments: Sedimentology , v.5, p.211-233.

Fairbridge, R.W., and Jablonski, D., 1979, The Encyclopedia of Palaeontology: Stroudsburg, Dowden, Hutchinson and Ross, Inc., 886p.

Fairchild, I.J., 1980, Sedimentation and origin of a Late Precambrian dolomite from Scotland: Jour. Sed. Petrology, v.50, p.0423–0446.

Finkel, E.A., and Wilkinson, B.M., 1990, Stylolitization as source of cement in Mississippian Salem Limestone, West-Central Indiana: Am. Assoc. Petroleum Geologists Bull., v.74, p.174-186.

Flugel, E., 1982, Microfacies Analysis of Limestone: Berlin, Springer-Verlag, 633p.

Folk, R.L., 1959, Practical petrographic classification of limestones: Am. Assoc. Petrol. Geol. Bull., v.43, p.1–38.

Folk, R.L., 1962, Spectral subdivision of limestone types: Am. Assoc. Petrol. Geol. Mem. v.1,p.62–84.

Folk, R.L., 1965, Some aspects of recrystallization in ancient limestones, *in* Pray, L.C., and Murray, R.C., eds, Dolomitization and Limestone Diagenesis: Soc. Econ. Paleont. Mineral. Spec. Pub. No.13, p.14–48.

Folk, R.L., 1974, The natural history of crystalline calcium carbonate: effects of magnesium content and salinity: Jour. Sed. Petrology, v.44, p.40-53.

Fortey, R.F., 1984, Global earlier Ordovician transgression and regression and their biological implication, *in* Bruton, D.L., ed., Aspects of the Ordovician System, Palaeontological Contributions from the University of Oslo: Oslo, Universitets forlaget 295, p.37-50.

Friedman G.M., 1965, Occurrence and stability relationships of aragonite, high-magnesian calcite, and low-magnesian calcite under deep-sea conditions: Geol. Soc. Am. Bull., v.76, p.1191–1196.

Frost, J.G., 1974, Subtidal algal stromatolites from the Florida blackreef environment: Jour. Sed. Petrology, v.44, p.532-537.

Füchtbauer, H., and Hardie, L.A., 1976, Experimentally determined homogeneous distribution coefficients for precipitated magnesium calcites: Ann. Progr. Meeting Geol. Soc. Am. Absts., p.877.

Garrison, R.E., and Fischer, A.G., 1969, Deep-water limestone and radiolarites of the Alpine Jurassic: Soc. Econ. Paleont. Mineral. Spec. Publ., v.14, p.20-56.

Gasiewier, A., Gerdes, G., and Krumbein, W.E., 1987, The peritidal Sabkha type stromatolites of the Platy Dolomite (Ca 3) of the Leba Elevation (North Poland), *in* Perty, T.M., ed., The Zechstein Facies in Europe, Lecture Notes in Earth Sciences. Vol.10: Berlin, Springer-Verlag, p.253–272.

Gebelein, C.D., 1969, Distribution, morphology, and accretion rate of recent subtidal algal stromatolite, Bermuda: Jour. Sed. Petrology, v.39, p.49-69.

Gebelein, C.D., 1974, Biological control of stromatolite microstructure: Implications for Precambrian time stratigraphy: Am. Jour. Science, v.274, p.556-574.

Gebelein, G.D., and Hoffman, P., 1973, Algal origin of dolomite laminations in stromatolitic limestone: Jour. Sed. Petrology, v.43, p.603–613.

Ginsburg, R.N., 1955, Recent stromatolitic sediments from South Florida, absts :Jour. Palaeontology, v.29, p.723.

Ginsburg, R.N., 1960, Ancient analogues of recent stromatolites: Int. Geol. Congress XXI, Nordex, part 22, p.26-35.

Ginsburg, R.N., 1971, Landward movement of carbonate mud: new model for regressive cycles in carbonates (abstract): Am. Assoc. Petrol. Geol. Bull., v.55, p.340.

Ginsburg, R.N., and Hardie, L.A., 1975, Tidal and storm deposits, northwest Andros Island, Bahamas, *in* Ginsburg, R.N., ed., Tidal Deposits: Berlin,Springer-Verlag, p.201–208.

Ginsburg, R.N., and James, N.P., 1974, Holocene carbonate sediments of continental shelves, *in* Burke, C.A., and Drake, C.L., eds, The Geology of Continental Margins: New York, Springer-Verlag, p.137-155.

Glover, E.D., and Pray, L.C., 1971, High-magnesian calcite and aragonite cementation within modern subtidal carbonate sediment grains, *in* Bricker, O.P., ed., Carbonate Cements: Baltimore, Johns Hopkins Press, p.80–118.

Godfrey, J.S., and Lindstrom, E.J., 1989, The heat butget of the Equatorial Western Pacific Surface Mixed Layer: Jour. Geolphysical Research, v.94, p.8007-8017.

Golubic, S., and Focke, J.W., 1978, *Phormidium Hendersonii Howe* : identity and significance of a modern stromatolite building microorganism: Jour. Sed. Petrology, v.48, p.751-764.

Gordon, A.L., and Baker, T.N., 1982, Southern Ocean Atlas: Thermohaline and Chemical Distributions and the Atlas Data Set: New Delhi, Amerind Publ. Co. P.V.T. Ltd., 12p./233plate.

Gregg, J.M., 1983, On the formation and occurrence of saddle dolomite — discussion: Jour. Sed. Petrology, v.53, p.1025–1033.

Gregg, J.M., and Sibley, D.F., 1984, Epigenetic dolomitization and the origin of xenotopic dolomite texture: Jour. Sed. Petrology, v.54, p.0908–0931.

Grotzinger, J.P., 1986, Cyclicity and palaeoenvironmental dynamics, Rocknest platform, northwest Canada: Geol. Soc. Am. Bull., v.97, p.1208-1231.

Grover, G., and Read, J.F., 1983, Sedimentology and diagenesis of Middle Ordovician carbonate, Virginia: Soc. Econ. Palaeont. Mineral., Core Workshop No.4, p.2–25.

Grover, G., and Read, J.F., 1983, Paleoaquifer and deep burial related cements defined by regional cathodoluminescent patterns, Middle Ordovician carbonates, Virginia: Am. Assoc. Petrol. Geol. Bull., v.67, p.1275–1303.

Grunder, J., and Roster, H., 1963, Zur Entstehung der oberdovonischen Kalknollengesteine Thuringens: Geologie, v.12, p.1009-1038.

Gunatilaka, H.A., and Shearman, D.J., 1988, Gypsum-carbonate laminites in a Recent Sabkha, Kuwait, *in* Friedman, G.M., ed., Carbonates and Evaporite, v.3(1), p.67–73.

Gunatilaka, H.A., Salels, A.A., and Al-Temeemi, A.Y., 1980, Plant controlled supratidal anhydrite from Al-Khiran, Kuwait: Nature, v.288, p.257–160.

Hagan, G.M., and Logan, G.M., 1975, Prograding tidal flat sequence: Hutchison Embayment, Shark Bay, Western Australia, *in* Ginsburg, R.N., ed., Tidal Deposit: New York, Springer-Verlag, p.215–222.

Halbach, P., 1986, Process controlling the heavy metal distribution in Pacific ferromanganese nodules and crusts: Geol. Rdsh., v.75, p.253-247.

Halley, R.B., 1976, Textural variation within Great Salt Lake algal mounds, in Walter, M:R., ed., Stromatolites: Developments in Sedimentology 20: Amsterdam, Elsevier, p.436-445.

Handford, G.R., 1985, Facies and bedding sequence in shelf-storm-deposited carbonates – Fayetteville shale and Pitkin Limestone (Mississipian, Arkansas): Jour. Sed. Petrology, v.56, p.123–137.

Hanshaw, B.C., Beck, W. and Deika, R.G., 1971, A geochemical hypothesis for dolomitization by groundwater: Econ. Geol., v.66, p.710–724.

Hamada, T., Zgo, H., Kobayashi, T., and Koika, T., 1975, Older and Middle Palaeozoic formation and fossils of Thailand and Malaysia: Geol. Palaentol. SE Asia, v.15, p.1–37.

Hardie, L.A., and Ginsburg, G.N., 1977, Layering: the origin and environmental significance of lamination and thin bedding, *in* Hardie, L.A., ed., Sedimentation on the Modern Carbonate Tidal flats of Northwest Andros Island, Bahamas: Johns Hopkins Studies in Geology , v.22, p.50-123.

Harland, T. L., 1981, Middle Ordovician reefs of Norway: Lethaia, v.3, p.169-188.

Harland, T. L., Pickerill, R.K., and Fillion, D., 1987, Establishment and development of patch reefs in the intracratonic Ordovician sequence near Chicoutimi: Lethaia , v.20, p.189-208.

Harms, J.C., Southard, J.B., Spearing, D.R., and Walker, R.G., 1975, Depositional environments as interpreted from primary sedimentary structures and stratification sequence: Soc. Econ. Paleont. Mineral. Short Course Notes, No.2, 161 pp.

Harwood, G.M., and Moore, C.H., 1984, Comparative sedimentology and diagenesis of Upper Jurassic ooid grainstone sequences, East Texas Basin, *in* Harris, P.M., ed., Carbonate Sands - a Core workshop: Soc. Econ. Paleont. Mineral. Core Workshop no. 5, p.176-232.

Havlicek, V., 1989, Climatic changes and development of benthic communities through the Mediterranean Ordovician: Sbor. Geol. Ved. Geologie, v.44, p.79-116.

Heller, P.L., Komar, P.O., and Pevear, R.D., 1980, Transport process in ooids genesis: Jour. Sed. Petrology, v.50, p.952.

Hoffman, P., 1974, Shallow and deep water stromatolites in Lower Proterozoic platform-to-basin facies change, Great Slave Lake, Canada: Am. Assoc. Petroleum Geologists, v.58, p.856–867.

Hoffman, P.F., 1967, Algal stromatolite: use in stratigraphic correlation and paleocurrent determination: Science, v.157, p.1043–1045.

Hofmann, H.J., 1969, Attributes of stromatolites: Geol. Surv. Canada Paper 69-39, p.58.

Hollmann, R., 1962, Über Subsolution und die "Knollen Kalk" des Calcare Ammonitico Rosso Superiore, *in* Monte Baldo(Maln, Norditalien): N. Jb. Geol. Palaont. Mh., v.4, p.163-179.

Horowitz, A.S., and Potter, P.E., 1971, Introductory Petrography of Fossils: Berlin, Springer-Verlag, p,13-33.

Houghton, R.W., 1986, Thermal structure along 4°W in the gulf of Guinea during 1983-1984: Jour. Geophysical Research, v.91, p.11,727-11,739.

Hudson, J.D., 1962, Pseudo-palaeochroic calcite in recrystallized shell limestones: Geol. Magazine, v.99, p.492-500.

Hudson, J.D., 1965, Preservation and recrystallization in some Jurassic mollusc shells from Scotland, abstr: Spec. Pap. Geol. Soc. Am., v.82, p.98.

Hudson, J.D., 1975, Carbon isotopes and limestone cement: Geology, v.3, p.19-22.

Hudson, J.D., 1977, Stable isotope and limestone lithification: Geol. Soc. London, v.133, p.637–660.

Humphrey,J.D., 1988, Late Pleistocene mixing zone dolomitization, southeastern Barbados, West Indies: Sedimentology, v.35, p.327-348.

Hsü, K.J., and Siegenthaler, C., 1969, Preliminary experiments on hydrodynamic movement induced by evaporation and their bearing on the dolomite problem: Sedimentology, v.12, p.11-25.

Illing, L.V., 1954, Bahamian calcareous sands: Am. Ass. Petrol. Geol. Bull., v.38, p.1-95.

Inden, R.F., and Moore, C.H., 1983, Beach environment, *in* Scholle, D.A., Bebout, D.G., and Moore, C.H., eds., Carbonate Depositional Environments: Am. Ass. Petrol. Geol. Mem., v.33, p.212-265.

Irwin, H., 1980, Early diagenesis carbonate precipitation and pore fluid migration in the Kimmeridge Clay of Dorset, England: Sedimentology, v.27, p.577–591.

Irwin, H., Curtis, C., and Coleman, M., 1977, Isotopic evidences for source of diagenetic carbonates form during burial of organic-rich sediments: Nature London, v.269, p.209-213.

James, N.P., 1984, Shallowing-upward sequence in carbonates, *in* Walker, R.G., ed., Facies Models: Geoscience Canada, Reprint Series 1, p.213–228.

James, N.P., and Choquette, P.W., 1983, The sea-floor diagenetic environment: Geoscience Canada, v.10, p.162–179.

James, N.P., and Choquette, P.W., 1984, Diagenesis 9 Limestone — the meteoric diagenetic environment: Geoscience Canada, v.11, p.161–194.

James, N.P., and Ginsburg, R.N., 1979, The seaward margin of Belize barrier and atoll reefs: Spec. Publ. Int. Ass. Sediment, v.3, p.191 p.

James, N.P., Ginsburg, R.N., Morszalek, D.S., and Choquette, P.W., 1976, Facies and fabric specification of early subsea cements in shallow Berlize (British Honduras) reefs: Jour. Sed. Petrology, v.46, p.523–544.

Javanaphet, J.C., 1969, Geological Map of Thailand, 1:1,000,000: Department of Mineral Resources, Bangkok, Thailand.

Jell, P.A., Burrett, C.F., Stait, B., and Yochelson, E.L., 1984, The Early Ordovician bellerophontoid Peelerophon oehlerti (Bergeron) from Argentina, Australia, and Thailand: Alcheringa, v.8, p.169–176.

Jenkyns, H.C.,1971, The genesis of condensed sequences in the Tethyan Jurassic: Lethaia, v.4, p.327-352.

Jenkyns, H.C., 1974, Origin of red nodular limestone (Ammonitico Rosso, Knollenkalka) in the Mediterranean Jurassic: a diagenetic model: Spec. Publ. Int. Assoc. Sediment., v.1, p.249–271.

Jenkyns, H.C.,1977, Fossil nodules, *in* Glasby, G.P., ed., Marine Manganese Deposits: New York, Elsevier Sci. Publ. Co., p.87-108.

Jones, C.R., 1968, Lower Palaeozoic rocks of the Malay Peninsula: Am. Assoc. Petrol. Geol. Bull.,v.52, p.1259–1278.

Jones, C.R., 1973, Lower Palaeozoic, *in* Gobbet, D.J., and Hutchison, C.S., eds, Geology of Malaysia Peninsula: New York, Wiley, p.25–60.

Jones, C.R., 1981, The geology and mineral resources of Perlis, north Kedah and the Langkawi Island: Geol. Surv. Malaysian District Mem., v.17, p.1–256.

Jones, J.R., and Cameron, B., 1988, Modern coastal back-barrier environment : Analog for coal basin or for carbonaceous black shale?: Geology, v.16, p.345-348.

Jozef, W., 1980, Relations between stromatolites and burrowing organisms, abst: Am. Assoc. Petroleum Geologists Bull., v.64, p.803.

Kaldi, J., and Gidman, J., 1982, Early diagenetic dolomite cements: Examples from the Permian Lower Magnesian Limestone of England and the Pleistocene carbonates of the Bahamas: Jour. Sed. Petrology, v.52, p.1073–1085.

Kalkowsky, E., 1908, Oolith und stromatolith in norddentschen Bundsandstein: Z. Dtsch. Geol. Ges., v.60, p.68–125.

Kempe,S., and Kazmierczak, J., 1990, Calcium carbonate supersaturation and the formation of *in situ* calcified stromatolites, *in* Ittekkot, V., Kempe,S., Michaelis, W., and Spitzy, A., eds., Facets of Modern Chemistry: Berlin, Springer-Verlag, p.255-278.

Kendal, C.g.St.C., and Skipwith, P.A.d'.E., 1969, Holocene shallow water carbonate and evaporite sediment of Khor at Bazam, Abu Dhabi, southwest Persian Gulf: Am. Assoc. Petroleum Geologists, v.53 p.841-869.

Kendall, A.C., 1977, Origin of dolomite motting in Ordovician limestones from Saskstchewan and Manitoba: Canadian Petroleum Geology Bull., V.25, p.480-504.

Kendall, A.C., 1984, Evaporites, *in* Walker, R.G., ed., Facies Models: Second edition, Geoscience Canada Reprint Series 1, p.259–296.

Kendall, A.C., 1985, Radaxial fibrous calcite: A reappraisal, *in* Schneidermann, N., and Harris, P.M., eds, Carbonate Cements: Soc. Econ. Paleont. Mineral. Spec. Publ. No.36, p.59–77.

Kennard, J.M., and James, N.P., 1986, Thrombolites and stromatolites: two distinct types of microbial structures: Palaios, v.1, p.492–503.

Kepper, Jr, J.C., 1966, Primary dolostone patterns in the Utah-Nevada Middle Cambrian: Jour. Sed. Petrology, v.36, p.548–562.

King Jr., D.T., 1990, Upper Cretaceous marl-limestone sequence of Albama: possible products of sea level change, not climate forcing: Geology, v.18, p.19-22.

Kinsman, D.J.J., 1969, Interpretation of Sr^{2+} concentrations in carbonate minerals and rocks: Jour. Sed. Petrology,v.39, p.486-508.

Kirschvink, J.L., and Chang, S.B.R., 1984, Ultrafine-grained magnetite in deep-sea sediments: possible bacterial magnetofossils: Geology, v.12, p.559-562.

Knauth, L.P., and Epstein, S., 1976, Hydrogen and oxygen isotope ratios in nodular and bedded cherts: Geochim. Cosmochim. Acta, v.40, p.1095–1108.

Knoll, A.H., Sweett, K., and Burkhardt, E., 1989, Palaeoenvironmental distribution of microfossils and stromatolites in the Upper Proterozoic Backlundtoppen Formation, Spitsbergen: Jour. Palaeontology, v.63, p.129-145.

Kobayashi, T., 1957, Upper Cambrian fossils from peninsular Thailand: Jour. Fac. Sci. Univ. Tokyo, Ser. 2, v.10, p.367–382.

Kobayashi, T., 1958, Some Ordovician fossils from the Thailand-Malayan borderland: Japan. Jour. Geol. Geog., v.24, p.223–231.

Kobayashi, T., 1959, On some Ordovician fossils from northern Malaysia and her adjacence: Jour. Fac. Sci. Kokyo Univ., Ser.2, v.11, p.387–407.

Kobayashi, T., 1964, Geology of Thailand: Geol. Paleont. S.E. Asia, v.1, p.1-15.

Kobayashi, T., 1973, The Early and Middle Palaeozoic history of the Burmese-Malayan geosyncline: Geol. Palaeont. S.E. Asia, v.11, p.93–107.

Kobayashi, T., 1984a, On the geological history of Thailand and West Malaysia: Geol. Palaeont. S.E. Asia, v.25, p.3–24.

Kobayashi, T., 1984b, Older Palaeozoic gastropods and cephalopods of Thailand and Malaysia: Geol. Palaeont. S.E. Asia, v.25, p.195–199.

Kobayashi, T., and Hamada, T., 1964, On the Middle Ordovician fossils from Satun, the Malaysian Frontier of Thailand: Geol. Paleont. S.E. Asia, v.1, p.269-277.

Kobluk, D.R., and Risk, M.J., 1977, Calcification of exposed filaments of endolithic algae, micrite envelope formation and sediment production: Jour. Sed. Petrology, v.47, p.517-528.

Krumbein, W.E., 1983, Stromatolites — the challenge of a term in space and time: Precambrian Research, v.20, p.493–531.

Ku, J.L., 1977, Rate of accretion, *in* Glasby, G.I., ed., Marine Manganese Deposits: Amsterdam, Elsevier Sci. Publ. Co., p.249-267.

Kumar, S., 1988, Mineralogy and element variations in the Vindhyan stromatolites, Central India: Jour. Geol. Soc. India, v.31, p.398-403.

Kuss, J., and Lepping, U., 1989, The early Tertiary (middle-late Paleocene) limestones from the western Gulf of Suez, Egypt: N. Jb. Geol. Palaeont. Abh., v.177, p.289-332.

Lancelot, Y., Hathaway, J.C., and Hollister, C.D., 1972, Lithology of sediments from the western North Atlantic, leg XI, Deep Sea Drilling Project, *in* Hollister, C.D., and Ewing, J.I., et al., eds, Init. Repts. DSDP, UXI: Washington, U.S. Government Printing Office, p.901-949.

Land, L.S., 1971, Phreatic versus meteoric diagenesis of limestones: evidence from a fossil water table in Bermuda, *in* Bricker, O.P., ed., Carbonate Cements: Baltimore, Johns Hopkins, p.133–136.

Land, L.S., 1973, Contemporaneous dolomitization of Middle Pleistocene reefs by meteoric water, North Jamaica: Bull. Marine Sci., v.23, p.64–92.

Land, L.S., 1980, The isotopic and trace element geochemistry of dolomite: the state of the art: Soc. Econ. Paleont. Mineral. Spec. Publ. No.28, p.87–110.

Land, L.S., 1986, Limestone diagenesis - some geochemical considerations, *in* Mumpton, F.A., ed., Studies in diagenesis: U.S. Geol. Survey Bull. 1578, p.129-137.

Lanier, W.P., 1988, Structure and morphogenesis of microstromatolites from the Transvaal Supergroup, South Africa: Jour. Sed. Petrology, v.58, p.84-99.

Laporte, L.F., 1967, Carbonate deposition near sea-level and resultant facies mosaic : Manlius Formation (Lower Devonian) of New York State: Am. Ass. Petrol. Geol. Bull., v.51, p.73-101.

Lasemi, Z., and Sandberg, P.A., 1984, Transformation of aragonite-dominated lime muds to microcrystalline limestone: Geology, v.12, p.420–423.

Le Campion-Alsumard, L., Campbell, S.E., and Golubic, S., 1982, Endoliths and the depth of the Photic zone - discussion: Jour. Sed. Petrology, v.52, p.1333.

Lee, C.P., 1983, Stratigraphy of the Tarutao and Machinchang Formation, *in* Natalaya, P., ed., Stratigraphic Correlation of Thailand and Malaysia: Geol. Soc. Thailand, Bangkok, v.1, p.20–38.

Lees, A., 1975, Possible influence of salinity and temperature on modern shelf carbonate sedimentation: Marine Geology, v.19, p.159-198.

Lindstrom, M., 1984, The Ordovician climate based on the study of carbonate rocks, *in* Bruton, D.L., ed., Aspects of the Ordovician System: Palaeontoligical Contributions from the University of Oslo, Oslo, Universitetsforlaget, v.295, p.37-50.

Logan, B.W., 1961, Cryptozoon and associated stromatolites from the Recent Shark Bay, Western Australia: Jour. Geology, v.69, p.517-533.

Logan, B.W., 1974, Inventory of diagenesis in Holocene-Recent carbonate sediment, Shark Bay, Western Australia, *in* Logan, B.W., Read, J.W., Hagan, G.M., Hoffman, P., Brown, R.G., Woods, P.J., and Gebelein, C.D., eds, Evolution and Diagenesis of Quaternary Carbonate Sequences, Shark Bay, Western Australia: Am. Assoc. Petrol. Geol. Mem. v.22, p.195–249.

Logan, B.W., and Semeniuk, V., 1976, Dynamic metamorphism: Process and products in Devonian carbonate rocks, Canning Basin, Western Australia: Spec. Publ. Geol. Soc. Australia, v.6, p.1-138.

Logan, B.W., Hoffman, P., and Gebelein, C.D., 1974, Algal mats, cryptalgal fabrics, and structures, Hamelin Pool, Western Australia, in Logan, B.W., Read, J.W., Hagan, G.M., Hoffman, P., Brown, R.G., Woods, P.J. and Gebelein, C.D., eds, Evolution and Diagenesis of Quaternary Carbonate Sequences, Shark Bay, Western Australia: Am. Assoc. Petrol. Geol. Mem., v.22, p.141–193.

Logan, B.W., Read, J.F., Hagen, G.M., and Hoffman, P., 1974, Evolution and diagenesis of Quaternary carbonate sequence, Shark Bay, Western Australia: Am. Assoc. Petrol. Geol. Mem., v.22, p.140–144.

Logan, B.W., Rezak, R., and Ginsburg, R.N., 1964, Classification and environmental significance of algal stromatolites: Jour. Geology, v.72, p.68-83.

Lohmann, K.C., and Meyers, W.J., 1977, Microdolomite inclusions in cloudy prismatic calcite: A proposed criteria for former high-magnesian calcite: Jour. Sed. Petrology, v.47, p.1078–1088.

Longman, M.W., 1980, Carbonate diagenetic textures from near-surface diagenetic environments: Am. Assoc. Petrol. Geol. Bull., v.64, p.461–487.

Loreau, J.P., and Purser, B.H., 1973, Distribution and Ultrastructure of Holocene Ooids in the Persian Gulf, *in* Purser, B.H., ed., The Persian Gulf: Holocene Carbonate Sedimentation and Diagenesis in a Shallow Epicontinental Sea: Berlin, Springer-Verlag, p.279-328.

Loucks, R.G., 1977, Porosity development and distribution in shoal-water carbonate complexes-subsurface Pearsall Formation (Lower Cretaceous), South Texas, *in* Cretaceous Carbonates of Texas and Mexico, applications to subsurface exploration: Texas Univ. Bur. Econ. Geol. Rept. Inv., v.89, p.97–126.

Lowenstam, H.A., 1981, Minerals formed by organisms: Sciences, v.211, p.1126-1131.

Lucia, M. 1972, Recognition of evaporite-carbonate shoreline sedimentation: Soc. Econ. Paleont. Mineral. Publ. No.16, p.160–191.

Lyons, W.B., Long, D.T., Hines, M.E., Guadette, H.E., and Armstrong, P.E., 1984, Calcification of cyanobacterial mats in Solar Lake, Sinai: Geology, v.12, p.623-626.

Machel, H.G., 1987, Saddle dolomite as a by-product of chemical compaction and thermochemical sulfate reduction: Geology, v.15, p.936–940.

Majid, A.H., and Veizer, J., 1987, Deposition and chemical diagenesis of Tertiary Carbonates, Kirkuk Oil Field, Iraq: Am. Assoc. Petroleum Geologists Bull., v.70, p.898-913.

Malbach, P., 1986, Process controlling the heavy metal distribution in Pacific ferromanganese nodules and crusts: Geologische Rundschau, v.75, p.235-247.

Malcolm, W.W., 1987, Sedimentology and diagenesis of Upper Devonian carbonates, Canning Basin, western Australia: Unpubl. Ph.D thesis, University of Tasmania, Australia, 184p.

Marshall, J.D., and Middleton, P.D., 1990, Changes in marine isotopic composition and the Late Ordovician glaciation: Jour. Geological Soc. London, v.147, p.1-4.

Mason, R.C., 1986, Lithostratigraphy, sedimentology and structure of the Lower Palaeozoic Thung Song Limestone, Tarutao Island, Thailand: Unpubl. B.Sc. Honours thesis, University of Tasmmania, Australia, 91 p.

Matter, A., 1967, Tidal flat deposits in the Ordovician of Western Maryland: Jour. Sed. Petrology, v.37, p.601-609.

Matter, A., 1968, Tidal flat deposits in the Ordovician of Western Maryland, *in* Muller, G., and Friedman, G.M., eds, Recent Developments in Carbonate Sedimentology in Central Europe: New York, Springer-Verlag, p.172–174.

Mattes, B.W., and Mountjoy, E.W., 1980, Burial dolomitization of the Upper Devonian Miette Buildup, Jasper National Park, Alberta: Soc. Econ. Paleont. Mineral. Spec. Publ. No.28, p.259–297.

McCave, I.N., 1988, Biological pumping upwards of the coarse fraction of deep-sea sediments: Jour. Sed. Petrology, v.58, p.148-158.

McKenzie, J.A., 1980, Holocene dolomitization of calcium carbonate sediments from the coastal Sabkhas of Abu Dhabi, UAE: A stable isotope study: Jour. Geol., v.89, p.185–198.

McKenzie, J.A., Hsü, K.J., and Schneider, J.F., 1980, Movement of subsurface water under the Sabkha, Abu Dhabi, UAE, and its relation to evaporative dolomite genetic, *in* Zenger, D.H., Dunham, J.B., and Ethington, R.L., eds, Concepts and Models of Dolomitization: Soc. Econ. Paleont. Mineral. Spec. Pub. No.28, p.11–30.

McMaster, R.L., and Conover, J.T. 1966, Recent algal stromatolites from the Canary Islands: Jour. Geology, v.74, p.647-652.

McRae, S.G., 1972, Glauconite: Earth Science Reviews, v.8, p.397-440.

McNeil, D.F.,1990, Biogenic Magnetite from surface Holocene carbonate sediments, Great Bahama Bank: Jour. Geographical Research, v.99, p.4363-4371.

Meyers, W., 1974, Carbonate cement stratigraphy of the Lake Valley Formation (Mississippian) Sacramento Mountains, New Mexico: Jour. Geol. Petrol., v.44, p.837–861.

Meyers, W.J., 1978, Carbonate cement: their regional distribution and interpretation in Mississippian limestones of southeastern New Mexico: Sedimentology, v.25, p.371-400.

Meyers, W.J., 1980, Compaction in Mississippian skeletal limestones, southwestern New Mexico: Jour. Sed. Petrology, v.50, p.0457–0474.

Meyers, W.J., and Hill, B.E., 1983, Quantitative studies of compaction in Mississippian skeletal limestones, New Mexico: Jour. Sed. Petrology, v.53, p.0231–0242.

Milliman, J.D., 1974, Marine carbonate: Berlin, Springer-Verlag, 375p.

Milliman, J.D., Ross, D.A., Teh-Lung, K., 1969, Precipitation and lithification of deep-sea carbonates in the Red Sea: Jour. Sed. Petrology, v.39, p.724-736.

Mills, P.C., 1983, Genesis and diagnostic value of soft-sediment deformation structures – a review. Sediment: Geol., v.35, p.83–104.

Mitchell, J.T., Land, L.S. and Miser, D.E., 1987, Modern marine dolomite cement in a north Jamaican fringing reef: Geology, v.15, p.557–560.

Moller, N.K., and Kvingan, K., 1988, The genesis of nodular limestones in the Ordovician and Silurian of the Oslo Region (Norway): Sedimentology, v.35, p.405–420.

Monty, C.L., 1972, Recent algal stromatolitic deposits, Andros Island, Bahamas: Geol. Rdsch, v.61, p.742-783.

Monty, C.L., 1973, Precambrian background and Phanerozoic history of stromatolitic communities, an overview: Am. Soc. Geol. Belg., v.96, p.585-624.

Monty, Cl., 1977, Evolving concepts on the nature and the ecological significance of stromatolites, *in* Fugel, E., ed., Fossil Algal: Berlin, Springer-Verlag, p.15-35.

Monty, C.L.V., Rouchy, J.M., Maurin, A., Bernett-Rollande, M.C., and Perthuisot, J.P., 1987, Reef-stromatolites facies relationships from Middle Miocene examples of the Gulf of Suez and the Red Sea, *in* Peryt, T.M., ed., Evaporite Basins: Lecture Notes in Earth Science, v.13, p.133-188.

Mook, W.G., and Grootes, P.M., 1973, The measuring procedure for high-precision mass-spectrometric analysis of isotopic abundance ratios, specially referring to carbon, oxygen and nitrogen: Jour. Mass Spectrometry Ion Physics, v.12, p.273–298.

Morgan, W.A., 1985, Silurian Reservoirs in Upward-shoaling cycles of the Hunton Group, Mt. Everette and southwest Reeding Field, Kingfisher County, Oklahoma, *in* Roehl, P.O., and Choquette, P.W., eds, Carbonate Petroleum Reservoirs. New York, Spriger-Verlag, p.109-120.

Morrow, D.W., 1982, Dolomite — Part 2, Dolomitization Models and Ancient Dolostones: Geoscience Canada, v.9, p.95–106.

Morrow, D.W., 1987, Dolomitization of Lower Paleozoic burrow-fillings: Jour. Sed. Petrology, v.48, p.295–306.

Moshier, S.O., 1989, Microporosity in micritic limestones: Sedimentary Geology, v.63, p.191-213.

Mount, J.F., and Ward, P., 1986, Origin of limestone/marl alternations in the Upper Maastrichtion of Zumaya, Spain: Jour. Geol. Petrol., v.56, p.228–236.

Mullins, H.T., Neumann, A.C., and Wilbur, R.J., 1980, Nodular submarine cementation on Bahamian slope — possible model for origin of some nodular limestones (abstract): Am. Ass. Petrol. Geol., v.64, p.755.

Murray, J.W., 1979, Iron oxides, *in* Burns, R.G., ed., Marine Minerals, Review in Mineralogy: Min. Soc. Am., p.47-97.

Nancy, C., and James, N.P., 1987, Cambrian grand cycles: A northern Appalachian perspective: Geol. Soc. Am. Bull., v.98, p.418–429.

Nelson, C.S., 1978, Temperate shelf carbonate sediments in the Cenozoic of New Zealand: Sedimentology, v.25, p.737-771.

Nelson, C.S., 1988, An introductory perspective on non-tropical shelf carbonates: Sed. Geology, v.60, p.3-12.

Nelson, C.S., Harris, G.J., and Young, H.R., 1988, Burial-dominated cementation in non-tropical carbonates of the Oligocene Te Kulti Group, New Zealand: Sed. Geology, v.60, p.233-250.

Neumann, A.C., 1968, Biological erosion of limestones coasts, *in* Fairbridge, R.W. ed., Encyclopedia of Geomorphology: New York, Reinhold Book Co., p.75-81.

Neumann, A.C., Gebelein, C.D., and Scoffin, T.P., 1970, The composition, structure and erodability of subtidal mat, Abaco, Bahamas: Jour. Sed. Petrology, v.40, p.274-297.

Nicoll, R.S., and Gorter, J.D., 1984, Interpretation of additional conodont colour alteration date and the thermal maturation and geothermal history of the Canning Basin, Western Australia, *in* Percell, P.G., ed., The Canning Basin, W.A. : Proceeding Geol. Soc. Australia Petroleum Explolation Symposium, Perth, p.411-425.

Nier, A.O., and Gulbransen, E.A., 1939, Variations in the relation abundance of carbon isotopes: Jour. Am. Chem. Soc., v.61, p.697–698.

Odin, G.S., and Letolle, R. 1980, Glauconitization and phosphotization environments: A tentative comparison: Soc. Econ. Palaeontologists Spec. Publ. 29, p.227-237.

Odin, G.S., and Matter, A., 1981, De glauniarum origin: Sedimentology, v.28, p.611-641.

Olausson, E., 1985, The glacial oceans: Palaeongeogr. Palaeoclim. Palaeoecol., v.50, p.291-301.

Parker, W.C., Ragland, P.C., and Textoris, D.A., 1985, Controls on trace elements in the Ordovician Black River Group; New York, U.S.A.: Chem, Geology, v.53, p.83-94.

Perkins, R.D., 1968, Primary rhombic calcite in sedimentary carbonates: Jour. Sed. Petrology,v.38, p.371-375.

Peryt, T.M., and Peryt, D., 1975, Association of sessile tubular foraminifera and cyanophytic algae: Geol. Mag., v.112, p.612-614.

Piyasin, S., 1980, Tentative correlation of Lower Palaeozoic stratigraphy of western part of southern Shan State, Burma and northwestern through Peninsular of Thailand: Geol. Palaeont. SE Asia, v.21, p.19–24.

Playford, P.E., 1979, Environmental controls on the morphology of modern stromatolites at Hamelin Pool, Western Australia: Geol. Sur. Ann. Report, p.73-77.

Playford, P.E., 1980, Devonian "Great Barrier Reef" of Canning Basin, Western Australia: Am. Assoc. Petrol. Geol. Bull., v.64, p.814–840.

Playford, P.E., and Cockbain, A.E., 1969, Algal stromatolites: deepwater forms in the Devonian of Western Australia: Science, v.165, p.1008–1010.

Playford, P.E., and Cockbain, A.E., 1976, Modern algal stromatolites at Hamelin Pool, a hypersaline barred basin in Shark Bay, Western Australia, *in* Walter, M.R., ed., Stromatolites, Development in Sedimentology : Amsterdam, Elsevier 20, p.389-412.

Playford, P.E., Cockbain, A.E., Druce, E.C., and Wray, J.L., 1976, Devonian stromatolites from the Canning Basin, Western Australia, *in* Walter, M.R., ed., Stromatolites,Development in Sedimentology : Amsterdam, Elsevier 20, p.543–563.

Poncet, J., 1984, Microfabric and origin of Cambrian carbonate ooids — examples from the Cambrian oolite of Carteret (Northeastern Armorican Massif, France). Sediment; Geol., v.39, p.273–280.

Pratt, B.R., 1982a, Stromatolitic framework of carbonate mud-mounds: Jour. Sed. Petrology, v.52, p.1203-1227.

Pratt, B.R., 1982b, Stromatolite decline - a reconsideration: Geology, v.10, p.512-515.

Pratt, B.R., and James, N.P., 1982, Cryptalgal-metazoan bioherms of early Ordovician age in the St George Group, western Newfoundland: Sedimentology, v.29, p.543-569.

Purdy, E.G., 1963, Recent calcium carbonate facies of the Great Bahama Bank: Jour. Geology, v.71, p.472-497.

Purser, B.H., 1975, Tidal sediments and their evolution in the Bathonian Carbonates of Burgundy, France, *in* Ginsburg, R.N., ed., Tidal Deposits: New York, Springer-Verlag, p.335-343.

Purser, B.H., and Evans, G., 1973, Regional sedimentation along the Trucial Coast, SE Persian Gulf, *in* Purser, B.H., ed., The Persian Gulf: Holocene Carbonate Sedimentation and Diagenesis in a Shallow Epicontinental Sea: Berlin, Springer-Verlag, p.211-231.

Radke, B.H., and Mathis, R.L., 1980, On the formation and occurrence of saddle dolomite: Jour. Sed. Petrology., v.50, p.1149–1168.

Railsback, L.B., Ackerly, S.C., Anderson, T.F., and Cisne, J.L., 1990, Palaeontological and isotope evidence for warm saline deep waters in Ordovician oceans: Nature, v.343, p.156-159.

Rao, C.P., 1979, Glaciomarine carbonate sedimentation-Berriedale Limestone (Permian), Hobart, Tasmania, Australia (abst.): Am. Assoc. Petroleum Geologists Bull.,v.63, p.513.

Rao, C.P.,1981a, Criteria for recognition of cold-water carbonate sedimentation: Berriedale Limestone (Lower Permian), Tasmania, Australia: Jour. Sed. Petrology, v.51, p.491-506.

Rao, C.P.,1981b, Geochemical differences between tropical (Ordovician) and subpolar (Permian) carbonates, Tasmania, Australia: Geology, v.9, p.205-209.

Rao, C.P.,1986, Geochemistry of temperate-water carbonates, Tasmania, Australia: Marine Geology, v.71, p.363-370.

Rao, C.P., 1989, Geochemistry of the Gordon Limestone (Ordovician), Mole Creek, Tasmania. Aust: Jour. Earth Sci., v.36, p.65–71.

Rao, C.P., 1989, Mixing zone dolomitization in the peritidal carbonates: the Gordon Group (Ordovician), Mole Creek, Tasmania, Australia, submitted.

Rao, C.P.,1990a, Geochemical differences between subtropical (Ordovician), cool temperate (Recent and Pleistocene) and subpolar (Permian) Carbonates,Tasmania, Australia: Jour. Sed. Petrology (submitted).

Rao, C.P.,1990b, Petrography, trace elements and oxygen and carbon isotope of Gordon Group Carbonates (Ordovician), Florentine Valley, Tasmania, Australia: Sed. Geology, v.66, p.83-97.

Rao, C.P., and Green, D.C., 1982, Oxygen and carbon isotopes of early Permian cold-water carbonates, Tasmania, Australia: Jour. Sed. Petrology, v.52, p.1111–1125.

Rao, C.P., and Green, D.C.,1983, Oxygen and carbon isotope composition of Cold shallow-marine carbonates of Tasmania, Australia: Marine Geology, v.53, p.117-129.

Rao, C.P., and Wang, B., 1990, Oxygen and carbon isotope composition of Gordon Group carbonates (Ordovician), Florentine Valley, Tasmania, Australia: Aus. Jour. Earth Science, v.37, p.305-316.

Ratcliffe, K.T., 1988, Oncoids as environmental indicators in the Much Wenlock Limestone Formation of the English Midlands: Jour. Geol. Soc. London, v.145, p.117-124.

Read, J.F., 1980, Carbonate ramp-to-basin transitions and foreland basin evolution, Middle Ordovician, Virginia Appalachians: Am. Assoc. Petrol. Geol. Bull., v.64, p.1575–1612.

Read, J.F., 1982, Carbonate platforms of passive (extensional) continental margins: types, characteristics and evolution: Tectonophysics, v.81, p.195–212.

Read, J.F., 1985, Carbonate platform facies models: Am. Assoc. Petrol. Geol. Bull., v.69, p.1–81.

Reijers, T.J.A., and ten Have, A.H.M., 1983, Ooid zonation as indication for environmental conditions in a Givetian-Frasnian carbonate shelf-slope transition, *in* Peryt, T.M., ed., Coated Grains: Berlin, Springer-Verlag, p.188-198.

Rejebian, V.A., Harris, A.G., and Huebner, J.S., 1987, Conodont color and textural alteration: an index to regional metamorphism, contact metamorphism, and hydrothermal alteration: Geol. Soc. Am. Bull., v.99, p.471-479.

Ricken, W., 1986, Diagenetic bedding: Berlin, Springer-Verlag, 210p.

Riding, R., 1975, Girvanella and other algae as depth indicators: Lethaia, v.8, p.173-179.

Riding, R., 1977, Calcified Plectonema (blue-green algae), a Recent example of Girvanella from Aldabra Atoll: Palaeontology, v.20, p.33-46.

Riding, R., and Wright, V.P., 1981, Paleosols and tidal-flat/lagoon sequence on a carboniferous carbonate shelf : sedimentary associations of triple disconformities: Jour. Sed. Petrology, v.51, p.1323-1339.

Robardet, M., and Dore, F., 1988, The Late Ordovician diamictic formations from southwestern Europe: North Gondwana glaciomarine deposits: Palaeogeogr. Palaeoclim. Palaeoecol., v.66, p.19-31.

Robinson, P., 1980, Determination of calcium, magnesium, manganese, strontium, sodium and iron in the fraction of limestones and dolomites: Chemical Geology, 28, p.135–146.

Rosen, M.R., and Holdren, Jr, G.R., 1986, Origin of dolomite cement in Chesapeake Group (Miocene) siliciclastic sediments: An alternation model to burial dolomitization: Jour. Sed. Petrology, v.56, p.788–798.

Ross Jr, R.J., Jaanusson, V. and Friedman, I., 1975, Lithology and origin of Middle Ordovician calcareous mudmound of Meiklejohn Peak, Southern Nevada. U.S. Geol: Surv. Prof. Pap. 871, 48p.

Ross Jr, R.J., Valusek, J.E., and James, N.P., 1988, Nuia and its environmental significance. New Mexico Bur: Mines Mineral Resources Mem., v.44, p.115-121.

Saller, A.H., 1984, Petrologic and geochemical constraints on the origin of subsurface dolomite, Enewetak Atoll : An example of dolomitization by normal seawater: Geology, v.12, p.217-220.

Saller, A.H., 1986, Radiaxial calcite in Lower Miocene strata, subsurface Enewetak Atoll: Jour. Sed. Petrology, v.56, p.743-762.

Sandberg, P.A., and Hudson, J.D., 1983, Aragonite relic preservation in Jurassic calcite-replaced bivalves: Sedimentology, v.30, p.879-892.

Schenk, P.E., 1967, The Macumber Formation of the Maritime Province, Canada-A Misissippian analogue to Recent strand-line Carbonates of the Persian Gulf; Jour. Sed. Petrology, v,37, p.365-376.

Schidlowski, M., 1988, A 3,800-million-year isotopic record of life from carbon in sedimentary rocks: Nature, v.333, p.313–318.

Schlager, W., and James, N.P., 1978, Low-magnesian calcite limestones forming at the deep-sea floor, Tongue of the Ocean, Bahamas: Sedimentology, v.25, p.675-702.

Schlanger, S.O., 1964, Petrology of the limestone of Guam: U.S. Geol. Surv. Prof. Papers 403D, p.1-52.

Scholle, P.A., and Arthur, M.A., 1976, Carbon-isotopic fluctuations in Upper Cretaceous sediments; an indicator of palaeo-oceanic circulation : Geol. Soc. Am. Abstracts with Programs, v.8, p.1089.

Scoffin, T.P., 1970, The trapping and binding of subtidal carbonate sediments by marine vegetation in Bimini Lagoon, Bahamas: Jour. Sed. Petrology, v.40, p.249-273.

Scoffin, T.P., 1987, An Introduction to Carbonate Sediments and Rocks: London, Blackie, 274 p.

Scotese, C.R., and McKerrow, W.S., 1990, Revised World maps and introduction, *in* McKerrow, W.S., and Scotese, C.R., eds., Palaeozoic Palaeogeography and Biogeography: Geological Society Memoir no.12, p.19-21.

Seibold, E., and Berger, W.H., 1982, The Sea Floor: Berlin, Springer-Verlag, 228p.

Serebryakov, S.N., and Semikhatov, M.A., 1974, Riphean and Recent stromatolites: A comparison: Am. Jour. Science, v.274, p.556-574.

Shanmugam, G., and Benedict III, G.L., 1983, Manganese distribution in the carbonate fraction of shallow and deep marine lithofacies, Middle Ordovician, Eastern Tennesee: Sed. Geology, v.35, p.159-175.

Sheppard, S.M.F., and Schwarcz, H.P., 1970, Fractionation of carbon and oxygen isotopes and magnesium between co-existing metamorphic calcite and dolomite: Contrib. Mineral. Petrol., v.26, p. 161-198.

Shergold, J., Burrett, C., Akerman, T. and Stait, B., 1988, Late Cambrian trilobites from Tarutao Island, Thailand: New Mexico Bur. Mines Mineral Resources Mem., v.44, p.303–320.

Shinn, E.A., 1983, Tidal flat environment, *in* Scholle, D.A., Bebout, D.G., and Moore, C.H., eds, Carbonate Depositional Environments; Am. Assoc. Petrol. Geol. Mem., v.33, p.171–210.

Shinn, E.A., and Robbin, D.M., 1983, Mechanical and chemical compaction in fine-grained shallow-water limestones: Jour. Sed. Petrology, v.53, p.595–618.

Shukla, V., and Friedman, G.M., 1983, Dolomitization and diagenesis in a shallowing-upward sequence: the Lockport Formation (Middle Silurian), New york State: Jour. Sed. Petrology, v.53, p.707-717.

Sibley, D.F., 1980, Climatic control of dolomitization, Seroe Domi Formation (Pliocene), Bonaire, N.A, *in* Zenger, D.H., Dunham, J.B., and Ethington, R.L., eds, Concepts and Models of Dolomitization: Soc. Econ. Paleont. Mineral. Spec. Publ., v.28, p.247–258.

Sibley, D.F., 1982, The origin of common dolomite fabrics: clue from the Pliocene. J. Sediment: Petrol., v.52, p.1087–1100.

Sibley, D.F., and Murray, R.C., 1972, Marine diagenesis of carbonate sediment, Bonair, Netherlands Antills: Jour. Sed. Petrology, v.42, p.168-178.

Sorokin, Y.I., 1972, Role of biological factors in the sedimentation of iron, manganese, and cobalt in the formation of nodules: Oceanology, v.12, p.1-11.

Southgate, P.N., 1989, Relationship between cyclicity and stromatolite form in the Late Proterozoic Bitter Spring Formation, Australia: Sedimentology, v.36, p.323-339.

Srivastava, N.K., 1977, Sedimentology and geochemical studies of the Late Precambrian stromatolites of India, *in* Flugel, E., Fossil Algae-Recent Results and Develoments: Berlin, Springer-Verlag, p.107-112.

Stait, B., and Burrett, C., 1984a, Early Ordovician polyplacophoran Chelodes whitehousei from Tarutao Island, Southern Thailand: Alcheringa, v.8, p.112.

Stait, B., and Burrett, C., 1984b, Ordovician nautiloid fauna of Central and Southern Thailand: Geol. Mag., v.121(2), p.115–124.

Stait, B., Burrett, C., and Wongwanich, T., 1984, Ordovician trilobites from the Tarutao Formation, Southern Thailand: N. Jb. Geol. Palaeont. Mh.,: p.53–64.

Steinen, R.P., 1978, On the diagenesis of lime mud: scanning electron microscopic observation of subsurface material from Barbados, W.I. : Jour. Sed. Petrology, v.48, p.1131–1188.

Stewart, W.N., and Taylor, T.N., 1965, The peel technique, *in* Kummel, B. and Raup, D., eds, Handbook of Palaeontological Techniques: San Francisco, Freeman, p.224–232.

Stoessell, R.K., Ward, W.C., Ford, B.H., and Schuffert , 1989, Water chemistry and $CaCO_3$ dissolution in the saline part of an open-flow mixing zone, coastal Yucatan Peninsula,Mexico: Geol. Soc. Am. Bull., v.101, p.159-169.

Stolz, J.F., Lovley, D.R., and Haggerty, S.E., 1990, Biogenic magnetite and the magnetization of sediments: Jour. Geophysical Research, v.95, p.4355-4361.

Suchecki, R.K., and Hubert, J.F., 1984, Stable isotopic and elemental relationships of ancient shallow-marine and slope carbonates, Cambro-Ordovician Cow Head Group, Newfoundland: Implications for fluid flux: Jour. Sed. Petrology, v.54, p.1062–1080.

Sweet, W.C., 1984, Graphic correlation of upper Middle and Upper Ordovician rocks, North American Midcontinent Province, USA, *in* Bruton, D.L., ed., Aspects of the Ordovician System, Palaeontological Contributions from the University of Oslo: Oslo, Universitets forlaget 295, p.23-35.

Tansuwan, W., Chaodumrong, P., and Teansiri, P., 1982, Report on the geology of Satun Province Quadrangle with geological map, scale 1:250,000: Geol. Surv. Div., Dept of Mineral Resources, Bangkok, Thailand: 71p.

Taylor, M.E., and Forester, R.M., 1979, Distributional model for marine isopod crustaceans and its bearing on early Palaeozoic palaeozoogeography and continental drift : Geological Society of America Bulletin, Part 1, v.90, p.405-413.

Teraoka, Y., Sawata, H., Yoshida, T., and Pungrassami, T., 1982, Lower Palaeozoic Formation of the Tarutao Islands, Southern Thailand: Prince of Songkhla Univ., Geol. Res. Project Publ. No.6, 54 p.

Textoris, D.A., and Carrozzi, A.V., 1966, Petrography of a Caxygan (Silurian) stromatolite mound and associated facies,Ohio: Am. Ass. Petrol. Geol. Bull., v.50, p.1375-1388.

Thornton, S.E., Pilkey, O.H., and Lynts, G.L., 1978, A lagoonal crustose coralline algal micro-ridge : Bahiret EL Bibane, Tunisia: Jour. Sed. Petrology, v.48, p.743-750.

Trompette; R., and Boudzoumou, F., 1988, Palaeogeographic significance of stromatolitic buildup on Late Proterozoic Platforms: example of the West Congo Basin: Palaeogeogr. Palaeoclim. Palaeoecol., v.66, p.102-112.

Tsien, H.H., 1985, Algal-bacterial origin of micrites in mud mounds, *in* Toomey, D.F., and Nitecki, M.H., Paleoalgology: Contemporary Research and Applications: Berlin, Springer-Verlag, p.290-296.

Tucker, M.E., 1973, Ferromanganese nodules from the Devonian of the Montague Noira (S.France) and West Germany: Geol. Rdsch., v.62, p.137-153.

Tucker, M.E., 1974, Sedimentology of Palaeozoic pelagic limestone : the Devonian Griotte (southern France) and Cephalopodenkalk (Germany): Spec. Publ. Int. Assoc. Sed., v.1, p.71-92.

Tucker, M.E., 1977, Stromatolitic biostromes and associated facies in the Late Precambrian Porsanger Dolomite Formation of Finnmark, Arctic Norway: Palaeogeography, Palaeoclimatology, Palaeoecology, v.21, p.55-83.

Tucker, M.E., and Wright, V.P., 1990, Carbonate Sedimentology: Oxford, Blackwell Scientific Pub., 482p.

Udomratn, C., Muenlek, S., and Wongwanich, T., 1981, Preliminary report on the stratigraphy of Southern Thailand: Geol. Surv. Div., Dept of Mineral Resources, Bangkok, Thailand.

Usui, A., 1983/1984, Regional variation of manganese nodule facies on the Wake-Tahiti Transect: morphological, chemical and mineralogical study: Marine Geology, v.54, p.27-51.

Veizer, J., 1977, Geochemistry of lithographic limestone and dark marls from the Jurassic of southern Germany: Neues Jahrbuch für Geologie and Paläontologie Abh., v.153, p.129-146.

Veizer, J., 1978, Simulation of limestone diagenesis - a model based on strontium depletion: Discussion: Can. Jour. Earth Science, v.15, p.1683-1685.

Veizer, J., 1983, Trace elements and isotopes in sedimentary carbonates, *in* Reeder, R.J., ed., Carbonate: Mineralogy and Chemistry: Mineral. Soc. Am. Rev. in Mineral.11, p.165-199.

Veizer, J., and Demovic, R., 1973, Environmental and climatic controlled fractionation of elements in the Mesozoic carbonate sequences of the Western Carpathians: Jour. Sed. Petrology, v.43, p.258-271.

Veizer, J., and Demovic, R., 1974, Strontium as a tool in facies analysis: Jour. Sed. Petrology, v.44,p.93-115.

Veizer, J. and Hoef, J., 1976, The nature of O^{18}/O^{16} and C^{13}/C^{12} secular trands in sedimentary carbonate rocks: Geochim. Cosmochim Acta, v.40, p.1387–1395.

Veizer, J., Friz, P., and Jones, B., 1986, Geochemistry of brachiopods: Oxygen and carbon isotopic record of Paleozoic oceans: Geochim. Cosmochim. Acta, v.50, p.1679–1696.

Von der Borch, C.C., 1970, Amorphous iron oxide precipitates in sediments cores during leg 5, deep Sea Drilling Project, In. Rep. Deep Sea Drilling Proj., v.5, p.541-544.

Vukovich, F.M., Crissman, B.W., Bushnell, M., and King, W.J., 1979, Some aspects of the Oceanography of the Gulf of Mexico using satellite and in situ data: Jour. Geophysical Research, v.84, p.7749-7768.

Wagener, K., 1975, Kinetic isotope effects of oxygen in photosynthesis and respiration, *in* Goldberg, E.D., ed., The Nature of Seawater, Principal and Chemical Sciences Research Report 1: Berlin, Bahlem Konferenzen, 719p.

Wagener, K., 1975, Kinetic isotope effects of oxygen in photosynthesis and respiration, *in* Goldberg, E.D., ed., The Nature of Seawater, Principal and

Chemical Sciences Research Report 1: Berlin, Bahlem Konferenzen, p.433-451.

Wallace, M.W., 1987, Sedimentology and diagenesis of Upper Devonian carbonates, Canning Basin, Western Australia: Unpli. Ph.D. thesis, Univ. Tasm., Australia: 184p.

Walter, M.R., 1976, Introduction, *in* Walter, M.R., ed., Stromatolites: Amsterdam, Elsevier, p.1–3.

Walter, M.R.,and Bauld, J., 1986, Subtidal stromatolites of Shark Bay, in 12th Int. Cong. Sedimentology, Canberra, p.315.

Walter, M.R., Krylov, Z.N., and Muir, M.D., 1988, Stromatolite from Middle and Late Proterozoic sequences in the McArthur and Georgena Basin and the Mount Isa Province, Australia: Alcheringa, v.12, p.79-106.

Wang, B., and Rao, C.P., 1990, Diagenesis of Gordon Limestone (Ordovician), Florentine Valley, Tasmania, Australia: Sediment. Geol., in press.

Wanless, H.R., 1979, Limestone response to stress : pressure solution and dolomitization: Jour. Sed. Petrology, v.49, p.437-462.

Wanless, H.R., 1983, Burial diagenesis in limestones, *in* Parker, A., and Sellwood, B.W., eds., Sediment Diagenesis: Dordrecht, Reidel Publ. Co., p.379-417.

Ward, W.C., and Brady, M.J., 1979, Strandline sedimentation of carbonate grainstones, Upper Pleistocene, Yucatan Peninsular, Mexico: Am. Ass. Petrol. Geol. Bull., v.63, p.362-369.

Wass, R.E., Conolly, J.R., and Macintyre, R.J., 1970, Bryozoan carbonate sand continuous along Southern Australia: Marine Geology, v.9, p. 63-73.

Waters, B.B., Spencer, R.J., and Demicco, R.V., 1989, Three-dimensional architecture of shallowing-upward carbonate cycles : Middle and Upper Cambrian Waterfowl Formation, Canmore, Alberta. Can: Petroleum Geol. Bull., v.37, p.198-209.

Weaver, C.E., 1989, Clays, Muds, and Shales, Developments in Sedimentology 44: Amsterdam, Elsevier, 819p.

Webby, B.D., 1984, Ordovician reefs and climate : a review, *in* Bruton, D.L., ed., Aspects of the Ordovician System, Palaeontoligical Contributions from the University of Oslo: Oslo, Universitets forlaget, 295, p.89-100.

Weiss, C.P., and Wilkinson, B.H., 1988, Holocene cementation along the Central Texas Coast: Jour. Sed. Petrology, v.58, p.468–478.

West, I.M., Brandon, A., and Smith, M., 1968, A tidal flat evaporitic facies in the Visean of Ireland: Jour. Sed. Petrology, v.38, p.1079-1093.

Wiggins, W.D., 1986, Geochemical signatures in carbonate matrix and their relation to deposition and diagenesis, Pennsylvanian Marble Falls Limestone, Central Texas: Jour. Sed. Petrology, v.56, p.771–783.

Wilkinson, B.H., 1982, Cyclic cratonic carbonates and Phanerozoic calcite seas: Jour. Geol. Educ., v.30 , p.189-203.

Wilkinson, B.H., Janecke, S.U., and Brett, C.E., 1982, Low-magnesian calcite marine cement in Middle Ordovician hardgrounds from Kirkfield, Ontario: Jour. Sed. Petrology, v.52, p.47–57.

Williams, L.A., 1983, Deposition of the Bear Gulch limestone: a carboniferous Plattenkalk from Central Montana: Sedimentology, v.30, p.843-860.

Williams, L.A., 1984, Subtidal stromatolites in Monterey Formation and other organic-rich rock as suggested source contributors to petroleum formation: Am. Assoc. Petroleum Geologists Bull., v.68, p.1879-1893.

Williams, L.A., and Reimers, C., 1982, Recognizing organic mats in deep water environments: Geol. Soc. Am. Abstracts with Programs, v.14, p.647.

Wilson, J.L., 1974, Characteristic of Carbonate-Platform Margins: Am. Ass. Petrol. Geologist Bull., v.58, p.810-824.

Wolfart, R., U. Myo Win, Saw Boitian, U. Myo Wai, U. Peter, U.K. Cung, and U. Thit Lwin, 1984, Stratigraphy of the Western Shan Massif, Burma; Geol. Jb., B57, 92 p.

Wongwanich, T., and Burrett, C., 1983, The lower Palaeozoic of Thailand: Jour. Geol. Soc. Thailand, v.6, p.21–29.

Wongwanich, T., Wyatt, D., Stait, B., and Burrett, C., 1983, The Ordovician System in Southern Thailand and Northern Malaysia, *in* Nutalaya, P., ed., Stratigraphic Correlation of Thailand and Malaysia: Geol. Soc. Thailand, Bangkok, v.1, p.77–95.

Wongwanich, T., Burrett, C.F., Tansathein, W., and Chaodamrong, P., 1990, Lower to Mid Palaeozoic stratigraphy of mainland Satun province, southern Thailand: Jour. Southeast Asian Earth Science, v.4, p.1-9.

Wongwanich, T., and Rao, C.P., 1990, Cold-water carbonate sedimentation during Late Ordovician, the Pa Kae Formation, southern Thailand: tropical deep setting versus shallow temperate origin?, *in* Roberts, J.H., and Brown, V.A., eds., Gondwana : Terranes and Resources, abstracts no.25: Geological Society of Australia, p.73-74.

Wray, T.L., 1977, Calcareous algae: Amsterdam, Elsevier, 185p.

Wright, V.P., and Wright, J.M., 1985, A stromatolite built by a Phormidium - like alga from the Lower Carboniferous of South Wales, *in* Toomey, D.F., and

Nitecki, M.H., eds., Paleoalgology Contemporary Research and Applications: Berlin, Springer-Verlag, p.40-54.

Wyatt, D.J., 1983, Lithostratigraphy and sedimentology of the Ordovician, Lower Setul Limestone, Pulau Langkawi, Malaysia: Unpubl. B.Sc. Hons. thesis, Univ. Tasm., Australia, 126 p.

Young, G.M., and Long, D.G.F., 1976, Stromatolites and basin analyses: an example from the Upper Proterozoic of northwestern Canada: Palaeogeogr. Palaeoclimatol. Palaeoecol., v.19, p.303–318.

Zamarreno, I., 1981, Lower cambrian stromatolites from northwest Spain and their palaeoenvironmental significance, *in* Monty, C., ed., Phanerozoic Stromatolites: Berlin, Springer-Verlag, p.5-18.